

Mustafa Ashry<sup>1</sup> 



*TEV SCALE LEFT-RIGHT SYMMETRIC MODEL WITH  
MINIMAL HIGGS SECTOR*

By

Mustafa Ashry Ibrahim Seif

SUBMITTED IN PARTIAL FULFILLMENT OF THE  
REQUIREMENTS FOR THE DEGREE OF  
MASTER OF SCIENCE  
AT  
CAIRO UNIVERSITY  
CAIRO, EGYPT  
JUNE 2015

© Copyright by Mustafa Ashry Ibrahim Seif, 2015

---

<sup>1</sup>mustafa@sci.cu.edu.eg , mustafa@cu.edu.eg

CAIRO UNIVERSITY

DEPARTMENT OF MATHEMATICS

The undersigned hereby certify that they have read and recommend to the Faculty of Graduate Studies for acceptance a thesis entitled "***TeV Scale Left-Right Symmetric Model with Minimal Higgs Sector***" by **Mustafa Ashry Ibrahim Seif** in partial fulfillment of the requirements for the degree of **Master of Science**.

Dated: June 2015

---

**External Referees:**

---

Prof. Qaisar Shafi  
Department of Physics and Astronomy,  
Delaware University, USA

---

**Research Supervisors:**

---

Prof. Tarek Ibrahim  
Department of Physics,  
Alexandria University, Egypt

---

Prof. Ahmad A. Amer  
Department of Mathematics,  
Faculty of Science, Cairo University, Egypt

---

Prof. Shaaban S. Khalil  
Department of Mathematics,  
Faculty of Science, Ain Shams University, Egypt  
and  
Center for Fundamental Physics (CFP),  
Zewail City of Science and Technology, Egypt

# CAIRO UNIVERSITY

Date: **June 2015**

Author: **Mustafa Ashry Ibrahim Seif**

Title: **TeV Scale Left-Right Symmetric Model with  
Minimal Higgs Sector**

Department: **Mathematics**

Degree: **M.Sc.** Convocation: **June** Year: **2015**

Permission is herewith granted to cairo university to circulate and to have copied for non-commercial purposes, at its discretion, the above title upon the request of individuals or institutions.

---

Signature of Author

THE AUTHOR RESERVES OTHER PUBLICATION RIGHTS, AND NEITHER THE THESIS NOR EXTENSIVE EXTRACTS FROM IT MAY BE PRINTED OR OTHERWISE REPRODUCED WITHOUT THE AUTHOR'S WRITTEN PERMISSION.

THE AUTHOR ATTESTS THAT PERMISSION HAS BEEN OBTAINED FOR THE USE OF ANY COPYRIGHTED MATERIAL APPEARING IN THIS THESIS (OTHER THAN BRIEF EXCERPTS REQUIRING ONLY PROPER ACKNOWLEDGEMENT IN SCHOLARLY WRITING) AND THAT ALL SUCH USE IS CLEARLY ACKNOWLEDGED.

**To**  
*my family: my beloved parents*



*The peaceful souls of my late brothers:*

*Mohamed Ashry (1976-2008)*

*and*

*Ahmed Ashry (1983-2004)*



*The smart souls of my late friends and colleagues:*

*Waleed A. Elsayed<sup>2</sup> (1986-2015)*

*and*

*Ahmed Elsayed<sup>3</sup> (1986-2013)*

---

<sup>2</sup> Research (<https://inspirehep.net/authors/2430962>)

<sup>3</sup> Research (<https://inspirehep.net/authors/1078349>)

# Table of Contents

<b>Table of Contents</b>	v
<b>List of Tables</b>	viii
<b>List of Figures</b>	ix
<b>List of Abbreviations</b>	xii
<b>Abstract</b>	xiii
<b>Acknowledgements</b>	xiv
<b>Introduction</b>	1
<b>1 LEFT-RIGHT SYMMETRIC MODEL</b>	7
1.1 Introduction . . . . .	7
1.2 The Standard Model . . . . .	8
1.2.1 The SM Lagrangian . . . . .	10
1.2.2 Spontaneous Symmetry Breaking in the SM . . . . .	13
1.2.3 Electroweak Interactions in the SM . . . . .	16
1.2.4 Higgs Interactions in the SM . . . . .	20
1.3 Description of the LRSM . . . . .	21
1.3.1 Gauge Lagrangian . . . . .	23
1.3.2 Kinetic Lagrangian . . . . .	24
1.3.3 Scalar Lagrangian . . . . .	25
1.3.4 Yukawa Lagrangian . . . . .	28
1.3.5 The Left-Right Symmetry . . . . .	28
1.4 Spontaneous Symmetry Breaking in the LRSM . . . . .	29
1.4.1 Gauge Boson Masses in the LRSM . . . . .	31
1.4.2 Fermion Masses in the LRSM . . . . .	43
1.5 Electroweak Interactions in the LRSM . . . . .	45
1.6 Higgs Sector in the LRSM . . . . .	50

1.6.1	Doubly-Charged Scalars . . . . .	53
1.6.2	Singly Charged Scalars . . . . .	55
1.6.3	Neutral Pseudoscalars . . . . .	57
1.6.4	Neutral Scalars . . . . .	59
1.6.5	Higgs Numerical Session in the LRSM . . . . .	64
1.6.6	Higgs Interactions in the LRSM . . . . .	68
<b>2</b>	<b>ALTERNATIVE LEFT-RIGHT SYMMETRIC MODEL</b>	<b>73</b>
2.1	Introduction . . . . .	73
2.2	Description of the ALRM . . . . .	74
2.2.1	Kinetic Lagrangian . . . . .	75
2.2.2	Scalar Lagrangian . . . . .	76
2.2.3	Yukawa Lagrangian . . . . .	78
2.2.4	Ghost Lagrangian . . . . .	78
2.3	Spontaneous Symmetry Breaking in the ALRM . . . . .	79
2.3.1	Gauge Boson Masses in the ALRM . . . . .	80
2.3.2	Fermion Masses in the ALRM . . . . .	86
2.4	Higgs Sector in the ALRM . . . . .	88
2.4.1	Higgs Masses and Mixing in the ALRM . . . . .	88
2.4.2	Higgs Numerical Session in the ALRM . . . . .	98
2.4.3	Higgs Interactions in the ALRM . . . . .	100
<b>3</b>	<b>PHENOMENOLOGICAL ASPECTS OF THE ALRM</b>	<b>107</b>
3.1	Introduction . . . . .	107
3.2	The $h \rightarrow \gamma\gamma$ Decay in the ALRM . . . . .	108
3.2.1	Higgs Production . . . . .	110
3.2.2	Higgs Decays . . . . .	114
3.2.3	The $h \rightarrow \gamma\gamma$ Decay . . . . .	118
3.3	ALRM Signatures at the LHC . . . . .	131
<b>4</b>	<b>Conclusion</b>	<b>138</b>
<b>A</b>	<b>Pauli, Dirac and Gell-Mann Matrices</b>	<b>139</b>
<b>B</b>	<b>The Electric Charge Formula and Gauge Coupling Relations</b>	<b>142</b>
<b>C</b>	<b>Gauge Transformations and Covariant Derivatives</b>	<b>145</b>

<b>D The Higgs Potential in the ALRM</b>	<b>148</b>
D.1 Boundedness From Below Conditions of the ALRM Potential . . . . .	148
D.2 Minimization of the ALRM Potential . . . . .	155
<b>E Mass Matrix Diagonlization</b>	<b>157</b>
E.1 Eigenvalues . . . . .	157
E.2 Nonsingular Mass Matrix Diagonlization . . . . .	159
E.2.1 Example: $n = 2$ . . . . .	160
E.2.2 Example: $n = 3$ . . . . .	161
E.2.3 Example: $n = 4$ . . . . .	162
E.3 Singular Mass Matrix Diagonlization . . . . .	163
E.3.1 Example: $n = 2$ . . . . .	165
E.3.2 Example: $n = 3$ . . . . .	165
E.3.3 Example: $n = 4$ . . . . .	166
E.4 MATHEMATICA® Codes . . . . .	167
<b>Bibliography</b>	<b>173</b>

# List of Tables

1.1	Field content of the SM and respective quantum numbers. . . . .	9
1.2	Field content of the LRSM and respective quantum numbers. . . . .	22
1.3	A LRSM benchmark point. Gauge coupling and spectra. . . . .	42
1.4	A LRSM benchmark point. Scalar potential parameters. . . . .	65
1.5	A LRSM benchmark point. Higgs spectra. . . . .	66
1.6	Higgs parameter dependence. . . . .	67
1.7	A LRSM benchmark point. Scalar and Pseudoscalar Higgs mixing. .	67
1.8	A LRSM benchmark point. Doubly and Singly charged Higgs mixing.	68
2.1	Field content of the ALRM and respective quantum numbers. . . . .	75
2.2	An ALRM benchmark point. Scalar potential parameters. . . . .	98
2.3	An ALRM benchmark point. Higgs and Gauge spectra. . . . .	99
2.4	An ALRM benchmark. Scalar, Pseudoscalar and Charged Higgs mixing.	100
3.1	Signal vs background for the process $pp \rightarrow d'\bar{d}' \rightarrow (l^-l^+) + (u\bar{u}) + (n\bar{n})$ . .	136

# List of Figures

1.1	The potential $V$ of the scalar field $\phi$ in the cases $\mu^2 \gtrless 0$ .	13
1.2	Feynman diagram and rule of electromagnetic interactions in the SM.	18
1.3	Feynman diagram and rule of neutral current interactions in the SM.	18
1.4	Feynman diagrams and rules of charged current in the SM.	20
1.5	Feynman diagrams and rules of Higgs-gauge interactions in the SM.	21
1.6	Feynman diagram and rule of Higgs-fermion interactions in the SM.	21
1.7	$g_{BL}$ vs $g_R$ in the LRSM.	33
1.8	$v_R$ and $v_L$ vs $\varepsilon$ , $t_\beta$ and $g_R$ in the LRSM.	40
1.9	$M_{W'}$ and $M_{Z'}$ vs $\varepsilon$ , $t_\beta$ and $g_R$ in the LRSM.	40
1.10	Feynman diagram and rule of electromagnetic interactions in the LRSM.	47
1.11	Feynman diagrams and rules of neutral current interactions in the LRSM.	48
1.12	Feynman diagrams and rules of charged currents in the LRSM.	49
1.13	$m_{\pm\pm}$ in the LRSM for the fixed benchmark point in Table 1.4.	54
1.14	$m_\pm$ in the LRSM for the fixed benchmark point in Table 1.4.	57
1.15	$m_{A1,2}$ in the LRSM for the fixed benchmark point in Table 1.4.	59
1.16	$m_{h_i}$ in the LRSM for the fixed benchmark point in Table 1.4.	62
1.17	$\lambda_1$ in the LRSM for the fixed benchmark point in Table 1.4.	63
1.18	Feynman diagrams and rules of quarks and neutral Higgs the LRSM.	71
2.1	$M_{Z'}, M_{W'}, v_R$ with $s_w^2$ .	84
2.2	Weinberg angle in the ALRM.	86
2.3	$t_\beta$ vs $m_t$ in the ALRM	87
2.4	$m_\pm$ in the ALRM for the fixed benchmark point in Tab. 2.2	90
2.5	$m_{A1,2}$ in the ALRM for the fixed benchmark point in Tab. 2.2	92

2.6	$\lambda_1$ in the ALRM for the fixed benchmark point in Tab. 2.2 . . . . .	94
2.7	$m_{h_i}$ in the ALRM for the fixed benchmark point in Tab. 2.2 . . . . .	95
2.8	$T_{\phi h}, T_{Lh}, T_{Rh}$ in the ALRM for the fixed benchmark point in Tab. 2.2 . . . . .	97
2.9	Feynman diagrams and rules of Higgs-gauge interactions in the ALRM. . . . .	103
2.10	Feynman diagrams and rules of trilinear and quartic terms in ALRM . . . . .	104
2.11	Feynman diagrams and rules of quarks and neutral Higgs in the ALRM	106
3.1	Higgs boson mass, production and decays. . . . .	108
3.2	ATLAS and CMS signal strength of Higgs decays. . . . .	109
3.3	The dominant SM Higgs production mechanisms in hadronic collisions. . . . .	110
3.4	Gluon luminosity for Higgs production at the LHC. . . . .	112
3.5	Higgs production cross section at the LHC and Tevatron. . . . .	113
3.6	SM Higgs decays at $m_h = 125$ GeV. . . . .	114
3.7	ATLAS and CMS Higgs decay channel $h \rightarrow \tau\tau$ . . . . .	115
3.8	ATLAS and CMS Higgs decay channel $h \rightarrow bb$ . . . . .	115
3.9	ATLAS and CMS Higgs decay channels $h \rightarrow WW^* \rightarrow 2l2\nu$ . . . . .	116
3.10	ATLAS and CMS Higgs decay channels $h \rightarrow ZZ^* \rightarrow 4l$ . . . . .	117
3.11	ATLAS and CMS Higgs discovery via the decay channel $h \rightarrow \gamma\gamma$ . . . . .	118
3.12	Feynman rules for the decay $h \rightarrow \gamma\gamma$ at the one W-loop level in the SM	120
3.13	One-loop diagrams with $W^*$ which contribute to the $h \rightarrow \gamma\gamma$ in the SM	121
3.14	Vanishing $h \rightarrow \gamma\gamma$ diagrams mediated by $W^\pm$ and $h^\pm$ in the ALRM .	122
3.15	$\Gamma(H \rightarrow \gamma\gamma)$ at $m_h = 125$ GeV vs $t_\beta, \lambda_3$ . . . . .	123
3.16	$W^\pm$ -, $t$ - and $h^\pm$ -mediated diagrams for $h \rightarrow \gamma\gamma$ . . . . .	124
3.17	Higgs coupling ratios. . . . .	125
3.18	Higgs coupling ratios. . . . .	125
3.19	Relation between the coupling ratios mixing parameters . . . . .	126
3.21	Signal strength $\mu_{\gamma\gamma}$ and correlation between $\mu_{\gamma\gamma}$ and $\mu_{ZZ}$ in the ALRM	126
3.20	$\kappa_{\gamma\gamma}$ and $\kappa_{gg}$ as functions of $t_\beta, \lambda_3, \alpha_1, \alpha_2, m_{h_{1,2}^\pm}$ . . . . .	127
3.22	$gg \rightarrow h \rightarrow \gamma\gamma$ and $pp \rightarrow \gamma\gamma$ in the ALRM and the SM. . . . .	127
3.23	$qq \rightarrow \gamma\gamma$ and $gg \rightarrow h \rightarrow \gamma\gamma$ in the ALRM. . . . .	128

3.24 Higgs coupling ratios . . . . .	129
3.25 Differential production cross section of exotic quark vs its invariant mass	133
3.26 Creation and decay of an exotic quark $d'$ . . . . .	134
3.27 Reconstructed invariant mass of $d'$ and background without cuts . . .	135
3.28 Reconstructed invariant mass of $d'$ and background with cuts . . . . .	136

## List of Abbreviations

ALRM	Alternative Left-Right Symmetric Model
EM	Electromagnetic
EW	Electroweak
FCNC	Flavor-Changing Neutral Current
GeV	Giga Electron Volt
LH	Left-Handed
LHC	Large Hadron Collider
LR	Left-Right
LRSM	Left-Right Symmetric Model
MeV	Mega Electron Volt
RH	Right-Handed
SM	Standard Model
SSB	Spontaneous Symmetry Breaking
TeV	Tera Electron Volt
VEV	Vacuum Expectation Value

# Abstract

Nonvanishing neutrino masses represents one of the firm observational evidences of new physics beyond the Standard Model. The fact that neutrinos are massless in the SM is a reflection to the chiral structure of weak interaction that leads to a complete asymmetry between left and right. Left-right models, which are based on the gauge symmetry  $SU(3)_C \times SU(2)_L \times SU(2)_R \times U(1)_{B-L}$ , are well motivated extensions of the SM since they automatically contain the ingredients to explain the observed neutrino masses and mixings. We analyse the Left-Right Model in which the left-right symmetry is broken by triplets at a high scale. We also study the implications of this model for particle physics. In particular, we show that this conventional Left-Right Model suffering from tree-level flavor-changing neutral currents and the scale of breaking the  $SU(2)_R$  must be at very high scale.

Our analysis focus on the alternative left-right symmetric model, motivated by the superstring-inspired  $E_6$  model. We reconstruct the model and systematically analyze the constraints imposed by theoretical and experimental bounds on the parameter space of this class of models. We discuss the bounds on the right-handed gauge boson masses and possible ways of detecting the  $W_R^\pm$  and  $Z_R$ . We also discuss neutrino masses, lepton numbers violation, and other implications. We perform a comprehensive analysis of the Higgs sector and show that three neutral  $CP$ -even and two  $CP$ -odd Higgs bosons in addition to two charged Higgs bosons can be light, of  $\mathcal{O}(100)$  GeV. We emphasize that the predictions of this model for the signal strengths of Higgs decays are consistent with the standard model expectations. We also explore discovery signatures of the exotic down-type quark, which is one of the salient predictions of this model.

# Acknowledgements

I would like to start by expressing my sincere gratitude and appreciation to my advisor Prof. *Ahmad Amer* for his support, encouragement and guidance notes.

It is with gratitude that I acknowledge my advisor Prof. *Shaaban Khalil* for his support for my M.Sc. study and research. His guidance helped me in research and in writing this thesis.

I hope that my Prof. *Ahmed Khalil* is resting in peace. My sincere gratefulness to him for motivating me towards modern fields of science. I am indebted to Prof. *Hamdy Abdalgawad* and Prof. *Nabil Youssef* for helping me in the first steps of research. Also thanking both Prof. *Adel awad* and Prof. *Elsayed Lashin* is necessary for their deep and fundamental discussions.

I want to thank my late colleague *Ahmed Elsayed*, whom I really miss, for his creative discussions. I will be forever grateful for his assistance. My deep thanks to my colleagues *Ahmad Moursy*, who answers almost all of my questions, and *Waleed Abdallah*, the man of precise numerics, for their fruitful discussions and sagacious opinions. My deep thanks to my colleagues *Ebtsam Taha* and *Waleed Elsayed* for their kind support.

I wish to express deep gratitude to the Mathematics Department, Faculty of Science, Cairo University. I had the honor of being an undergraduate student in such a department. Luckily, I became a junior member of staff there. Also I would like to thank the Center for Fundamental Physics (CFP) at Zewail City for Science and Technology for providing everything I need to complete my work.

Last but not least, I would like to thank my family: my parents for their endless love and care, and for supporting me spiritually throughout my life.

Cairo, Egypt.  
May 5, 2015

*Mustafa Ashry*

# Introduction

The discovery of neutrino masses and oscillations confirmed the fact that although the standard model (SM) is extremely accurate, it is still incomplete. The left-right symmetric model (LRSM) is the most natural extension of the SM that accounts for the measured neutrino masses and provides an elegant understanding for the origin of the parity violation in low energy weak interactions [12, 19, 33, 54, 59, 61, 66, 74]. The LRSM is based on the gauge group  $SU(3)_C \times SU(2)_L \times SU(2)_R \times U(1)_{B-L} \times P$ , where  $P$  is the discrete parity symmetry. In the LRSM, the SM fermions are assigned in left-handed (LH) and right-handed (RH) doublets:

$$Q_L = \begin{pmatrix} u_L \\ d_L \end{pmatrix}, \quad L_L = \begin{pmatrix} \nu_L \\ e_L \end{pmatrix} \quad \& \quad Q_R = \begin{pmatrix} u_R \\ d_R \end{pmatrix}, \quad L_R = \begin{pmatrix} \nu_R \\ e_R \end{pmatrix}. \quad (0.0.1)$$

The parity symmetry:  $Q_L, L_L \leftrightarrow Q_R, L_R$  implies that the gauge couplings of left and right handed  $SU(2)$  are equal, *i.e.*,  $g_L = g_R = g$ . The Higgs sector of the LRSM consists of (*i*) bidoublet  $\Phi(1, 2, 2^*, 0)$ , which is required to construct SM Yukawa couplings of quarks and leptons. (*ii*) two scalar triplets  $\Delta_L(1, 3, 0, +2)$  and  $\Delta_R(1, 0, 3, +2)$  that break  $U(1)_{B-L}$  and generate neutrino Majorana masses. At high energy scale, well above the electroweak (EW) breaking scale, the  $SU(2)_R \times U(1)_{B-L} \times P$  symmetry is broken down to  $U(1)_Y$  by the *vacuum expectation value* (VEV) of the neutral component of  $\Delta_R$ , hence the RH Majorana neutrino mass is generated. In this type of models, the hypercharge  $Y$  is defined as  $Y = T_R^3 + (B - L)/2$ , where  $T_R^3$  is the third component of the RH isospin. At lower energy scales,  $\Phi$  and  $\Delta_L$  acquire VEVs that break  $SU(2)_L \times U(1)_Y$  down to  $U(1)_{\text{EM}}$ . It is worth mentioning that in the conventional LRSM, one gets the following estimate for the associated VEVs:  $\langle \Delta_L \rangle = v_L \lesssim \mathcal{O}(1)$

---

GeV,  $\langle \Delta_R \rangle = v_R \gtrsim \mathcal{O}(10^{11})$  GeV, and  $\langle \Phi \rangle = \text{diag}(k', k)$  with  $k \ll k'$  and  $k' \sim \mathcal{O}(100)$  GeV [33, 59, 61].

It turns out that the Higgs sector of the LRSM may induce tree level flavor violating processes that contradict the current experimental limits. Therefore, it is usually assumed that  $SU(2)_R \times U(1)_{B-L}$  is broken at a very high energy scale. In this case, it is not possible to detect any residual effect for  $SU(2)_R$  gauge symmetry at TeV scale in the Large Hadron Collider (LHC). This has motivated Ernest Ma, in his pioneering work in 1987 [51], to study variants of the conventional LRSM. He has shown that the superstring inspired  $E_6$  model may lead to two types of left-right models. The first one is the canonical LRSM, while the second one is what is known as alternative left-right Model (ALRM) [13, 52], where the fermion assignments are different from those in the conventional LRSM in the following: (i) an extra quark,  $d'_R$ , instead of  $d_R$ , is combined with  $u_R$  and form  $SU(2)_R$  doublet. (ii) an extra lepton,  $n_R$ , instead of  $\nu_R$ , is combined with  $e_R$  and form  $SU(2)_R$  doublet. Therefore, the RH neutrino  $\nu_R$  is a true singlet and is no longer a part of the RH doublet.

It is remarkable that  $E_6$  is a complex Lie group of rank 6. It includes the  $SO(10)$  group, so it is a good candidate for grand unification. Some string theories (Heterotic string) predict that the low energy effective model is symmetric under  $E_6$ . Depending on the string model,  $E_6$  may be broken to  $SO(10)$  and then to conventional LRSM or it may have another branch of symmetry breaking that lead to the Alternative Left-Right model that we consider. The particle content of ALRM, derived from  $E_6$  model, contains more particles than those in the conventional LRSM obtained from  $SO(10)$ . This can be simply understood from the fact that the fundamental representation 27 of  $E_6$  is equivalent to the fundamental representation 16 of  $SO(10)$  plus its 10 and singlet representations. In the conventional LRSM all non-SM particles are decoupled and can be quite heavy. However, in the ALRM they are involved with SM fermions and will have low energy consequences. Furthermore, another important difference

---

between ALRM and the conventional LRSM is the fact that tree-level flavor-changing neutral current (FCNC) are naturally absent, so that the  $SU(2)_R$  breaking scale can be of order TeV, allowing to several interesting signatures at the LHC. As ALRM is a low energy effective model of supersymmetric  $E_6$  model, the gauge couplings are not unified within the ALRM. They are unified in the underling  $E_6$  model, similar to the unification of SM gauge couplings in supersymmetric  $SU(5)$ .

In this thesis we aim at providing a comprehensive analysis for the phenomenological implications of ALRM, with emphasis on the possible signatures of this model at the LHC. There are couple of recent papers [44, 52] that discuss specific phenomenological aspects of ALRM, namely the Dark Matter search and  $Z'$  and  $W'$  signals at the LHC. Our goal here is twofold. Firstly, to analyze the Higgs sector of the ALRM and check if the recent results reported by ATLAS and CMS experiments on Higgs production and decays can be accommodated. Secondly, to explore the discovery signature of the exotic down-type quarks associated with this type of models at the LHC.

The latest results of ATLAS and CMS collaborations [4, 43], confirmed the Higgs discovery with mass around 125 GeV, through Higgs decay channels:  $h \rightarrow \gamma\gamma$ ,  $H \rightarrow ZZ^{(*)} \rightarrow 4l$ , and  $h \rightarrow WW^{(*)} \rightarrow l\nu l\nu$  at integrated luminosities of  $5.1 \text{ fb}^{-1}$  taken at energy  $\sqrt{s} = 7 \text{ TeV}$  and  $19.6 \text{ fb}^{-1}$  taken at  $\sqrt{s} = 8 \text{ TeV}$ . These results still indicate for possible discrepancies between their results for signal strengths in these channels [1, 2, 29, 30]. We show that our ALRM has a rich Higgs sector, consists of one bidoublet and two LH and RH doublets. Therefore, one obtains four neutral  $CP$ -even and two  $CP$ -odd Higgs bosons, in addition to two charged Higgs bosons. It turns out that most of these Higgs bosons can be light, of order EW scale, and can be accessible at the LHC. We also find that the contributions of the charged Higgs bosons to decay rate of  $h \rightarrow \gamma\gamma$  are not significant. Furthermore, we show that due to the mixing among the neutral  $CP$ -even Higgs bosons, the couplings of SM-like Higgs, which is

---

the lightest one, with the top quark and  $W$ -gauge boson are slightly modified respect to SM ones. Therefore, ALRM predictions for signal strengths of Higgs decays, in particular  $h \rightarrow \gamma\gamma$  and  $h \rightarrow W^+W^-$  are consistent with SM expectation.

Another salient feature of ALRM is the presence of an extra down-type quark,  $d'$ . We analyze the striking signature of this exotic quark at the LHC. We show that the most promising  $d'$ -production channel is  $gg \rightarrow \bar{d}'d'$ , due to the direct coupling of  $d'$  to gluons with strong coupling constant and color factor. Then  $d'$  decays to jet and lepton plus missing energy. We find that the cross section of this process is of  $\mathcal{O}(1)$  fb, which can be probed at the LHC with 14 TeV center of mass energy.

**The thesis has the following structure:**

1. In chapter 1, we review the SM. We then review the LRSM in detail. We wrote the field content of the LRSM and respective quantum numbers in the LR gauge group strucutre. In accordance the kinetic terms of fermions are determined. We discussed the scalar sector in a detail motivating the structure of the Higgs multiplets to be a bidoublet and two LH and RH triplets. The Yukawa type interactions are discussed. The spontaneous symmetry breaking (SSB) yields to generating masses for gauge bosons and all fermions. At this point, we discussed the generating of a Majorana mass for the neutrinos via the so-called seesaw mechanism as Majorana particles. Finally, we focused in this chapter on the EW interactions of the LRSM and the mixing in the charged weak currents in both quark and leptonic sectors and showing that the LRSM suffers from the problem of the tree-level FCNC interactions.
2. In chapter 2, we review an  $E_6$ -inspired superstring TeV-scale alternative left-right symmetric model. We wrote the field content of the ALRM and respective quantum numbers in the LR gauge group strucutre. A new discrete symmetry

---

$S$  is introduced to distinguish between scalar fields and their dual scalars. This symmetry is motivated by letting another symmetry  $L = T_R^3 + S$  to be a residual symmetry after breaking the LR symmetry. This minimized the Higgs sector of the model and cancelled the existence of the tree-level FCNC that appeared in the LRSM. The triplets of the LRSM are replaced by doublets in the ALRM. Extra particles in the ALRM are introduced and their interactions with the SM fermions are discussed. We analyzed the scalar sector in a detail. The Yukawa type interactions are shown and extracted to deduce the interactions between scalars and fermions. The SSB is discussed in detail yielding to generating masses for gauge bosons and all fermions. At this point, we discussed the generating of a mass for the neutrinos via the so-called seesaw mechanism as Majorana particles. The study of the boundedness from below imposed theoretical conditions on the potential parameters. Finally, we focused on the Higgs sector showing the existence of two  $\mathcal{O}(100)$  GeV charged Higgs bosons and four neutral  $CP$ -even Higgs bosons three of which are light of  $\mathcal{O}(100)$  GeV and the forth one is of  $\mathcal{O}(1)$  TeV. One of these neutral Higgs bosons is identified to be a SM-like one whose mass is fixed to be 125 GeV. The rotation of this neutral Higgs mass matrix affects the mixing of the SM-like Higgs with SM fermions and gauge bosons. We show these new coupling as well as the couplings with the charged Higgs bosons.

3. In chapter 3, we focus on the Higgs decay into diphoton in the ALRM and the discovery signatures of extra quark  $d'$  at the LHC. The new particles of ALRM have negligible contributions to the Higgs decays channels. Charged Higgs contribution is suppressed because of the smallness of its coupling with the SM-like Higgs. The contribution of the RH gauge boson  $W_R$  as well as the contribution of the exotic down-type quark  $d'$  is suppressed because of its

---

large mass. We emphasize that the predictions of this model for the signal strengths of Higgs decays are consistent with the SM expectations. We also explore discovery signatures of the exotic down-type quark, which is one of the salient predictions of this model. Then, we give our conclusions in chapter 4.

Finally, we insert the set of appendices and the set of references referred to which throughout the thesis.

**The main work of the thesis is based on the following paper [11]:**

M. Ashry and S. Khalil, “*Phenomenological aspects of a TeV-scale alternative left-right model*”, Phys.Rev. D91 (2015) 015009 ([arXiv: 1310.3315](#))

**The ALRM was implemented by the author into FeynRules:**

Mustafa Ashry, *Implementation of an Alternative Left-Right Symmetric Model into the FeynRules package*

(FeynRules Database: <https://feynrules.irmp.ucl.ac.be/wiki/ALRM>),

(GitHub: <https://github.com/Mustafa-Ashry/ALRM-FeynRules>).

**This Thesis can be found at [9, 10]:**

Mustafa Ashry, *TeV-Scale Left-Right Symmetric Model with Minimal Higgs Sector, MSc Thesis, Cairo University (2015)*

([https://scholar.cu.edu.eg/?q=science\\_math\\_mashry/files/mashry\\_msc\\_thesis.pdf](https://scholar.cu.edu.eg/?q=science_math_mashry/files/mashry_msc_thesis.pdf)),

(<https://inspirehep.net/literature/2708563>).

# 1

## LEFT-RIGHT SYMMETRIC MODEL

### 1.1 Introduction

The Left-Right Symmetric Model (LRSM) is mainly motivated by treating the RH particles and their interactions on an equal footing with the left ones. Parity is broken maximally in the SM. That is, all the fermions in the model are chiral Weyl fermions which means that the weak gauge bosons  $W^\pm$  and  $Z$  only couple to LH fermions. While the SM breaks parity maximally, it is an explicit exact symmetry of the LRSM until SSB takes place. Because of the vector-axialvector (V-A) structure of the weak interactions, we know parity must be broken at some point. Also, in the SM, neutrinos are massless because of the absence of the RH neutrinos and Majorana mass terms for the LH neutrinos would break the  $U(1)$  symmetry. The recent experiments showed that neutrinos do have small masses indeed  $m_\nu < 1$  eV [57]. In the context of the LRSM neutrinos can have masses through both Majorana and Dirac mass terms, as the RH neutrinos are accommodated naturally with the RH charged leptons in RH doublets under an  $SU(2)$  group in analogy with the LH doublets in the SM. The gauged  $U(1)_{B-L}$  symmetry is another peculiar feature of the LRSM. That is, the difference between baryon and lepton number  $B - L$  is a conserved quantity but, again, only until SSB takes place. The  $B - L$  gauge is a more attractive choice as it makes

more physical sense than the hypercharge from the SM. Another reason is that  $B - L$  automatically appears as a gauged symmetry in  $SO(10)$  grand unification [60]. Since the LRSM can be embedded in  $SO(10)$ , one is in some sense looking at a low energy limit of this GUT. Following these motivations; the LRSM, being a natural extension of the SM, can fulfill the above requirements and also may give some interesting consequences.

The left-right symmetric models were first introduced around 1974 by Pati and Salam [67]. Later, Rabindra N. Mohapatra and Goran Senjanovic actively analyzed the phenomenology of these models. This chapter is based on the articles [33, 41, 63].

Before we go in the details of the LRSM, we review some elements of the SM in the next section.

## 1.2 The Standard Model

The Standard Model of elementary particle physics is a quantum field theory that has the gauge symmetry group

$$SU(3)_C \times SU(2)_L \times U(1)_Y \quad (1.2.1)$$

It describes strong, weak and electromagnetic (EM) interactions at low energy via the exchange of the corresponding spin-1 gauge fields: eight massless gluons for the strong interactions, three massive bosons for the weak interactions and one massless photon for the EM interaction. Unifying three of four fundamental interactions of nature and precisely explaining almost all known phenomena in elementary particle physics, the SM is an extremely successful theoretical framework. The field content of the SM and their quantum numbers are given in Table 1.1. It contains three generations of fermions and their antiparticles as elementary particles, electron ( $e$ ), muon ( $\mu$ ) and tau ( $\tau$ ) lepton with their associated neutrinos, electron neutrino ( $\nu_e$ ), muon neutrino ( $\nu_\mu$ ) and tau neutrino ( $\nu_\tau$ ) in lepton sector (six leptons) and up ( $u$ ),

## 1.2 The Standard Model

---

<b>Fields</b>	<b>Components</b>	$SU(3)_C \times SU(2)_L \times U(1)_Y$		
<b>Fermions</b>				
$L$	$\begin{pmatrix} \nu \\ e \end{pmatrix}_L$	1	2	$-\frac{1}{2}$
$E$	$e_R$	1	1	-1
$Q$	$\begin{pmatrix} u \\ d \end{pmatrix}_L$	3	2	$+\frac{1}{6}$
$U$	$u_R$	3	1	$+\frac{2}{3}$
$D$	$d_R$	3	1	$-\frac{1}{3}$
<b>Gauge bosons</b>				
$B_\mu$	$B_\mu$	singlet	singlet	singlet
$W_\mu$	$W_\mu^+, W_\mu^-, W_\mu^3$	singlet	triplet	singlet
$G_\mu^a$	$(a = 1...8)$	octet	singlet	singlet
<b>Higgs</b>				
$\phi$	$\begin{pmatrix} \phi^+ \\ \phi^0 \end{pmatrix}$	1	2	$+\frac{1}{2}$

Table 1.1: Field content of the SM and respective quantum numbers.

down ( $d$ ), charm ( $c$ ), strange ( $s$ ), top ( $t$ ) and bottom ( $b$ ) quarks in quark sector (six quarks). Different fermion generations or families are of identical quantum numbers but different masses.

Quarks are triplets under the gauge group  $SU(3)_C$ . All LH fermions are doublets under the gauge group  $SU(2)_L$ : a charged lepton with its corresponding neutrino form a doublet, and a LH up-type and a down-type quarks form a doublet. Right-handed fermions are all singlets under the group  $SU(2)_L$ . The chiral projectors  $\psi_L$  and  $\psi_R$  for any four-component Dirac spinor field and the Dirac matrices  $\gamma_\mu$  are defined in Appendix A.

At high energies the gauge bosons of corresponding symmetry groups are mathematically seen to be virtual massless fields, however at low energies the spontaneous

breaking of symmetries

$$SU(3)_C \times SU(2)_L \times U(1)_Y \longrightarrow SU(3)_C \times U(1)_{\text{EM}} \quad (1.2.2)$$

gives rise to physical massive gauge bosons *i.e.*, neutral  $Z$  and charged  $W^\pm$  bosons. This symmetry breaking at low energies relates the corresponding quantum numbers: the EM charge ( $Q$ ) of  $U(1)_{\text{EM}}$  gauge group with the weak isospin ( $T^3$ ) of  $SU(2)_L$  and the hypercharge ( $Y$ ) of  $U(1)_Y$ . This relation is formulated in the so called Gell-Mann-Nishijima formula

$$Q = T^3 + Y \quad (1.2.3)$$

### 1.2.1 The SM Lagrangian

The interactions and dynamics of the SM fields are prescribed in the Lagrangian density

$$\mathcal{L}_{\text{SM}} = \mathcal{L}_{\text{YM}} + \mathcal{L}_K + \mathcal{L}_{\text{Higgs}} + \mathcal{L}_Y. \quad (1.2.4)$$

The Yang-Mills part  $\mathcal{L}_{\text{YM}}$  contains the gauge bosons kinetic energy terms as well as the three and four-point self interactions for the gauge fields  $G_\mu^a$  and  $W_\mu^i$  via field strength tensors

$$\mathcal{L}_{\text{YM}} = -\frac{1}{4}G_{\mu\nu}^a G^{\mu\nu a} - \frac{1}{4}W_{\mu\nu}^i W^{\mu\nu i} - \frac{1}{4}B_{\mu\nu} B^{\mu\nu}, \quad (1.2.5)$$

where the gauge field strengths are

$$G_{\mu\nu}^a = \partial_\mu G_\nu^a - \partial_\nu G_\mu^a - g_s f^{abc} G_\mu^b G_\nu^c, \quad (1.2.6)$$

$$W_{\mu\nu}^i = \partial_\mu W_\nu^i - \partial_\nu W_\mu^i - g \epsilon^{ijk} W_\mu^j W_\nu^k, \quad (1.2.7)$$

$$B_{\mu\nu} = \partial_\mu B_\nu - \partial_\nu B_\mu, \quad (1.2.8)$$

and we have denoted  $g_s$  and  $g$  with the  $SU(3)_C$  and  $SU(2)_L$  coupling constants, respectively. The spin-1 gauge fields  $G_\mu^a$  ( $a = 1, \dots, 8$ ) are gluons associated with the strong interactions,  $W_\mu^i$  ( $i = 1, 2, 3$ ) and  $B_\mu$  are the gauge bosons associated

with the EW interactions. The structure constants  $f^{abc}$  and  $\epsilon^{ijk}$  are defined by the commutation relations of the (Hermitian)  $SU(3)_C$  and  $SU(2)_L$  generators,  $\Lambda^a$ 's and  $T^i$ 's, respectively (see Appendix A). The following set of gauge transformations of the gauge fields makes the complete frame work consistent [28]

$$\Lambda \cdot G_\mu \rightarrow V(\Lambda \cdot G_\mu)V^\dagger - \frac{i}{g_s}(\partial_\mu V)V^\dagger, \quad (1.2.9)$$

$$T \cdot W_\mu \rightarrow U(T \cdot W_\mu)U^\dagger - \frac{i}{g}(\partial_\mu U)U^\dagger, \quad (1.2.10)$$

$$B_\mu \rightarrow B_\mu - \frac{1}{g_Y}\partial_\mu \alpha. \quad (1.2.11)$$

In this previous set of equations the matrices  $V$  and  $U$  are local  $SU(3)$  and  $SU(2)$  transformations, respectively, and  $\alpha$  is the parameter of any local  $U(1)$  transformation. Details on these equations can be found in Appendix C.

The gauge invariant Lagrangian containing the kinetic terms for the fermion fields and their interactions with the gauge bosons is given by

$$\mathcal{L}_K = i \sum_{j=1}^3 (\bar{L}_j \gamma^\mu D_\mu L_j + \bar{E}_j \gamma^\mu D_\mu E_j + \bar{Q}_j \gamma^\mu D_\mu Q_j + \bar{U}_j \gamma^\mu D_\mu U_j + \bar{D}_j \gamma^\mu D_\mu D_j) \quad (1.2.12)$$

where the covariant derivative is

$$D_\mu \equiv \partial_\mu - ig_s \Lambda^a G_\mu^a - ig_Y T^i W_\mu^i - ig_Y Y B_\mu \quad (1.2.13)$$

and  $g_Y$  is the  $U(1)_Y$  coupling constant. According to the charge assignments in Table 1.1, the covariant derivative ( $D_\mu$ ) takes the following forms for each term

$$\bar{L} \gamma^\mu D_\mu L = \bar{L} \gamma^\mu (\partial_\mu - \frac{ig}{2} \sigma \cdot W_\mu + \frac{ig_Y}{2} B_\mu) L \quad (1.2.14)$$

$$\bar{E} \gamma^\mu D_\mu E = \bar{E} \gamma^\mu (\partial_\mu + ig_Y B_\mu) E \quad (1.2.15)$$

$$\bar{Q} \gamma^\mu D_\mu Q = \bar{Q}^\alpha \gamma^\mu [(\partial_\mu - \frac{ig}{2} \sigma \cdot W_\mu - \frac{ig_Y}{6} B_\mu) \delta_{\alpha\beta} - \frac{ig_s}{2} \lambda_{\alpha\beta} \cdot G_\mu] Q^\beta \quad (1.2.16)$$

$$\bar{U} \gamma^\mu D_\mu U = \bar{U}^\alpha \gamma^\mu [(\partial_\mu - \frac{2ig_Y}{3} B_\mu) \delta_{\alpha\beta} - \frac{ig_s}{2} \lambda_{\alpha\beta} \cdot G_\mu] U^\beta \quad (1.2.17)$$

$$\bar{D} \gamma^\mu D_\mu D = \bar{D}^\alpha \gamma^\mu [(\partial_\mu + \frac{ig_Y}{3} B_\mu) \delta_{\alpha\beta} - \frac{ig_s}{2} \lambda_{\alpha\beta} \cdot G_\mu] D^\beta \quad (1.2.18)$$

where  $\alpha$  and  $\beta$  are color indices for quarks ( $\alpha, \beta = 1, 2, 3$  or  $r, g, b$ ) and  $\sigma$  and  $\lambda$  are  $2 \times 2$  Pauli spin and  $3 \times 3$  Gell-Mann matrices, respectively (see Appendix A).

The Higgs Lagrangian  $\mathcal{L}_{\text{Higgs}}$  contains the kinetic term of the Higgs field as well as its potential

$$\mathcal{L}_{\text{Higgs}} = \mathcal{L}_{\text{Higgs}}^{\text{K}} - V(\phi), \quad (1.2.19)$$

The kinetic Higgs Lagrangian contains the interaction of the Higgs field with the EW gauge bosons as well as the mass terms of the gauge bosons

$$\mathcal{L}_{\text{Higgs}}^{\text{K}} = (D^\mu \phi)^\dagger (D_\mu \phi) \quad (1.2.20)$$

where the covariant derivative of the Higgs field is given by

$$D_\mu \phi = (\partial_\mu - \frac{ig}{2} \sigma \cdot W_\mu - \frac{ig_Y}{2} B_\mu) \phi, \quad (1.2.21)$$

The scalar potential contains the Higgs field self interactions and mass terms for the Higgs field. The most general renormalizable and gauge invariant Higgs potential is

$$V(\phi) = \mu^2 \phi^\dagger \phi + \lambda (\phi^\dagger \phi)^2. \quad (1.2.22)$$

Finally, the Yukawa interaction terms of fermions and Higgs field are given by

$$\mathcal{L}_Y = - \sum_{i,j=1}^3 (y_{ij}^e \bar{L}_i \phi E_j + y_{ij}^u \bar{Q}_i \tilde{\phi} U_j + y_{ij}^d \bar{Q}_i \phi D_j) + h.c. \quad (1.2.23)$$

where the dual field

$$\tilde{\phi} \equiv i\sigma^2 \phi^* = \begin{pmatrix} \phi^{0*} \\ -\phi^- \end{pmatrix} \quad (1.2.24)$$

transforms in the same way as  $\phi$  does, with opposite hypercharge.

The scalar squared mass  $\mu^2$  and the self-interaction coupling constant  $\lambda$  are real parameters, whereas the Yukawa couplings  $y^e$ ,  $y^u$ ,  $y^d$  are, in general, complex  $3 \times 3$  matrices.

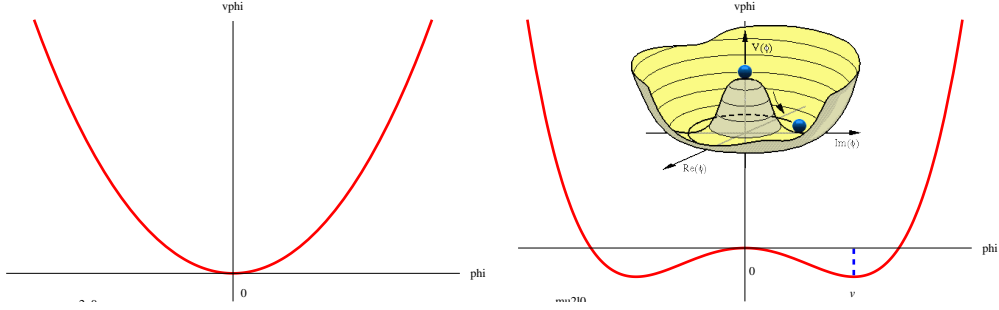


Figure 1.1: The potential  $V$  of the scalar field  $\phi$  in the cases  $\mu^2 \gtrless 0$ .

### 1.2.2 Spontaneous Symmetry Breaking in the SM

Some of Gauge bosons and fermions become massive as a result of *spontaneous symmetry breaking*, via the so-called *Higgs mechanism*. The gauge symmetry-breaking pattern of the SM is

$$SU(2)_L \times U(1)_Y \xrightarrow{\langle\phi\rangle} U(1)_{\text{EM}}, \quad (1.2.25)$$

where  $U(1)_{\text{EM}}$  is associated with the EM interactions.

At the tree level, the potential eq. (1.2.22) is bounded from below if  $\lambda > 0$ . It exhibits symmetry breaking if and only if  $\mu^2 < 0$ , where its minimum occurs at a Higgs VEV of the form (see Fig. 1.1)

$$\langle\phi\rangle = \frac{1}{\sqrt{2}} \begin{pmatrix} 0 \\ v \end{pmatrix}, \quad v^2 = \frac{-\mu^2}{\lambda} \quad (1.2.26)$$

For simplicity, we choose the unitary gauge, in which the Higgs field is

$$\phi(x) = \frac{1}{\sqrt{2}} \begin{pmatrix} 0 \\ h(x) + v \end{pmatrix}. \quad (1.2.27)$$

Substituting eq. (1.2.27) into the potential eq. (1.2.22), we can find the quadratic terms in  $h$  identify the Higgs boson mass

$$m_h^2 = -2\mu^2. \quad (1.2.28)$$

## Gauge Boson Masses in the SM

Gauge boson mass terms are contained in the scalar kinetic term (1.2.20)

$$\mathcal{L}_{\text{Higgs}}^{\text{K}} \supset M_W^2 W_\mu^+ W^{-\mu} + \frac{M_Z^2}{2} Z_\mu Z^\mu, \quad (1.2.29)$$

where the gauge boson mass eigenstates are

$$W_\mu^\pm = \frac{1}{\sqrt{2}}(W_\mu^1 \mp iW_\mu^2), \quad (1.2.30)$$

$$Z_\mu = \cos \theta_W W_\mu^3 - \sin \theta_W B_\mu, \quad (1.2.31)$$

$$A_\mu = \sin \theta_W W_\mu^3 + \cos \theta_W B_\mu, \quad (1.2.32)$$

and their corresponding physical masses are

$$M_W = \frac{gv}{2}, \quad M_Z = \frac{M_W}{\cos \theta_W}, \quad M_A = 0. \quad (1.2.33)$$

The Weinberg angle  $\theta_W$  is defined in terms of the EM charge  $e$  and gauge couplings  $g$  and  $g_Y$  by

$$s_W \equiv \sin \theta_W = \frac{e}{g} = \frac{g_Y}{\sqrt{g^2 + g_Y^2}}, \quad (1.2.34)$$

and hence

$$c_W \equiv \cos \theta_W = \frac{g}{g_Y} = \frac{1}{\sqrt{g^2 + g_Y^2}}. \quad (1.2.35)$$

The EM charge  $e$  is (see Appendix B)

$$e = \frac{gg_Y}{\sqrt{g^2 + g_Y^2}}. \quad (1.2.36)$$

In the SM, the Weinberg angle is fixed by

$$s_W^2 = 1 - \frac{M_W^2}{M_Z^2}. \quad (1.2.37)$$

### Fermion Masses in the SM

When a standard mass term for fermions  $m\bar{\psi}\psi$  is expressed in  $\psi_{L,R}$ , only fields of opposite chirality couple together. Consequently, two types of mass terms are possible: the Dirac mass terms

$$m_D \overline{\psi}_L \psi_R + \text{h.c.} \quad (1.2.38)$$

and the Majorana mass terms

$$M_L \overline{\psi}_L (\psi_L)^c + M_R \overline{(\psi_R)^c} \psi_R + \text{h.c.} \quad (1.2.39)$$

The charge conjugate field is defined in Appendix A.

At this point it is worth emphasizing that because of electric charge conservation, the existence of Majorana type masses for all charged fermions in the SM is forbidden. So, the only allowed mass term for the charged fermions is the Dirac mass term (1.2.38).

In the unitary gauge, the Yukawa Lagrangian eq. (1.2.23) becomes

$$\mathcal{L}_Y = -\frac{h(x) + v}{\sqrt{2}} (y_{ij}^e \overline{e}_{Li} e_{Rj} + y_{ij}^u \overline{u}_{Li} u_{Rj} + y_{ij}^d \overline{d}_{Li} d_{Rj}) + \text{h.c.} \quad (1.2.40)$$

The fermion mass matrices are given by

$$m^f = \frac{y^f v}{\sqrt{2}}, \quad f = e, u, d. \quad (1.2.41)$$

The Yukawa matrices coefficients  $y^f$  ( $f = e, u, d$ ) are not diagonal, in general, and hence not all the fermions  $f$  are in their physical eigenstates. By suitable unitary transformations (without any loss of generality, we can consider that the RH fermions are already in their physical eigenstates)

$$f_L \rightarrow V^f f_L, \quad \nu_L \rightarrow V^e \nu_L, \quad (1.2.42)$$

the Yukawa coupling matrices are then simultaneously diagonalized and the fermion masses take the form

$$m_f = y_f^{\text{diag}} \frac{v}{\sqrt{2}}, \quad y_f^{\text{diag}} = V^{f\dagger} y^f. \quad (1.2.43)$$

### 1.2.3 Electroweak Interactions in the SM

Electroweak interactions of leptons and quarks in the SM arise from the kinetic part of the Lagrangian (eq. (1.2.12))

$$\mathcal{L}_K = i \sum_{j=1}^3 (\bar{L}_j \gamma^\mu D_\mu L_j + \bar{E}_j \gamma^\mu D_\mu E_j + \bar{Q}_j \gamma^\mu D_\mu Q_j + \bar{U}_j \gamma^\mu D_\mu U_j + \bar{D}_j \gamma^\mu D_\mu D_j)$$

For any RH-fermion  $\psi_R$  in the SM,  $Q(\psi_R) = Y(\psi_R)$ .

Substituting the physical eigenstates for the neutral gauge bosons from Eqs. (1.2.30)-(1.2.32), we can simply extract all the three types of the EW interactions, namely, the EM, neutral and charged currents of weak interactions. The kinetic terms of the LH and RH fermions contain the following terms

$$\begin{aligned} \bar{\psi}_L i\gamma^\mu D_\mu \psi_L &\supset \bar{\psi}_L \gamma^\mu \left( \frac{g}{\sqrt{2}} (W_\mu^+ T^+ + W_\mu^- T^-) + g W_\mu^3 T^3 + g_Y B_\mu Y \right) \psi_L \\ &= \bar{\psi} \gamma^\mu \left( \frac{g}{\sqrt{2}} (W_\mu^+ T^+ + W_\mu^- T^-) \right) P_L \psi \\ &\quad + \bar{\psi} \gamma^\mu \left( e Q A_\mu + e \left( \frac{g}{g_Y} T^3 - \frac{g_Y}{g} Y \right) Z_\mu \right) P_L \psi, \end{aligned} \quad (1.2.44)$$

$$\bar{\psi}_R i\gamma^\mu D_\mu \psi_R \supset \bar{\psi}_R \gamma^\mu (g_Y B_\mu Y) \psi_R = \bar{\psi} \gamma^\mu (e Q A_\mu - \frac{e g_Y}{g} Q Z_\mu) P_R \psi. \quad (1.2.45)$$

Where  $P_{L,R}$  and  $T^\pm$  are in Appendix A. Finally, the EW interactions are

$$\begin{aligned} \bar{\psi}_L i\gamma^\mu D_\mu \psi_L + \bar{\psi}_R i\gamma^\mu D_\mu \psi_R &\supset \bar{\psi} \gamma^\mu \left( \frac{g}{\sqrt{2}} (W_\mu^+ T^+ + W_\mu^- T^-) \right) P_L \psi \\ &\quad + \bar{\psi} \gamma^\mu \left( e Q A_\mu + \frac{g}{\cos \theta_W} (T^3 P_L - \sin^2 \theta_W Q) Z_\mu \right) \psi. \end{aligned} \quad (1.2.46)$$

Or in compact form

$$\bar{\psi}_L i\gamma^\mu D_\mu \psi_L + \bar{\psi}_R i\gamma^\mu D_\mu \psi_R \supset \mathcal{L}_{EM} + \mathcal{L}_{NC} + \mathcal{L}_{CC} \quad (1.2.47)$$

where the EM interaction Lagrangian  $\mathcal{L}_{EM}$ , neutral weak interaction Lagrangian  $\mathcal{L}_{NC}$  and charged weak interaction Lagrangian  $\mathcal{L}_{CC}$  are defined as follows

$$\mathcal{L}_{EM} = e A_\mu J_A^\mu, \quad (1.2.48)$$

$$\mathcal{L}_{\text{NC}} = \frac{g}{\cos \theta_w} Z_\mu J_Z^\mu, \quad (1.2.49)$$

$$\mathcal{L}_{\text{CC}} = \frac{g}{\sqrt{2}} (W_\mu^+ J_W^\mu + W_\mu^- J_W^{\mu\dagger}). \quad (1.2.50)$$

The EM current  $J_A^\mu$ , neutral weak current  $J_Z^\mu$  and charged weak current  $J_W^\mu$  are defined as follows

$$J_A^\mu = \bar{\psi} \gamma^\mu Q \psi, \quad (1.2.51)$$

$$J_Z^\mu = \bar{\psi} \gamma^\mu (T^3 P_L - \sin^2 \theta_w Q) \psi, \quad (1.2.52)$$

$$J_W^\mu = \bar{\psi} \gamma^\mu T^+ P_L \psi, \quad J_W^{\mu\dagger} = \bar{\psi} \gamma^\mu T^- P_L \psi. \quad (1.2.53)$$

Where summation over  $\psi$  is involved over leptons and quarks.

### Electromagnetic Interactions in the SM

Electromagnetic interactions in the SM are mediated by photons. They only couple to electrically charged fermions with their electric charges.

The compact form of the EM interactions is simply written

$$\mathcal{L}_{\text{EM}} = e A_\mu J_A^\mu. \quad (1.2.54)$$

In terms of fermion components the EM current  $J_A^\mu$  which covers the three flavors of fermions is given by

$$J_A^\mu = \sum_i Q^i \bar{f}_i \gamma^\mu f_i = -\bar{e} \gamma^\mu e + \frac{2}{3} \bar{u} \gamma^\mu u - \frac{1}{3} \bar{d} \gamma^\mu d \quad (1.2.55)$$

Summation over generations adds similar terms for the other generations.

### Neutral Weak Current Interactions in the SM

Neutral current in the SM is mediated by  $Z$  gauge boson and this expression can be summarized in terms of neutral current

$$\mathcal{L}_{\text{NC}} = \frac{g}{\cos \theta_w} Z_\mu J_Z^\mu, \quad (1.2.56)$$

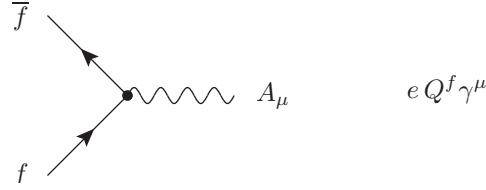


Figure 1.2: Feynman diagram and rule of electromagnetic interactions in the SM.

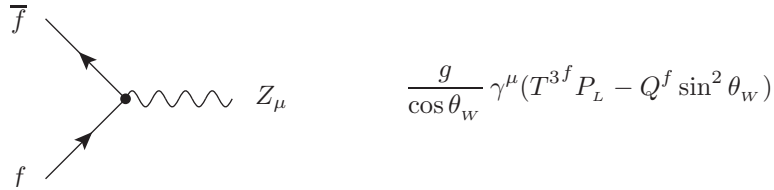


Figure 1.3: Feynman diagram and rule of neutral current interactions in the SM.

In terms of fermion components the neutral weak current  $J_Z^\mu$  which covers the three flavors of fermions is given by

$$\begin{aligned} J_Z^\mu &= \sum_i \bar{f}_i \gamma^\mu (T^{3i} P_L - Q^i \sin^2 \theta_w) f_i \\ &= \frac{1}{2} \bar{\nu}_e \gamma^\mu P_L \nu_e + \bar{e} \gamma^\mu \left( -\frac{1}{2} P_L + \sin^2 \theta_w \right) e \\ &\quad + \bar{u} \gamma^\mu \left( \frac{1}{2} P_L - \frac{2}{3} \sin^2 \theta_w \right) u + \bar{d} \gamma^\mu \left( -\frac{1}{2} P_L + \frac{1}{3} \sin^2 \theta_w \right) d \end{aligned} \quad (1.2.57)$$

Where again summation over generations adds similar terms for the other generations.

### Charged Weak Current Interactions in the SM

Charged current in the SM is mediated by  $W^\pm$  gauge bosons and this expression can be summarized in terms of charged current

$$\mathcal{L}_{CC} = \frac{g}{\sqrt{2}} (W_\mu^+ J_W^\mu + W_\mu^- J_W^{\mu\dagger}). \quad (1.2.58)$$

## 1.2 The Standard Model

---

The charged currents  $J_W^\mu$  and its conjugate  $J_W^{\mu\dagger}$  are given in terms of the fermions components as follows

$$J_W^\mu = \sum_{i,j} (\bar{v}_{Lj} \gamma^\mu e_{Li} \delta_{ij} + \bar{u}_{Li} \gamma^\mu d_{Lj} V_{ij}) \quad (1.2.59)$$

$$J_W^{\mu\dagger} = \sum_{i,j} (\bar{e}_{Lj} \gamma^\mu \nu_{Li} \delta_{ij} + \bar{d}_{Lj} \gamma^\mu u_{Li} V_{ij}^\dagger). \quad (1.2.60)$$

Where the CKM matrix is

$$V_{\text{CKM}} \equiv V \equiv V^{u\dagger} V^d \quad (1.2.61)$$

The  $V_{\text{CKM}}$  is the Cabibbo-Kobayashi-Maskawa matrix, which describes the quark mixing in the weak charged currents.

One may wonder why there is no an analogous mixing in the leptonic sector in the SM. In fact, the absence of any mass terms (Dirac and Majorana) for neutrinos in the SM permits (without loss of generality) the choice of the matrix  $V^\nu = V^e$  in eq. (1.2.42), which keeps the leptonic charged currents in eq. (1.2.59) unchanged. The absence of RH-neutrinos in the SM causes the absence of Dirac mass terms  $y_{ij}^\nu \bar{\nu}_{Li} \nu_{Rj}$  for neutrinos in the leptonic sector, that would be analogous to that of the up-quarks  $y_{ij}^u \bar{u}_{Li} u_{Rj}$  in quark sector in eq. (1.2.40). Also Majorana mass terms  $y_{Mij}^\nu \bar{\nu}_{Li} \nu_{Lj}^c$  for neutrinos wouldn't be invariant under the gauge group  $U(1)_Y$ .

The standard parametrization of the CKM matrix is [83]

$$V_{\text{CKM}} = \begin{pmatrix} c_{12}c_{13} & s_{12}c_{13} & s_{13}e^{-i\delta} \\ -s_{12}c_{23} - c_{12}s_{23}s_{13}e^{i\delta} & c_{12}c_{23} - s_{12}s_{23}s_{13}e^{i\delta} & s_{23}c_{13} \\ s_{12}s_{23} - c_{12}c_{23}s_{13}e^{i\delta} & -c_{12}s_{23} - s_{12}c_{23}s_{13}e^{i\delta} & c_{23}c_{13} \end{pmatrix}, \quad (1.2.62)$$

in terms of the 4 parameters:  $\theta_{12}, \theta_{23}, \theta_{13}$  and  $\delta$  ( $s_{ij} = \sin \theta_{ij}$ ,  $c_{ij} = \cos \theta_{ij}$ ;  $s_{ij}, c_{ij} \geq 0$ ), the values extracted from recent experimental data are [83]

$$\sin \theta_{12} = 0.2229 \pm 0.0022, \quad (1.2.63)$$

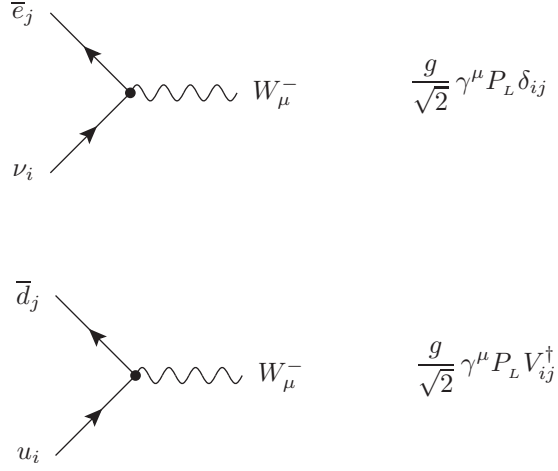


Figure 1.4: Feynman diagrams and rules of leptons charged current interactions (up) and quarks charged current interactions (down) in the SM.

$$\sin \theta_{23} = 0.0412 \pm 0.0002, \quad (1.2.64)$$

$$\sin \theta_{13} = 0.0036 \pm 0.0007, \quad (1.2.65)$$

$$\delta = 1.02 \pm 0.22. \quad (1.2.66)$$

### 1.2.4 Higgs Interactions in the SM

#### Higgs-Gauge Boson Interactions in the SM

The kinetic Lagrangian (1.2.20) of the Higgs field contains the following interaction terms of Higgs field and gauge bosons [28]

$$\mathcal{L}_{\text{Higgs}}^K \supset W_\mu^+ W^{-\mu} \left( \frac{g^2}{4} h^2 + g M_W h \right) + Z_\mu Z^\mu \left( \frac{g^2}{8 \cos^2 \theta_W} h^2 + \frac{g M_Z}{2 \cos \theta_W} h \right) \quad (1.2.67)$$

#### Higgs-Fermion Interactions in the SM

In the unitary gauge [28], after substituting from Eqs. (1.2.42) and (1.2.43), the Yukawa Lagrangian eq. (1.2.40) contains the following interaction terms of the Higgs

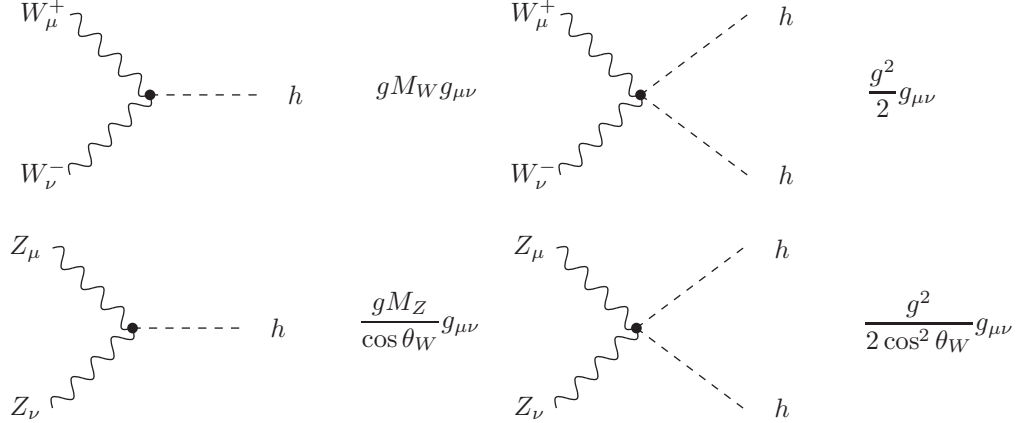


Figure 1.5: Feynman diagrams and rules of Higgs-gauge interactions in the SM.

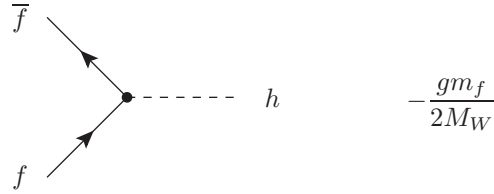


Figure 1.6: Feynman diagram and rule of Higgs-fermion interactions in the SM.

field with fermions

$$-\mathcal{L}_Y \supset \frac{h}{v} \sum_f m_f \bar{f} f = \frac{h}{v} (m_e \bar{e} e + m_u \bar{u} u + m_d \bar{d} d) \quad (1.2.68)$$

As the neutrino is massless, it doesn't interact with the Higgs field.

### 1.3 Description of the LRSM

The LRSM is based on the gauge group

$$SU(3)_C \times SU(2)_L \times SU(2)_R \times U(1)_{B-L}. \quad (1.3.1)$$

At low energies, it is required that the LRSM gauge group (1.3.1) be broken spontaneously to the SM gauge group (1.2.1). The complete EW symmetry breaking pattern

of the LRSM is accomplished in the following two stages

$$SU(2)_L \times SU(2)_R \times U(1)_{B-L} \longrightarrow SU(2)_L \times U(1)_Y \longrightarrow U(1)_{\text{EM}}, \quad (1.3.2)$$

where the EM charge is defined by the modified Gell-Mann-Nishijima formula

$$Q = T_L^3 + T_R^3 + Q_{BL}, \quad Q_{BL} \equiv \frac{1}{2}(B - L). \quad (1.3.3)$$

The derivation of the EM charge modified Gell-Mann-Nishijima formula and the coupling relations are in detail in Appendix B.

Fields	Components	$SU(2)_L \times SU(2)_R \times U(1)_{B-L}$			
<b>Fermions</b>					
$L_L$	$\begin{pmatrix} \nu \\ e \end{pmatrix}_L$	2	1	- $\frac{1}{2}$	
$L_R$	$\begin{pmatrix} \nu \\ e \end{pmatrix}_R$	1	2	- $\frac{1}{2}$	
$Q_L$	$\begin{pmatrix} u \\ d \end{pmatrix}_L$	2	1	+ $\frac{1}{6}$	
$Q_R$	$\begin{pmatrix} u \\ d \end{pmatrix}_R$	1	2	+ $\frac{1}{6}$	
<b>Gauge bosons</b>					
$W_L$	$W_L^+, W_L^-, W_L^3$	triplet	singlet	singlet	
$W_R$	$W_R^+, W_R^-, W_R^3$	singlet	triplet	singlet	
$V$	$V$	singlet	singlet	singlet	
<b>Higgs</b>					
$\Phi$	$\begin{pmatrix} \Phi_1^0 & \Phi_1^+ \\ \Phi_2^- & \Phi_2^0 \end{pmatrix}$	2	2	0	
$\Delta_L$	$\begin{pmatrix} \frac{\Delta^+}{\sqrt{2}} & \Delta^{++} \\ \Delta^0 & -\frac{\Delta^+}{\sqrt{2}} \end{pmatrix}_L$	3	1	+1	
$\Delta_R$	$\begin{pmatrix} \frac{\Delta^+}{\sqrt{2}} & \Delta^{++} \\ \Delta^0 & -\frac{\Delta^+}{\sqrt{2}} \end{pmatrix}_R$	1	3	+1	

Table 1.2: Field content of the LRSM and respective quantum numbers.

As in the SM, the strong interactions in the LRSM are based on the gauge group  $SU(3)_C$ . The weak interactions of the LRSM are based on the gauge group  $SU(2)_L \times SU(2)_R \times U(1)_{B-L}$ . We expect three extra gauge bosons, two charged  $W_R^\pm$  analogous to the  $W^\pm$  boson, and one neutral  $Z_R$  analogous to the  $Z$  boson (we will denote gauge bosons  $W^\pm$  and  $Z$  hereafter by  $W_L^\pm$  and  $Z_L$ , respectively, in order to keep the historical symmetric notation). The field content of the model and quantum numbers are given in Table 1.2. Contrary to the SM, all RH component of fermion fields transform as doublets under  $SU(2)_R$  symmetry in the LRSM and the corresponding gauge bosons of this new symmetry only couple to RH fermions. This Left-Right (LR) symmetry emerged from the idea that the physical laws must be as valid for RH dynamics as they are for the LH ones. It was shown by Mohapatra and Senjanovic [74] in 1975 that the LR symmetry can be spontaneously broken to give a chiral low energy theory which is the SM at the weak scale and it also connects the small neutrino masses to the breaking of LR symmetry via the seesaw mechanism.

The Lagrangian density of the LRSM can be summarized as in the same way in the SM (see eq. (1.2.4)); gauge, kinetic, scalar and Yukawa parts.

$$\mathcal{L}_{\text{LRSM}} = \mathcal{L}_{\text{Gauge}} + \mathcal{L}_{\text{Kinetic}} + \mathcal{L}_{\text{Scalar}} + \mathcal{L}_{\text{Yukawa}}. \quad (1.3.4)$$

### 1.3.1 Gauge Lagrangian

The gauge part of the Lagrangian density contains the gauge bosons kinetic energy terms as well as the three and four-point self interactions for the gauge fields  $G_\mu^a$ ,  $W_{L\mu}^i$  and  $W_{R\mu}^i$ .

$$\mathcal{L}_{\text{Gauge}} = -\frac{1}{4}G_{\mu\nu}^a G^{\mu\nu a} - \frac{1}{4}W_{L\mu\nu}^i W_L^{\mu\nu i} - \frac{1}{4}W_{R\mu\nu}^i W_R^{\mu\nu i} - \frac{1}{4}V_{\mu\nu} V^{\mu\nu}, \quad (1.3.5)$$

where the field strength tensors for  $SU(3)_C$ ,  $SU(2)_L$ ,  $SU(2)_R$  and  $U(1)_{B-L}$  are respectively

$$G_{\mu\nu}^a = \partial_\mu G_\nu^a - \partial_\nu G_\mu^a - g_s f^{abc} G_\mu^b G_\nu^c, \quad a, b, c = 1 \dots 8, \quad (1.3.6)$$

$$W_{L\mu\nu}^i = \partial_\mu W_{L\nu}^i - \partial_\nu W_{L\mu}^i - g_L \epsilon^{ijk} W_{L\mu}^j W_{L\nu}^k, \quad i, j, k = 1 \dots 3, \quad (1.3.7)$$

$$W_{R\mu\nu}^i = \partial_\mu W_{R\nu}^i - \partial_\nu W_{R\mu}^i - g_R \epsilon^{ijk} W_{R\mu}^j W_{R\nu}^k, \quad i, j, k = 1 \dots 3, \quad (1.3.8)$$

$$V_{\mu\nu} = \partial_\mu V_\nu - \partial_\nu V_\mu. \quad (1.3.9)$$

The gauge couplings  $g_L \equiv g$  and  $g_R$  are of  $SU(2)_L$  and  $SU(2)_R$  groups respectively.

The following set of gauge transformations of the gauge fields makes the complete frame work consistent [28]

$$\Lambda \cdot G_\mu \rightarrow V(\Lambda \cdot G_\mu)V^\dagger - \frac{i}{g_s}(\partial_\mu V)V^\dagger, \quad (1.3.10)$$

$$T_L \cdot W_{L\mu} \rightarrow U_L(T_L \cdot W_{L\mu})U_L^\dagger - \frac{i}{g_L}(\partial_\mu U_L)U_L^\dagger, \quad (1.3.11)$$

$$T_R \cdot W_{R\mu} \rightarrow U_R(T_R \cdot W_{R\mu})U_R^\dagger - \frac{i}{g_R}(\partial_\mu U_R)U_R^\dagger, \quad (1.3.12)$$

$$V_\mu \rightarrow V_\mu - \frac{1}{g_{BL}}\partial_\mu \beta, \quad (1.3.13)$$

where  $g_{BL}$  is the coupling of the  $U(1)_{B-L}$  group. Details on the previous set of equations can be found in Appendix C.

### 1.3.2 Kinetic Lagrangian

The kinetic part of the Lagrangian density constitutes the kinetic terms of fermions and interactions to gauge bosons

$$\mathcal{L}_{\text{Kinetic}} = i \sum_{j=1}^3 (\bar{L}_{Lj} \gamma^\mu D_\mu L_{Lj} + \bar{L}_{Rj} \gamma^\mu D_\mu L_{Rj} + \bar{Q}_{Lj} \gamma^\mu D_\mu Q_{Lj} + \bar{Q}_{Rj} \gamma^\mu D_\mu Q_{Rj}) \quad (1.3.14)$$

The action of a group element of  $SU(2)_L \times SU(2)_R$  on the fermion doublets is as follows

$$Q_\hbar \rightarrow U_\hbar Q_\hbar = e^{-i\sigma \cdot \alpha_\hbar(x)/2} Q_\hbar, \quad (1.3.15)$$

$$L_\hbar \rightarrow U_\hbar L_\hbar = e^{-i\sigma \cdot \alpha_\hbar(x)/2} L_\hbar, \quad (1.3.16)$$

where the index  $\mathcal{H}$  is a ‘LR’ index valued either L or R. The matrix  $U_{\mathcal{H}}$  is any local  $SU(2)_{\mathcal{H}}$  transformation. The quarks have  $B - L = +1/3$  and the leptons  $-1$ , so that under  $U(1)_{B-L}$  the doublets transform as

$$Q_{\mathcal{H}} \rightarrow e^{-i\alpha(x)(B-L)/2} Q_{\mathcal{H}} = e^{-i\alpha(x)/6} Q_{\mathcal{H}}, \quad (1.3.17)$$

$$L_{\mathcal{H}} \rightarrow e^{-i\alpha(x)(B-L)/2} L_{\mathcal{H}} = e^{i\alpha(x)/2} L_{\mathcal{H}}. \quad (1.3.18)$$

Accordingly, the covariant derivative takes the following forms for each term

$$\bar{L}_L \gamma^\mu D_\mu L_L = \bar{L}_L \gamma^\mu (\partial_\mu - \frac{ig_L}{2} \sigma \cdot W_{L\mu} + \frac{ig_{BL}}{2} V_\mu) L_L, \quad (1.3.19)$$

$$\bar{L}_R \gamma^\mu D_\mu L_R = \bar{L}_R \gamma^\mu (\partial_\mu - \frac{ig_R}{2} \sigma \cdot W_{R\mu} + \frac{ig_{BL}}{2} V_\mu) L_R, \quad (1.3.20)$$

$$\bar{Q}_L \gamma^\mu D_\mu Q_L = \bar{Q}_L^\alpha \gamma^\mu [(\partial_\mu - \frac{ig_L}{2} \sigma \cdot W_{L\mu} - \frac{ig_{BL}}{6} V_\mu) \delta_{\alpha\beta} - \frac{ig_s}{2} \lambda_{\alpha\beta} \cdot G_\mu] Q_L^\beta, \quad (1.3.21)$$

$$\bar{Q}_R \gamma^\mu D_\mu Q_R = \bar{Q}_R^\alpha \gamma^\mu [(\partial_\mu - \frac{ig_R}{2} \sigma \cdot W_{R\mu} - \frac{ig_{BL}}{6} V_\mu) \delta_{\alpha\beta} - \frac{ig_s}{2} \lambda_{\alpha\beta} \cdot G_\mu] Q_R^\beta, \quad (1.3.22)$$

where the strong and weak interactions of fermions and bosons are encoded in these kinetic terms.

### 1.3.3 Scalar Lagrangian

The Higgs fields are required for two main jobs

1. It should lead to an appropriate SSB of the LR EW symmetry  $SU(2)_L \times SU(2)_R \times U(1)_{B-L}$ . *i.e.*, at high energy, breaking the LR EW symmetry to the SM EW symmetry  $SU(2)_L \times U(1)_Y$ , and then, at low energy, breaking this later one to the EM symmetry  $U(1)_{EM}$ ,
2. generating masses for the SM massive particles as well as giving the neutrino its light mass. It also generates heavy masses for non-SM particles, like  $W_R$  and  $Z_R$ .

As fermions in the LRSM are grouped in doublets under the  $SU(2)$  groups, a gauge invariant Yukawa term  $\bar{\psi}_L \Phi \psi_R$  implies that the scalar field  $\Phi$  is a  $2 \times 2$  matrix that transforms nontrivially under the  $SU(2)$  groups and has  $B - L = 0$ . In fact,  $\Phi$  is made out of two columns which are doublets of  $SU(2)_L$  and at the same time the rows form two doublets of  $SU(2)_R$ . Hence  $U(1)_{B-L}$  would be an exact symmetry after SSB by  $\Phi$  only and, unfortunately, the first job couldn't be achieved completely. So we have to add an extra Higgs field that transforms nontrivially under  $SU(2)_R \times U(1)_{B-L}$  to break the LR symmetry to the SM one. In the LRSM we add a RH Higgs triplet  $\Delta_R$  under the gauge group  $SU(2)_R$ . The LH Higgs triplet ( $\Delta_L$ ) is only responsible for maintaining the discrete parity symmetry [67] in the theory.

The Higgs fields  $\Phi$ ,  $\Delta_L$  and  $\Delta_R$  are scalar fields grouped in matrices. The Higgs field  $\Phi$  is a bidoublet under the LR EW symmetry group. The Higgs fields  $\Delta_{L,R}$  are triplets written in the adjoint representation. They are parameterized, for gauge invariance, as in Table 1.2. Gauge invariance implies that the action of a group element of  $SU(2)_L \times SU(2)_R$  on the Higgs multiplets is as follows

$$\Phi \rightarrow U_L \Phi U_R^\dagger, \quad \Delta_\hbar \rightarrow U_\hbar \Delta_\hbar U_\hbar^\dagger \quad (1.3.23)$$

The bidoublet is a singlet under the  $U(1)_{B-L}$  group. The triplets  $\Delta_\hbar$  have  $B - L = +2$  so that they transform under  $U(1)_{B-L}$  as

$$\Delta_\hbar \rightarrow e^{-i\alpha(x)(B-L)/2} \Delta_\hbar = e^{-i\alpha(x)} \Delta_\hbar \quad (1.3.24)$$

Accordingly, the covariant derivative takes the following forms for each term

$$D_\mu \Phi = \partial_\mu \Phi - \frac{ig_L}{2} (\sigma \cdot W_{L\mu}) \Phi + \frac{ig_R}{2} \Phi (\sigma \cdot W_{R\mu}) \quad (1.3.25)$$

$$D_\mu \Delta_\hbar = \partial_\mu \Delta_\hbar - \frac{ig_\hbar}{2} [\sigma \cdot W_{\hbar\mu}, \Delta_\hbar] - ig_{BL} V_\mu \Delta_\hbar \quad (1.3.26)$$

The scalar part of the Lagrangian contains the kinetic terms  $\mathcal{L}_{\text{Scalar}}^{\text{Kin}}$  and potential  $V(\Phi, \Delta_L, \Delta_R)$  of Higgs multiplets

$$\mathcal{L}_{\text{Scalar}} = \mathcal{L}_{\text{Scalar}}^{\text{Kin}} - V(\Phi, \Delta_L, \Delta_R) \quad (1.3.27)$$

Before we proceed with the kinetic terms of the Higgs fields we note the following. For a square matrix  $A = (a_{ij})$ , we have  $\text{Tr}(A^\dagger A) = \sum_{i,j} |a_{ij}|^2$ . *i.e.*, the outcome is the sum of the absolute value squared of all matrix elements. According to this note and the definitions of the Higgs multiplets  $\Phi$ ,  $\Delta_L$  and  $\Delta_R$ , it follows that if we take the kinetic Lagrangian of the scalars in the form

$$\mathcal{L}_{\text{Scalar}}^{\text{Kin}} = \text{Tr}[|D_\mu \Phi|^2] + \text{Tr}[|D_\mu \Delta_L|^2] + \text{Tr}[|D_\mu \Delta_R|^2] \quad (1.3.28)$$

we get the ‘standard’ complex scalar field kinetic term (*i.e.*,  $(\partial_\mu \phi)^\dagger (\partial^\mu \phi)$ ) for the separate components of the matrix fields plus of course some interaction terms between Higgs fields and the various gauge fields. Using the cyclic property of the trace operation, it is easily checked that these are indeed gauge invariant. Explicitely,

$$\text{Tr}[|D_\mu \Phi|^2] \rightarrow \text{Tr}[U_R (D_\mu \Phi)^\dagger U_L^\dagger U_L (D_\mu \Phi) U_R^\dagger] = \text{Tr}[|D_\mu \Phi|^2], \quad (1.3.29)$$

$$\text{Tr}[|D_\mu \Delta_H|^2] \rightarrow \text{Tr}[U_H (D_\mu \Delta_H)^\dagger U_H^\dagger U_H (D_\mu \Delta_H) U_H^\dagger] = \text{Tr}[|D_\mu \Delta_H|^2], \quad (1.3.30)$$

where the different  $U_L$  and  $U_R$  matrices all combine to unit matrices.

The most general gauge invariant and renormalizable Higgs potential is [14, 33]

$$\begin{aligned} V(\Phi, \Delta_L, \Delta_R) = & -\mu_1^2 \text{Tr}(\Phi^\dagger \Phi) - \mu_2^2 \text{Tr}(\tilde{\Phi}^\dagger \Phi + \Phi^\dagger \tilde{\Phi}) - \mu_3^2 \text{Tr}(\Delta_L^\dagger \Delta_L + \Delta_R^\dagger \Delta_R) \\ & + \lambda_1 [\text{Tr}(\Phi^\dagger \Phi)]^2 + \lambda_2 \{[\text{Tr}(\tilde{\Phi}^\dagger \Phi)]^2 + [\text{Tr}(\Phi^\dagger \tilde{\Phi})]^2\} + \lambda_3 \text{Tr}(\tilde{\Phi}^\dagger \Phi) \text{Tr}(\Phi^\dagger \tilde{\Phi}) \\ & + \lambda_4 \text{Tr}(\Phi^\dagger \Phi) \text{Tr}(\tilde{\Phi}^\dagger \Phi + \Phi^\dagger \tilde{\Phi}) + \rho_1 \{[\text{Tr}(\Delta_L^\dagger \Delta_L)]^2 + [\text{Tr}(\Delta_R^\dagger \Delta_R)]^2\} \\ & + \rho_2 \{\text{Tr}(\Delta_L^\dagger \Delta_L^\dagger) \text{Tr}(\Delta_L \Delta_L) + \text{Tr}(\Delta_R^\dagger \Delta_R^\dagger) \text{Tr}(\Delta_R \Delta_R)\} + \rho_3 \{\text{Tr}(\Delta_L^\dagger \Delta_L) \\ & \times \text{Tr}(\Delta_R^\dagger \Delta_R)\} + \rho_4 \{\text{Tr}(\Delta_L \Delta_L) \text{Tr}(\Delta_R^\dagger \Delta_R^\dagger) + \text{Tr}(\Delta_R \Delta_R) \text{Tr}(\Delta_L^\dagger \Delta_L^\dagger)\} \\ & + \alpha_1 \text{Tr}(\Phi \Phi^\dagger) [\text{Tr}(\Delta_L^\dagger \Delta_L + \Delta_R^\dagger \Delta_R)] + \alpha_2 \{\text{Tr}(\Phi^\dagger \tilde{\Phi}) \text{Tr}(\Delta_L^\dagger \Delta_L) \\ & + \text{Tr}(\Phi \tilde{\Phi}^\dagger) \text{Tr}(\Delta_R^\dagger \Delta_R)\} + \alpha_2^* \{\text{Tr}(\Phi^\dagger \tilde{\Phi}) \text{Tr}(\Delta_R^\dagger \Delta_R) + \text{Tr}(\Phi \tilde{\Phi}^\dagger) \text{Tr}(\Delta_L^\dagger \Delta_L)\} \\ & + \alpha_3 \text{Tr}(\Phi \Phi^\dagger \Delta_L \Delta_L^\dagger + \Phi^\dagger \Phi \Delta_R \Delta_R^\dagger) + \beta_1 \text{Tr}(\Delta_L^\dagger \Phi \Delta_R \Phi^\dagger + \Delta_R^\dagger \Phi^\dagger \Delta_L \Phi) \\ & + \beta_2 \text{Tr}(\Delta_L^\dagger \tilde{\Phi} \Delta_R \Phi^\dagger + \Delta_R^\dagger \tilde{\Phi}^\dagger \Delta_L \Phi) + \beta_3 \text{Tr}(\Delta_L^\dagger \Phi \Delta_R \tilde{\Phi}^\dagger + \Delta_R^\dagger \Phi^\dagger \Delta_L \tilde{\Phi}), \end{aligned} \quad (1.3.31)$$

where the conjugate Higgs bidoublet is defined as

$$\tilde{\Phi} = \sigma_2 \Phi^* \sigma_2 = \begin{pmatrix} \Phi_2^{0*} & -\Phi_2^+ \\ -\Phi_1^- & \Phi_1^{0*} \end{pmatrix} \quad (1.3.32)$$

and transforms in the same way as  $\Phi$  does.

The scalar potential contains the mass terms as well as the three and four-point self interactions for the Higgs fields. It is worth mentioning that, unless we demand the potential (1.3.31) to be  $CP$ -invariant, it would be a source of  $CP$  violation by allowing some parameters (e.g.,  $\alpha_2$ ) to be complex. If all parameters are real, some VEV's could still acquire complex phases. In [33] it is argued that if one chooses real parameters in the Higgs Potential, the VEV's can generally be taken real. A general overview of the Higgs sector of the LRSM will be given in section 1.6.

### 1.3.4 Yukawa Lagrangian

This part of the Lagrangian contains Yukawa type interactions of fermions with Higgs multiplets [33, 63]

$$-\mathcal{L}_{\text{Yukawa}} = \sum_{i,j=1}^3 \left[ y_{ij}^L \bar{L}_{Li} \Phi L_{Rj} + \tilde{y}_{ij}^L \bar{L}_{Li} \tilde{\Phi} L_{Rj} + y_{ij}^Q \bar{Q}_{Li} \Phi Q_{Rj} + \tilde{y}_{ij}^Q \bar{Q}_{Li} \tilde{\Phi} Q_{Rj} + iy_{ij}^M (L_{Li}^T C \sigma^2 \Delta_L L_{Rj} + L_{Ri}^T C \sigma^2 \Delta_R L_{Rj}) + h.c. \right] \quad (1.3.33)$$

here  $y^L, \tilde{y}^L, y^Q, \tilde{y}^Q$  and  $y^M$  are  $3 \times 3$  Yukawa matrices which again will determine fermion masses and mixings.

### 1.3.5 The Left-Right Symmetry

As mentioned in the introduction, the main motivation of the LR symmetry is parity. Parity relates the two groups  $SU(2)$ , *i.e.*, relates only the LH sector with the RH one. There are two ways to realize the parity symmetry: as generalized parity  $\mathcal{P}$  or as generalized charge conjugation  $\mathcal{C}$ . For fermions they coincide with the usual

parity and charge conjugation. For gauge boson and scalar fields, they are chosen in such a way as to keep the gauge interactions and Yukawa interactions invariant, respectively [55, 79]. The obvious way to impose the discrete parity symmetry is to demand invariance under either the parity:

$$\mathcal{P} : \{Q_L, L_L, W_L, \Delta_L, \Phi\} \leftrightarrow \{Q_R, L_R, W_R, \Delta_R, \Phi^\dagger\}, \quad (1.3.34)$$

or the charge conjugation:

$$\mathcal{C} : \{Q_L, L_L, W_L, \Delta_L, \Phi\} \leftrightarrow \{(Q_R)^c, (L_R)^c, -W_R^\dagger, \Delta_R^*, \Phi^T\}. \quad (1.3.35)$$

The Lagrangian that appeared in bits and pieces in this section contains many parameters. The parity symmetry will put some restrictions on them. One of them we have already encountered is that the Majorana couplings of the left and right handed fields must be the same ( $y^M$ ). The most obvious consequence of LR symmetry is that the gauge couplings of the left and right handed  $SU(2)$  are equal ( $g_L = g = g_R$ ). Looking at the Dirac Yukawa couplings (1.3.33) it can be seen that under (1.3.34) each term must transform into its hermitian conjugate. Therefore, the matrices  $y^L$ ,  $\tilde{y}^L$ ,  $y^Q$  and  $\tilde{y}^Q$  should be taken Hermitian. On the other hand, invariance of (1.3.33) under (1.3.35) makes the matrices  $y^L$ ,  $\tilde{y}^L$ ,  $y^Q$  and  $\tilde{y}^Q$  to be taken symmetric [55, 79]. Reference [55] argued that (1.3.34) and (1.3.35) are the only realistic possibilities of the LR symmetry relating mass matrices.

## 1.4 Spontaneous Symmetry Breaking in the LRSM

As a consequence of the LRSM Lagrangian gauge invariance, all the fermions and gauge bosons are massless before SSB. The symmetry breaking of the LRSM is spontaneously achieved in two stages and the symmetry breaking mechanism is similar to that of the SM. That is, it occurs via VEV of scalar Higgs multiplets. The symmetry

breaking scheme is as following

$$SU(2)_L \times SU(2)_R \times U(1)_{B-L} \xrightarrow{\langle \Delta_R \rangle} SU(2)_L \times U(1)_Y \quad (1.4.1)$$

at this stage RH scalar Higgs triplet gets a VEV and breaks LR symmetry to the EW symmetry. Physical  $W_{R\mu}^\pm$  and  $Z_{R\mu}$  gauge bosons gain their masses through interacting with RH Higgs triplet. After this stage of symmetry breaking, the hypercharge operator is the linear combination of the third component of the RH isospin and the difference between baryon and lepton numbers

$$Y = T_R^3 + Q_{BL} \quad (1.4.2)$$

where  $Q_{BL}$  is the generator of the  $U(1)_{B-L}$  group, defined in eq. (1.3.3). The values of the new gauge couplings  $g_R$  and  $g_{BL}$  are related to the known coupling  $g_Y$  by:

$$g_Y = \frac{g_R g_{BL}}{\sqrt{g_R^2 + g_{BL}^2}} \quad (1.4.3)$$

As shown in Appendix B,  $Y(\Delta_R^0) = 0$  and as  $\Delta_R$  is a singlet under the gauge group  $SU(2)_L$ , the desired pattern (1.4.1) of SSB is achieved.

The next stage is the breaking of the SM EW symmetry which is exactly the same as in the SM

$$SU(2)_L \times U(1)_Y \xrightarrow{\langle \Phi \rangle, \langle \Delta_L \rangle} U(1)_{EM} \quad (1.4.4)$$

where the neutral components of the bidoublet Higgs and (possibly but not necessarily) LH Higgs triplet get VEV and break the SM EW symmetry to electromagnetism. In consequence physical  $W_{L\mu}^\pm$  and  $Z_{L\mu}$  gauge bosons acquire their masses. The EM charge is defined by the modified Gell-Mann-Nishijima formula

$$Q = T_L^3 + T_R^3 + Q_{BL} \quad (1.4.5)$$

The values of the new gauge couplings  $g_R$  and  $g_{BL}$  are related to the EM charge  $e$  and the known coupling  $g_L$  by:

$$\frac{1}{e^2} = \frac{1}{g_L^2} + \frac{1}{g_R^2} + \frac{1}{g_{BL}^2} = \frac{1}{g_L^2} + \frac{1}{g_Y^2} \quad (1.4.6)$$

Which retain again relation (1.2.36). The derivation of the EM charge modified Gell-Mann-Nishijima formula and the coupling relations are in detail in Appendix B.

The VEVs of Higgs scalars are given to their neutral components

$$\langle \Phi \rangle = \frac{1}{\sqrt{2}} \begin{pmatrix} k_1 & 0 \\ 0 & k_2 \end{pmatrix}, \quad \langle \Delta_R \rangle = \frac{1}{\sqrt{2}} \begin{pmatrix} 0 & 0 \\ v_R & 0 \end{pmatrix}, \quad \langle \Delta_L \rangle = \frac{1}{\sqrt{2}} \begin{pmatrix} 0 & 0 \\ v_L & 0 \end{pmatrix} \quad (1.4.7)$$

The hierarchy between VEVs is like  $v_R \gg (k_1, k_2) \gg v_L$ . Since the EW analysis lead to the constraint  $v_L \leq 10$  GeV and the seesaw mechanism for small LH neutrino masses requires  $v_L \leq$  a few MeV. If we work at the limit  $v_L \rightarrow 0$ , then  $\sqrt{k_1^2 + k_2^2} = v = 246$  GeV is chosen to be compatible with the SM. [58]

### 1.4.1 Gauge Boson Masses in the LRSM

Gauge bosons masses are generated after SSB from Higgs fields kinetic terms. At the first stage, RH Higgs triplet takes a VEV  $\langle \Delta_R \rangle = v_R$  and breaks the LR symmetry as in eq. (1.4.1). The corresponding Higgs kinetic terms are

$$\text{Tr}|D_\mu \langle \Delta_R \rangle|^2 = \frac{g_R^2 v_R^2}{2} W_R^{\mu-} W_{R\mu}^+ + \frac{v_R^2}{2} (g_R W_R^{\mu 3} - g_{BL} V^\mu) (g_R W_{R\mu}^3 - g_{BL} V_\mu) \quad (1.4.8)$$

In general, as the  $U(1)_{\text{EM}}$  is an exact symmetry, there are no mixed mass terms between charged and neutral gauge bosons. The Neutral fields can be diagonalized by an orthogonal transformation and then the compositions of physical gauge bosons in terms of gauge eigenstates become

$$W_{R\mu}^\pm = \frac{W_{R\mu}^1 \mp i W_{R\mu}^2}{\sqrt{2}}, \quad \begin{pmatrix} Z_{R\mu} \\ B_\mu \end{pmatrix} = \begin{pmatrix} c_\varphi & -s_\varphi \\ s_\varphi & c_\varphi \end{pmatrix} \begin{pmatrix} W_{R\mu}^3 \\ V_\mu \end{pmatrix} \quad (1.4.9)$$

where  $\varphi$  is a mixing angle which has a similar role with the SM Weinberg angle  $\theta_W$ ,

$$s_\varphi = \frac{g_{BL}}{\sqrt{g_R^2 + g_{BL}^2}} = \frac{g_Y}{g_R}, \quad c_\varphi = \frac{g_R}{\sqrt{g_R^2 + g_{BL}^2}} = \frac{g_Y}{g_{BL}}. \quad (1.4.10)$$

At this stage of  $SU(2)_R \times U(1)_{B-L}$  breaking, the neutral gauge eigenstates  $W_{R\mu}^3$  and  $V_\mu$  mix to give a physical massless state which will be identified as the hypercharge

$B_\mu$  field and a physical massive  $Z_{R\mu}$  boson which will decouple from the further breakdown process.

The second stage is controlled by the Higgs bidoublet getting a non zero VEV  $\langle \Phi \rangle = \text{diag}(k_1, k_2)$  and possibly, but not necessarily by the left triplet VEV  $\langle \Delta_L \rangle = v_L$ . The LH Higgs triplet ( $\Delta_L$ ) is only responsible for maintaining the discrete parity symmetry [67] in the theory, whereas the Higgs bidoublet is needed to give masses to leptons, quarks and the SM gauge bosons. The kinetic terms for left triplet and bidoublet Higgs fields are

$$\begin{aligned} \text{Tr}|D_\mu\langle\Delta_L\rangle|^2 &= \frac{g_L^2 v_L^2}{2} W_L^{\mu-} W_{L\mu}^+ + \frac{v_L^2}{2} (g_L W_L^{\mu 3} - g_{BL} V^\mu) (g_L W_{L\mu}^3 - g_{BL} V_\mu) \\ &\supset \frac{g_L^2 v_L^2}{2} W_L^{\mu-} W_{L\mu}^+ + \frac{v_L^2}{2} (g_L W_L^{\mu 3} - g_Y B^\mu) (g_L W_{L\mu}^3 - g_Y B_\mu) \end{aligned} \quad (1.4.11)$$

and

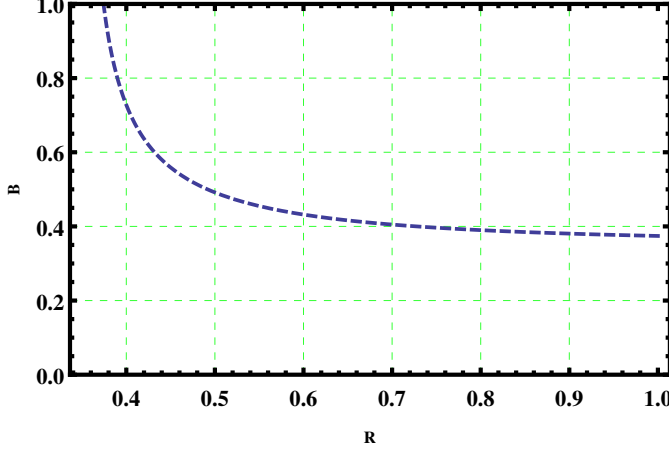
$$\begin{aligned} \text{Tr}|D_\mu\langle\Phi\rangle|^2 &= \text{Tr}[(D^\mu\langle\Phi\rangle)^\dagger(D_\mu\langle\Phi\rangle)] \\ &= \frac{v^2}{8} (g_L W_L^{\mu 3} - g_R W_R^{\mu 3}) (g_L W_{L\mu}^3 - g_R W_{R\mu}^3) \\ &\quad + \frac{v^2}{4} (g_L^2 W_L^{\mu+} W_{L\mu}^- + g_R^2 W_R^{\mu+} W_{R\mu}^-) \\ &\quad - \frac{g_L g_R k_1 k_2}{2} (W_L^{\mu+} W_{R\mu}^- + W_R^{\mu+} W_{L\mu}^-) \\ &\supset \frac{v^2}{8} (g_L W_L^{\mu 3} - g_Y B_\mu) (g_L W_{L\mu}^3 - g_Y B_\mu) \\ &\quad + \frac{v^2}{4} (g_L^2 W_L^{\mu+} W_{L\mu}^- + g_R^2 W_R^{\mu+} W_{R\mu}^-) \\ &\quad - \frac{g_L g_R k_1 k_2}{2} (W_L^{\mu+} W_{R\mu}^- + W_R^{\mu+} W_{L\mu}^-) \end{aligned} \quad (1.4.12)$$

and the composition of physical gauge bosons at this stage are

$$W_{L\mu}^\pm = \frac{W_{L\mu}^1 \mp i W_{L\mu}^2}{\sqrt{2}}, \quad \begin{pmatrix} Z_{L\mu} \\ A_\mu \end{pmatrix} = \begin{pmatrix} \cos \theta_W & -\sin \theta_W \\ \sin \theta_W & \cos \theta_W \end{pmatrix} \begin{pmatrix} W_{L\mu}^3 \\ B_\mu \end{pmatrix} \quad (1.4.13)$$

where the Weinberg mixing angle is defined here as in eq. (1.2.34) in the SM

$$\sin \theta_W = \frac{g_Y}{\sqrt{g_L^2 + g_Y^2}} = \frac{e}{g_L}, \quad \cos \theta_W = \frac{g_L}{\sqrt{g_L^2 + g_Y^2}} = \frac{e}{g_Y} \quad (1.4.14)$$


 Figure 1.7:  $g_{BL}$  vs  $g_R$  in the LRSM.

From (1.4.6), (1.4.10) and (1.4.14), we have the following relations

$$g_{BL} = \frac{g_L g_R s_w}{\sqrt{c_w^2 g_R^2 - s_w^2 g_L^2}}, \quad g_Y = t_w g_L \quad (1.4.15)$$

where  $t_w = \tan \theta_w$ . From eq. (1.4.15), for  $c_w^2 g_R^2 - s_w^2 g_L^2 \geq 0$ , and for perturbation for  $g_{BL}$ , we have, respectively, the following limits for  $g_R$

$$g_R \geq t_w g_L \gtrsim 0.35, \quad g_R \gtrsim 0.375, \quad (1.4.16)$$

i.e., for perturbation

$$1 \geq g_R \gtrsim 0.375. \quad (1.4.17)$$

For  $g_L = g_R = g$ , a case which satisfies the above limits, we have

$$g_{BL} = \frac{g s_w}{\sqrt{c_w^2 - s_w^2}}, \quad g_Y = t_w g. \quad (1.4.18)$$

Now it is easy to extract the neutral and charged gauge bosons mass matrices from those Higgs kinetic terms above. The mass squared matrix for neutral gauge

bosons in the basis  $\{W_{L\mu}^3, W_{R\mu}^3, V_\mu\}$  is [64]

$$M_{V^0}^2 = \frac{1}{4} \begin{pmatrix} g_L^2 (4v_L^2 + v^2) & -g_L g_R v^2 & -4g_L g_{BL} v_L^2 \\ -g_L g_R v^2 & g_R^2 (4v_R^2 + v^2) & -4g_R g_{BL} v_R^2 \\ -4g_L g_{BL} v_L^2 & -4g_R g_{BL} v_R^2 & g_{BL}^2 (4v_R^2 + 4v_L^2) \end{pmatrix} \quad (1.4.19)$$

By using eq. (1.4.9) and eq. (1.4.13), it is diagonalized by the rotation of gauge fields into physical eigenstates by

$$\begin{pmatrix} W_{L\mu}^3 \\ W_{R\mu}^3 \\ V_\mu \end{pmatrix} = \begin{pmatrix} \cos \theta_W & \sin \theta_W & 0 \\ -s_\varphi \sin \theta_W & s_\varphi \cos \theta_W & c_\varphi \\ -c_\varphi \sin \theta_W & c_\varphi \cos \theta_W & -s_\varphi \end{pmatrix} \begin{pmatrix} Z_{L\mu} \\ A_\mu \\ Z_{R\mu} \end{pmatrix} \quad (1.4.20)$$

or in terms of the EM coupling constant  $e$  and gauge coupling constants  $g_L, g_R, g_{BL}$  and  $g_Y$

$$\begin{pmatrix} W_{L\mu}^3 \\ W_{R\mu}^3 \\ V_\mu \end{pmatrix} = \begin{pmatrix} \frac{e}{g_Y} & \frac{e}{g_L} & 0 \\ \frac{-eg_Y}{g_L g_R} & \frac{e}{g_R} & \frac{g_Y}{g_{BL}} \\ \frac{-eg_Y}{g_L g_{BL}} & \frac{e}{g_{BL}} & \frac{-g_Y}{g_R} \end{pmatrix} \begin{pmatrix} Z_{L\mu} \\ A_\mu \\ Z_{R\mu} \end{pmatrix}. \quad (1.4.21)$$

### Charged Gauge Bosons in the LRSM

Since  $\Phi$  transforms non-trivially under both  $SU(2)_L$  and  $SU(2)_R$ , it mixes the  $W_R$  and  $W_L$  gauge bosons with the following mass-squared matrix in the basis  $\{W_{L\mu}^\pm, W_{R\mu}^\pm\}$

$$M_{V^\pm} = \begin{pmatrix} M_{LL}^\pm & M_{LR}^\pm \\ M_{LR}^\pm & M_{RR}^\pm \end{pmatrix} = \frac{1}{4} \begin{pmatrix} g_L^2 (k_1^2 + k_2^2 + 2v_L^2) & -2g_L g_R k_1 k_2 \\ -2g_L g_R k_1 k_2 & g_R^2 (k_1^2 + k_2^2 + 2v_R^2) \end{pmatrix} \quad (1.4.22)$$

where the two mass eigenstates are  $W_1^\pm$  and  $W_2^\pm$ . The corresponding squared masses satisfy

$$M_{W'}^2 + M_W^2 = T^{g\pm}, \quad M_{W'}^2 M_W^2 = D^{g\pm}, \quad (1.4.23)$$

where  $T^{g\pm} = \text{Tr}(M_{V^\pm})$  and  $D^{g\pm} = \text{Det}(M_{V^\pm})$ . Thus we have the following relations between masses

$$M_{W'}^2 = T^{g\pm} - M_W^2 = \frac{D^{g\pm}}{M_W^2}, \quad (1.4.24)$$

and the masses are given by

$$M_{W,W'}^2 = \frac{1}{2} \left( T^{g\pm} \mp \sqrt{(T^{g\pm})^2 - 4D^{g\pm}} \right), \quad (1.4.25)$$

where

$$T^{g\pm} = \frac{1}{4} ((g_L^2 + g_R^2)(k_1^2 + k_2^2) + 2(g_L^2 v_L^2 + g_R^2 v_R^2)) \quad (1.4.26)$$

$$D^{g\pm} = \frac{1}{16} g_L^2 g_R^2 ((k_1^2 + k_2^2 + 2v_L^2)(k_1^2 + k_2^2 + 2v_R^2) - 4k_1^2 k_2^2). \quad (1.4.27)$$

We define two parameters, the angle  $\beta$  and the deviation-from-electroweak parameter  $\varepsilon$ , such that

$$k_1 = (v + \varepsilon) c_\beta, \quad k_2 = (v + \varepsilon) s_\beta. \quad (1.4.28)$$

where  $s_\beta = \sin \beta$  and  $c_\beta = \cos \beta$ . Thus

$$t_\beta \equiv \tan \beta = \frac{k_2}{k_1} \quad (1.4.29)$$

and

$$\sqrt{k_1^2 + k_2^2} - \varepsilon = v \equiv 246 \text{ GeV}. \quad (1.4.30)$$

In terms of  $t_\beta, s_w^2, \varepsilon$ , (1.4.26) and (1.4.27) can be rewritten in the form

$$T^{g\pm} = \frac{1}{4} ((g_L^2 + g_R^2)(v + \varepsilon)^2 + 2(g_L^2 v_L^2 + g_R^2 v_R^2)), \quad (1.4.31)$$

$$D^{g\pm} = \frac{1}{16} g_L^2 g_R^2 (((v + \varepsilon)^2 + 2v_L^2)((v + \varepsilon)^2 + 2v_R^2) - 4(v + \varepsilon)^4 s_\beta^2 c_\beta^2). \quad (1.4.32)$$

Since  $M_W^2$  is a zero for the characteristic polynomial

$$P^{g\pm}(x) = x^2 - T^{g\pm}x + D^{g\pm}, \quad (1.4.33)$$

then we have

$$M_W^4 - T^{g\pm} M_W^2 + D^{g\pm} = 0. \quad (1.4.34)$$

We notice from (1.4.26) and (1.4.27) that both  $T^{g\pm}$  and  $D^{g\pm}$  are linear in  $v_R^2$ . We thus solve eq. (1.4.34) for  $v_R^2$  in terms of  $M_W^2, t_\beta, s_w^2, \varepsilon$  and  $v_L$  as follows

$$v_R^2 = -\frac{M_W^4 - T^{g\pm(0)} M_W^2 + D^{g\pm(0)}}{-T^{g\pm(1)} M_W^2 + D^{g\pm(1)}}, \quad (1.4.35)$$

that is

$$v_R^2 = -\frac{M_W^4 - \frac{1}{4}((g_L^2 + g_R^2)(v + \varepsilon)^2 + 2g_L^2 v_L^2) M_W^2 + \frac{1}{16}g_L^2 g_R^2(v + \varepsilon)^2 \left((v + \varepsilon)^2 c_{2\beta}^2 + 2v_L^2\right)}{-\frac{1}{2}g_R^2 M_W^2 + \frac{1}{8}g_L^2 g_R^2((v + \varepsilon)^2 + 2v_L^2)}, \quad (1.4.36)$$

where  $c_{2\beta} = \cos 2\beta$ . Substituting from eq. (1.4.36) into eq. (1.4.24) for  $v_R^2$  gives  $M_{W'}^2$ , in terms of  $M_W^2, t_\beta, s_w^2, \varepsilon$  and  $v_L$  as

$$M_{W'}^2 = \frac{g_L^2((v + \varepsilon)^2 + 2v_L^2) M_W^2 - g_L^2 g_R^2(v + \varepsilon)^4 s_\beta^2 c_\beta^2 - \frac{1}{4}g_L^4((v + \varepsilon)^2 + 2v_L^2)^2}{4M_W^2 - g_L^2((v + \varepsilon)^2 + 2v_L^2)}. \quad (1.4.37)$$

The two mass eigenstates are  $W_1^\pm$  and  $W_2^\pm$ , and they mix with an orthogonal rotation matrix to construct physical W gauge bosons

$$\begin{pmatrix} W_{1\mu}^\pm \\ W_{2\mu}^\pm \end{pmatrix} = \begin{pmatrix} \cos \xi & e^{-i\omega} \sin \xi \\ -\sin \xi & e^{-i\omega} \cos \xi \end{pmatrix} \begin{pmatrix} W_{L\mu}^\pm \\ W_{R\mu}^\pm \end{pmatrix} \quad (1.4.38)$$

where  $\xi$  is a mixing angle which has already some natural bounds on it ( $\xi < 10^{-3}$ ) [47] and  $\omega$  is a phase. The mixing angle and two mass eigenstates are defined by

$$\tan 2\xi = \frac{2M_{LR}}{M_{LL} - M_{RR}} \quad (1.4.39)$$

and

$$\cos \xi = \frac{-\text{sign}(M_{LR})(M_{RR} - M_{LL} + \sqrt{4M_{LR}^2 + (M_{RR} - M_{LL})^2})}{\sqrt{4M_{LR}^2 + (M_{RR} - M_{LL} + \sqrt{4M_{LR}^2 + (M_{RR} - M_{LL})^2})^2}}, \quad (1.4.40)$$

$$\sin \xi = \frac{-2|M_{\text{LR}}|}{\sqrt{4M_{\text{LR}}^2 + (M_{\text{RR}} - M_{\text{LL}} + \sqrt{4M_{\text{LR}}^2 + (M_{\text{RR}} - M_{\text{LL}})^2})^2}}. \quad (1.4.41)$$

The mixing angle and two mass eigenstates in the predefined VEV hierarchy limit are defined

$$\tan 2\xi = \frac{2M_{\text{LR}}}{M_{\text{LL}} - M_{\text{RR}}} = \frac{4g_{RL}k_1k_2}{2g_{RL}^2v_R^2 + (g_{RL}^2 - 1)v^2} \quad (1.4.42)$$

$$M_{W_1}^2 = \frac{g_L^2}{4}[v^2 \cos^2 \xi - 2g_{RL}k_1k_2 \sin 2\xi + g_{RL}^2(2v_R^2 + v^2) \sin^2 \xi], \quad (1.4.43)$$

$$M_{W_2}^2 = \frac{g_L^2}{4}[v^2 \sin^2 \xi + 2g_{RL}k_1k_2 \sin 2\xi + g_{RL}^2(2v_R^2 + v^2) \cos^2 \xi], \quad (1.4.44)$$

where we have introduced a new parameter  $g_{RL} = g_R/g_L$  (for our numerical purposes) and the shorthand notation  $v^2 = k_1^2 + k_2^2$ . Notice that, in the case of no mixing ( $\xi \rightarrow 0$ ) the mass eigenstates will exactly be as  $M_{W_1} = M_{W_L}$  and  $M_{W_2} = M_{W_R}$ .

$$M_{W_L} = \frac{vg_L}{2}, \quad M_{W_R} = \frac{v_R g_R}{\sqrt{2}} \quad (1.4.45)$$

### Neutral Gauge Bosons in the LRSM

Now it is easy to extract the neutral and charged gauge bosons mass matrices from those Higgs kinetic terms above. The mass squared matrix for neutral gauge bosons in the basis  $\{W_{L\mu}^3, W_{R\mu}^3, V_\mu\}$  is [64]

$$M_{V^0}^2 = \frac{1}{4} \begin{pmatrix} g_L^2(4v_L^2 + k_1^2 + k_2^2) & -g_L g_R (k_1^2 + k_2^2) & -4g_L g_{BL} v_L^2 \\ -g_L g_R (k_1^2 + k_2^2) & g_R^2(4v_R^2 + k_1^2 + k_2^2) & -4g_R g_{BL} v_R^2 \\ -4g_L g_{BL} v_L^2 & -4g_R g_{BL} v_R^2 & g_{BL}^2(4v_R^2 + 4v_L^2) \end{pmatrix} \quad (1.4.46)$$

The eigenvalues of this matrix are  $M_Z^2, M_{Z'}^2$  and for the photon  $M_A = 0$ . Thus we have  $D^{ZZ'} = \text{Det}(M_{ZZ'}) = 0$  and moreover

$$T^{ZZ'} = \text{Tr}(M_{ZZ'}) = M_{Z'}^2 + M_Z^2 = M_{W'}^2 + M_W^2 + \frac{1}{2}\{(g_L^2 + 2g_{BL}^2)v_L^2 + (g_R^2 + 2g_{BL}^2)v_R^2\}. \quad (1.4.47)$$

Since the determinant  $D^{ZZ'} = 0$ , the characteristic polynomial  $P_{ZZ'}^3$  of the matrix  $M_{ZZ'}^2$  has the form

$$P^{ZZ'}(x) = x(-x^2 + T^{ZZ'}x - D_2^{ZZ'}), \quad (1.4.48)$$

where

$$T^{ZZ'} = \frac{1}{4}(g_L^2 + g_R^2)(v + \varepsilon)^2 + (g_L^2 + g_{BL}^2)v_L^2 + (g_R^2 + g_{BL}^2)v_R^2, \quad (1.4.49)$$

$$D_2^{ZZ'} = \frac{1}{4}(g_L^2 g_R^2 + g_{BL}^2(g_L^2 + g_R^2))((v + \varepsilon)^2(v_L^2 + v_R^2) + 4v_L^2 v_R^2). \quad (1.4.50)$$

and the masses are given by

$$M_{Z,Z'}^2 = \frac{1}{2} \left( T^{ZZ'} \mp \sqrt{(T^{ZZ'})^2 - 4D_2^{ZZ'}} \right). \quad (1.4.51)$$

Substituting from eqs. (1.4.15), (1.4.36) and eq. (1.4.37) into eq. (1.4.47) for  $g_{BL}$ ,  $v_R^2$  and  $M_{W'}^2$  gives  $M_{Z'}^2$  in terms of  $M_Z^2$ ,  $M_W^2$ ,  $t_\beta$ ,  $s_w^2$ ,  $\varepsilon$ ,  $v_L$  and  $g_R$  as

$$M_{Z'}^2 = M_{W'}^2 + M_W^2 - M_Z^2 + \frac{1}{2}\{(g_L^2 + 2g_{BL}^2)v_L^2 + (g_R^2 + 2g_{BL}^2)v_R^2\}. \quad (1.4.52)$$

Since the squared mass  $M_Z^2$  is a zero of  $P^{ZZ'}$ , we have

$$-M_Z^4 + T^{ZZ'}M_Z^2 - D_2^{ZZ'} = 0. \quad (1.4.53)$$

Since, as it is clear from eqs. (1.4.49) and (1.4.50), both  $T^{ZZ'}$  and  $D_2^{ZZ'}$  are linear in  $v_R^2$ , we solve eq. (1.4.53) for  $v_R^2$  in terms of  $M_Z^2$ ,  $M_W^2$ ,  $t_\beta$  and  $s_w^2$  to obtain

$$v_R^2 = -\frac{-M_Z^4 + M_Z^2 T^{ZZ'(0)} - D_2^{ZZ'(0)}}{M_Z^2 T^{ZZ'(1)} - D_2^{ZZ'(1)}}, \quad (1.4.54)$$

where

$$T^{ZZ'} = T^{ZZ'(1)}v_R^2 + T^{ZZ'(0)}, \quad D_2^{ZZ'} = D_2^{ZZ'(1)}v_R^2 + D_2^{ZZ'(0)}. \quad (1.4.55)$$

i.e.,

$$v_R^2 = -\frac{-M_Z^4 + M_Z^2 \{\frac{1}{4}(g_L^2 + g_R^2)(v + \varepsilon)^2 + (g_L^2 + g_{BL}^2)v_L^2\} - \frac{1}{4}(g_L^2 g_R^2 + g_{BL}^2(g_L^2 + g_R^2))(v + \varepsilon)^2 v_L^2}{M_Z^2(g_R^2 + g_{BL}^2) - \frac{1}{4}(g_L^2 g_R^2 + g_{BL}^2(g_L^2 + g_R^2))((v + \varepsilon)^2 + 4v_L^2)}. \quad (1.4.56)$$

We solve eq. (1.4.36) and eq. (1.4.56) for  $v_L$  in terms of  $M_W^2, M_Z^2, s_w^2, \varepsilon, t_\beta$  and  $g_R$ .

From eq. (1.4.36) and eq. (1.4.56), we have

$$\frac{A_1 v_L^2 + A_2}{A_3 v_L^2 + A_4} = \frac{B_1 v_L^2 + B_2}{B_3 v_L^2 + B_4}, \quad (1.4.57)$$

from which we obtain

$$Av_L^4 + Bv_L^2 + C = 0, \quad (1.4.58)$$

i.e.,

$$v_L^2 = \frac{-B \pm \sqrt{B^2 - 4AC}}{2A}, \quad (1.4.59)$$

where

$$A_1 = -\frac{1}{8}g_L^2\{4M_W^2 - g_R^2(v + \varepsilon)^2\}, \quad (1.4.60)$$

$$A_2 = M_W^4 - \frac{1}{4}(g_L^2 + g_R^2)(v + \varepsilon)^2 M_W^2 + \frac{1}{16}g_L^2 g_R^2(v + \varepsilon)^4 c_{2\beta}^2, \quad (1.4.61)$$

$$A_3 = \frac{1}{4}g_L^2 g_R^2, \quad (1.4.62)$$

$$A_4 = -\frac{1}{2}g_R^2 M_W^2 + \frac{1}{8}g_L^2 g_R^2(v + \varepsilon)^2, \quad (1.4.63)$$

$$B_1 = M_Z^2(g_L^2 + g_{BL}^2) - \frac{1}{4}(g_L^2 g_R^2 + g_{BL}^2(g_L^2 + g_R^2))(v + \varepsilon)^2, \quad (1.4.64)$$

$$B_2 = -M_Z^4 + \frac{1}{4}M_Z^2(g_L^2 + g_R^2)(v + \varepsilon)^2, \quad (1.4.65)$$

$$B_3 = -(g_L^2 g_R^2 + g_{BL}^2(g_L^2 + g_R^2)), \quad (1.4.66)$$

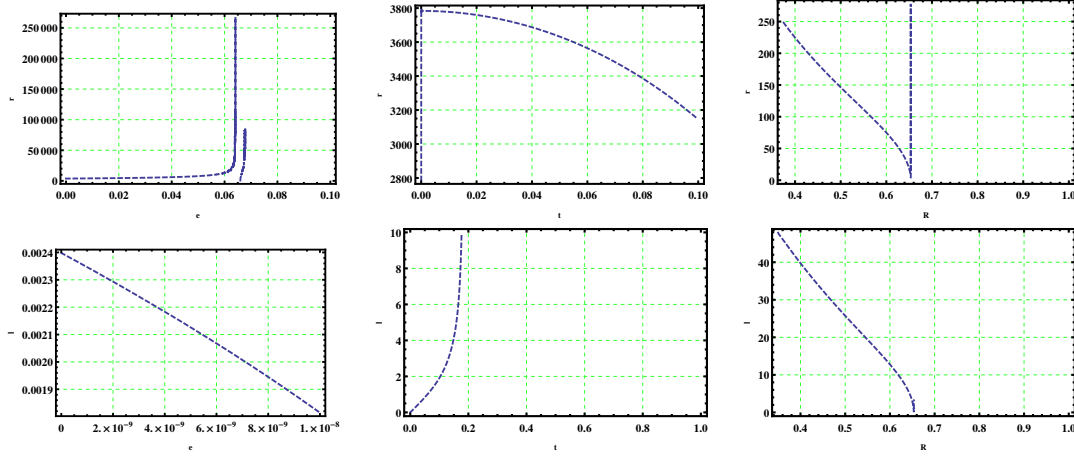
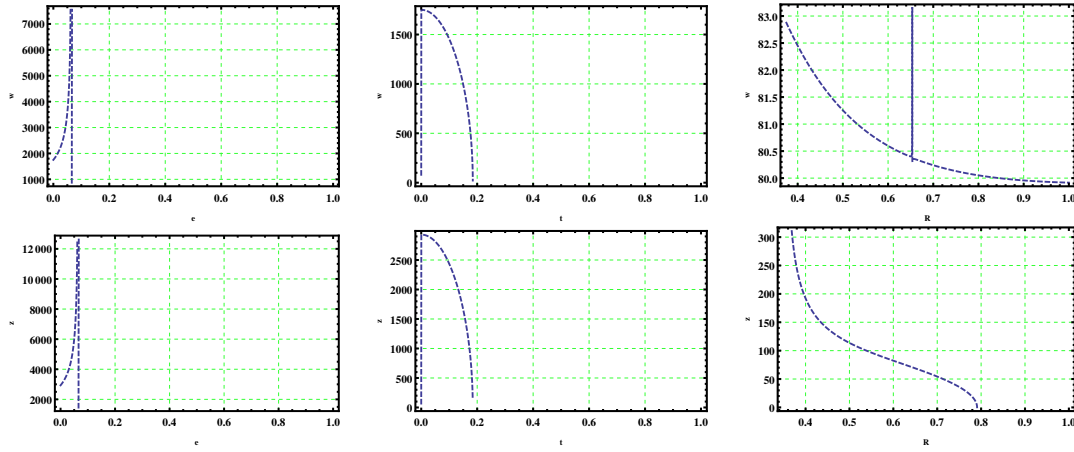
$$B_4 = M_Z^2(g_R^2 + g_{BL}^2) - \frac{1}{4}(g_L^2 g_R^2 + g_{BL}^2(g_L^2 + g_R^2))(v + \varepsilon)^2, \quad (1.4.67)$$

and

$$A = A_1 B_3 - A_3 B_1, \quad (1.4.68)$$

$$B = (A_1 B_4 + A_2 B_3) - (A_3 B_2 + A_4 B_1), \quad (1.4.69)$$

$$C = A_2 B_4 - A_4 B_2. \quad (1.4.70)$$


 Figure 1.8:  $v_R$  and  $v_L$  vs  $\epsilon$ ,  $t_\beta$  and  $g_R$  in the LRSM.

 Figure 1.9:  $M_{W'}$  and  $M_{Z'}$  vs  $\epsilon$ ,  $t_\beta$  and  $g_R$  in the LRSM.

By using eq. (1.4.9) and eq. (1.4.13), it is diagonalized by the rotation of gauge fields into physical eigenstates by

$$\begin{pmatrix} W_{L\mu}^3 \\ W_{R\mu}^3 \\ V_\mu \end{pmatrix} = \begin{pmatrix} \cos \theta_W & \sin \theta_W & 0 \\ -s_\varphi \sin \theta_W & s_\varphi \cos \theta_W & c_\varphi \\ -c_\varphi \sin \theta_W & c_\varphi \cos \theta_W & -s_\varphi \end{pmatrix} \begin{pmatrix} Z_{L\mu} \\ A_\mu \\ Z_{R\mu} \end{pmatrix} \quad (1.4.71)$$

or in terms of the EM coupling constant  $e$  and gauge coupling constants  $g_L, g_R, g_{BL}$

and  $g_Y$

$$\begin{pmatrix} W_{L\mu}^3 \\ W_{R\mu}^3 \\ V_\mu \end{pmatrix} = \begin{pmatrix} \frac{e}{g_Y} & \frac{e}{g_L} & 0 \\ \frac{-eg_Y}{g_L g_R} & \frac{e}{g_R} & \frac{g_Y}{g_{BL}} \\ \frac{-eg_Y}{g_L g_{BL}} & \frac{e}{g_{BL}} & \frac{-g_Y}{g_R} \end{pmatrix} \begin{pmatrix} Z_{L\mu} \\ A_\mu \\ Z_{R\mu} \end{pmatrix}. \quad (1.4.72)$$

The bidoublet  $\Phi$  also mixes the  $Z_R$  and  $Z_L$  gauge bosons with the following mass-squared matrix in the basis  $\{Z_{L\mu}, Z_{R\mu}\}$

$$M_{Z_L Z_R}^2 = \begin{pmatrix} M_{LL}^0 & M_{LR}^0 \\ M_{LR}^0 & M_{RR}^0 \end{pmatrix} \quad (1.4.73)$$

where

$$\begin{aligned} M_{LL}^0 &= \frac{e^2(g_L^2 + g_Y^2)^2(k_1^2 + k_2^2 + 4v_L^2)}{4g_L^2 g_Y^2} \\ M_{LR}^0 &= -\frac{e(g_L^2 + g_Y^2)(g_R^2(k_1^2 + k_2^2) - 4g_{BL}^2 v_L^2)}{4g_L g_R g_{BL}} \\ M_{RR}^0 &= \frac{g_Y^2(g_R^4(k_1^2 + k_2^2 + 4v_R^2) + 4g_{BL}^4(v_L^2 + v_R^2) + 8g_R^2 g_{BL}^2 v_R^2)}{4g_R^2 g_{BL}^2} \end{aligned}$$

The exact eigenstates  $Z$  and  $Z'$  are obtained as

$$\begin{pmatrix} Z \\ Z' \end{pmatrix} = \begin{pmatrix} \cos \vartheta & e^{-i\omega^0} \sin \vartheta \\ -\sin \vartheta & e^{-i\omega^0} \cos \vartheta \end{pmatrix} \begin{pmatrix} Z_L \\ Z_R \end{pmatrix}. \quad (1.4.74)$$

The mixing angle  $\vartheta$  is defined as

$$\tan 2\vartheta = \frac{2M_{LR}^0}{M_{LL}^0 - M_{RR}^0}, \quad (1.4.75)$$

The eigenvalues  $M_Z^2$  and  $M_{Z'}^2$  are given by

$$M_{Z,Z'}^2 = \frac{1}{2}(M_{LL}^2 + M_{RR}^2 \mp (M_{RR}^2 - M_{LL}^2)\sqrt{1 + \tan^2 2\vartheta}). \quad (1.4.76)$$

Spectrum	Domain	Value
<b>Gauge Coupling</b>		
$g_L$	$0 \leq g_L \leq 1$	0.653488
$g_R$	$0 \leq g_R \leq 1$	0.653488
$g_{BL}$	$0 \leq g_{BL} \leq 1$	0.415328
$g_Y$	$0 \leq g_Y \leq 1$	0.350524
$e$	$0 \leq e \leq 1$	0.313451
$s_w^2$	Exp. SM	0.22343
<b>Gauge Spectrum</b>		
$M_{W'}$	$\sim \mathcal{O}(10)$ TeV	1749.82
$M_{Z'}$	$\sim \mathcal{O}(10)$ TeV	2929.81
$M_W$	SM	80.379
$M_Z$	SM	91.1876
$M_A$	0	0

Table 1.3: A LRSM benchmark point. Gauge coupling and spectra.

It is clear that if  $v_R \gg v$ , *i.e.*,  $\vartheta \rightarrow 0$ , then  $Z \simeq Z_L$  and  $Z' \simeq Z_R$ . The LHC search for the  $Z'$  gauge boson is rather model dependent. However, one may consider  $M_{Z'} \gtrsim 2$  TeV as a conservative lower bound [3, 27]. In addition, the mixing between  $Z$  and  $Z'$  should be less than  $\mathcal{O}(10^{-3})$ .

### Gauge Numerical Session in the LRSM

Table 1.3 gives A LRSM benchmark point for gauge coupling and spectrum.

Fig. 1.7 exhibits the dependence

$$g_{BL}(g_R), \quad (1.4.77)$$

Fig. 1.8 exhibits the dependence

$$v_R(\varepsilon, t_\beta, g_R), \quad v_L(\varepsilon, t_\beta, g_R), \quad (1.4.78)$$

Fig. 1.9 exhibits the dependence

$$M_{W'}(\varepsilon, t_\beta, g_R), \quad M_{Z'}(\varepsilon, t_\beta, g_R). \quad (1.4.79)$$

### 1.4.2 Fermion Masses in the LRSM

Similar to the SM, three generations of leptons and quarks acquire their masses through Yukawa interactions of Higgs multiplets.

$$\begin{aligned} -\mathcal{L}_{\text{Yukawa}} \supset & \sum_{i,j=1}^3 \left[ \bar{L}_L^i (y_{ij}^L \langle \Phi \rangle + \tilde{y}_{ij}^L \langle \tilde{\Phi} \rangle) L_R^j + \bar{Q}_L^i (y_{ij}^Q \langle \Phi \rangle + \tilde{y}_{ij}^Q \langle \tilde{\Phi} \rangle) Q_R^j \right. \\ & \left. + i y_{ij}^M (L_L^T C \sigma^2 \langle \Delta_L \rangle L_R^j + L_R^T C \sigma^2 \langle \Delta_R \rangle L_R^j) + h.c. \right] \end{aligned} \quad (1.4.80)$$

$\Phi$  and  $\tilde{\Phi}$  couple to both leptons and quarks, they generate Dirac masses for fermions, their Yukawa matrices are independent allowing nontrivial quark and lepton mixings in the charged current interactions.  $\Delta_L$  and  $\Delta_R$  only couple to leptons generating light Majorana masses to the LH neutrinos and heavy Majorana masses to the RH neutrinos according to seesaw mechanism. The Yukawa Lagrangian leads the following Dirac mass matrices for leptons and quarks

$$M_u = \frac{1}{\sqrt{2}} (y^Q k_1 + \tilde{y}^Q k_2), \quad M_d = \frac{1}{\sqrt{2}} (y^Q k_2 + \tilde{y}^Q k_1) \quad (1.4.81)$$

$$M_\nu = \frac{1}{\sqrt{2}} (y^L k_1 + \tilde{y}^L k_2), \quad M_e = \frac{1}{\sqrt{2}} (y^L k_2 + \tilde{y}^L k_1) \quad (1.4.82)$$

and Majorana mass matrices for neutrinos

$$M_{\nu_L} = \frac{1}{\sqrt{2}} y^M v_L, \quad M_{\nu_R} = \frac{1}{\sqrt{2}} \tilde{y}^M v_R \quad (1.4.83)$$

The charged leptons and quarks mass matrices can be diagonalized just as in the SM by the biunitary transformations

$$V_L^{u\dagger} M_u V_R^u = M_u^{\text{diag}}, \quad V_L^{d\dagger} M_d V_R^d = M_d^{\text{diag}}, \quad V_L^{e\dagger} M_e V_R^e = M_e^{\text{diag}}. \quad (1.4.84)$$

Neutrino mass terms are derived both from the  $y^L$  and  $\tilde{y}^L$  terms, which lead to Dirac mass terms, and from the  $y^M$  term, which leads to Majorana mass terms. It is more convenient to employ the self-conjugate spinors [33, 62, 63]

$$\nu = \frac{\nu_L + \nu_L^c}{\sqrt{2}}, \quad N = \frac{\nu_R^c + \nu_R}{\sqrt{2}} \quad (1.4.85)$$

We also define

$$y_D \equiv \frac{1}{\sqrt{2}} \frac{y^L k_1 + \tilde{y}^L k_2}{v} = \frac{M_\nu}{v} \quad (1.4.86)$$

This quantity governs the size of the Dirac-type neutrino mass term. In terms of  $y_D$  and  $y^M$ , the neutrino mass matrix can be written in the form

$$\begin{pmatrix} \bar{\nu} \\ \bar{N} \end{pmatrix}^T \begin{pmatrix} \sqrt{2}y^M v_L & y_D v \\ y_D v & \sqrt{2}y^M v_R \end{pmatrix} \begin{pmatrix} \nu \\ N \end{pmatrix} \quad (1.4.87)$$

Normally, we expect  $y^M$  and  $y_D$  to be similar in size,  $y^M \sim y_D \sim M_e/v$ . In such a case, since we require  $v_R \gg v, v_L$  (for  $M_{W_R} \gg M_{W_L}$ ),  $\nu$  and  $N$  will be approximate flavor eigenstates with the well known seesaw mass matrices [33]

$$m_N \simeq \sqrt{2}y^M v_R, \quad m_\nu \simeq \sqrt{2}(y^M v_L - \frac{v^2}{2v_R} y_D (y^M)^{-1} y_D^T) \quad (1.4.88)$$

After this stage of diagonalization and obtaining the flavor (approximate) eigenstates  $\nu$  and  $N$  and the flavor mass matrices (1.4.88), we diagonalize both  $m_N$  and  $m_\nu$  by unitary transformations  $V_R^N$  and  $V_L^\nu$ , respectively

$$V_R^{N\dagger} m_N V_R^N = m_N^{\text{diag}}, \quad V_L^{\nu\dagger} m_\nu V_L^\nu = m_\nu^{\text{diag}} \quad (1.4.89)$$

Other possibilities for obtaining light neutrino masses are argued in [33].

## 1.5 Electroweak Interactions in the LRSM

As in the SM, the EW interactions of leptons and quarks arise in the LRSM from the kinetic part of the Lagrangian (eq. (1.3.14))

$$\mathcal{L}_{\text{Kinetic}} = i \sum_{j=1}^3 (\bar{L}_{Lj} \gamma^\mu D_\mu L_{Lj} + \bar{L}_{Rj} \gamma^\mu D_\mu L_{Rj} + \bar{Q}_{Lj} \gamma^\mu D_\mu Q_{Lj} + \bar{Q}_{Rj} \gamma^\mu D_\mu Q_{Rj})$$

For any  $\mathcal{H}$ -handed fermion  $\psi_{\mathcal{H}}$  in the LRSM,

$$Q(\psi_{\mathcal{H}}) = T_L^3(\psi_{\mathcal{H}}) + T_R^3(\psi_{\mathcal{H}}) + Q_{BL}(\psi_{\mathcal{H}}) = T_{\mathcal{H}}^3(\psi_{\mathcal{H}}) + Q_{BL}(\psi_{\mathcal{H}}), \quad (1.5.1)$$

Substituting the physical eigenstates for the neutral gauge bosons from eq. (1.4.21), we extract all the three types of the EW interactions, namely, the EM, neutral and charged currents of weak interactions. Following eq. (1.5.1), the kinetic terms of the LH and RH fermions contain the following terms

$$\begin{aligned} \bar{\psi}_L i \gamma^\mu D_\mu \psi_L &\supset \bar{\psi}_L \gamma^\mu \left( \frac{g_L}{\sqrt{2}} (W_{L\mu}^+ T_L^+ + W_{L\mu}^- T_L^-) + g_L W_{L\mu}^3 T_L^3 + g_{BL} V_\mu Q_{BL} \right) \psi_L \\ &= \bar{\psi} \gamma^\mu \left( \frac{g_L}{\sqrt{2}} (W_{L\mu}^+ T_L^+ + W_{L\mu}^- T_L^-) \right) P_L \psi \\ &\quad + \bar{\psi} \gamma^\mu \left( e Q A_\mu + e \left( \frac{g_L}{g_Y} T_L^3 - \frac{g_Y}{g_L} Q_{BL} \right) Z_{L\mu} - \frac{g_{BL} g_Y}{g_R} Q_{BL} Z_{R\mu} \right) P_L \psi, \end{aligned} \quad (1.5.2)$$

$$\begin{aligned} \bar{\psi}_R i \gamma^\mu D_\mu \psi_R &\supset \bar{\psi}_R \gamma^\mu \left( \frac{g_R}{\sqrt{2}} (W_{R\mu}^+ T_R^+ + W_{R\mu}^- T_R^-) + g_R W_{R\mu}^3 T_R^3 + g_{BL} V_\mu Q_{BL} \right) \psi_R \\ &= \bar{\psi} \gamma^\mu \left( \frac{g_R}{\sqrt{2}} (W_{R\mu}^+ T_R^+ + W_{R\mu}^- T_R^-) \right) P_R \psi \\ &\quad + \bar{\psi} \gamma^\mu \left( e Q A_\mu - \frac{e g_Y}{g_L} Q Z_{L\mu} + \left( \frac{g_Y g_R}{g_{BL}} T_R^3 - \frac{g_{BL} g_Y}{g_R} Q_{BL} \right) Z_{R\mu} \right) P_R \psi. \end{aligned} \quad (1.5.3)$$

Following Eqs. (1.4.14), (1.5.2) and (1.5.3), the EW interactions are

$$\begin{aligned} &\bar{\psi}_L i \gamma^\mu D_\mu \psi_L + \bar{\psi}_R i \gamma^\mu D_\mu \psi_R \\ &\supset \bar{\psi} \gamma^\mu \left( \frac{g_L}{\sqrt{2}} (W_{L\mu}^+ T_L^+ + W_{L\mu}^- T_L^-) P_L + \frac{g_R}{\sqrt{2}} (W_{R\mu}^+ T_R^+ + W_{R\mu}^- T_R^-) P_R \right) \psi \\ &\quad + \bar{\psi} \gamma^\mu \left( e Q A_\mu + \frac{g_L}{\cos \theta_W} (T_L^3 P_L - \sin^2 \theta_W Q) Z_{L\mu} + \frac{g_Y}{\tan \varphi} (T_R^3 P_R - \tan^2 \varphi Q_{BL}) Z_{R\mu} \right) \psi. \end{aligned} \quad (1.5.4)$$

Or in compact form

$$\bar{\psi}_L i\gamma^\mu D_\mu \psi_L + \bar{\psi}_R i\gamma^\mu D_\mu \psi_R \supset \mathcal{L}_{EM} + \mathcal{L}_{NC} + \mathcal{L}_{CC} \quad (1.5.5)$$

where the EM interaction Lagrangian  $\mathcal{L}_{EM}$ , neutral weak interaction Lagrangian  $\mathcal{L}_{NC}$  and charged weak interaction Lagrangian  $\mathcal{L}_{CC}$  are defined as follows

$$\mathcal{L}_{EM} = eA_\mu J_A^\mu, \quad (1.5.6)$$

$$\mathcal{L}_{NC} = \frac{g_L}{\cos \theta_W} Z_{L\mu} J_{Z_L}^\mu + \frac{g_Y}{\tan \varphi} Z_{R\mu} J_{Z_R}^\mu, \quad (1.5.7)$$

$$\mathcal{L}_{CC} = \frac{g_L}{\sqrt{2}} (W_{L\mu}^+ J_{W_L}^\mu + W_{L\mu}^- J_{W_L}^{\mu\dagger}) + \frac{g_R}{\sqrt{2}} (W_{R\mu}^+ J_{W_R}^\mu + W_{R\mu}^- J_{W_R}^{\mu\dagger}). \quad (1.5.8)$$

The EM current  $J_A^\mu$ , neutral weak currents  $J_{Z_L}^\mu$ ,  $J_{Z_R}^\mu$  and charged weak currents  $J_{W_L}^\mu$ ,  $J_{W_R}^\mu$  are defined as follows

$$J_A^\mu = \bar{\psi} \gamma^\mu Q \psi, \quad (1.5.9)$$

$$J_{Z_L}^\mu = \bar{\psi} \gamma^\mu (T_L^3 P_L - \sin^2 \theta_W Q) \psi, \quad (1.5.10)$$

$$J_{Z_R}^\mu = \bar{\psi} \gamma^\mu (T_R^3 P_R - \tan^2 \varphi Q_{BL}) \psi, \quad (1.5.11)$$

$$J_{W_L}^\mu = \bar{\psi} \gamma^\mu T_L^+ P_L \psi, \quad J_{W_L}^{\mu\dagger} = \bar{\psi} \gamma^\mu T_L^- P_L \psi, \quad (1.5.12)$$

$$J_{W_R}^\mu = \bar{\psi} \gamma^\mu T_R^+ P_R \psi, \quad J_{W_R}^{\mu\dagger} = \bar{\psi} \gamma^\mu T_R^- P_R \psi. \quad (1.5.13)$$

Where summation over  $\psi$  is involved over leptons and Quarks multiplets ( $\psi = L, Q$ ).

### Electromagnetic Interactions in the LRSM

Electromagnetic interactions in the LRSM are mediated by photons as in the SM.

They only couple to electrically charged fermions with their electric charges.

The compact form of the EM interactions is simply written

$$\mathcal{L}_{EM} = eA_\mu J_A^\mu. \quad (1.5.14)$$

In terms of fermion components the EM current  $J_A^\mu$  which covers the three flavors of fermions is given by

$$J_A^\mu = \sum_i Q^i \bar{f}_i \gamma^\mu f_i = -\bar{e} \gamma^\mu e + \frac{2}{3} \bar{u} \gamma^\mu u - \frac{1}{3} \bar{d} \gamma^\mu d \quad (1.5.15)$$

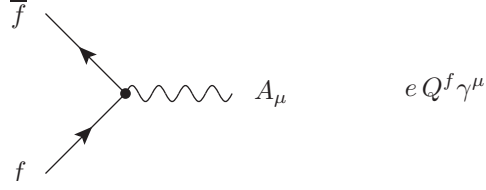


Figure 1.10: Feynman diagram and rule of electromagnetic interactions in the LRSM.

Summation over generations adds similar terms for the other generations.

### Neutral Current Interactions in the LRSM

Neutral currents in the LRSM are mediated by  $Z_L$  and  $Z_R$  gauge bosons. Mixing of neutral gauge eigenstates ensure that both  $Z_L$  and  $Z_R$  are involved in left and right neutral currents. and this expression can be summarized in terms of neutral currents

$$\mathcal{L}_{NC} = \frac{g_L}{\cos \theta_W} Z_{L\mu} J_{Z_L}^\mu + \frac{g_Y}{\tan \varphi} Z_{R\mu} J_{Z_R}^\mu \quad (1.5.16)$$

In terms of fermion components the neutral weak currents  $J_{Z_L}^\mu$  and  $J_{Z_R}^\mu$  which covers the three flavors of fermions are given by

$$\begin{aligned} J_{Z_L}^\mu &= \sum_i \bar{f}_i \gamma^\mu (T_L^{3i} P_L - Q^i \sin^2 \theta_W) f_i \\ &\simeq \frac{1}{2} \bar{\nu}_e \gamma^\mu P_L \nu_e + \bar{e} \gamma^\mu \left( -\frac{1}{2} P_L + \sin^2 \theta_W \right) e \\ &\quad + \bar{u} \gamma^\mu \left( \frac{1}{2} P_L - \frac{2}{3} \sin^2 \theta_W \right) u + \bar{d} \gamma^\mu \left( -\frac{1}{2} P_L + \frac{1}{3} \sin^2 \theta_W \right) d \end{aligned} \quad (1.5.17)$$

$$\begin{aligned} J_{Z_R}^\mu &= \sum_i \bar{f}_i \gamma^\mu (T_R^{3i} P_R - Q_{BL}^i \tan^2 \varphi) f_i \\ &\simeq \bar{N}_e \gamma^\mu \left( \frac{1}{2} P_R + \frac{1}{2} \tan^2 \varphi \right) N_e + \bar{e} \gamma^\mu \left( -\frac{1}{2} P_R + \frac{1}{2} \tan^2 \varphi \right) e \\ &\quad + \bar{u} \gamma^\mu \left( \frac{1}{2} P_R - \frac{1}{6} \tan^2 \varphi \right) u + \bar{d} \gamma^\mu \left( -\frac{1}{2} P_R - \frac{1}{6} \tan^2 \varphi \right) d \end{aligned} \quad (1.5.18)$$

Where again summation over generations adds similar terms for the other generations.

The semi-equal signs ‘ $\simeq$ ’ in Eqs. (1.5.17) and (1.5.18) are due to neglecting the  $\nu - N$

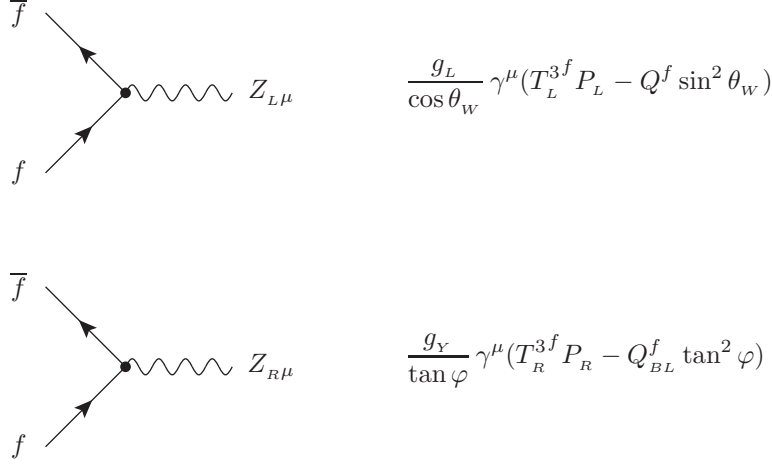


Figure 1.11: Feynman diagrams and rules of neutral current interactions in the LRSM.

seesaw mixing.

### Charged Current Interactions in the LRSM

$$\mathcal{L}_{CC} = \frac{g_L}{\sqrt{2}} (W_{L\mu}^+ J_{W_L}^\mu + W_{L\mu}^- J_{W_L}^{\mu\dagger}) + \frac{g_R}{\sqrt{2}} (W_{R\mu}^+ J_{W_R}^\mu + W_{R\mu}^- J_{W_R}^{\mu\dagger}) \quad (1.5.19)$$

The left and right charged currents  $J_{W_L}^\mu, J_{W_R}^\mu$  and their conjugates  $J_{W_L}^{\mu\dagger}, J_{W_R}^{\mu\dagger}$  are given in terms of the fermions components as follows

$$J_{W_L}^\mu \simeq \sum_{i,j} (\bar{\nu}_{Li} \gamma^\mu e_{Lj} U_{ij}^L + \bar{u}_{Li} \gamma^\mu d_{Lj} V_{ij}^L) \quad (1.5.20)$$

$$J_{W_L}^{\mu\dagger} \simeq \sum_{i,j} (\bar{e}_{Lj} \gamma^\mu \nu_{Li} U_{ij}^{L\dagger} + \bar{d}_{Lj} \gamma^\mu u_{Li} V_{ij}^{L\dagger}) \quad (1.5.21)$$

$$J_{W_R}^\mu \simeq \sum_{i,j} (\bar{N}_{Ri} \gamma^\mu e_{Rj} U_{ij}^R + \bar{u}_{Ri} \gamma^\mu d_{Rj} V_{ij}^R) \quad (1.5.22)$$

$$J_{W_R}^{\mu\dagger} \simeq \sum_{i,j} (\bar{e}_{Rj} \gamma^\mu N_{Ri} U_{ij}^{R\dagger} + \bar{d}_{Rj} \gamma^\mu u_{Ri} V_{ij}^{R\dagger}) \quad (1.5.23)$$

The semi-equal signs ‘ $\simeq$ ’ in these equations are due to neglecting the  $\nu - N$  seesaw mixing.

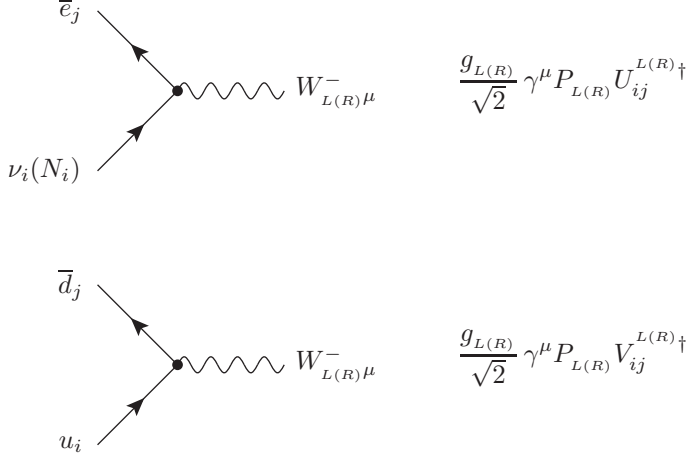


Figure 1.12: Feynman diagrams and rules of leptons charged current interactions (up) and quarks charged current interactions (down) in the LRSM.

The left and right CKM and PMNS matrices are

$$V^{L,R} \equiv V_{\text{CKM}}^{L,R} \equiv V_{L,R}^{u\dagger} V_{L,R}^d, \quad U^{L,R} \equiv U_{\text{PMNS}}^{L,R} \equiv V_{L,R}^{\nu,N\dagger} V_{L,R}^e \quad (1.5.24)$$

and the matrices  $V_{L,R}^u$ ,  $V_{L,R}^d$  and  $V_{L,R}^e$  are those in eq. (1.4.84) diagonalizing the mass matrices of up-quarks, down-quarks and charged leptons, respectively. The matrices  $V_L^\nu$  and  $V_R^N$  diagonalize the mass matrices of neutrinos  $\nu$  and  $N$  in eq. (1.4.89), respectively. In the context of the LRSM both left and right handed neutrinos can have masses, and they are also subject to mix under proper circumstances. Therefore,  $U^{L,R}$  represent corresponding left and right lepton mixing matrices as well as  $V^{L,R}$  in quark sector. where  $U^L$  and  $U^R$  are in generic form

$$U^L = \begin{pmatrix} U_{\nu_e e} & U_{\nu_e \mu} & U_{\nu_e \tau} \\ U_{\nu_\mu e} & U_{\nu_\mu \mu} & U_{\nu_\mu \tau} \\ U_{\nu_\tau e} & U_{\nu_\tau \mu} & U_{\nu_\tau \tau} \end{pmatrix}_L, \quad U^R = \begin{pmatrix} U_{N_e e} & U_{N_e \mu} & U_{N_e \tau} \\ U_{N_\mu e} & U_{N_\mu \mu} & U_{N_\mu \tau} \\ U_{N_\tau e} & U_{N_\tau \mu} & U_{N_\tau \tau} \end{pmatrix}_R \quad (1.5.25)$$

In quark sector,  $W_L$  gauge boson mixes left handed quarks in a same way as in the SM with the same CKM quark mixing matrix ( $V_{\text{CKM}}^L$ ). However the mixing of right handed quarks is left arbitrary in the most general form ( $V_{\text{CKM}}^R$ ). In this thesis we will adopt in a specific choice of  $V_{\text{CKM}}^R$  that is introduced in [49] which is constructed in such a way that is constrained by some well known low energy phenomenologies.

It is worth mentioning that till now we neglected the  $Z_L - Z_R$  mixing and  $W_L - W_R$  mixing in the EW interactions calculations. For more precise calculations, the neutral weak interaction Lagrangian  $\mathcal{L}_{\text{NC}}$  and charged weak interaction Lagrangian  $\mathcal{L}_{\text{CC}}$  are

$$\mathcal{L}_{\text{NC}} = Z_\mu J_Z^\mu + Z'_\mu J_{Z'}^\mu \quad (1.5.26)$$

$$\mathcal{L}_{\text{CC}} = W_{1\mu}^+ J_{W_1}^\mu + W_{1\mu}^- J_{W_1}^{\mu\dagger} + W_{2\mu}^+ J_{W_2}^\mu + W_{2\mu}^- J_{W_2}^{\mu\dagger} \quad (1.5.27)$$

The neutral weak currents  $J_Z^\mu$ ,  $J_{Z'}^\mu$  and charged weak currents  $J_{W_1}^\mu$ ,  $J_{W_2}^\mu$  are

$$J_Z^\mu = \frac{g_L}{\cos \theta_W} \cos \vartheta J_{Z_L}^\mu + \frac{g_Y}{\tan \varphi} e^{i\omega^0} \sin \vartheta J_{Z_R}^\mu \quad (1.5.28)$$

$$J_{Z'}^\mu = -\frac{g_L}{\cos \theta_W} \sin \vartheta J_{Z_L}^\mu + \frac{g_Y}{\tan \varphi} e^{i\omega} \cos \vartheta J_{Z_R}^\mu \quad (1.5.29)$$

$$J_{W_1}^\mu = \frac{g_L}{\sqrt{2}} \cos \xi J_{W_L}^\mu + \frac{g_R}{\sqrt{2}} e^{i\omega} \sin \xi J_{W_R}^\mu \quad (1.5.30)$$

$$J_{W_1}^{\mu\dagger} = \frac{g_L}{\sqrt{2}} \cos \xi J_{W_L}^{\mu\dagger} + \frac{g_R}{\sqrt{2}} e^{i\omega} \sin \xi J_{W_R}^{\mu\dagger} \quad (1.5.31)$$

$$J_{W_2}^\mu = -\frac{g_L}{\sqrt{2}} \sin \xi J_{W_L}^\mu + \frac{g_R}{\sqrt{2}} e^{i\omega} \cos \xi J_{W_R}^\mu \quad (1.5.32)$$

$$J_{W_2}^{\mu\dagger} = -\frac{g_L}{\sqrt{2}} \sin \xi J_{W_L}^{\mu\dagger} + \frac{g_R}{\sqrt{2}} e^{i\omega} \cos \xi J_{W_R}^{\mu\dagger} \quad (1.5.33)$$

## 1.6 Higgs Sector in the LRSM

As mentioned before, the Higgs sector of the LRSM consists of one bidoublet ( $\Phi$ ) and two triplets ( $\Delta_{L,R}$ ) complex scalar Higgs fields. The RH triplet ( $\Delta_R$ ) is responsible for the first stage of symmetry breaking

$$SU(2)_L \times SU(2)_R \times U(1)_{B-L} \rightarrow SU(2)_L \times U(1)_Y \quad (1.6.1)$$

and the bidoublet ( $\Phi$ ) accomplishes the second stage

$$SU(2)_L \times U(1)_Y \rightarrow U(1)_{\text{EM}} \quad (1.6.2)$$

whereas the LH triplet ( $\Delta_L$ ) is only present to maintain the discrete parity symmetry in the theory.

Neutral component of Higgs fields are expanded around the vacuum as

$$\Phi_1^0 = \frac{k_1 + h_1^0 + i\varphi_1^0}{\sqrt{2}}, \quad \Phi_2^0 = \frac{k_2 + h_2^0 + i\varphi_2^0}{\sqrt{2}}, \quad \Delta_\text{H}^0 = \frac{v_\text{H} + h_\text{H}^0 + i\varphi_\text{H}^0}{\sqrt{2}}. \quad (1.6.3)$$

The potential to minimize is

$$\begin{aligned} V(k_1, k_2, v_L, v_R) = & \frac{1}{4} \left[ \lambda_1(k_1^4 + k_2^4) + 4\lambda_4 k_1 k_2 (k_1^2 + k_2^2) + 2k_1^2 k_2^2 (\lambda_1 + 2\lambda_{23}^+) \right. \\ & + k_1^2 (2\mu_1 + \alpha_1(v_L^2 + v_R^2) + 2\beta_2 v_L v_R) \\ & + k_2^2 (2\mu_1 + \alpha_{13}(v_L^2 + v_R^2) + 2\beta_3 v_L v_R) \\ & + 2k_1 k_2 (4\mu_2 + 2\alpha_2(v_L^2 + v_R^2) + \beta_1 v_L v_R) \\ & \left. + \rho_1(v_L^4 + v_R^4) + 2\mu_3(v_L^2 + v_R^2) + \rho_3 v_L^2 v_R^2 \right]. \end{aligned} \quad (1.6.4)$$

The minimization conditions are

$$\begin{aligned} \frac{\partial V}{\partial k_1} = & \lambda_1 k_1^3 + 3k_1^2 k_2 \lambda_4 + \frac{1}{2} k_1 \left( 2(k_2^2(\lambda_1 + 2\lambda_{23}^+) + \mu_1) + \alpha_1 v_+^2 + 2\beta_2 v_\times^2 \right) \\ & + k_2 \left( k_2^2 \lambda_4 + 2\mu_2 + \alpha_2 v_+^2 + \frac{\beta_1 v_\times^2}{2} \right) = 0, \end{aligned} \quad (1.6.5)$$

$$\begin{aligned} \frac{\partial V}{\partial k_2} = & \frac{1}{2} \left[ k_2 \left( 2(k_1^2(\lambda_1 + 2\lambda_{23}^+) + \mu_1) + \alpha_{13} v_+^2 + 2\beta_3 v_\times^2 \right) \right. \\ & \left. + k_1 \left( 2k_1^2 \lambda_4 + 4\mu_2 + 2\alpha_2 v_+^2 + \beta_1 v_\times^2 \right) + 6k_1 k_2^2 \lambda_4 + 2\lambda_1 k_2^3 \right] = 0, \end{aligned} \quad (1.6.6)$$

$$\begin{aligned} \frac{\partial V}{\partial v_L} = & \frac{1}{2} \left[ k_1^2 (\alpha_1 v_L + \beta_2 v_R) + k_1 k_2 (4\alpha_2 v_L + \beta_1 v_R) + k_2^2 (v_L \alpha_{13} + \beta_3 v_R) \right. \\ & \left. + v_L (2\mu_3 + 2\rho_1 v_L^2 + \rho_3 v_R^2) \right] = 0, \end{aligned} \quad (1.6.7)$$

$$\begin{aligned} \frac{\partial V}{\partial v_R} = & \frac{1}{2} \left[ k_1^2 (\beta_2 v_L + \alpha_1 v_R) + k_1 k_2 (\beta_1 v_L + 4\alpha_2 v_R) + k_2^2 (\beta_3 v_L + v_R \alpha_{13}) \right. \\ & \left. + v_R (2\mu_3 + \rho_3 v_L^2 + 2\rho_1 v_R^2) \right] = 0. \end{aligned} \quad (1.6.8)$$

From minimization conditions, we solve (1.6.5) and (1.6.6) for  $\mu_1^2$  and  $\mu_2^2$ , and solve (1.6.7) and (1.6.8) for  $\mu_3^2$  and  $\beta_3$ , and we obtain

$$\beta_3 = -\frac{\beta_2 k_1^2 + \beta_1 k_1 k_2 - v_{\times}^2 \rho_{13}^-}{k_2^2}, \quad (1.6.9)$$

$$\mu_3^2 = \frac{1}{2} (\alpha_1 k_1^2 + 4\alpha_2 k_1 k_2 + k_2^2 \alpha_{13} + 2\rho_1 v_+^2), \quad (1.6.10)$$

$$\mu_1^2 = \frac{-2\lambda_1 k_1^4 - 4k_1^3 k_2 \lambda_4 - k_1^2 (\alpha_1 v_+^2 + 2\beta_2 v_{\times}^2) + 4k_1 k_2^3 \lambda_4 + k_2^2 (2\lambda_1 k_2^2 + \alpha_{13} v_+^2 + 2\beta_3 v_{\times}^2)}{2(k_2^2 - k_1^2)}, \quad (1.6.11)$$

$$\begin{aligned} \mu_2^2 &= \frac{1}{4(k_2^2 - k_1^2)} \left[ -2\lambda_4 k_1^4 - 4k_1^3 k_2 \lambda_{23} - k_1^2 (2\alpha_2 v_+^2 + \beta_1 v_{\times}^2) + 4k_1 k_2^3 \lambda_{23} \right. \\ &\quad \left. + k_2^2 (2\lambda_4 k_2^2 + 2\alpha_2 v_+^2 + \beta_1 v_{\times}^2) + k_1 k_2 (-\alpha_3 v_+^2 + 2v_{\times}^2 (\beta_2 - \beta_3)) \right], \end{aligned} \quad (1.6.12)$$

where  $\alpha_{13} = \alpha_1 + \alpha_3$ ,  $\lambda_{23}^{\pm} = 2\lambda_2 \pm \lambda_3$ ,  $\rho_{13}^{\pm} = 2\rho_1 \pm \rho_3$ ,  $v_+^2 = v_L^2 + v_R^2$ ,  $v_{\times}^2 = v_L v_R$ . From eqs. (1.6.9) and (1.6.10)

$$v_{\times}^2 = v_L v_R = \frac{\beta_2 k_1^2 + \beta_1 k_1 k_2 + \beta_3 k_2^2}{\rho_{13}^-}, \quad (1.6.13)$$

$$v_+^2 = v_L^2 + v_R^2 = \frac{1}{2\rho_1} (2\mu_3^2 - \alpha_1 k_1^2 - 4\alpha_2 k_1 k_2 - \alpha_{13} k_2^2). \quad (1.6.14)$$

Thus

$$v_R \pm v_L = \sqrt{v_+^2 \pm 2v_{\times}^2} = \sqrt{\frac{2\mu_3^2 - \alpha_1 k_1^2 - 4\alpha_2 k_1 k_2 - \alpha_{13} k_2^2}{2\rho_1} \pm \frac{2(\beta_2 k_1^2 + \beta_1 k_1 k_2 + \beta_3 k_2^2)}{\rho_{13}^-}} \quad (1.6.15)$$

from which we obtain simply  $v_L$  and  $v_R$  in terms of  $k_1$ ,  $k_2$  and the potential parameters.

After substitution from eqs. (1.6.13) and (1.6.14) into eq. (1.6.11), it can be written in the quartic form

$$a_0 k_1^4 + a_1 k_1^3 + a_2 k_1^2 + a_3 k_1 + a_4 = 0, \quad (1.6.16)$$

where  $a_i$ 's are all functions of the potential parameters in addition to  $k_2$ . This equations can be generally solved for  $k_1$  then to substituted for  $k_1$  into eq. (1.6.12) and then to solve for  $k_2$ .

There are four neutral scalar, four neutral pseudo scalar, four singly charged scalar and 2 doubly charged scalar Higgs fields in the theory. They mix appropriately with

unitary transformations to construct the physical Higgs spectrum of the LRSM (See. Appendix E).

### 1.6.1 Doubly-Charged Scalars

$$(D_i^{\pm\pm})^T = (\Delta_L^{\pm\pm} \ \Delta_R^{\pm\pm}), \quad (H_i^{\pm\pm})^T = (H_1^{\pm\pm} \ H_2^{\pm\pm}), \quad D_i^{\pm\pm} = (Z_D)_{ij} \ H_j^{\pm\pm}. \quad (1.6.17)$$

The doubly-charged Higgs mass matrix corresponds to the basis  $\begin{pmatrix} \Delta_L^{\pm\pm} & \Delta_R^{\pm\pm} \end{pmatrix}$ :

$$M^{\pm\pm} = \begin{pmatrix} M_{11}^{\pm\pm} & M_{12}^{\pm\pm} \\ . & M_{22}^{\pm\pm} \end{pmatrix}, \quad (1.6.18)$$

where

$$M_{11}^{\pm\pm} = \frac{1}{2} (4\rho_2 v_L^2 + (k_1^2 - k_2^2)\alpha_3 - v_R^2 \rho_{13}^-), \quad (1.6.19)$$

$$M_{12}^{\pm\pm} = \frac{1}{2} \left( -\frac{(\beta_2 k_1^2 + k_2 \beta_1 k_1 - v_\times^2 \rho_{13}^-) k_1^2}{k_2^2} + k_2 \beta_1 k_1 + k_2^2 \beta_2 + 4v_\times^2 \rho_4 \right), \quad (1.6.20)$$

$$M_{22}^{\pm\pm} = \frac{1}{2} (-\rho_{13}^- v_L^2 + (k_1^2 - k_2^2)\alpha_3 + 4v_R^2 \rho_2). \quad (1.6.21)$$

The doubly-charged Higgs boson masses are the solutions of the characteristic polynomial

$$P^{\pm\pm}(x) = x^2 - T^{\pm\pm}x + D^{\pm\pm}. \quad (1.6.22)$$

The mass squared eigenvalues are

$$m_{\pm\pm}^2 = \frac{1}{2} \left( T^{\pm\pm} \pm \sqrt{(T^{\pm\pm})^2 - 4D^{\pm\pm}} \right), \quad (1.6.23)$$

where

$$T^{\pm\pm} = \text{Tr}(M^{\pm\pm}) = M_{11}^{\pm\pm} + M_{22}^{\pm\pm}, \quad (1.6.24)$$

$$D^{\pm\pm} = \text{Det}(M^{\pm\pm}) = M_{11}^{\pm\pm} M_{22}^{\pm\pm} - (M_{12}^{\pm\pm})^2. \quad (1.6.25)$$

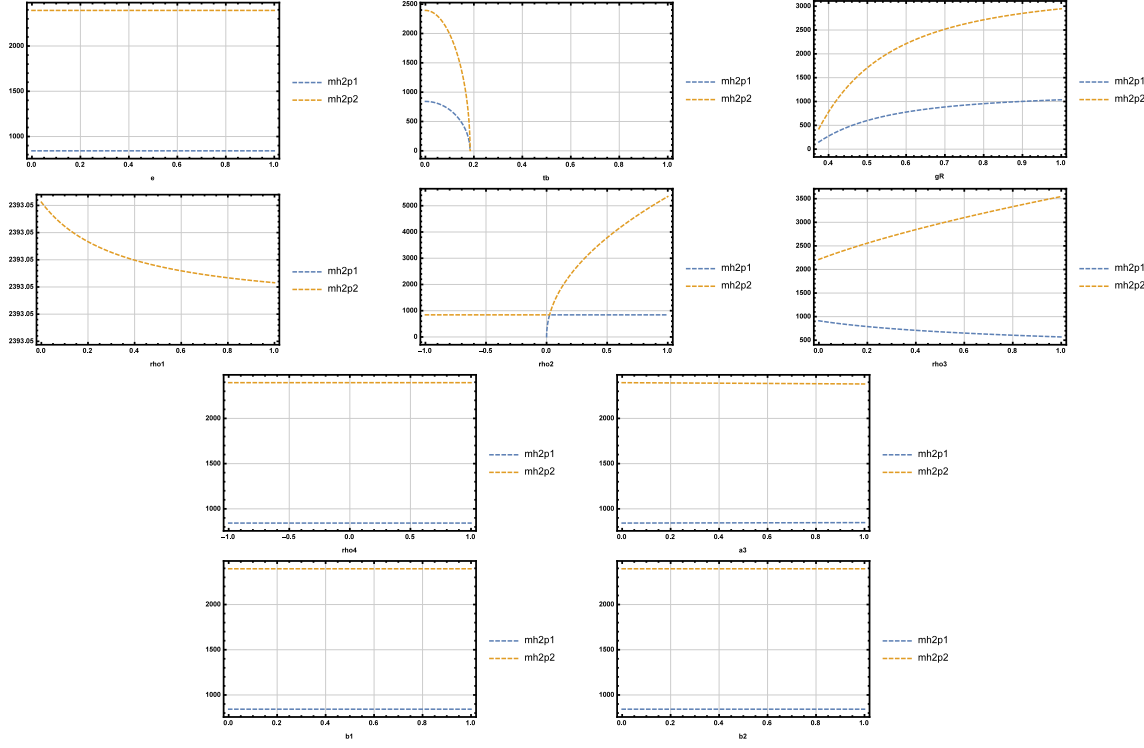


Figure 1.13:  $m_{\pm\pm}$  in the LRSM for the fixed benchmark point in Table 1.4.

Moreover, we have the following relations between eigenvalues

$$m_{2\pm\pm}^2 = T^{\pm\pm} - m_{1\pm\pm}^2 = \frac{D^{\pm\pm}}{m_{1\pm\pm}^2}. \quad (1.6.26)$$

For the rotation matrix, we define the function

$$f(x) = \frac{x - M_{22}^{\pm\pm}}{M_{12}^{\pm\pm}}. \quad (1.6.27)$$

The rotation matrix  $Z_D$  is

$$\begin{pmatrix} \frac{f_1}{\sqrt{1+f_1^2}} & -\frac{s_{12}}{\sqrt{1+f_1^2}} \\ \frac{1}{\sqrt{1+f_1^2}} & \frac{s_{12}f_1}{\sqrt{1+f_1^2}} \end{pmatrix}, \quad (1.6.28)$$

where  $s_{12} = \text{sign}(f_1 - f_2) = \text{sign}(f(m_{1\pm\pm}^2) - f(m_{2\pm\pm}^2)) = \text{sign}(M_{12}^{\pm\pm})$ .

We could equally well define the function

$$g(x) = \frac{M_{11}^{\pm\pm} - x}{M_{12}^{\pm\pm}}, \quad (1.6.29)$$

and use the equalities

$$f(m_{1\pm\pm}^2) = g(m_{2\pm\pm}^2), \quad f(m_{2\pm\pm}^2) = g(m_{1\pm\pm}^2). \quad (1.6.30)$$

See App. E.

### 1.6.2 Singly Charged Scalars

$$(C_i^\pm)^T = (\Phi_1^\pm \Phi_2^{\mp*} \Delta_L^\pm \Delta_R^\pm), \quad (H_i^\pm)^T = (H_1^\pm H_2^\pm G_1^\pm G_2^\pm), \quad C_i^\pm = (Z_C)_{ij} H_j^\pm. \quad (1.6.31)$$

The charged Higgs mass matrix corresponds to the basis  $\begin{pmatrix} \phi_1^\pm & \phi_2^\pm & \Delta_L^\pm & \Delta_R^\pm \end{pmatrix}$ :

$$M^\pm = \begin{pmatrix} M_{11}^\pm & M_{12}^\pm & M_{13}^\pm & M_{14}^\pm \\ . & M_{22}^\pm & M_{23}^\pm & M_{24}^\pm \\ . & . & M_{33}^\pm & M_{34}^\pm \\ . & . & . & M_{44}^\pm \end{pmatrix}, \quad (1.6.32)$$

where

$$M_{11}^\pm = \frac{k_2^2 \alpha_3 v_L^2 - 2k_1 k_2 v_\times^2 \beta_1 + ((v_R^2 \alpha_3 - 4v_\times^2 \beta_2) k_1^2 + 2v_\times^4 \rho_{13}^-)}{2(k_1^2 - k_2^2)}, \quad (1.6.33)$$

$$M_{12}^\pm = -\frac{2v_\times^2 \beta_2 k_1^3 + k_2 v_\times^2 \beta_1 k_1^2 - ((v_+^2 \alpha_3 - 2v_\times^2 \beta_2) k_2^2 + 2v_\times^4 \rho_{13}^-) k_1 + k_2^3 v_\times^2 \beta_1}{2k_2(k_1^2 - k_2^2)}, \quad (1.6.34)$$

$$M_{13}^\pm = \frac{v_L \alpha_3 k_2^2 - k_1 v_R \beta_1 k_2 + 2v_R (v_\times^2 \rho_{13}^- - k_1^2 \beta_2)}{2\sqrt{2} k_2}, \quad (1.6.35)$$

$$M_{14}^\pm = \frac{k_1 v_R \alpha_3 - k_2 v_L \beta_1 - 2k_1 v_L \beta_2}{2\sqrt{2}}, \quad (1.6.36)$$

$$M_{22}^\pm = \frac{v_L (v_L \alpha_3 - 4v_R \beta_2) k_1^2 - 2k_2 v_\times^2 \beta_1 k_1 + v_R^2 (\alpha_3 k_2^2 + 2v_L^2 \rho_{13}^-)}{2(k_1^2 - k_2^2)}, \quad (1.6.37)$$

$$M_{23}^{\pm} = \frac{k_1 v_L \alpha_3 - k_2 v_R \beta_1 - 2k_1 v_R \beta_2}{2\sqrt{2}}, \quad (1.6.38)$$

$$M_{24}^{\pm} = \frac{v_R \alpha_3 k_2^2 - k_1 v_L \beta_1 k_2 + 2v_L (v_{\times}^2 \rho_{13}^- - k_1^2 \beta_2)}{2\sqrt{2} k_2}, \quad (1.6.39)$$

$$M_{33}^{\pm} = \frac{1}{4} (-2\rho_{13}^- v_R^2 + (k_1^2 - k_2^2) \alpha_3), \quad (1.6.40)$$

$$M_{34}^{\pm} = \frac{-2\beta_2 k_1^3 + 2(\beta_2 k_2^2 + v_{\times}^2 \rho_{13}^-) k_1 + k_2^3 \beta_1 - k_1^2 k_2 \beta_1}{4k_2}, \quad (1.6.41)$$

$$M_{44}^{\pm} = \frac{1}{4} (-2\rho_{13}^- v_L^2 + (k_1^2 - k_2^2) \alpha_3). \quad (1.6.42)$$

The charged Higgs boson masses are the solutions of the characteristic polynomial

$$P^{\pm}(x) = x^4 - T^{\pm} x^3 + D_2^{\pm} x^2 - D_3^{\pm} x + D^{\pm} = x^2(x^2 - T^{\pm} x + D_2^{\pm}). \quad (1.6.43)$$

The mass squared eigenvalues are

$$m_{\pm}^2 = \frac{1}{2} \left( T^{\pm} \pm \sqrt{(T^{\pm})^2 - 4D_2^{\pm}} \right). \quad (1.6.44)$$

Moreover, we have the following relations between eigenvalues

$$m_{2\pm}^2 = T^{\pm} - m_{1\pm}^2. \quad (1.6.45)$$

This matrix can be diagonalized by the unitary transformation:

$$V^{\pm\dagger} M^{\pm} V^{\pm} = \text{diag} (m_{1\pm}^2, m_{2\pm}^2, 0, 0), \quad (1.6.46)$$

where

$$\begin{pmatrix} \phi_1^{\pm} \\ \phi_2^{\pm} \\ \Delta_L^{\pm} \\ \Delta_R^{\pm} \end{pmatrix} = \underbrace{\begin{pmatrix} Z_{11}^{\pm} & Z_{12}^{\pm} & Z_{13}^{\pm} & Z_{14}^{\pm} \\ Z_{21}^{\pm} & Z_{22}^{\pm} & Z_{23}^{\pm} & Z_{24}^{\pm} \\ Z_{31}^{\pm} & Z_{32}^{\pm} & Z_{33}^{\pm} & Z_{34}^{\pm} \\ Z_{41}^{\pm} & Z_{42}^{\pm} & Z_{43}^{\pm} & Z_{44}^{\pm} \end{pmatrix}}_{V^{\pm}} \begin{pmatrix} H_1^{\pm} \\ H_2^{\pm} \\ G_1^{\pm} \\ G_2^{\pm} \end{pmatrix}. \quad (1.6.47)$$

See App. E for explicit expressions for  $Z_{ij}^{\pm}$  and  $D_k^{\pm}$ .

## 1.6 Higgs Sector in the LRSM

---

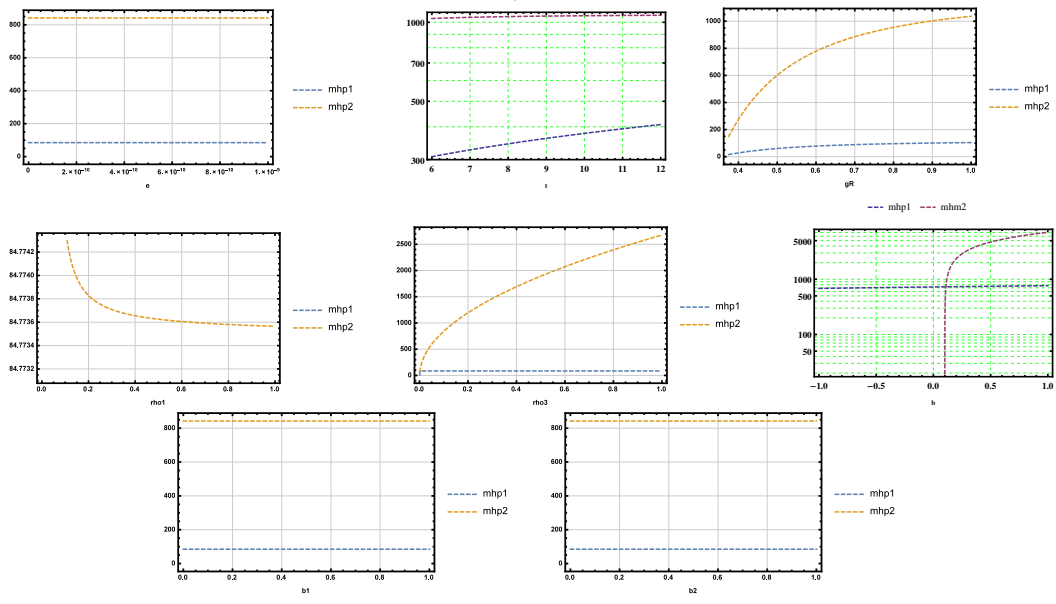


Figure 1.14:  $m_{\pm}$  in the LRSM for the fixed benchmark point in Table 1.4.

### 1.6.3 Neutral Pseudoscalars

$$(P_i^0)^T = (\varphi_1^0 \varphi_2^0 \varphi_L^0 \varphi_R^0), \quad (A_i^0)^T = (A_1^0 A_2^0 G_1^0 G_2^0), \quad P_i^0 = (Z_P)_{ij} A_j^0. \quad (1.6.48)$$

The pseudoscalar Higgs mass matrix corresponds to the basis  $\begin{pmatrix} \phi_1^{im} & \phi_2^{im} & \Delta_L^{im} & \Delta_R^{im} \end{pmatrix}$ :

$$M^P = \begin{pmatrix} M_{11}^P & M_{12}^P & M_{13}^P & M_{14}^P \\ \cdot & M_{22}^P & M_{23}^P & M_{24}^P \\ \cdot & \cdot & M_{33}^P & M_{34}^P \\ \cdot & \cdot & \cdot & M_{44}^P \end{pmatrix}, \quad (1.6.49)$$

where

$$M_{11}^P = \frac{4\lambda_{23}^- k_2^4 + (-4\lambda_{23}^- k_1^2 + v_+^2 \alpha_3 + 2v_\times^2 \beta_2) k_2^2 - 2k_1 v_\times^2 \beta_1 k_2 + 2v_\times^2 (v_\times^2 \rho_{13}^- - 3k_1^2 \beta_2)}{2(k_1^2 - k_2^2)}, \quad (1.6.50)$$

$$M_{12}^P = \frac{-2(2\lambda_{23}^- k_2^2 + v_\times^2 \beta_2) k_1^3 + (4\lambda_{23}^- k_2^4 + (v_+^2 \alpha_3 - 2v_\times^2 \beta_2) k_2^2 + 2v_\times^4 \rho_{13}^-) k_1 - 2k_2^3 v_\times^2 \beta_1}{2k_2(k_1^2 - k_2^2)}, \quad (1.6.51)$$

$$M_{13}^P = -\frac{1}{2} v_R (k_2 \beta_1 + 2k_1 \beta_2), \quad (1.6.52)$$

$$M_{14}^P = \frac{k_2 v_L \beta_1}{2} + k_1 v_L \beta_2, \quad (1.6.53)$$

$$M_{22}^P = \frac{1}{2k_2^2(k_1^2 - k_2^2)} \left[ 2(-2\lambda_{23}^- k_2^2 + v_\times^2 \beta_2) k_1^4 + 2k_2 v_\times^2 \beta_1 k_1^3 + (4\lambda_{23}^- k_2^2 + v_+^2 \alpha_3 - 6v_\times^2 \beta_2) k_1^2 k_2^2 - 2v_\times^4 \rho_{13}^- k_1^2 - 4k_2^3 v_\times^2 \beta_1 k_1 + 4k_2^2 v_\times^4 \rho_{13}^- \right], \quad (1.6.54)$$

$$M_{23}^P = -\frac{v_R (2\beta_2 k_1^2 + k_2 \beta_1 k_1 - 2v_\times^2 \rho_{13}^-)}{2k_2}, \quad (1.6.55)$$

$$M_{24}^P = \frac{v_L (2\beta_2 k_1^2 + k_2 \beta_1 k_1 - 2v_\times^2 \rho_{13}^-)}{2k_2}, \quad (1.6.56)$$

$$M_{33}^P = -\frac{1}{2} v_R^2 \rho_{13}^-, \quad (1.6.57)$$

$$M_{34}^P = \frac{1}{2} v_\times^2 \rho_{13}^-, \quad (1.6.58)$$

$$M_{44}^P = -\frac{1}{2} v_L^2 \rho_{13}^-. \quad (1.6.59)$$

The pseudoscalar Higgs boson masses are the solutions of the characteristic polynomial

$$P^P(x) = x^4 - T^P x^3 + D_2^P x^2 - D_3^P x + D^P = x^2(x^2 - T^P x + D_2^P). \quad (1.6.60)$$

The mass squared eigenvalues are

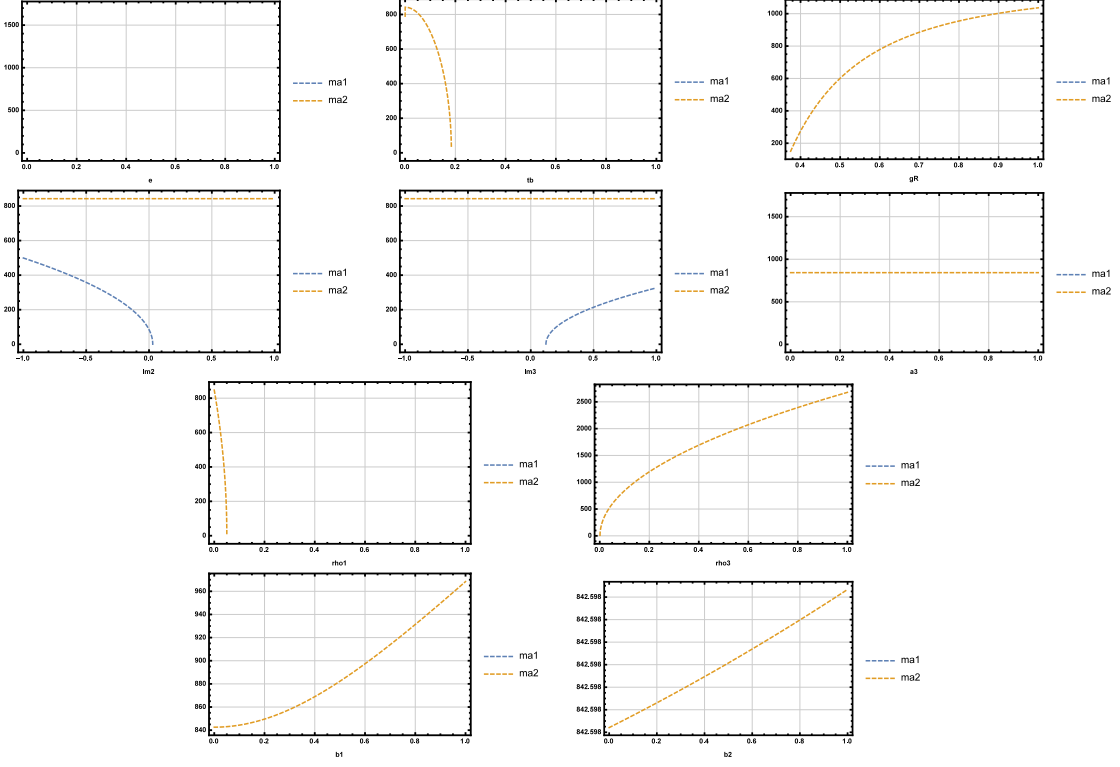
$$m_A^2 = \frac{1}{2} \left( T^P \pm \sqrt{(T^P)^2 - 4D_2^P} \right). \quad (1.6.61)$$

Moreover, we have the following relations between eigenvalues

$$m_{2A}^2 = T^P - m_{1A}^2. \quad (1.6.62)$$

The mass matrix can be diagonalized by the unitary transformation:

$$V^{P\dagger} M^P V^P = \text{diag}(m_{A1}^2, m_{A2}^2, 0, 0), \quad (1.6.63)$$


 Figure 1.15:  $m_{A1,2}$  in the LRSM for the fixed benchmark point in Table 1.4.

where

$$\begin{pmatrix} \phi_1^{\text{im}} \\ \phi_2^{\text{im}} \\ \Delta_L^{\text{im}} \\ \Delta_R^{\text{im}} \end{pmatrix} = \underbrace{\begin{pmatrix} Z_{11}^P & Z_{12}^P & Z_{13}^P & Z_{14}^P \\ Z_{21}^P & Z_{22}^P & Z_{23}^P & Z_{24}^P \\ Z_{31}^P & Z_{32}^P & Z_{33}^P & Z_{34}^P \\ Z_{41}^P & Z_{42}^P & Z_{43}^P & Z_{44}^P \end{pmatrix}}_{V^P} \begin{pmatrix} A_1 \\ A_2 \\ G_1^0 \\ G_2^0 \end{pmatrix}. \quad (1.6.64)$$

See App. E for explicit expressions for  $Z_{ij}^P$  and  $D_k^P$ .

#### 1.6.4 Neutral Scalars

$$(S_i^0)^T = (h_1^0 \ h_2^0 \ h_L^0 \ h_R^0), \quad (H_i^0)^T = (H_1^0 \ H_2^0 \ H_3^0 \ H_4^0), \quad S_i^0 = (Z_S)_{ij} \ H_j^0. \quad (1.6.65)$$

The neutral scalar Higgs mass matrix

$$M^H = \begin{pmatrix} m_{11} & m_{12} & m_{13} & m_{14} \\ . & m_{22} & m_{23} & m_{24} \\ . & . & m_{33} & m_{34} \\ . & . & . & m_{44} \end{pmatrix}, \quad (1.6.66)$$

where

$$\begin{aligned} m_{11} = & \frac{1}{2(k_1^2 - k_2^2)} \left[ 4\lambda_1 k_1^4 - 2v_{\times}^2 \beta_2 k_1^2 - 8k_2^3 \lambda_4 k_1 - 4k_2^4 \lambda_{23}^+ + k_2^2 (4(-\lambda_1 + \lambda_{23}^+) k_1^2 + v_+^2 \alpha_3 - 2v_{\times}^2 \beta_2) \right. \\ & \left. + k_2 (8k_1^3 \lambda_4 - 2k_1 v_{\times}^2 \beta_1) + 2v_{\times}^4 \rho_{13}^- \right], \end{aligned} \quad (1.6.67)$$

$$\begin{aligned} m_{12} = & \frac{1}{2k_2(k_1^2 - k_2^2)} \left[ -4\lambda_4 k_2^5 + 2k_1^2 v_{\times}^2 \beta_1 k_2 + 4k_1^4 \lambda_4 k_2 + 2k_1^3 (2(\lambda_1 + \lambda_{23}^+) k_2^2 + v_{\times}^2 \beta_2) \right. \\ & \left. - k_1 (4(\lambda_1 + \lambda_{23}^+) k_2^4 + (v_+^2 \alpha_3 - 2v_{\times}^2 \beta_2) k_2^2 + 2v_{\times}^4 \rho_{13}^-) \right], \end{aligned} \quad (1.6.68)$$

$$m_{13} = k_1 v_L \alpha_1 + 2k_2 v_L \alpha_2 + \frac{k_2 v_R \beta_1}{2} + k_1 v_R \beta_2, \quad (1.6.69)$$

$$m_{14} = k_1 v_R \alpha_1 + 2k_2 v_R \alpha_2 + \frac{k_2 v_L \beta_1}{2} + k_1 v_L \beta_2, \quad (1.6.70)$$

$$\begin{aligned} m_{22} = & \frac{1}{2k_2^2(k_1^2 + k_2^2)} \left[ 4\lambda_1 k_2^6 + 8k_1 \lambda_4 k_2^5 + 2k_1^4 (v_{\times}^2 \beta_2 - 2k_2^2 \lambda_{23}^+) + k_1^3 (2k_2 v_{\times}^2 \beta_1 - 8k_2^3 \lambda_4) \right. \\ & \left. - k_1^2 (4(\lambda_1 - 2\lambda_2 - \lambda_3) k_2^4 + (v_+^2 \alpha_3 - 2v_{\times}^2 \beta_2) k_2^2 + 2v_{\times}^4 \rho_{13}^-) \right], \end{aligned} \quad (1.6.71)$$

$$m_{23} = \left( 2v_L \alpha_2 - \frac{v_R \beta_1}{2} \right) k_1 + k_2 v_L \alpha_{13} + \frac{v_R (v_{\times}^2 \rho_{13}^- - k_1^2 \beta_2)}{k_2}, \quad (1.6.72)$$

$$m_{24} = \left( 2v_R \alpha_2 - \frac{v_L \beta_1}{2} \right) k_1 + k_2 v_R \alpha_{13} + \frac{v_L (v_{\times}^2 \rho_{13}^- - k_1^2 \beta_2)}{k_2}, \quad (1.6.73)$$

$$m_{33} = 2\rho_1 v_L^2 - \frac{1}{2} v_R^2 \rho_{13}^-, \quad (1.6.74)$$

$$m_{34} = \frac{1}{2} v_{\times}^2 \rho_{13}^+, \quad (1.6.75)$$

$$m_{44} = -\frac{1}{2} \rho_{13}^- v_L^2 + 2v_R^2 \rho_1. \quad (1.6.76)$$

The mass squared eigenvalues are the roots of the characteristic polynomial

$$P(x) = x^4 - Tx^3 + D_2 x^2 - D_3 x + D. \quad (1.6.77)$$

The Higgs mass squared eigenvalues are [37, 38, 50, 73, 82]

$$m^2 = \frac{T}{4} - S \mp \frac{1}{2} \sqrt{-2p + \frac{q}{S} - 4S^2}, \quad \frac{T}{4} + S \mp \frac{1}{2} \sqrt{-2p - \frac{q}{S} - 4S^2}, \quad (1.6.78)$$

where

$$p = \frac{1}{8} (8D_2 - 3T^2), \quad (1.6.79)$$

$$q = \frac{1}{8} (-T^3 + 4TD_2 - 8D_3), \quad (1.6.80)$$

$$S = \frac{1}{2} \sqrt{\frac{1}{3} \left( \frac{\Delta_0}{Q} + Q \right) - \frac{2p}{3}}, \quad (1.6.81)$$

$$Q = \sqrt[3]{\frac{1}{2} \left( \sqrt{\Delta_1^2 - 4\Delta_0^3} + \Delta_1 \right)}, \quad (1.6.82)$$

$$\Delta_0 = -3TD_3 + D_2^2 + 12D, \quad (1.6.83)$$

$$\Delta_1 = 27T^2D - 9TD_2D_3 + 2D_2^3 - 72D_2D + 27D_3^2. \quad (1.6.84)$$

Moreover, we have the following relations between eigenvalues

$$m_{3,4}^2 = \frac{1}{2} \left( T - m_1^2 - m_2^2 \pm \sqrt{(T - m_1^2 - m_2^2)^2 - \frac{4D}{m_1^2 m_2^2}} \right), \quad (1.6.85)$$

and

$$m_4^2 = T - m_1^2 - m_2^2 - m_3^2 = \frac{D}{m_1^2 m_2^2 m_3^2}. \quad (1.6.86)$$

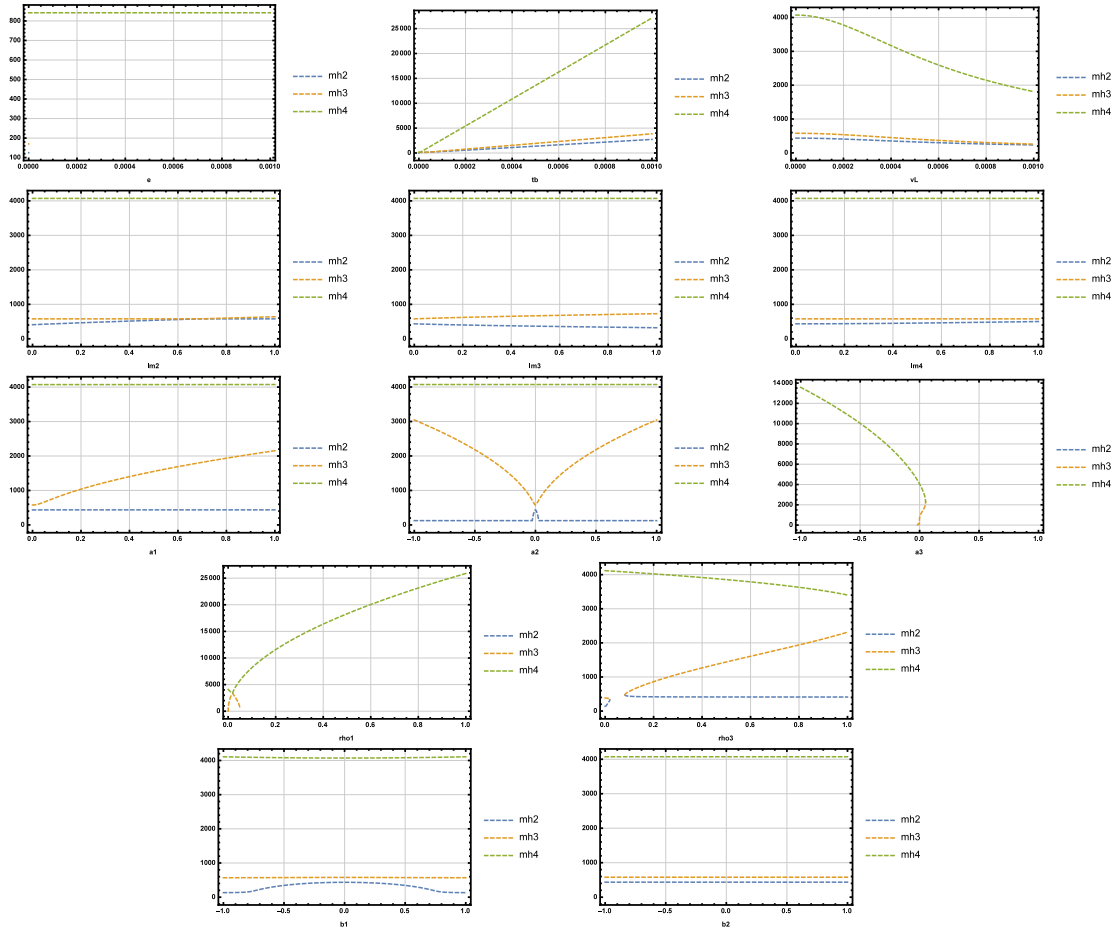


Figure 1.16:  $m_{h_i}$  in the LRSM for the fixed benchmark point in Table 1.4.

## 1.6 Higgs Sector in the LRSM

---

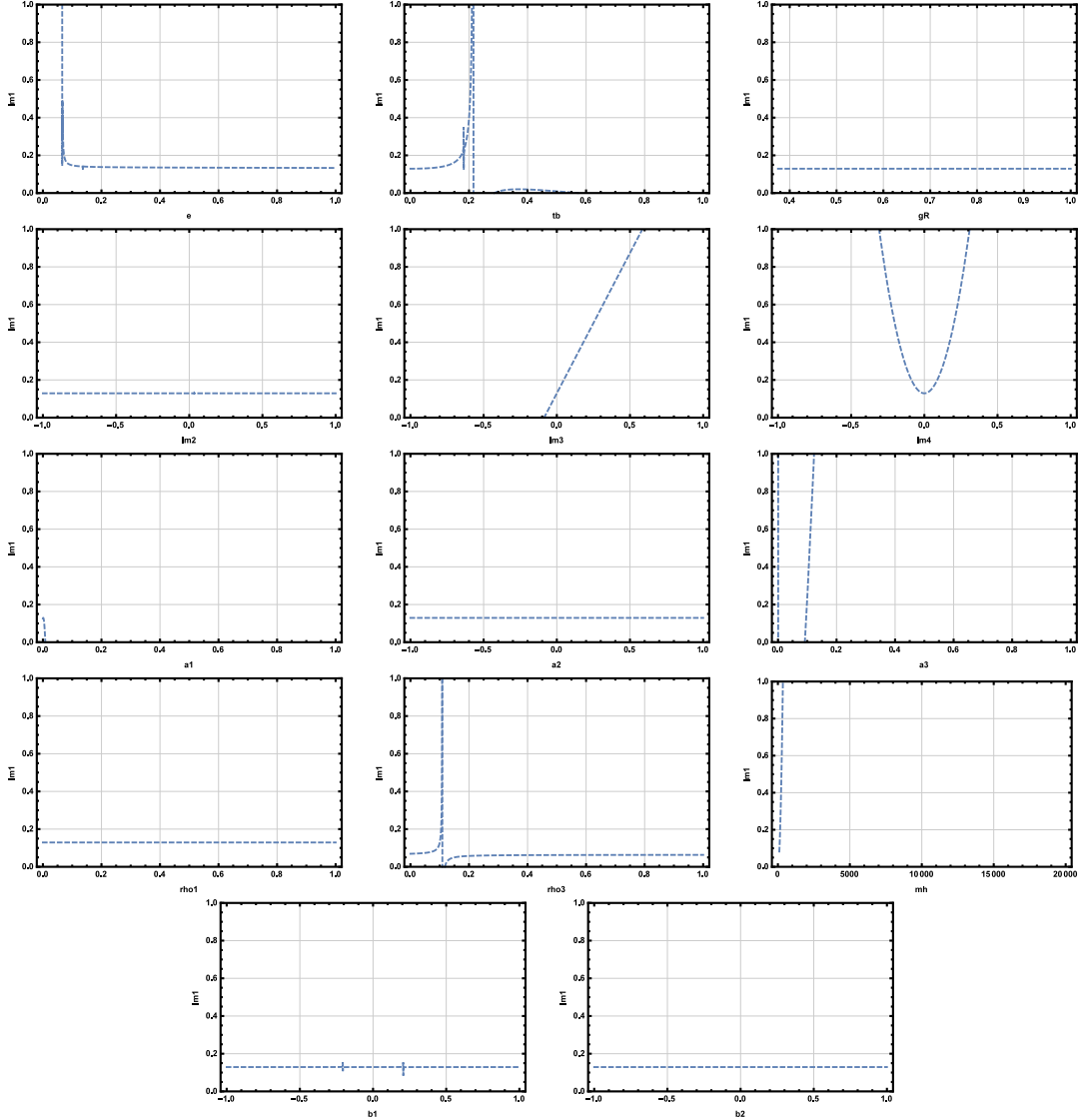


Figure 1.17:  $\lambda_1$  in the LRSM for the fixed benchmark point in Table 1.4.

The Higgs matrix (1.6.66) can be diagonalized by the unitary transformation:

$$V^\dagger M^H V = \text{diag} (m_1^2, m_2^2, m_3^2, m_4^2), \quad (1.6.87)$$

where

$$\begin{pmatrix} \phi_1^r \\ \phi_2^r \\ \Delta_L^r \\ \Delta_R^r \end{pmatrix} = \underbrace{\begin{pmatrix} Z_{11} & Z_{12} & Z_{13} & Z_{14} \\ Z_{21} & Z_{22} & Z_{23} & Z_{24} \\ Z_{31} & Z_{32} & Z_{33} & Z_{34} \\ Z_{41} & Z_{42} & Z_{43} & Z_{44} \end{pmatrix}}_V \begin{pmatrix} H_1 \\ H_2 \\ H_3 \\ H_4 \end{pmatrix}. \quad (1.6.88)$$

The characteristic polynomial (1.6.77) can be solved to give

$$\lambda_1 = -\frac{m_h^8 - T^{(0)}m_h^6 + D_2^{(0)}m_h^4 - D_3^{(0)}m_h^2 + D^{(0)}}{-T^{(1)}m_h^6 + D_2^{(1)}m_h^4 - D_3^{(1)}m_h^2 + D^{(1)}} \quad (1.6.89)$$

See App. E for explicit expressions for  $Z_{ij}$  and  $D_k$ .

### 1.6.5 Higgs Numerical Session in the LRSM

Table 1.4 gives A LRSM benchmark point for scalar potential parameters.

Table 1.5 gives A LRSM benchmark point for Higgs spectra.

Table 1.7 gives A LRSM benchmark point for scalar and Pseudoscalar Higgs mixing.

Table 1.8 gives A LRSM benchmark point for doubly and singly charged Higgs mixing.

Potential Parameters and VEVs	Domain	Value
$\mu_1^2$	$\mu_1^2 > 0$	7812.51
$\mu_2^2$	$\mu_2^2 > 0$	45.512
$\mu_3^2$	$\mu_3^2 > 0$	167478.
$\varepsilon = \sqrt{k_1^2 + k_2^2} - v$	$\sim 0$	$10^{-9}$
$v$	$SM \sim \mathcal{O}(100) \text{ GeV}$	246
$t_\beta = \frac{k_1}{k_2}$	$\sim 0$	$1.5 \times 10^{-4}$
$k_1$	$k_1 > 0$	0.0369
$k_2$	$k_2 > 0$	245.99
$v_L$	$v_L > 0$	0.00234621
$v_R$	$v_R > 0$	3787.19
$\lambda_1$	$0 \leq \lambda_1 \leq 1$	0.129098
$\lambda_2$	$-1 \leq \lambda_2 \leq 1$	0.09
$\lambda_3$	$-1 \leq \lambda_3 \leq 1$	0.3
$\lambda_4$	$-1 \leq \lambda_4 \leq 1$	0.001
$\rho_1$	$0 \leq \rho_1 \leq 1$	0.0005
$\rho_2$	$-1 \leq \rho_2 \leq 1$	0.2
$\rho_3$	$0 \leq \rho_3 \leq 1$	0.1
$\rho_4$	$-1 \leq \rho_4 \leq 1$	0.4
$\alpha_1$	$0 \leq \alpha_1 \leq 1$	0.001
$\alpha_2$	$ \alpha_2  \leq 1$	$-10^{-8}$
$\alpha_3$	$0 \leq \alpha_3 \leq 1$	-0.001
$\beta_1$	$-1 \leq \beta_1 \leq 1$	0.001
$\beta_2$	$-1 \leq \beta_2 \leq 1$	0.01
$\beta_3$	$-1 \leq \beta_3 \leq 1$	-0.0000704455

Table 1.4: A LRSM benchmark point. Scalar potential parameters.

Spectrum	Domain	Value	Spectrum	Domain	Value
$m_h$	$\sim \mathcal{O}(100)$ GeV	125.	$m_{1\pm}$	$\sim \mathcal{O}(100)$ GeV	84.7726
$m_{h_2}$	$\sim \mathcal{O}(100)$ GeV	119.762	$m_{2\pm}$	$\sim \mathcal{O}(1)$ TeV	842.607
$m_{h_3}$	$\sim \mathcal{O}(100)$ GeV	255.474	$m_{1\pm\pm}$	$\sim \mathcal{O}(1)$ TeV	842.616
$m_{h_4}$	$\sim \mathcal{O}(1)$ TeV	842.598	$m_{2\pm\pm}$	$\sim \mathcal{O}(10)$ TeV	2395.24
$m_{A_1}$	$\sim \mathcal{O}(100)$ GeV	147.292	$m_{A_2}$	$\sim \mathcal{O}(1)$ TeV	842.598

Table 1.5: A LRSM benchmark point. Higgs spectra.

Fig. 1.13 exhibits the dependence

$$m_{1,2\pm\pm}(\varepsilon, t_\beta, g_R, \rho_1, \rho_2, \rho_3, \rho_4, \alpha_3, \beta_1, \beta_2), \quad (1.6.90)$$

Fig. 1.14 exhibits the dependence

$$m_{1,2\pm}(\varepsilon, t_\beta, g_R, \rho_1, \rho_3, \alpha_3, \beta_1, \beta_2), \quad (1.6.91)$$

Fig. 1.15 exhibits the dependence

$$m_{1,2A}(\varepsilon, t_\beta, g_R, \lambda_2, \lambda_3, \rho_1, \rho_3, \alpha_3, \beta_1, \beta_2), \quad (1.6.92)$$

Fig. 1.16 exhibits the dependence

$$m_{h_i}(\varepsilon, t_\beta, g_R, \lambda_2, \lambda_3, \lambda_4, \rho_1, \rho_3, \alpha_1, \alpha_2, \alpha_3, \beta_1, \beta_2, m_h = 125.), \quad (1.6.93)$$

Fig. 1.17 exhibits the dependence

$$\lambda_1(\varepsilon, t_\beta, g_R, \lambda_2, \lambda_3, \lambda_4, \rho_1, \rho_3, \alpha_1, \alpha_2, \alpha_3, \beta_1, \beta_2, m_h = 125.). \quad (1.6.94)$$

Finally, table 1.6 recaps the Higgs parameter dependence of eqs. (1.6.90-1.6.94).

## 1.6 Higgs Sector in the LRSM

---

Par Mass \	$\varepsilon, t_\beta, g_R$	$\lambda_1$	$\lambda_2$	$\lambda_3$	$\lambda_4$	$\rho_1$	$\rho_2$	$\rho_3$	$\rho_4$	$\alpha_1$	$\alpha_2$	$\alpha_3$	$\beta_1$	$\beta_2$
$m_{1,2\pm\pm}$	✓	✗	✗	✗	✗	✓	✓	✓	✓	✗	✗	✓	✓	✓
$m_{1,2\pm}$	✓	✗	✗	✗	✗	✓	✗	✓	✗	✗	✗	✓	✓	✓
$m_{1,2A}$	✓	✗	✓	✓	✗	✓	✗	✓	✗	✗	✗	✓	✓	✓
$m_{h_i}$	✓	✓	✓	✓	✓	✓	✗	✓	✗	✓	✓	✓	✓	✓

Table 1.6: Higgs parameter dependence.

Higgs Mixing	Value	Higgs Mixing	Value
$Z_{11}^P$	-0.00067883	$Z_{11}$	0.000724704
$Z_{12}^P$	0.9999997583	$Z_{12}$	0.9999999999919308
$Z_{13}^P$	-0.00015	$Z_{13}$	-0.00263936
$Z_{14}^P$	$4.76146 \times 10^{-23}$	$Z_{14}$	$-2.37875 \times 10^{-6}$
$Z_{21}^P$	-0.0000192031	$Z_{21}$	-0.0000194953
$Z_{22}^P$	0.000149987	$Z_{22}$	0.00263938
$Z_{23}^P$	0.9999999886	$Z_{23}$	0.999997
$Z_{24}^P$	$1.89524 \times 10^{-20}$	$Z_{24}$	$2.44987 \times 10^{-7}$
$Z_{31}^P$	0.9999997694	$Z_{31}$	0.9999997372
$Z_{32}^P$	0.000678833	$Z_{32}$	-0.00072465
$Z_{33}^P$	0.0000191013	$Z_{33}$	0.000021408
$Z_{34}^P$	$6.20369 \times 10^{-7}$	$Z_{34}$	$-6.44349 \times 10^{-7}$
$Z_{41}^P$	$-6.20369 \times 10^{-7}$	$Z_{41}$	$6.46077 \times 10^{-7}$
$Z_{42}^P$	$-4.21127 \times 10^{-10}$	$Z_{42}$	$2.37762 \times 10^{-6}$
$Z_{43}^P$	$-1.18499 \times 10^{-11}$	$Z_{43}$	$-2.51251 \times 10^{-7}$
$Z_{44}^P$	0.9999999999	$Z_{44}$	0.9999999999

Table 1.7: A LRSM benchmark point. Scalar and Pseudoscalar Higgs mixing.

Higgs Mixing	Value	Higgs Mixing	Value
$Z_{11}^\pm$	-0.0000135772	$Z_{12}^\pm$	0.000149836
$Z_{13}^\pm$	0.9999999525	$Z_{14}^\pm$	0.00026895
$Z_{21}^\pm$	-0.000470086	$Z_{22}^\pm$	0.998947
$Z_{23}^\pm$	-0.000162024	$Z_{24}^\pm$	0.0458822
$Z_{31}^\pm$	0.9999998892	$Z_{32}^\pm$	0.000470583
$Z_{33}^\pm$	0.0000135067	$Z_{34}^\pm$	$3.72557 \times 10^{-9}$
$Z_{41}^\pm$	0.0000215912	$Z_{42}^\pm$	-0.0458823
$Z_{43}^\pm$	-0.000261792	$Z_{44}^\pm$	0.998947
$Z_{11}^{\pm\pm}$	0.0000616058	$Z_{12}^{\pm\pm}$	0.9999999981
$Z_{21}^{\pm\pm}$	0.9999999981	$Z_{22}^{\pm\pm}$	-0.0000616058

Table 1.8: A LRSM benchmark point. Doubly and Singly charged Higgs mixing.

### 1.6.6 Higgs Interactions in the LRSM

#### Higgs-Gauge Boson Interactions in the LRSM

The kinetic Lagrangian (1.3.28) of the Higgs fields contains the interaction terms of the Higgs fields and gauge bosons. In terms of the physical gauge bosons, the covariant derivatives (1.3.25) and (1.3.26) of the Higgs multiplets  $\Phi$ ,  $\Delta_L$  and  $\Delta_R$  are

$$D_\mu \Phi = \partial_\mu \Phi - ig_L (W_{L\mu} \cdot T_L) \Phi + ig_R \Phi (W_{R\mu} \cdot T_R)$$

$$= \begin{pmatrix} \partial_\mu \Phi_1^0 & \partial_\mu \Phi_1^+ \\ \partial_\mu \Phi_2^- & \partial_\mu \Phi_2^0 \end{pmatrix} - i \begin{pmatrix} \frac{g_L}{\sqrt{2}} W_{L\mu}^+ \Phi_2^- - \frac{g_R}{\sqrt{2}} W_{R\mu}^- \Phi_1^+ & \frac{g_L}{\sqrt{2}} W_{L\mu}^+ \Phi_2^0 - \frac{g_R}{\sqrt{2}} W_{R\mu}^+ \Phi_1^0 \\ \frac{g_L}{\sqrt{2}} W_{L\mu}^- \Phi_1^0 - \frac{g_R}{\sqrt{2}} W_{R\mu}^- \Phi_2^0 & \frac{g_L}{\sqrt{2}} W_{L\mu}^- \Phi_1^+ - \frac{g_R}{\sqrt{2}} W_{R\mu}^+ \Phi_2^- \end{pmatrix}$$

$$-i \begin{pmatrix} \frac{1}{2}(\frac{g_L}{\cos \theta_W} Z_{L\mu} - \frac{g_Y}{\tan \varphi} Z_{R\mu}) \Phi_1^0 & (eA_\mu + \frac{g_L \cos 2\theta_W}{2 \cos \theta_W} Z_{L\mu} + \frac{g_Y}{2 \tan \varphi} Z_{R\mu}) \Phi_1^+ \\ -(eA_\mu + \frac{g_L \cos 2\theta_W}{2 \cos \theta_W} Z_{L\mu} + \frac{g_Y}{2 \tan \varphi} Z_{R\mu}) \Phi_2^- & -\frac{1}{2}(\frac{g_L}{\cos \theta_W} Z_{L\mu} - \frac{g_Y}{\tan \varphi} Z_{R\mu}) \Phi_2^0 \end{pmatrix} \quad (1.6.95)$$

$$\begin{aligned} D_\mu \Delta_L &= \partial_\mu \Delta_L - ig_L [W_{L\mu} \cdot T_L, \Delta_L] - ig_{BL} V_\mu \Delta_L \\ &= \begin{pmatrix} \frac{\partial_\mu \Delta_L^+}{\sqrt{2}} & \partial_\mu \Delta_L^{++} \\ \partial_\mu \Delta_L^0 & -\frac{\partial_\mu \Delta_L^+}{\sqrt{2}} \end{pmatrix} - i \frac{g_L}{\sqrt{2}} \begin{pmatrix} W_{L\mu}^+ \Delta_L^0 - W_{L\mu}^- \Delta_L^{++} & -\sqrt{2} W_{L\mu}^+ \Delta_L^+ \\ \sqrt{2} W_{L\mu}^- \Delta_L^+ & W_{L\mu}^- \Delta_L^{++} - W_{L\mu}^+ \Delta_L^0 \end{pmatrix} \\ &\quad - i \begin{pmatrix} (eA_\mu - e \tan \theta_W Z_{L\mu} - g_Y \tan \varphi Z_{R\mu}) \frac{\Delta_L^+}{\sqrt{2}} & (2eA_\mu + \frac{g_L \cos 2\theta_W}{\cos \theta_W} Z_{L\mu} - g_Y \tan \varphi Z_{R\mu}) \Delta_L^{++} \\ -(\frac{g_L}{\cos \theta_W} Z_{L\mu} + g_Y \tan \varphi Z_{R\mu}) \Delta_L^0 & -(eA_\mu - e \tan \theta_W Z_{L\mu} - g_Y \tan \varphi Z_{R\mu}) \frac{\Delta_L^+}{\sqrt{2}} \end{pmatrix} \end{aligned} \quad (1.6.96)$$

$$\begin{aligned} D_\mu \Delta_R &= \partial_\mu \Delta_R - ig_R [W_{R\mu} \cdot T_R, \Delta_R] - ig_{BL} V_\mu \Delta_R \\ &= \begin{pmatrix} \frac{\partial_\mu \Delta_R^+}{\sqrt{2}} & \partial_\mu \Delta_R^{++} \\ \partial_\mu \Delta_R^0 & -\frac{\partial_\mu \Delta_R^+}{\sqrt{2}} \end{pmatrix} - i \frac{g_R}{\sqrt{2}} \begin{pmatrix} W_{R\mu}^+ \Delta_R^0 - W_{R\mu}^- \Delta_R^{++} & -\sqrt{2} W_{R\mu}^+ \Delta_R^+ \\ \sqrt{2} W_{R\mu}^- \Delta_R^+ & W_{R\mu}^- \Delta_R^{++} - W_{R\mu}^+ \Delta_R^0 \end{pmatrix} \\ &\quad - i \begin{pmatrix} (eA_\mu - e \tan \theta_W Z_{L\mu} - g_Y \tan \varphi Z_{R\mu}) \frac{\Delta_R^+}{\sqrt{2}} & (2eA_\mu - 2e \tan \theta_W Z_{L\mu} + \frac{2g_Y}{\tan 2\varphi} Z_{R\mu}) \Delta_R^{++} \\ -\frac{2g_Y}{\sin 2\varphi} Z_{R\mu} \Delta_R^0 & -(eA_\mu - e \tan \theta_W Z_{L\mu} - g_Y \tan \varphi Z_{R\mu}) \frac{\Delta_R^+}{\sqrt{2}} \end{pmatrix}. \end{aligned} \quad (1.6.97)$$

The kinetic terms are then

$$\begin{aligned} \text{Tr}[|D_\mu \Phi|^2] &= \left| \partial_\mu \Phi_1^0 - i(\frac{g_L}{\sqrt{2}} W_{L\mu}^+ \Phi_2^- - \frac{g_R}{\sqrt{2}} W_{R\mu}^- \Phi_1^+ + \frac{1}{2}(\frac{g_L}{\cos \theta_W} Z_{L\mu} - \frac{g_Y}{\tan \varphi} Z_{R\mu}) \Phi_1^0) \right|^2 \\ &\quad + \left| \partial_\mu \Phi_1^+ - i(\frac{g_L}{\sqrt{2}} W_{L\mu}^+ \Phi_2^0 - \frac{g_R}{\sqrt{2}} W_{R\mu}^+ \Phi_1^0 + (eA_\mu + \frac{g_L \cos 2\theta_W}{2 \cos \theta_W} Z_{L\mu} + \frac{g_Y}{2 \tan \varphi} Z_{R\mu}) \Phi_1^+) \right|^2 \\ &\quad + \left| \partial_\mu \Phi_2^- - i(\frac{g_L}{\sqrt{2}} W_{L\mu}^- \Phi_1^0 - \frac{g_R}{\sqrt{2}} W_{R\mu}^- \Phi_2^0 - (eA_\mu + \frac{g_L \cos 2\theta_W}{2 \cos \theta_W} Z_{L\mu} + \frac{g_Y}{2 \tan \varphi} Z_{R\mu}) \Phi_2^-) \right|^2 \end{aligned}$$

$$+ \left| \partial_\mu \Phi_2^0 - i \left( \frac{g_L}{\sqrt{2}} W_{L\mu}^- \Phi_1^+ - \frac{g_R}{\sqrt{2}} W_{R\mu}^+ \Phi_2^- - \frac{1}{2} \left( \frac{g_L}{\cos \theta_W} Z_{L\mu} - \frac{g_Y}{\tan \varphi} Z_{R\mu} \right) \Phi_2^0 \right) \right|^2 \quad (1.6.98)$$

$$\begin{aligned} \text{Tr}[|D_\mu \Delta_L|^2] &= \left| \partial_\mu \Delta_L^+ - i(g_L (W_{L\mu}^+ \Delta_L^0 - W_{L\mu}^- \Delta_L^{++}) + (eA_\mu - e \tan \theta_W Z_{L\mu} - g_Y \tan \varphi Z_{R\mu}) \Delta_L^+) \right|^2 \\ &\quad + \left| \partial_\mu \Delta_L^{++} - i(-g_L \sqrt{2} W_{L\mu}^+ \Delta_L^+ + (2eA_\mu + \frac{g_L \cos 2\theta_W}{\cos \theta_W} Z_{L\mu} - g_Y \tan \varphi Z_{R\mu}) \Delta_L^{++}) \right|^2 \\ &\quad + \left| \partial_\mu \Delta_L^0 - i(g_L W_{L\mu}^- \Delta_L^+ - (\frac{g_L}{\cos \theta_W} Z_{L\mu} + g_Y \tan \varphi Z_{R\mu}) \Delta_L^0) \right|^2 \end{aligned} \quad (1.6.99)$$

$$\begin{aligned} \text{Tr}[|D_\mu \Delta_R|^2] &= \left| \partial_\mu \Delta_R^+ - i(g_R (W_{R\mu}^+ \Delta_R^0 - W_{R\mu}^- \Delta_R^{++}) + (eA_\mu - e \tan \theta_W Z_{R\mu} - g_Y \tan \varphi Z_{R\mu}) \Delta_R^+) \right|^2 \\ &\quad + \left| \partial_\mu \Delta_R^{++} - i(-g_R \sqrt{2} W_{R\mu}^+ \Delta_R^+ + (2eA_\mu - 2e \tan \theta_W Z_{L\mu} + \frac{2g_Y}{\tan 2\varphi} Z_{R\mu}) \Delta_R^{++}) \right|^2 \\ &\quad + \left| \partial_\mu \Delta_R^0 - i(g_R W_{R\mu}^- \Delta_R^+ - \frac{2g_Y}{\sin 2\varphi} Z_{R\mu} \Delta_R^0) \right|^2. \end{aligned} \quad (1.6.100)$$

Now, the Higgs-gauge bosons interactions can be extracted by substituting from Eqs. (1.6.17), (1.6.31), (1.6.48) and (1.6.65) for the physical Higgs fields in the above set of equations.

### Higgs-Fermion Interactions and Tree-level Flavor-Changing Neutral Currents in the LRSM

For  $k_1 \neq k_2$ , we can invert the first two equations of Eqs. (1.4.84) to solve for  $y^Q$  and  $\tilde{y}^Q$  in terms of the physical masses of the up and down quarks, after substitution from Eqs. (1.4.81):

$$y^Q = \frac{\sqrt{2}}{k_1^2 - k_2^2} (k_1 V_L^u M_u^{\text{diag}} V_R^{u\dagger} - k_2 V_L^d M_d^{\text{diag}} V_R^{d\dagger}) \quad (1.6.101)$$

$$\tilde{y}^Q = \frac{\sqrt{2}}{k_1^2 - k_2^2} (-k_2 V_L^u M_u^{\text{diag}} V_R^{u\dagger} + k_1 V_L^d M_d^{\text{diag}} V_R^{d\dagger}) \quad (1.6.102)$$

From Eqs. (1.4.84), the transformations to the physical quarks are

$$u_{L,R} \rightarrow V_{L,R}^u u_{L,R}, \quad d_{L,R} \rightarrow V_{L,R}^d d_{L,R} \quad (1.6.103)$$

The Yukawa Lagrangian (1.3.33) contains the following terms

$$\overline{Q}_L (y^Q \Phi + \tilde{y}^Q \tilde{\Phi}) Q_R + h.c. \supset \overline{u}_L (y^Q \Phi_1^0 + \tilde{y}^Q \Phi_2^{0*}) u_R + \overline{d}_L (y^Q \Phi_2^0 + \tilde{y}^Q \Phi_1^{0*}) d_R + h.c.$$

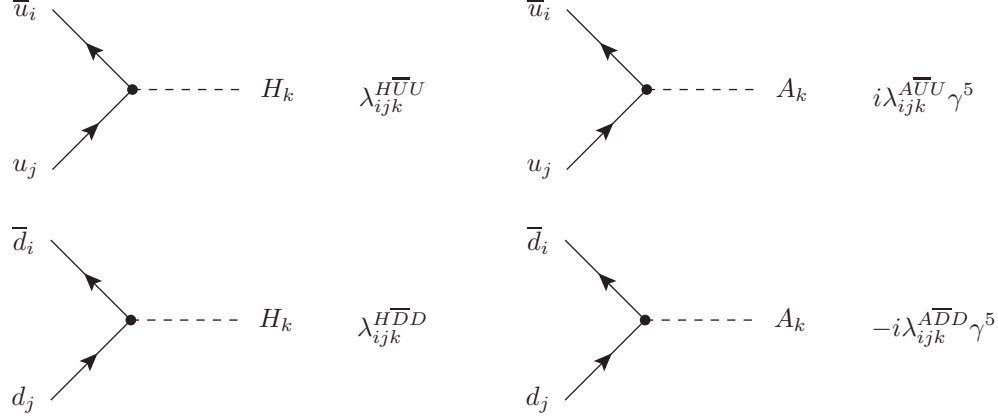


Figure 1.18: Feynman diagrams and rules of quarks and the neutral scalar and pseudoscalar Higgs fields in the LRSM.

Substituting from Eqs. (1.6.101) and (1.6.102) and using the transformations (1.6.103), we obtain the following

$$\begin{aligned} & \bar{u}_L (y^Q \Phi_1^0 + \tilde{y}^Q \Phi_2^{0*}) u_R \\ &= \frac{\sqrt{2}}{k_1^2 - k_2^2} \bar{u}_L (M_u^{\text{diag}}(k_1 \Phi_1^0 - k_2 \Phi_2^{0*}) + V^L M_d^{\text{diag}} V^{R\dagger} (-k_2 \Phi_1^0 + k_1 \Phi_2^{0*})) u_R \quad (1.6.104) \end{aligned}$$

$$\begin{aligned} & \bar{d}_L (y^Q \Phi_2^0 + \tilde{y}^Q \Phi_1^{0*}) d_R \\ &= \frac{\sqrt{2}}{k_1^2 - k_2^2} \bar{d}_L (M_d^{\text{diag}}(k_1 \Phi_1^{0*} - k_2 \Phi_2^0) + V^{L\dagger} M_u^{\text{diag}} V^R (-k_2 \Phi_1^{0*} + k_1 \Phi_2^0)) d_R \quad (1.6.105) \end{aligned}$$

Finally, substituting from Eqs. (1.6.65) and (1.6.48) and then substituting from eq. (1.6.3) and writing the Hermitian conjugate terms explicitly, we find that the neutral scalar and pseudoscalar Higgs-quarks interactions are

$$\begin{aligned} \bar{Q}_L (y^Q \Phi + \tilde{y}^Q \tilde{\Phi}) Q_R + h.c. \supset & \bar{u}_i (\lambda_{ijk}^{H\bar{U}U} H_k + i\lambda_{ijk}^{A\bar{U}U} A_k \gamma^5) u_j + \bar{d}_i (\lambda_{ijk}^{H\bar{D}D} H_k - i\lambda_{ijk}^{A\bar{D}D} A_k \gamma^5) d_j \\ & \quad (1.6.106) \end{aligned}$$

where the couplings are

$$\begin{aligned} \lambda_{ijk}^{H\bar{U}U} = & \frac{(k_1(Z_S)_{1k} - k_2(Z_S)_{2k})}{k_1^2 - k_2^2} M_{u_i} \delta_{ij} + \frac{(-k_2(Z_S)_{1k} + k_1(Z_S)_{2k})}{k_1^2 - k_2^2} \sum_{l=1}^3 V_{il}^L M_{d_l} V_{jl}^{R*} \\ & \quad (1.6.107) \end{aligned}$$

$$\lambda_{ijk}^{H\bar{D}D} = \frac{(k_1(Z_S)_{1k} - k_2(Z_S)_{2k})}{k_1^2 - k_2^2} M_{d_i} \delta_{ij} + \frac{(-k_2(Z_S)_{1k} + k_1(Z_S)_{2k})}{k_1^2 - k_2^2} \sum_{l=1}^3 V_{li}^L M_{u_l} V_{lj}^R \quad (1.6.108)$$

$$\lambda_{ijk}^{A\bar{U}U} = \frac{(k_1(Z_P)_{1k} + k_2(Z_P)_{2k})}{k_1^2 - k_2^2} M_{u_i} \delta_{ij} - \frac{(k_2(Z_P)_{1k} + k_1(Z_P)_{2k})}{k_1^2 - k_2^2} \sum_{l=1}^3 V_{il}^L M_{d_l} V_{jl}^{R*} \quad (1.6.109)$$

$$\lambda_{ijk}^{A\bar{D}D} = \frac{(k_1(Z_P)_{1k} + k_2(Z_P)_{2k})}{k_1^2 - k_2^2} M_{d_i} \delta_{ij} - \frac{(k_2(Z_P)_{1k} + k_1(Z_P)_{2k})}{k_1^2 - k_2^2} \sum_{l=1}^3 V_{li}^L M_{u_l} V_{lj}^R. \quad (1.6.110)$$

Note that the second terms of the couplings  $\lambda_{ijk}^{H\bar{U}U}$ ,  $\lambda_{ijk}^{H\bar{D}D}$ ,  $\lambda_{ijk}^{A\bar{U}U}$  and  $\lambda_{ijk}^{A\bar{D}D}$  are not diagonal (with respect to the indices  $i$  and  $j$ ), since the CKM matrices are not diagonal. This nondiagonality always yields powerful constraints. These terms are the source of the tree-level FCNC interactions in the LRSM [33]. A similar situation is involved in the leptonic sector due to the nondiagonality of the PMNS matrices.

# 2

## ALTERNATIVE LEFT-RIGHT SYMMETRIC MODEL

### 2.1 Introduction

The Higgs sector of the LRSM induces a tree-level FCNC processes that contradict the current experimental limits. Therefore, it is usually assumed that  $SU(2)_R \times U(1)_{B-L}$  is broken at a very high-energy scale. In this case, it is not possible to detect any residual effect for  $SU(2)_R$  gauge symmetry at the TeV scale in the LHC. This has motivated Ernest Ma, in his pioneering work in 1987 [51], to study variants of the conventional the LRSM. He has shown that the superstring-inspired  $E_6$  model may lead to two types of left-right models. The first one is the canonical the LRSM, while the second one is what is known as the ALRM [13, 52], where the fermion assignments are different from those in the conventional the LRSM.

The group  $E_6$  is a complex Lie group of rank 6. It contains  $SO(10) \times U(1)$  as a maximal subgroup, so it is a good candidate for grand unification. Some string theories (Heterotic string) predict that the low-energy effective model is symmetric under  $E_6$ . Depending on the string model,  $E_6$  may be broken to  $SO(10)$  and then to the conventional LRSM or it may have another branch of symmetry breaking that

leads to the ALRM that we consider. The particle content of the ALRM, derived from  $E_6$  model, contains more particles than those in the conventional the LRSM obtained from  $SO(10)$ . This can be simply understood from the fact that the fundamental representation 27 of  $E_6$  is equivalent to the fundamental representation 16 of  $SO(10)$  plus its 10 and singlet representations. In the conventional the LRSM, all non-the SM particles are decoupled and can be quite heavy. However, in the ALRM, they are involved with the SM fermions and will have low-energy consequences. Furthermore, another important difference between the ALRM and the conventional LRSM is the fact that tree-level flavor-changing neutral currents are naturally absent so that the  $SU(2)_R$  breaking scale can be of order TeV, allowing to several interesting signatures at the LHC. As the ALRM is a low-energy effective model of the supersymmetric  $E_6$  model, the gauge couplings are not unified within the ALRM. They are unified in the underling  $E_6$  model, similar to the unification of the SM gauge couplings in supersymmetric  $SU(5)$ .

## 2.2 Description of the ALRM

We consider an ALRM based on the symmetry

$$SU(3)_C \times SU(2)_L \times SU(2)_R \times U(1)_{B-L} \times S \quad (2.2.1)$$

where  $S$  is a discrete symmetry imposed to distinguish between scalar fields and their dual scalars. The particle content of this model, with their charge assignments, is presented in Table 2.1 [53]. As can be seen from this table, extra quarks and leptons are predicted as in all  $E_6$ -based left-right models. The Lagrangian density of the ALRM can be summarized as in the same way in the SM (see eq. (1.2.1)) or as in the LRSM (see eq. (1.3.1)); gauge, kinetic, scalar, Yukawa and Ghost parts.

$$\mathcal{L}_{\text{ALRM}} = \mathcal{L}_{\text{Gauge}} + \mathcal{L}_{\text{Kin}} + \mathcal{L}_S + \mathcal{L}_{\text{Yuk}} + \mathcal{L}_{\text{Ghost}}. \quad (2.2.2)$$

## 2.2 Description of the ALRM

---

Fields	$SU(3)_C \times SU(2)_L \times SU(2)_R \times U(1)_{B-L}$	$S$
<b>Fermions</b>		
$Q_L = \begin{pmatrix} u \\ d \end{pmatrix}_L$	$(3, 2, 1, +\frac{1}{6})$	0
$Q_R = \begin{pmatrix} u \\ d' \end{pmatrix}_R$	$(3, 1, 2, +\frac{1}{6})$	$-\frac{1}{2}$
$d'_L$	$(3, 1, 1, -\frac{1}{3})$	-1
$d_R$	$(3, 1, 1, -\frac{1}{3})$	0
$L_L = \begin{pmatrix} \nu \\ e \end{pmatrix}_L$	$(1, 2, 1, -\frac{1}{2})$	0
$L_R = \begin{pmatrix} n \\ e \end{pmatrix}_R$	$(1, 1, 2, -\frac{1}{2})$	$+\frac{1}{2}$
$n_L$	$(1, 1, 1, 0)$	+1
$\nu_R$	$(1, 1, 1, 0)$	0
<b>Higgs</b>		
$\Phi = \begin{pmatrix} \phi_1^0 & \phi_1^+ \\ \phi_2^- & \phi_2^0 \end{pmatrix}$	$(1, 2, 2^*, 0)$	$-\frac{1}{2}$
$\chi_L = \begin{pmatrix} \chi_L^+ \\ \chi_L^0 \end{pmatrix}$	$(1, 2, 1, +\frac{1}{2})$	0
$\chi_R = \begin{pmatrix} \chi_R^+ \\ \chi_R^0 \end{pmatrix}$	$(1, 1, 2, +\frac{1}{2})$	$+\frac{1}{2}$

Table 2.1: Field content of the ALRM and respective quantum numbers.

The gauge structure and its constituents of the ALRM wasn't changed than that of the LRSM. Hence the gauge part  $\mathcal{L}_{\text{Gauge}}$  of the ALRM Lagrangian density is defined as in the LRSM in eq. (1.3.5).

### 2.2.1 Kinetic Lagrangian

The kinetic part of the Lagrangian density constitutes the kinetic terms of fermions and the interaction of fermions to gauge bosons

$$\begin{aligned} \mathcal{L}_{\text{Kin}} = i \sum_{j=1}^3 & \left[ \bar{L}_{Lj} \gamma^\mu D_\mu L_{Lj} + \bar{L}_{Rj} \gamma^\mu D_\mu L_{Rj} + \bar{Q}_{Lj} \gamma^\mu D_\mu Q_{Lj} + \bar{Q}_{Rj} \gamma^\mu D_\mu Q_{Rj} \right. \\ & \left. + \bar{d}'_{Lj} \gamma^\mu D_\mu d'_{Lj} + \bar{d}_{Rj} \gamma^\mu D_\mu d_{Rj} + \bar{n}_{Lj} \gamma^\mu D_\mu n_{Lj} + \bar{\nu}_{Rj} \gamma^\mu D_\mu \nu_{Rj} \right] \end{aligned} \quad (2.2.3)$$

According to the charge assignments in Table 2.1, the covariant derivative of fermions takes the following forms for each term

$$\bar{L}_L \gamma^\mu D_\mu L_L = \bar{L}_L \gamma^\mu (\partial_\mu - \frac{ig_L}{2} \sigma \cdot W_{L\mu} + \frac{ig_{BL}}{2} V_\mu) L_L, \quad (2.2.4)$$

$$\bar{L}_R \gamma^\mu D_\mu L_R = \bar{L}_R \gamma^\mu (\partial_\mu - \frac{ig_R}{2} \sigma \cdot W_{R\mu} + \frac{ig_{BL}}{2} V_\mu) L_R, \quad (2.2.5)$$

$$\bar{Q}_L \gamma^\mu D_\mu Q_L = \bar{Q}_L^\alpha \gamma^\mu [(\partial_\mu - \frac{ig_L}{2} \sigma \cdot W_{L\mu} - \frac{ig_{BL}}{6} V_\mu) \delta_{\alpha\beta} - \frac{ig_s}{2} \lambda_{\alpha\beta} \cdot G_\mu] Q_L^\beta, \quad (2.2.6)$$

$$\bar{Q}_R \gamma^\mu D_\mu Q_R = \bar{Q}_R^\alpha \gamma^\mu [(\partial_\mu - \frac{ig_R}{2} \sigma \cdot W_{R\mu} - \frac{ig_{BL}}{6} V_\mu) \delta_{\alpha\beta} - \frac{ig_s}{2} \lambda_{\alpha\beta} \cdot G_\mu] Q_R^\beta, \quad (2.2.7)$$

$$\bar{n}_L \gamma^\mu D_\mu n_L = \bar{n}_L \gamma^\mu \partial_\mu n_L, \quad (2.2.8)$$

$$\bar{\nu}_R \gamma^\mu D_\mu \nu_R = \bar{\nu}_R \gamma^\mu \partial_\mu \nu_R, \quad (2.2.9)$$

$$\bar{d}'_L \gamma^\mu D_\mu d'_L = \bar{d}'_L^\alpha \gamma^\mu [(\partial_\mu + \frac{ig_{BL}}{3} V_\mu) \delta_{\alpha\beta} - \frac{ig_s}{2} \lambda_{\alpha\beta} \cdot G_\mu] d'_L^\beta, \quad (2.2.10)$$

$$\bar{d}_R \gamma^\mu D_\mu d_R = \bar{d}_R^\alpha \gamma^\mu [(\partial_\mu + \frac{ig_{BL}}{3} V_\mu) \delta_{\alpha\beta} - \frac{ig_s}{2} \lambda_{\alpha\beta} \cdot G_\mu] d_R^\beta, \quad (2.2.11)$$

where the strong and weak interactions of fermions and bosons are encoded in these kinetic terms. Here the indices  $\alpha, \beta = 1\dots 3$  are color indices.

## 2.2.2 Scalar Lagrangian

In the ALRM, LH and RH up-type quarks as well as LH and RH charged leptons are accommodated in left and right doublets under  $SU(2)$  groups, respectively, as in the LRSM. So we still need the bidoublet  $\Phi$  to generate mass for these particles after SSB. On the other hand, as in the SM, LH down-type quarks are in doublets under the gauge group  $SU(2)_L$  while RH down-type quarks are singlets under  $SU(2)$  groups and hence a mass term for the down-type quarks may be generated from a gauge invariant term Yukawa term  $\bar{Q}_L \chi_L d_R$  with an  $SU(2)_L$  doublet  $\chi_L$ . A similar situation is for the neutrino. The Higgs sector of the ALRM considered here consists of bidoublet  $\Phi$  with left and right doublets  $\chi_L$  and  $\chi_R$ . Unlike the LRSM, the LH scalar Higgs field  $\chi_L$  is necessary not only for maintaining the LR symmetry, but also

it plays a role in generating the fermion masses. The charge assignments of these Higgs fields are shown in Table 2.1.

The covariant derivative of the bidoublet  $\Phi$  is this in eq. (1.3.25) in the LRSM. As in the SM, the covariant derivative of doublets takes the following forms

$$D_\mu \chi_{\mathcal{H}} = (\partial_\mu - \frac{ig_{\mathcal{H}}}{2}(\sigma \cdot W_{\mathcal{H}\mu}) - \frac{ig_{BL}}{2}V_\mu)\chi_{\mathcal{H}}. \quad (2.2.12)$$

The scalar part of the Lagrangian contains the kinetic terms  $\mathcal{L}_S^{\text{Kin}}$  and the potential  $V(\Phi, \chi_L, \chi_R)$  of the Higgs multiplets

$$\mathcal{L}_S = \mathcal{L}_S^{\text{Kin}} - V(\Phi, \chi_L, \chi_R), \quad (2.2.13)$$

where

$$\mathcal{L}_S^{\text{Kin}} = \text{Tr}[|D_\mu \Phi|^2] + |D_\mu \chi_L|^2 + |D_\mu \chi_R|^2. \quad (2.2.14)$$

The most general Higgs potential that is invariant under the symmetry (2.2.1) is given by [19]

$$\begin{aligned} V(\Phi, \chi_L, \chi_R) = & -\mu_1^2 \text{Tr}[\Phi^\dagger \Phi] + \lambda_1 (\text{Tr}[\Phi^\dagger \Phi])^2 + \lambda_2 \text{Tr}[\Phi^\dagger \tilde{\Phi}] \text{Tr}[\tilde{\Phi}^\dagger \Phi] \\ & - \mu_2^2 (\chi_L^\dagger \chi_L + \chi_R^\dagger \chi_R) + \lambda_3 [(\chi_L^\dagger \chi_L)^2 + (\chi_R^\dagger \chi_R)^2] + 2\lambda_4 (\chi_L^\dagger \chi_L)(\chi_R^\dagger \chi_R) \\ & + 2\alpha_1 \text{Tr}(\Phi^\dagger \Phi)(\chi_L^\dagger \chi_L + \chi_R^\dagger \chi_R) + 2\alpha_2 (\chi_L^\dagger \Phi \Phi^\dagger \chi_L + \chi_R^\dagger \Phi \Phi^\dagger \chi_R) \\ & + 2\alpha_3 (\chi_L^\dagger \tilde{\Phi} \tilde{\Phi}^\dagger \chi_L + \chi_R^\dagger \tilde{\Phi}^\dagger \tilde{\Phi} \chi_R) + \mu_3 (\chi_L^\dagger \Phi \chi_R + \chi_R^\dagger \Phi^\dagger \chi_L). \end{aligned} \quad (2.2.15)$$

where the conjugate Higgs multiplets are defined as before, *i.e.*, as in the SM for doublets and as in the LRSM for the bidoublet, Eqs. (1.2.24) and (1.3.32).

The scalar potential contains the mass terms for the Higgs fields as well as the three and four-point self interactions for the Higgs fields. Since our interest is in the Higgs sector of the model, we will give a detailed analysis of the Higgs sector in section 2.4.

### 2.2.3 Yukawa Lagrangian

This part of the Lagrangian contains Yukawa type interactions of fermions with Higgs multiplets

$$\begin{aligned} -\mathcal{L}_{\text{Yuk}} = & \sum_{i,j=1}^3 \left[ \overline{Q}_L{}^i Y_{ij}^q \tilde{\Phi} Q_R{}_j + \overline{Q}_L{}^i Y_{Lij}^q \chi_L d_R{}_j + \overline{Q}_R{}^i Y_{Rij}^q \chi_R d'_L{}_j + \overline{L}_L{}^i Y_{ij}^\ell \Phi L_R{}_j \right. \\ & \left. + \overline{L}_L{}^i Y_{Lij}^\ell \tilde{\chi}_L \nu_R{}_j + \overline{L}_R{}^i Y_{Rij}^\ell \tilde{\chi}_R n_L{}_j + \overline{\nu}_R^c M_N{}^{ij} \nu_R{}_j + \text{h.c.} \right], \end{aligned} \quad (2.2.16)$$

where  $Y^q$ ,  $Y_L^q$ ,  $Y_R^q$ ,  $Y^\ell$ ,  $Y_L^\ell$  and  $Y_R^\ell$  are  $3 \times 3$  Yukawa matrices which again will determine fermion masses and mixings. The matrix  $M_N$  is the Majorana mass matrix for neutrino. Without loss of generality, here and in the rest of this thesis, we take  $M_N$  to be diagonal, real and positive [24]. Note that the Yukawa terms like  $\overline{L}_L \tilde{\Phi} L_R$  and  $\overline{Q}_L \Phi Q_R$  are forbidden by the discrete  $S$  symmetry only.

### 2.2.4 Ghost Lagrangian

The Faddeev-Popov gauge-fixing ghost fields of the ALRM model are in adjoint representations [69] of the corresponding groups

$$c^{0,a_L,a_R,a_c} = c^0, c^{1_L \dots 3_L}, c^{1_R \dots 3_R}, c^{1_c \dots 8_c} = B_{\text{gh}}, W_{L\text{gh}}^a, W_{R\text{gh}}^a, G_{\text{gh}}^a. \quad (2.2.17)$$

The Lagrangian of the ghost fields is

$$\mathcal{L}_{\text{Ghost}} = \mathcal{L}_{G_{\text{gh}}} + \mathcal{L}_{W_{L\text{gh}}} + \mathcal{L}_{W_{R\text{gh}}} + \mathcal{L}_{B_{\text{gh}}} + \mathcal{L}_{\text{gh}}^h. \quad (2.2.18)$$

The kinetic Lagrangians of the ghost fields are [69]

$$\mathcal{L}_{G_{\text{gh}}} = - \sum_{a_c, b_c} \bar{c}^a (\partial_\mu D^\mu)^{ab} c^b = -\overline{G_{\text{gh}}^a} \partial_\mu \partial^\mu G_{\text{gh}}^a - g_s f^{abc} \overline{G_{\text{gh}}^a} \partial_\mu \{G^{\mu b} G_{\text{gh}}^c\}, \quad (2.2.19)$$

$$\begin{aligned} \mathcal{L}_{W_{L,R\text{gh}}} = & - \sum_{a_{L,R}, b_{L,R}} \bar{c}^a (\partial_\mu D^\mu)^{ab} c^b = -\overline{W_{L,R\text{gh}}^a} \partial_\mu \partial^\mu W_{L,R\text{gh}}^a - g \epsilon^{abc} \overline{W_{L,R\text{gh}}^a} \partial_\mu \{W_{L,R}^{\mu b} W_{L,R\text{gh}}^c\}, \\ & \end{aligned} \quad (2.2.20)$$

$$\mathcal{L}_{B_{\text{gh}}} = -\bar{c}^0(\partial_\mu D^\mu)c^0 = -\overline{B_{\text{gh}}}\partial_\mu\partial^\mu B_{\text{gh}}, \quad (2.2.21)$$

and the covariant derivatives of the ghost fields are [69]

$$D^\mu c^{ac} = D^\mu G_{\text{gh}}^a = \partial^\mu G_{\text{gh}}^a + g_s f^{abc} G^{\mu b} G_{\text{gh}}^c, \quad (2.2.22)$$

$$D^\mu c^{a_{L,R}} = D^\mu W_{L,R\text{gh}}^a = \partial^\mu W_{L,R\text{gh}}^a + g \epsilon^{abc} W_{L,R}^{\mu b} W_{L,R\text{gh}}^c, \quad (2.2.23)$$

$$D^\mu c^0 = D^\mu B_{\text{gh}} = \partial^\mu B_{\text{gh}}. \quad (2.2.24)$$

The Lagrangian  $\mathcal{L}_{\text{gh}}^h$  represents the Higgs-ghost interaction Lagrangian [69]

$$\begin{aligned} \mathcal{L}_{\text{gh}}^h = & - \sum_{0,a_L,b_L} \bar{c}^a \{ \xi g^a g^b (T^a \chi_{L0}) \cdot (T^b \chi_L) \} c^b - \sum_{0,a_R,b_R} \bar{c}^a \{ \xi g^a g^b (T^a \chi_{R0}) \cdot (T^b \chi_R) \} c^b \\ & - \sum_{a_L,b_L} \bar{c}^a \{ \xi g^a g^b (T^a \Phi_0) \cdot (T^b \Phi) \} c^b - \sum_{a_R,b_R} \bar{c}^a \{ \xi g^a g^b (\Phi_0 T^a) \cdot (\Phi T^b) \} c^b \\ & + \sum_{a_L,b_R} \bar{c}^a \{ \xi g^a g^b (T^a \Phi_0) \cdot (\Phi T^b) \} c^b + \sum_{a_R,b_L} \bar{c}^a \{ \xi g^a g^b (\Phi_0 T^a) \cdot (T^b \Phi) \} c^b, \end{aligned} \quad (2.2.25)$$

and the gauge couplings  $g^0 = g_{BL}$ ,  $g^{L,R} = g$ . The matrices  $T^a$ 's are the groups' generators in the basis of real degrees of freedom of the Higgs fields [69, Ch. 20, p. 692-697, Ch. 21, 739-742].

## 2.3 Spontaneous Symmetry Breaking in the ALRM

As in the LRSM, the symmetry breaking of the ALRM is spontaneously achieved in two stages via VEVs of scalar Higgs multiplets. The symmetry breaking scheme is as following

$$SU(2)_L \times SU(2)_R \times U(1)_{B-L} \xrightarrow{\langle \chi_R \rangle} SU(2)_L \times U(1)_Y \xrightarrow{\langle \Phi \rangle, \langle \chi_L \rangle} U(1)_{\text{EM}}. \quad (2.3.1)$$

In Appendix D, we provide a detailed study for the conditions that keep the potential (2.2.15) bounded from below. It is remarkable that the copositivity conditions [42, 71] for this Higgs potential significantly depend on the signs of the following

parameters  $\alpha_{12} = \alpha_1 + \alpha_2$ ,  $\alpha_{13} = \alpha_1 + \alpha_3$ , and  $\lambda_{12} = \lambda_1 + 2\lambda_2$ . Here, we present the case with minimal constraints imposed on the potential parameters:

$$\lambda_1 \geq 0, \lambda_2 \leq 0, \lambda_3 \geq 0, \alpha_2 - \alpha_3 \geq 0, \alpha_{12} \geq 0, \alpha_{13} \geq 0, \lambda_{12} \geq 0. \quad (2.3.2)$$

Also for perturbativity the absolute value of any dimensionless potential parameter is assumed to be less than  $\sqrt{4\pi}$ .

The VEVs of Higgs scalars are given to their neutral components as follows

$$\langle \Phi \rangle = \frac{1}{\sqrt{2}} \begin{pmatrix} 0 & 0 \\ 0 & k \end{pmatrix}, \langle \chi_R \rangle = \frac{1}{\sqrt{2}} \begin{pmatrix} 0 \\ v_R \end{pmatrix}, \langle \chi_L \rangle = \frac{1}{\sqrt{2}} \begin{pmatrix} 0 \\ v_L \end{pmatrix}. \quad (2.3.3)$$

From the minimization conditions, one finds that the nonvanishing VEVs are given by (see Appendix D)

$$v_L v_R = \frac{-\mu_3 k}{\sqrt{2}(\lambda_4 - \lambda_3)}, \quad (2.3.4)$$

$$v_L^2 + v_R^2 = \frac{\mu_2^2 - (\alpha_1 + \alpha_2)k^2}{\lambda_3}, \quad (2.3.5)$$

$$k^2 = \frac{2(\lambda_3 \mu_1^2 - (\alpha_1 + \alpha_2) \mu_2^2) \lambda_4 - \lambda_3 + \lambda_3 \mu_3^2}{2(\lambda_1 \lambda_3 - (\alpha_1 + \alpha_2)^2)(\lambda_4 - \lambda_3)}. \quad (2.3.6)$$

It is always useful for numerical purposes to express nonphysical parameters in terms of physical ones, as those latter may be fixed by experiments. We use eqs (2.3.4-2.3.6) to express the three nonphysical parameters  $\mu_1, \mu_2$  and  $\lambda_4$  out of the ten free parameters in the Higgs potential (2.2.15) in terms of the VEVs  $k, v_L$  and  $v_R$ :

$$\mu_1^2 = (v_L^2 + v_R^2)(\alpha_1 + \alpha_2) + k^2 \lambda_1 + \frac{v_L v_R \mu_3}{\sqrt{2}k}, \quad (2.3.7)$$

$$\mu_2^2 = (v_L^2 + v_R^2)\lambda_3 + k^2(\alpha_1 + \alpha_2), \quad (2.3.8)$$

$$\lambda_4 = \lambda_3 - \frac{\mu_3 k}{\sqrt{2}v_L v_R}. \quad (2.3.9)$$

### 2.3.1 Gauge Boson Masses in the ALRM

At the first stage of SSB, the RH Higgs doublet  $\chi_R$  takes a VEV  $\langle \chi_R \rangle = v_R$  and breaks the LR symmetry as in eq. (2.3.1). The second stage is controlled by the

Higgs bidoublet getting a non zero VEV  $\langle \Phi \rangle = \text{diag}(0, k)$  and by the LH doublet VEV  $\langle \chi_L \rangle = v_L$ . The corresponding Higgs kinetic terms are

$$|D_\mu \langle \chi_R \rangle|^2 = \frac{g_R^2 v_R^2}{4} W_R^{\mu-} W_{R\mu}^+ + \frac{v_R^2}{8} (g_R W_R^{\mu 3} - g_{BL} V^\mu) (g_R W_{R\mu}^3 - g_{BL} V_\mu), \quad (2.3.10)$$

$$|D_\mu \langle \chi_L \rangle|^2 = \frac{g_L^2 v_L^2}{4} W_L^{\mu-} W_{L\mu}^+ + \frac{v_L^2}{8} (g_L W_L^{\mu 3} - g_{BL} V^\mu) (g_L W_{L\mu}^3 - g_{BL} V_\mu), \quad (2.3.11)$$

$$\begin{aligned} \text{Tr} |D_\mu \langle \Phi \rangle|^2 &= \frac{k^2}{4} (g_L^2 W_L^{\mu+} W_{L\mu}^- + g_R^2 W_R^{\mu+} W_{R\mu}^-) \\ &\quad + \frac{k^2}{8} (g_L W_L^{\mu 3} - g_R W_R^{\mu 3}) (g_L W_{L\mu}^3 - g_R W_{R\mu}^3). \end{aligned} \quad (2.3.12)$$

### Charged Gauge bosons

In contrast to the LRSM, the mixing between  $W_L$  and  $W_R$  gauge bosons vanishes identically and the  $\{W_{L\mu}^\pm, W_{R\mu}^\pm\}$  are themselves the mass eigenstates  $\{W_\mu^\pm$  and  $W'_\mu^\pm\}$  in the ALRM

$$W^\pm = \frac{W_L^1 \mp i W_L^2}{\sqrt{2}}, \quad W'^\pm = \frac{W_R^1 \mp i W_R^2}{\sqrt{2}} \quad (2.3.13)$$

with corresponding squared masses

$$M_W^2 = \frac{g_L^2}{4} (v_L^2 + k^2) \equiv \frac{g_L^2 v^2}{4}, \quad M_{W'}^2 = \frac{g_R^2}{4} (v_R^2 + k^2) \equiv \frac{g_R^2 v'^2}{4}. \quad (2.3.14)$$

We have the following relations

$$\frac{M_{W'}}{M_W} = \frac{g_R}{g_L} \frac{v'}{v}, \quad (2.3.15)$$

and for  $g_L = g_R$ , it reads

$$M_{W'} = \frac{v'}{v} M_W. \quad (2.3.16)$$

We define the two left-right analogous angles  $\beta$  and  $\zeta$  such that

$$v_L = v c_\beta, \quad v_R = v' c_\zeta, \quad k = v s_\beta = v' s_\zeta, \quad (2.3.17)$$

where  $s_\beta = \sin \beta$ ,  $c_\beta = \cos \beta$ ,  $s_\zeta = \sin \zeta$ ,  $c_\zeta = \cos \zeta$ . Thus

$$t_\beta \equiv \tan \beta = \frac{k}{v_L}, \quad t_\zeta \equiv \tan \zeta = \frac{k}{v_R}, \quad (2.3.18)$$

and

$$\sqrt{v_L^2 + k^2} = v \equiv 246 \text{ GeV}, \quad \sqrt{v_R^2 + k^2} = v' \sim \mathcal{O}(\text{TeV}). \quad (2.3.19)$$

### Neutral Gauge bosons and Weinberg Angle

The mass squared matrix for neutral gauge bosons in the basis  $\{W_{L\mu}^3, W_{R\mu}^3, V_\mu\}$  is [64]

$$M_{V^0}^2 = \frac{1}{4} \begin{pmatrix} g_L^2(v_L^2 + k^2) & -g_L g_R k^2 & -g_L g_{BL} v_L^2 \\ -g_L g_R k^2 & g_R^2(v_R^2 + k^2) & -g_R g_{BL} v_R^2 \\ -g_L g_{BL} v_L^2 & -g_R g_{BL} v_R^2 & g_{BL}^2(v_L^2 + v_R^2) \end{pmatrix}. \quad (2.3.20)$$

For  $g_L = g_R$ , this matrix takes the form

$$M_{ZZ'} = \begin{pmatrix} \frac{1}{4}g^2(k^2 + v_L^2) & -\frac{1}{4}g^2k^2 & -\frac{1}{4}gg_{BL}v_L^2 \\ -\frac{1}{4}g^2k^2 & \frac{1}{4}g^2(k^2 + v_R^2) & -\frac{1}{4}gg_{BL}v_R^2 \\ -\frac{1}{4}gg_{BL}v_L^2 & -\frac{1}{4}gg_{BL}v_R^2 & \frac{1}{4}g_{BL}^2(v_L^2 + v_R^2) \end{pmatrix}. \quad (2.3.21)$$

The eigenvalues of this matrix are  $M_Z^2, M_{Z'}^2$  and for the photon  $M_A = 0$ . Thus we have  $D^{ZZ'} = \text{Det}(M_{ZZ'}) = 0$  and moreover

$$T^{ZZ'} = \text{Tr}(M_{ZZ'}) = M_{Z'}^2 + M_Z^2 = M_{W'}^2 + M_W^2 + \frac{1}{4}g_{BL}^2(v_L^2 + v_R^2). \quad (2.3.22)$$

In terms of the Weinberg angle  $\theta_w$  and  $t_\beta$  we have

$$M_{Z'}^2 = (M_W^2 + M_{W'}^2)\left(\frac{1-s_w^2}{1-2s_w^2}\right) - \frac{2M_W^2 s_w^2}{1-2s_w^2} \frac{t_\beta^2}{1+t_\beta^2} - M_Z^2. \quad (2.3.23)$$

Since the determinant  $D^{ZZ'} = 0$ , the characteristic polynomial  $P_{ZZ'}^3$  of the matrix  $M_{ZZ'}^2$  has the form

$$P^{ZZ'}(x) = x(-x^2 + T^{ZZ'}x - D_2^{ZZ'}), \quad (2.3.24)$$

where

$$T^{ZZ'} = (M_W^2 + M_{W'}^2)\left(\frac{1-s_w^2}{1-2s_w^2}\right) - \frac{2M_W^2 s_w^2}{1-2s_w^2} \frac{t_\beta^2}{1+t_\beta^2}, \quad (2.3.25)$$

$$D_2^{ZZ'} = \frac{M_W^2}{1 - 2s_w^2} (M_{W'}^2 - \frac{M_W^2 t_\beta^4}{(1 + t_\beta^2)^2}). \quad (2.3.26)$$

Since the squared mass  $M_Z^2$  is a zero of  $P^{ZZ'}$ , we have

$$-M_Z^4 + T^{ZZ'} M_Z^2 - D_2^{ZZ'} = 0. \quad (2.3.27)$$

Since, as it is clear from eqs. (2.3.25) and (2.3.26), both  $T^{ZZ'}$  and  $D_2^{ZZ'}$  are linear in  $M_{W'}^2$ , we solve eq. (2.3.27) for  $M_{W'}^2$  in terms of  $M_Z^2, M_W^2, t_\beta$  and  $s_w^2$  to obtain<sup>1</sup>

$$M_{W'}^2 = -\frac{-M_Z^4 + M_Z^2 T^{ZZ'(0)} - D_2^{ZZ'(0)}}{M_Z^2 T^{ZZ'(1)} - D_2^{ZZ'(1)}}, \quad (2.3.28)$$

where

$$T^{ZZ'} = T^{ZZ'(1)} M_{W'}^2 + T^{ZZ'(0)}, \quad D_2^{ZZ'} = D_2^{ZZ'(1)} M_{W'}^2 + D_2^{ZZ'(0)}. \quad (2.3.29)$$

From eqs. (2.3.25) and (2.3.26), formula (2.3.28) can be written explicitly as

$$M_{W'}^2 = \frac{M_Z^4 (1 - 2s_w^2)(1 + t_\beta^2)^2 - M_Z^2 M_W^2 (1 + t_\beta^2)(1 + t_\beta^2 - s_w^2(1 + 3t_\beta^2)) - M_W^4 t_\beta^4}{(M_Z^2 (1 - s_w^2) - M_W^2)(1 + t_\beta^2)^2}. \quad (2.3.30)$$

From eqs. (2.3.16), (2.3.18), 2.3.19), and (2.3.30) we obtain  $v_R^2$  in terms of  $M_Z^2, M_W^2, t_\beta$  and  $s_w^2$  as follows

$$v_R^2 = v^2 \left( \frac{M_{W'}^2}{M_W^2} - \frac{t_\beta^2}{1 + t_\beta^2} \right). \quad (2.3.31)$$

It is worth noting that instead of the SM relation  $s_w^2 = 1 - M_W^2/M_Z^2$ , we have in the ALRM the following relation for the Weinberg angle

$$s_w^2 = \frac{M_W^4 t_\beta^4 + (M_Z^2 - M_W^2)(M_{W'}^2 - M_Z^2)(1 + t_\beta^2)^2}{M_Z^2 (1 + t_\beta^2)((M_{W'}^2 - 2M_Z^2)(1 + t_\beta^2) + M_W^2(1 + 3t_\beta^2))}. \quad (2.3.32)$$

This relation is used to constrain one of the new parameters, as  $M_{W'}^2$  in eq. (2.3.30), taking into account that the parameters

$$M_W = 80.387, \quad M_Z = 91.1876, \quad s_w^2 = 0.23129(5) \quad (2.3.33)$$

<sup>1</sup>Based on a notice by my late colleague A. Elsayed, and I dedicate its usage to his smart soul.

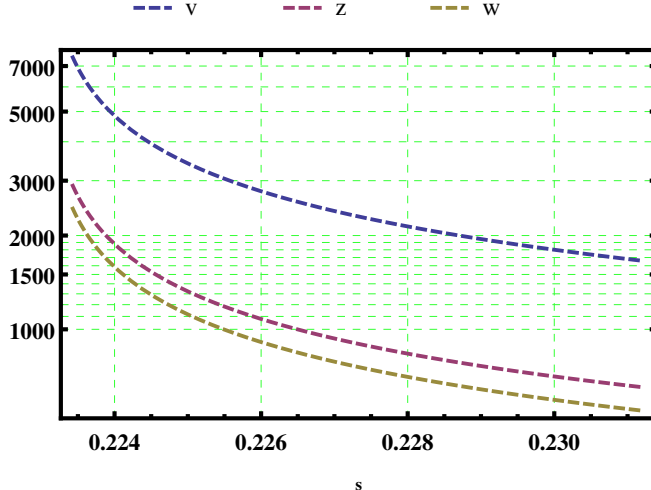


Figure 2.1:  $M_{Z'}$ ,  $M_{W'}$ ,  $v_R$  with  $s_w^2$ .

are fixed as SM inputs from experiments [68].

We notice also that  $M_{W'}^2 \rightarrow \infty$  when  $s_w^2 \rightarrow 1 - M_W^2/M_Z^2$  (as in the on-shell scheme [78]), i.e., when  $s_w^2$  approaches the SM value  $1 - M_W^2/M_Z^2$ . This explains why  $M_{W'}$  must be large. i.e., the high scale symmetry breaking is now dictated by the low scale phenomenology.

As in the LRSM, the matrix (2.3.20) is diagonalized by the rotation of gauge fields into physical eigenstates by

$$\begin{pmatrix} W_{L\mu}^3 \\ W_{R\mu}^3 \\ V_\mu \end{pmatrix} = \begin{pmatrix} c_w & s_w & 0 \\ -s_\varphi s_w & s_\varphi c_w & c_\varphi \\ -c_\varphi s_w & c_\varphi c_w & -s_\varphi \end{pmatrix} \begin{pmatrix} Z_{L\mu} \\ A_\mu \\ Z_{R\mu} \end{pmatrix}, \quad (2.3.34)$$

where the states  $Z_{L\mu}$ ,  $Z_{R\mu}$  and  $A_\mu$  and the angles  $\varphi$  and  $\theta_w$  are those defined in Eqs. (1.4.9), (1.4.10) and (1.2.34), respectively.

For  $g_L = g_R$ , for the diagonalization of the matrix (2.3.21), it is more convenient

### 2.3 Spontaneous Symmetry Breaking in the ALRM

---

to work in the basis  $(A, Z_L, Z_R)$ , where

$$\begin{pmatrix} A \\ Z_L \\ Z_R \end{pmatrix} = \begin{pmatrix} s_w & s_w & \sqrt{c_w^2 - s_w^2} \\ c_w & -s_w^2/c_w & -s_w\sqrt{c_w^2 - s_w^2}/c_w \\ 0 & \sqrt{c_w^2 - s_w^2}/c_w & -s_w/c_w \end{pmatrix} \begin{pmatrix} W_L^3 \\ W_R^3 \\ B \end{pmatrix}. \quad (2.3.35)$$

As in the LRSM, the bidoublet  $\Phi$  mixes the  $Z_L$  and  $Z_R$  gauge bosons with the following mass-squared matrix in the basis  $\{Z_{L\mu}, Z_{R\mu}\}$

$$\begin{pmatrix} Z_L \\ Z_R \end{pmatrix}^T \begin{pmatrix} M_{LL} & M_{LR} \\ M_{RL} & M_{RR} \end{pmatrix} \begin{pmatrix} Z_L \\ Z_R \end{pmatrix}. \quad (2.3.36)$$

where for  $g_L = g_R = g$ , the mixing coefficients are

$$M_{LL} = \frac{g^2 v^2}{4c_w^2} = \frac{M_W^2}{1 - s_w^2}, \quad (2.3.37)$$

$$M_{LR} = \frac{g^2(v^2 s_w^2 - k^2 c_w^2)}{4c_w^2 \sqrt{c_w^2 - s_w^2}} = \frac{M_W^2}{\sqrt{1 - 2s_w^2}} \left( \frac{s_w^2}{1 - s_w^2} - \frac{t_\beta^2}{1 + t_\beta^2} \right), \quad (2.3.38)$$

$$M_{RR} = \frac{g^2(v^2 s_w^4 + v'^2 c_w^4 - 2k^2 s_w^2 c_w^2)}{4c_w^2(c_w^2 - s_w^2)} = \frac{M_W^2 s_w^2}{1 - 2s_w^2} \left( \frac{s_w^2}{1 - s_w^2} + \frac{M_{W'}^2}{M_W^2} \frac{1 - s_w^2}{s_w^2} - \frac{2t_\beta^2}{1 + t_\beta^2} \right). \quad (2.3.39)$$

The exact mass eigenstates  $Z$  and  $Z'$  are obtained by

$$\begin{pmatrix} Z_L \\ Z_R \end{pmatrix} = \begin{pmatrix} \cos \vartheta & \sin \vartheta \\ -\sin \vartheta & \cos \vartheta \end{pmatrix} \begin{pmatrix} Z \\ Z' \end{pmatrix}, \quad (2.3.40)$$

where the mixing angle  $\vartheta$  is defined as

$$\tan 2\vartheta = \frac{2M_{LR}}{M_{LL} - M_{RR}} = \frac{2\sqrt{1 - 2s_w^2}}{s_w^2} \frac{\frac{s_w^2}{1 - s_w^2} - \frac{t_\beta^2}{1 + t_\beta^2}}{\frac{2(1 - 2s_w^2)}{s_w^2(1 - s_w^2)} - \left(1 + \frac{M_{W'}^2}{M_W^2}\right) \frac{1 - s_w^2}{s_w^2} + \frac{2t_\beta^2}{1 + t_\beta^2}}, \quad (2.3.41)$$

and

$$\cos \vartheta = \frac{-\text{sign}(M_{LR})(M_{RR} - M_{LL} + \sqrt{4M_{LR}^2 + (M_{RR} - M_{LL})^2})}{\sqrt{4M_{LR}^2 + (M_{RR} - M_{LL} + \sqrt{4M_{LR}^2 + (M_{RR} - M_{LL})^2})^2}}, \quad (2.3.42)$$

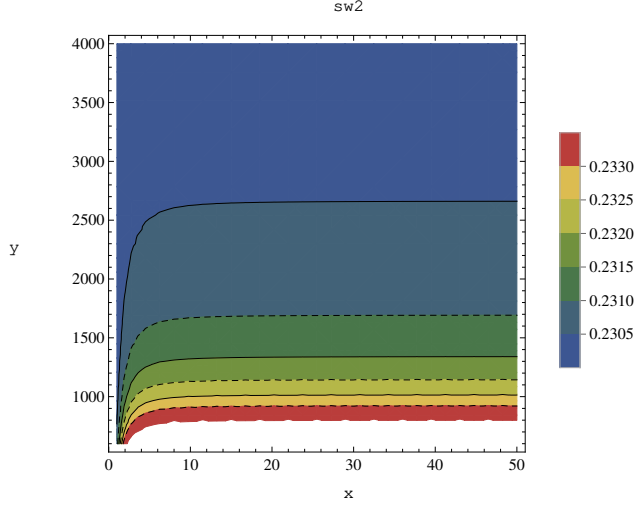


Figure 2.2: Weinberg angle in the ALRM.

$$\sin \vartheta = \frac{-2|M_{\text{LR}}|}{\sqrt{4M_{\text{LR}}^2 + (M_{\text{RR}} - M_{\text{LL}} + \sqrt{4M_{\text{LR}}^2 + (M_{\text{RR}} - M_{\text{LL}})^2})^2}}. \quad (2.3.43)$$

The squared mass eigenvalues  $M_Z^2$  and  $M_{Z'}^2$  are given by

$$M_{Z,Z'}^2 = \frac{1}{2}(M_{\text{LL}} + M_{\text{RR}} \mp (M_{\text{RR}} - M_{\text{LL}})\sqrt{1 + \tan^2 2\vartheta}). \quad (2.3.44)$$

It is clear that if  $v_R \gg v$ , i.e.,  $\vartheta \rightarrow 0$ , then  $Z \simeq Z_L$  and  $Z' \simeq Z_R$ . The LHC search for the  $Z'$  gauge boson is rather model dependent. However, one may consider  $M_{Z'} \gtrsim 2$  TeV as a conservative lower bound [3, 27]. In addition, the mixing between  $Z$  and  $Z'$  should be less than  $\mathcal{O}(10^{-3})$ . We notice from Fig. 2.2 that for wide ranges of the parameters  $t_\beta$  and  $M_{W'}$ , the Weinberg angle keeps within its experimental range  $s_w^2 = 0.231 \pm 0.00015$ .

### 2.3.2 Fermion Masses in the ALRM

Similar to the SM, three generations of fermions acquire their masses through Yukawa interactions of Higgs multiplets.

$$-\mathcal{L}_{\text{Yukawa}} \supset \sum_{i,j=1}^3 \left[ \overline{Q}_L^i Y_{ij}^q \langle \tilde{\Phi} \rangle Q_R^j + \overline{Q}_L^i Y_{Lij}^q \langle \chi_L \rangle d_R^j + \overline{Q}_R^i Y_{Rij}^q \langle \chi_R \rangle d_L^j + \overline{L}_L^i Y_{ij}^\ell \langle \Phi \rangle L_R^j \right]$$

### 2.3 Spontaneous Symmetry Breaking in the ALRM

---

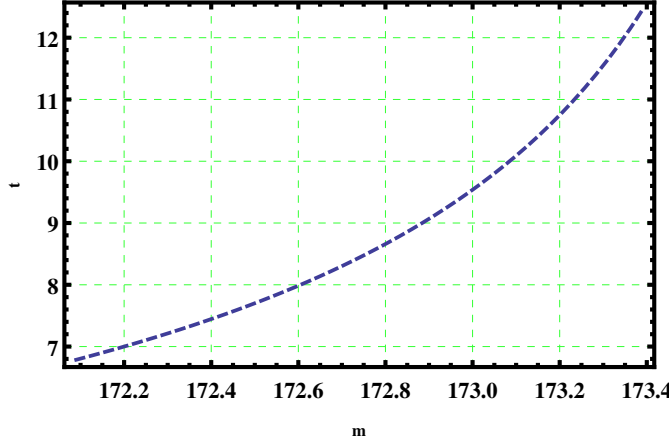


Figure 2.3:  $t_\beta$  vs  $m_t$  in the ALRM

$$+ \bar{L}_L^i Y_{Lij}^\ell \langle \tilde{\chi}_L \rangle \nu_{Rj} + \bar{L}_R^i Y_{Rij}^\ell \langle \tilde{\chi}_R \rangle n_{Lj} + \bar{\nu}_{Ri}^c M_{Nij} \nu_{Rj} + \text{h.c.} \Big], \quad (2.3.45)$$

The Yukawa Lagrangian leads to the following Dirac mass matrices for fermions

$$M_u = \frac{1}{\sqrt{2}} Y_L^q v s_\beta, \quad M_d = \frac{1}{\sqrt{2}} Y_L^q v c_\beta, \quad M_{d'} = \frac{1}{\sqrt{2}} Y_R^q v_{_R} \quad (2.3.46)$$

$$M_\nu = \frac{1}{\sqrt{2}} Y_L^\ell v c_\beta, \quad M_e = \frac{1}{\sqrt{2}} Y^\ell v s_\beta, \quad M_n = \frac{1}{\sqrt{2}} Y_R^\ell v_{_R} \quad (2.3.47)$$

and the Majorana mass matrix for neutrino is  $M_N$ .

The charged fermions and scotino mass matrices can be diagonalized by the following biunitary transformations

$$V_L^{u\dagger} M_u V_R^u = M_u^{\text{diag}}, \quad V_L^{d\dagger} M_d V_R^d = M_d^{\text{diag}}, \quad V_R^{d'\dagger} M_{d'} V_L^{d'} = M_{d'}^{\text{diag}} \quad (2.3.48)$$

$$V_L^{e\dagger} M_e V_R^e = M_e^{\text{diag}}, \quad V_R^{n\dagger} M_n V_L^n = M_n^{\text{diag}} \quad (2.3.49)$$

The top quark mass  $m_t$  is given in terms of  $t_\beta$  as

$$m_t = \frac{y_t v}{\sqrt{2}} s_\beta = \frac{y_t v}{\sqrt{2}} \frac{t_\beta}{\sqrt{1+t_\beta^2}} \quad (2.3.50)$$

Conversely, upper and lower bounds for  $t_\beta$  can be found from the experimental values

of the top quark mass  $m_t$ , where

$$t_\beta = \frac{\sqrt{2}m_t}{\sqrt{y_t^2 v^2 - 2m_t^2}}. \quad (2.3.51)$$

Since  $m_t = 172.74 \pm 0.33_{\text{exp}} \pm 0.32_{\text{th}}$  [78], then, for  $y_t = 1$ ,  $v = 246$ , we have

$$6.7864 \lesssim t_\beta \lesssim 12.4516, \quad (2.3.52)$$

as shown in Fig. 2.3.

The neutrino mass matrix in the basis  $\{\nu, N\}$ , defined in eq. (1.4.85), is [33, 62, 63]

$$\begin{pmatrix} \bar{\nu} \\ \bar{N} \end{pmatrix}^T \begin{pmatrix} 0 & M_\nu \\ M_\nu^T & M_N \end{pmatrix} \begin{pmatrix} \nu \\ N \end{pmatrix}. \quad (2.3.53)$$

Again, as in the LRSM,  $\nu$  and  $N$  will be approximate flavor eigenstates with the well known seesaw mass matrices

$$m_N \simeq M_N, \quad m_\nu \simeq M_\nu M_N^{-1} M_\nu^T \quad (2.3.54)$$

The matrix of the heavy neutrino  $m_N \simeq M_N$  is already taken diagonal. The flavor mass matrix of the light neutrinos is diagonalized by the unitary transformation

$$V_L^{\nu\dagger} m_\nu V_L^\nu = M_\nu^{\text{diag}} \quad (2.3.55)$$

## 2.4 Higgs Sector in the ALRM

### 2.4.1 Higgs Masses and Mixing in the ALRM

We begin by 16 degrees of freedom; 8 of  $\Phi$  and 8 of  $\chi_L$  and  $\chi_R$ . After symmetry breaking, two neutral components of these 16 degrees of freedom will be eaten by the neutral gauge bosons  $Z$  and  $Z'$  to acquire their masses. In addition, another four charged components will be eaten by the charged gauge bosons  $W^\pm$  and  $W'^\pm$  to acquire their masses. The neutral components of the Higgs multiplets  $\Phi$ ,  $\chi_L$  and

$\chi_R$  are expanded around their (nonvanishing) vacua into real and imaginary parts as follows

$$\phi_2^0 = \frac{k + \phi_2^{0R} + i\phi_2^{0I}}{\sqrt{2}}, \quad \chi_L^0 = \frac{v_L + \chi_L^{0R} + i\chi_L^{0I}}{\sqrt{2}}, \quad \chi_R^0 = \frac{v_R + \chi_R^{0R} + i\chi_R^{0I}}{\sqrt{2}}. \quad (2.4.1)$$

Ten scalars remain as physical Higgs bosons in this class of models. As we will explicitly show, four of them give the charged Higgs bosons, two lead to the pseudoscalar Higgs bosons, and the remaining four give the  $CP$ -even neutral Higgs bosons.

### Charged Higgs bosons

The mass matrix of the charged Higgs bosons, in the basis  $\{\phi_1^+, \chi_L^+, \phi_2^+, \chi_R^+\}$ , is a block diagonal matrix with the following two matrices, which, respectively, correspond to the bases  $\{\phi_1^+, \chi_L^+\}$  and  $\{\phi_2^+, \chi_R^+\}$ :

$$M_{1L}^\pm = (kv_L(\alpha_3 - \alpha_2) - \frac{\mu_3 v_R}{\sqrt{2}}) \begin{pmatrix} ct_\beta & -1 \\ -1 & t_\beta \end{pmatrix}, \quad (2.4.2)$$

$$M_{2R}^\pm = (kv_R(\alpha_3 - \alpha_2) - \frac{\mu_3 v_L}{\sqrt{2}}) \begin{pmatrix} ct_\zeta & -1 \\ -1 & t_\zeta \end{pmatrix}, \quad (2.4.3)$$

where  $ct_\beta = \cot\beta$  and  $ct_\zeta = \cot\zeta$ . These matrices  $M_{1L}^\pm$  and  $M_{2R}^\pm$  can be diagonalized by the unitary transformations:  $V_1^\dagger M_{1L}^\pm V_1 = \text{diag}(m_{h_1^\pm}, 0)$  and  $V_2^\dagger M_{2R}^\pm V_2 = \text{diag}(m_{h_2^\pm}, 0)$ , where

$$\begin{pmatrix} \phi_1^\pm \\ \chi_L^\pm \end{pmatrix} = \underbrace{\begin{pmatrix} c_\beta & s_\beta \\ -s_\beta & c_\beta \end{pmatrix}}_{V_1} \begin{pmatrix} h_1^\pm \\ G_1^\pm \end{pmatrix}, \quad \begin{pmatrix} \phi_2^\pm \\ \chi_R^\pm \end{pmatrix} = \underbrace{\begin{pmatrix} c_\zeta & s_\zeta \\ -s_\zeta & c_\zeta \end{pmatrix}}_{V_2} \begin{pmatrix} h_2^\pm \\ G_2^\pm \end{pmatrix}. \quad (2.4.4)$$

The massless eigenstates  $G_1^\pm$  and  $G_2^\pm$  are the charged Goldstone bosons eaten by the gauge bosons  $W^\pm$  and  $W'^\pm$  to acquire their masses. The charged Higgs bosons masses are

$$m_{h_1^\pm}^2 = \text{Tr}(M_{1L}^\pm) = (kv_L(\alpha_3 - \alpha_2) - \frac{\mu_3 v_R}{\sqrt{2}}) \frac{v^2}{kv_L}, \quad (2.4.5)$$

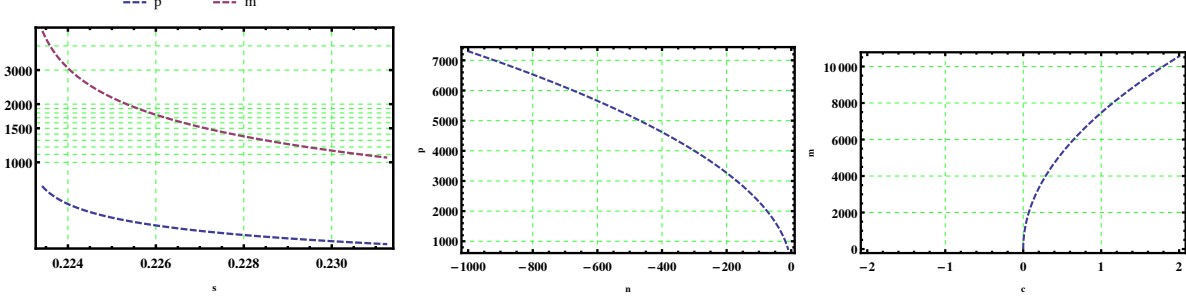


Figure 2.4: Charged Higgs Masses  $m_{1\pm}, m_{2\pm}$  with  $s_w^2$ ,  $\mu_3$  and  $\alpha_{32}$ .

$$m_{h_2^\pm}^2 = \text{Tr}(M_{2R}^\pm) = (kv_R(\alpha_3 - \alpha_2) - \frac{\mu_3 v_L}{\sqrt{2}}) \frac{v'^2}{kv_R}. \quad (2.4.6)$$

From these expressions, one can show that the mass of the charged Higgs can be of  $\mathcal{O}(100)$  GeV for a wide range of the parameter space. We express some of the parameters in terms of the physical Higgs masses

$$\alpha_3 = \alpha_2 - \frac{1}{v_R^2 - v_L^2} \left( \frac{v_L^2}{v^2} m_{h_1^\pm}^2 - \frac{v_R^2}{v'^2} m_{h_2^\pm}^2 \right), \quad (2.4.7)$$

$$\mu_3 = -\frac{\sqrt{2}kv_Lv_R}{v_R^2 - v_L^2} \left( \frac{1}{v^2} m_{h_1^\pm}^2 - \frac{1}{v'^2} m_{h_2^\pm}^2 \right). \quad (2.4.8)$$

### CP-odd Higgs bosons

We now turn to the neutral Higgs physical fields and their masses. This can be easily obtained if one develops the neutral components of the bidoublets  $\Phi$  and the doublets  $\chi_{L,R}$  around their vacua into real and imaginary parts, i.e.,

$$\phi_i^0 = \frac{1}{\sqrt{2}}(v_i + \phi_i^{0R} + i\phi_i^{0I}), \quad i = 1, 2, L, R, \quad (2.4.9)$$

where  $v_1 = 0$ ,  $v_2 = k$ , and  $\phi_{L,R} = \chi_{L,R}$ . In this case, the squared mass matrix of neutral Goldston and  $CP$ -odd Higgs bosons is given by

$$M_{P_{ij}}^2 = \frac{\partial^2 V(\Phi, \chi_{L,R})}{\partial \phi_i^{0I} \partial \phi_j^{0I}} \Big|_{\langle \phi_{i,j}^{0R} \rangle = \langle \phi_{i,j}^{0I} \rangle = 0}. \quad (2.4.10)$$

One finds that this mass matrix in the basis  $\{\phi_1^{0I}, \phi_2^{0I}, \chi_L^{0I}, \chi_R^{0I}\}$  is factored as a product of the squared mass of  $\phi_1^{0I}$ , which is totally decoupled due to the fact that we have  $v_1 = 0$ , times the following  $3 \times 3$  squared mass matrix of  $\{\phi_2^{0I}, \chi_L^{0I}, \chi_R^{0I}\}$ :

$$M_P^2 = -\frac{\mu_3}{2\sqrt{2}} \begin{pmatrix} \frac{v_L v_R}{k} & -v_R & v_L \\ -v_R & \frac{k v_R}{v_L} & -k \\ v_L & -k & \frac{k v_L}{v_R} \end{pmatrix}, \quad (2.4.11)$$

or in terms of the rotation angles

$$M_P^2 = -\frac{k\mu_3}{2\sqrt{2}} \begin{pmatrix} ct_\beta ct_\zeta & -ct_\zeta & ct_\beta \\ -ct_\zeta & t_\beta ct_\zeta & -1 \\ ct_\beta & -1 & t_\zeta ct_\beta \end{pmatrix}. \quad (2.4.12)$$

The mass of the first pseudoscalar Higgs boson  $\phi_1^{0I} \equiv A_1$  is given by

$$m_{A_1}^2 = 2k^2\lambda_2 + (\alpha_3 - \alpha_2)(v_L^2 + v_R^2) - \frac{v_L v_R \mu_3}{\sqrt{2}k}. \quad (2.4.13)$$

The matrix  $M_P^2$  can be diagonalized by the unitary transformation:  $U^\dagger M_P^2 U = \text{diag}(m_{A_2}^2, 0, 0)$ ,

$$\begin{pmatrix} \phi_2^{0I} \\ \chi_L^{0I} \\ \chi_R^{0I} \end{pmatrix} = \underbrace{\begin{pmatrix} \frac{1}{\sqrt{t_\beta^2 + t_\zeta^2 + 1}} & -\frac{t_\zeta}{\sqrt{t_\zeta^2 + 1}} & \frac{t_\beta}{\sqrt{(t_\zeta^2 + 1)(t_\beta^2 + t_\zeta^2 + 1)}} \\ -\frac{t_\beta}{\sqrt{t_\beta^2 + t_\zeta^2 + 1}} & 0 & \sqrt{\frac{t_\zeta^2 + 1}{t_\beta^2 + t_\zeta^2 + 1}} \\ \frac{t_\zeta}{\sqrt{t_\beta^2 + t_\zeta^2 + 1}} & \frac{1}{\sqrt{t_\zeta^2 + 1}} & \frac{t_\beta t_\zeta}{\sqrt{(t_\zeta^2 + 1)(t_\beta^2 + t_\zeta^2 + 1)}} \end{pmatrix}}_U \begin{pmatrix} A_2 \\ G_1^0 \\ G_2^0 \end{pmatrix}, \quad (2.4.14)$$

where the massless eigenstates  $G_1^0$  and  $G_2^0$  are the neutral Goldstone bosons eaten by the gauge bosons  $Z$  and  $Z'$  to acquire their masses. The other  $CP$ -odd Higgs boson mass is given by

$$m_{A_2}^2 = \text{Tr}(M_P^2) = -\frac{k\mu_3}{\sqrt{2}} \frac{1 + t_\beta^2 + t_\zeta^2}{t_\beta t_\zeta}. \quad (2.4.15)$$

It is worth mentioning that  $m_{A_2}^2$  constrains the parameter  $\mu_3$  to be negative. We find that the typical values of  $CP$ -odd Higgs masses are of  $\mathcal{O}(100)$  GeV.

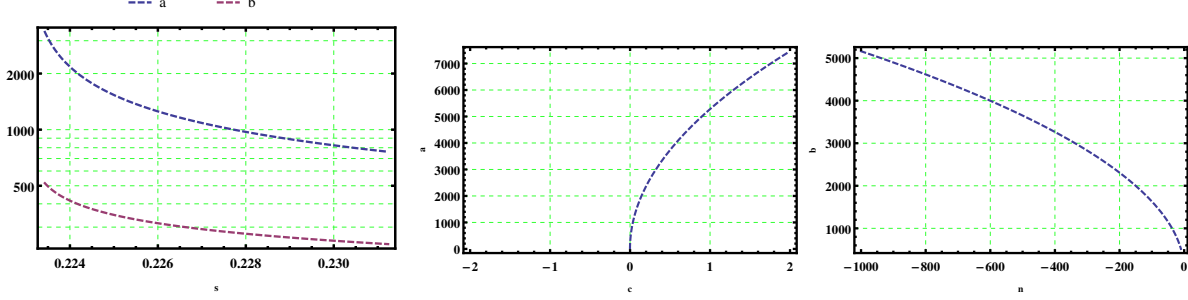


Figure 2.5: Pseudoscalar Higgs Masses  $m_{A1}, m_{A2}$  with  $s_w^2, \mu_3$  and  $\alpha_{32}$ .

### *CP*-even Higgs bosons

Finally, we consider the *CP*-even Higgs bosons. Similar to the *CP*-odd Higgs, the squared mass matrix of *CP*-even Higgs bosons is given by

$$M_{Sij}^2 = \frac{\partial^2 V(\Phi, \chi_{L,R})}{\partial \phi_i^{0R} \partial \phi_j^{0R}} \Big|_{\langle \phi_i^{0R} \rangle = \langle \phi_{i,j}^{0I} \rangle = 0}. \quad (2.4.16)$$

Again, one finds that  $h_1 = \phi_1^{0R}$  is decoupled with mass  $m_{h_1} = m_{A1}$ . The remaining squared mass matrix of the *CP*-even Higgs bosons is given in the basis  $\{\phi_2^{0R}, \chi_L^{0R}, \chi_R^{0R}\}$  by

$$M_S^2 = (m_{ij}) = \begin{pmatrix} 2k^2\lambda_1 - \frac{v_L v_R \mu_3}{\sqrt{2}k} & 2kv_L(\alpha_1 + \alpha_2) + \frac{v_R \mu_3}{\sqrt{2}} & 2kv_R(\alpha_1 + \alpha_2) + \frac{v_L \mu_3}{\sqrt{2}} \\ 2kv_L(\alpha_1 + \alpha_2) + \frac{v_R \mu_3}{\sqrt{2}} & 2v_L^2 \lambda_3 - \frac{kv_R \mu_3}{\sqrt{2}v_L} & 2v_L v_R \lambda_3 - \frac{k \mu_3}{\sqrt{2}} \\ 2kv_R(\alpha_1 + \alpha_2) + \frac{v_L \mu_3}{\sqrt{2}} & 2v_L v_R \lambda_3 - \frac{k \mu_3}{\sqrt{2}} & 2v_R^2 \lambda_3 - \frac{kv_L \mu_3}{\sqrt{2}v_R} \end{pmatrix}. \quad (2.4.17)$$

The squared Higgs masses are the zeros of the characteristic polynomial  $P_h^3$  of the matrix  $M_S^2$ . The characteristic polynomial  $P_h^3$  is the cubic polynomial

$$P_h^3(x) = \text{Det}(M_S^2 - xI) = -x^3 + T^h x^2 - D_2^h x + D^h, \quad (2.4.18)$$

where

$$T^h = \text{Tr}(M_S^2), \quad (2.4.19)$$

$$D_2^h = m_{11}m_{22} + m_{11}m_{33} + m_{22}m_{33} - m_{12}^2 - m_{13}^2 - m_{23}^2, \quad (2.4.20)$$

$$D^h = \text{Det}(M_S^2). \quad (2.4.21)$$

Explicitly, we have

$$T^h = 2k^2\lambda_1 + 2(v_L^2 + v_R^2)\lambda_3 - \frac{(v_L^2 v_R^2 + k^2(v_L^2 + v_R^2))\mu_3}{\sqrt{2}kv_L v_R}, \quad (2.4.22)$$

$$\begin{aligned} D_2^h &= -\frac{v_L^2 + v_R^2}{kv_L v_R} \{4k^3 v_L v_R ((\alpha_1 + \alpha_2)^2 - \lambda_1 \lambda_3) + \sqrt{2}k^4 \lambda_1 \mu_3 + \sqrt{2}v_L^2 v_R^2 \lambda_3 \mu_3\} \\ &\quad - \frac{\sqrt{2}k\mu_3}{v_L v_R} (4v_L^2 v_R^2 (\alpha_1 + \alpha_2) + (v_L^2 - v_R^2)^2 \lambda_3), \end{aligned} \quad (2.4.23)$$

$$D^h = \frac{2\sqrt{2}k^3(v_L^2 - v_R^2)^2((\alpha_1 + \alpha_2)^2 - \lambda_1 \lambda_3)\mu_3}{v_L v_R}. \quad (2.4.24)$$

We notice that the parameter  $\lambda_1$  appears only once in  $M_S^2$ . This enables picking out this parameter in terms of the Higgs mass  $m_h$  as follows. Assuming the parameters  $a(\lambda_1)$ ,  $b(\lambda_1)$ ,  $c(\lambda_1)$  as functions of  $\lambda_1$ , we notice that they are linear functions of the latter (i.e.,  $\lambda_1$ ) and the characteristic polynomial  $P_h^3$  is linear in these parameters, and hence it's linear in  $\lambda_1$ . We solve the following equation

$$P_h^3(m_h) = -m_h^6 + T^h m_h^4 - D_2^h m_h^2 + D^h = 0, \quad (2.4.25)$$

to obtain  $\lambda_1$  in terms of the Higgs mass  $m_h$  as

$$\lambda_1(m_h) = -\frac{-m_h^6 + T^{h(0)} m_h^4 - D_2^{h(0)} m_h^2 + D^{h(0)}}{m_h^4 T^{h(1)} - D_2^{h(1)} m_h^2 + D^{h(1)}}, \quad (2.4.26)$$

where

$$T^h = \lambda_1 T^{h(1)} + T^{h(0)}, \quad D_2^h = \lambda_1 D_2^{h(1)} + D_2^{h(0)}, \quad D^h = \lambda_1 D^{h(1)} + D^{h(0)}. \quad (2.4.27)$$

Explicitly, we have

$$\lambda_1(m_h) = -\frac{A(m_h)}{B(m_h)}, \quad (2.4.28)$$

where  $A(m_h)$  and  $B(m_h)$  are the polynomials

$$A(m_h) = -m_h^6 + \{2(v_L^2 + v_R^2)\lambda_3 - \frac{(v_L^2 v_R^2 + k^2(v_L^2 + v_R^2))\mu_3}{\sqrt{2}kv_L v_R}\}m_h^4$$

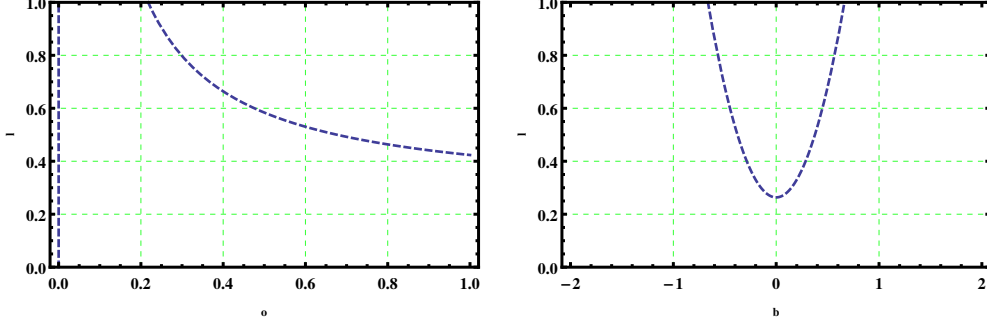


Figure 2.6:  $\lambda_1$  with  $\lambda_3$  and  $\alpha_{12}$  at fixed values of  $t_\beta, \mu_3, \lambda_3, s_w^2$  and  $m_h = 125$ .

$$\begin{aligned}
 & + \frac{1}{kv_L v_R} \{ (v_L^2 + v_R^2)(4k^3 v_L v_R (\alpha_1 + \alpha_2)^2 + \sqrt{2} v_L^2 v_R^2 \lambda_3 \mu_3) \\
 & + \sqrt{2} k^2 (4v_L^2 v_R^2 (\alpha_1 + \alpha_2) + (v_L^2 - v_R^2)^2 \lambda_3) \mu_3 \} m_h^2 \\
 & + \frac{2\sqrt{2} k^3 (v_L^2 - v_R^2)^2 (\alpha_1 + \alpha_2)^2 \mu_3}{v_L v_R}, \tag{2.4.29}
 \end{aligned}$$

$$B(m_h) = 2k^2 m_h^4 - (v_L^2 + v_R^2) \frac{4k^3 v_L v_R \lambda_3 - \sqrt{2} k^4 \mu_3}{kv_L v_R} m_h^2 - \frac{2\sqrt{2} k^3 (v_L^2 - v_R^2)^2 \lambda_3 \mu_3}{v_L v_R}. \tag{2.4.30}$$

Factorizing  $(x - m_h^2)$  out of  $P_h^3$ , it remains the quadratic polynomial

$$P_h^2(x) = -x^2 + (T^h - m_h^2)x + m_h^2(T^h - m_h^2) - D_2^h. \tag{2.4.31}$$

Hence, the other two squared Higgs masses are the solutions of the equation  $P_h^2(x) = 0$ :

$$m_{h3,2}^2 = \frac{1}{2} \{ T^h - m_h^2 \pm \sqrt{(T^h - m_h^2)^2 + 4(m_h^2(T^h - m_h^2) - D_2^h)} \}, \tag{2.4.32}$$

and we have

$$m_{h3}^2 = T^h - m_h^2 - m_{h2}^2 = \frac{D^h}{m_h^2 m_{h2}^2}. \tag{2.4.33}$$

This last relation is expected and clear being  $T^h = \text{Tr}(M_S^2)$  and the eigenvalues of the matrix  $M_S^2$  are themselves the squared masses. We notice that the masses  $m_{h3,2}$  are obtained in terms of the third one  $m_h$ . This idea is generic and we can obtain some of the eigenvalues in terms of others. This will be useful in models with multi Higgs fields and high-dimensions matrices.

## 2.4 Higgs Sector in the ALRM

---

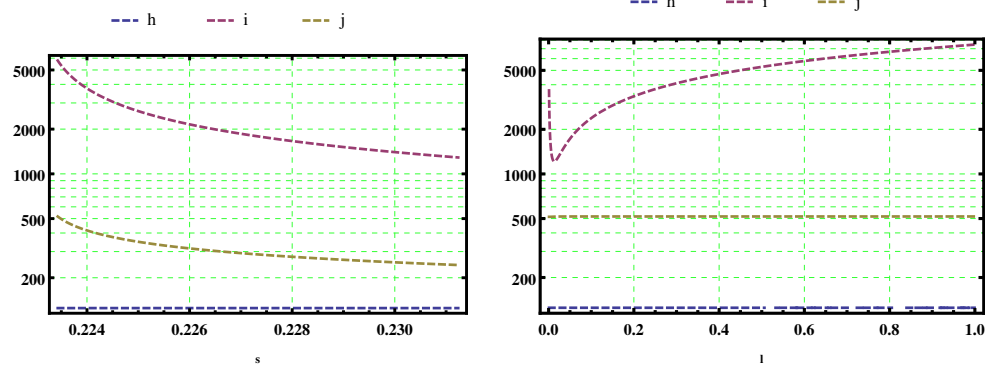


Figure 2.7: Scalar Higgs Masses  $m_{h2}, m_{h3}$  as functions of  $t_\beta$  and  $\mu_3$  at fixed values of  $\alpha_1, \alpha_2, \lambda_3, s_w^2$  and  $m_h = 125$  (left) and  $m_{h3}$  as functions of  $\lambda_3$  at fixed values of  $t_\beta, s_w^2, \mu_3, \alpha_1, \alpha_2$  (right).

The mass squared eigenvalues are the roots of the characteristic polynomial

$$P(x) = -x^3 + Tx^2 - D_2x + D. \quad (2.4.34)$$

The Higgs mass squared eigenvalues are [37, 38, 50, 73, 82]

$$m_k^2 = \frac{1}{3} \left( T - \xi^{k-1} C - \frac{\Delta_0}{\xi^{k-1} C} \right), \quad \xi = \frac{-1 + \sqrt{3}i}{2}, \quad k = 1, 2, 3, \quad (2.4.35)$$

where

$$\Delta_0 = T^2 - 3D_2, \quad (2.4.36)$$

$$\Delta_1 = 2T^3 - 9TD_2 + 27D, \quad (2.4.37)$$

$$C = \sqrt[3]{\frac{1}{2} \left( -\Delta_1 + \sqrt{\Delta_1^2 - 4\Delta_0^3} \right)}. \quad (2.4.38)$$

The discriminant is

$$\Delta = 18TD_2D - 4T^3D + T^2D_2^2 - 4D_2^3 - 27D^2. \quad (2.4.39)$$

If  $\Delta = 0$  and  $\Delta_0 = 0$ , then the equation has a single root (which is a triple root)  $\frac{T}{3}$ .

If  $\Delta = 0$  and  $\Delta_0 \neq 0$ , then there are both a double root  $\frac{TD_2 - 9D}{2\Delta_0}$  and a simple root  $\frac{4TD_2 - 9D + D_2^3}{-\Delta_0}$ .

The matrix  $M_S^2$  can be diagonalized by the unitary transformation:  $T^\dagger M_S^2 T = \text{diag}(m_h^2, m_{h2}^2, m_{h3}^2)$ ,

$$\begin{pmatrix} \phi_2^{0R} \\ \chi_L^{0R} \\ \chi_R^{0R} \end{pmatrix} = \underbrace{\begin{pmatrix} T_{\phi h} & T_{\phi h2} & T_{\phi h3} \\ T_{Lh} & T_{Lh2} & T_{Lh3} \\ T_{Rh} & T_{Rh2} & T_{Rh3} \end{pmatrix}}_T \begin{pmatrix} h \\ h_2 \\ h_3 \end{pmatrix}, \quad (2.4.40)$$

The lightest eigenstate  $h_0 \equiv h$  is the SM-like Higgs, whose mass will be fixed to be  $m_h = 125$  GeV. In general, from the numerical checks, we found that, for a wide range of the parameter space of the model, three  $CP$ -even Higgs bosons ( $h_1$  and  $h_2$ ) are light [of  $\mathcal{O}(100)$  GeV] and the other one ( $h_3$ ) is heavy [of  $\mathcal{O}(1)$  TeV].

It is well known that the eigenvector components are implicit functions of the corresponding eigenvalue. We used this fact to express these components in terms of the eigenvalues explicitly. This simplifies the expressions for eigenvectors a lot.

The eigenvectors are

$$v_h = (f(m_h), g(m_h), 1), \quad v_{h2} = (f(m_{h2}), g(m_{h2}), 1), \quad v_{h3} = (f(m_{h3}), g(m_{h3}), 1), \quad (2.4.41)$$

where we define the two functions:

$$f(x) = \frac{2x^4 v_L v_R + x^2(v_L^2 + v_R^2)(\sqrt{2}k\mu_3 - 4\lambda_3 v_L v_R) - 2\sqrt{2}k\lambda_3\mu_3(v_L^2 - v_R^2)^2}{v_R(x^2(4kv_L v_R(\alpha_1 + \alpha_2) + \sqrt{2}\mu_3 v_L^2) + 2\sqrt{2}\mu_3(k^2(\alpha_1 + \alpha_2) + v_L^2\lambda_3)(v_R^2 - v_L^2))}, \quad (2.4.42)$$

$$g(x) = \frac{v_L(x^2(4kv_L v_R(\alpha_1 + \alpha_2) + \sqrt{2}\mu_3 v_R^2) + 2\sqrt{2}\mu_3(k^2(\alpha_1 + \alpha_2) + v_R^2\lambda_3)(v_L^2 - v_R^2))}{v_R(x^2(4kv_L v_R(\alpha_1 + \alpha_2) + \sqrt{2}\mu_3 v_L^2) + 2\sqrt{2}\mu_3(k^2(\alpha_1 + \alpha_2) + v_L^2\lambda_3)(v_R^2 - v_L^2))}. \quad (2.4.43)$$

Then the rotation matrix  $T$  is the orthonormalization of the matrix of eigenvectors

$$(v_h^{\text{tr}} \ v_{h2}^{\text{tr}} \ v_{h3}^{\text{tr}}). \quad (2.4.44)$$

Thus we have the rotation coefficients

$$T_{\phi h} = \frac{f}{\sqrt{f^2 + g^2 + 1}}, \quad (2.4.45)$$

## 2.4 Higgs Sector in the ALRM

---

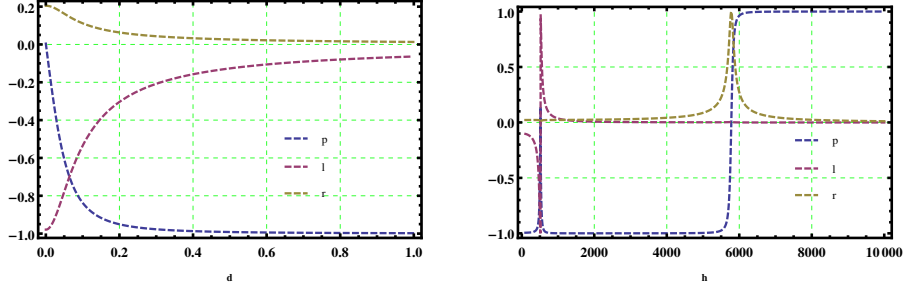


Figure 2.8:  $T_{\phi h}, T_{Lh}, T_{Rh}$  as functions of  $\lambda_3$  at fixed values of  $t_\beta, \mu_3, \alpha_1, \alpha_2, s_w^2$  and  $m_h = 125$ .

$$T_{\phi h2} = \frac{\{f_2(1+g^2) - f(1+gg_2)\}/\sqrt{1+f^2+g^2}}{\sqrt{f_2^2(1+g^2) + (g-g_2)^2 - 2f(f_2+f_2gg_2) + f^2(1+g_2^2)}}, \quad (2.4.46)$$

$$T_{\phi h3} = \frac{(\text{sgn})(-g+g_2)}{\sqrt{f_2^2(1+g^2) + (g-g_2)^2 - 2f(f_2+f_2gg_2) + f^2(1+g_2^2)}}, \quad (2.4.47)$$

$$T_{Lh} = \frac{g}{\sqrt{f^2+g^2+1}}, \quad (2.4.48)$$

$$T_{Lh2} = \frac{\{g_2(1+f^2) - g(1+ff_2)\}/\sqrt{1+f^2+g^2}}{\sqrt{f_2^2(1+g^2) + (g-g_2)^2 - 2f(f_2+f_2gg_2) + f^2(1+g_2^2)}}, \quad (2.4.49)$$

$$T_{Lh3} = \frac{-(\text{sgn})(-f+f_2)}{\sqrt{f_2^2(1+g^2) + (g-g_2)^2 - 2f(f_2+f_2gg_2) + f^2(1+g_2^2)}}, \quad (2.4.50)$$

$$T_{Rh} = \frac{1}{\sqrt{f^2+g^2+1}}, \quad (2.4.51)$$

$$T_{Rh2} = \frac{\{f(f-f_2) + g(g+g_2)\}/\sqrt{1+f^2+g^2}}{\sqrt{f_2^2(1+g^2) + (g-g_2)^2 - 2f(f_2+f_2gg_2) + f^2(1+g_2^2)}}, \quad (2.4.52)$$

$$T_{Rh3} = \frac{(\text{sgn})(f_2g-fg_2)}{\sqrt{f_2^2(1+g^2) + (g-g_2)^2 - 2f(f_2+f_2gg_2) + f^2(1+g_2^2)}}, \quad (2.4.53)$$

where

$$\text{sgn} = \text{sign}\{f_2g - f_3g - fg_2 + f_3g_2 + fg_3 - f_2g_3\}, \quad (2.4.54)$$

and  $f = f(m_h)$ ,  $f_{2,3} = f(m_{h2,3})$  and similarly  $g = g(m_h)$  and  $g_{2,3} = g(m_{h2,3})$ .

Direct calculations confirm that the matrix  $T$  is unitary (indeed, orthogonal), as it must be. See Appendix E for more details about the diagonalization of matrices.

Potential Parameters and VEVs	Domain	Value
$\mu_1^2$	$\mu_1^2 > 0$	$1.3391 \times 10^6$
$\mu_2^2$	$\mu_2^2 > 0$	$1.98637 \times 10^6$
$v$	$SM \sim \mathcal{O}(100) \text{ GeV}$	246
$s_w^2$	Experimental Average	0.231236
$t_\beta = \frac{k}{v_L}$	$\sim 0$	12
$k_1$	$k_1 = 0$	0.
$k$	$k > 0$	245.15
$v_L$	$v_L > 0$	20.4292
$v_R$	$v_R > 0$	1808.35
$\lambda_1$	$0 \leq \lambda_1 \leq 1$	0.531558
$\lambda_2$	$-1 \leq \lambda_2 \leq 1$	0.5
$\lambda_3$	$0 < \lambda_3 \leq 1$	0.6
$\lambda_4$	$0 < \lambda_4 \leq 1$	0.646923
$\alpha_1$	$-1 \leq \alpha_1 \leq 1$	0.3
$\alpha_2$	$-1 \leq \alpha_2 \leq 1$	0.1
$\alpha_3$	$-1 \leq \alpha_3 \leq 1$	0.3
$\mu_3$	$\mu_3 < 0$	-10.

Table 2.2: An ALRM benchmark point. Scalar potential parameters.

#### 2.4.2 Higgs Numerical Session in the ALRM

Table 2.2 gives an ALRM benchmark point for scalar potential parameters.

Table 2.3 gives an ALRM benchmark point for Higgs and gauge spectra.

Table 2.4 gives an ALRM benchmark point for scalar, Pseudoscalar and charged Higgs mixing.

Fig. 2.4 exhibits the dependences

$$m_{1,2\pm}(t_\beta, s_w^2, \lambda_2, \alpha_2, \alpha_3, \alpha_3, \mu_3). \quad (2.4.55)$$

Fig. 2.5 exhibits the dependences

$$m_{1A}(t_\beta, s_w^2, \lambda_2, \alpha_2, \alpha_3, \mu_3), \quad m_{2A}(t_\beta, s_w^2, \mu_3) \quad (2.4.56)$$

Fig. 2.7 exhibits the dependences

$$m_{h_i}(t_\beta, s_w^2, \lambda_1, \lambda_3, \alpha_1, \alpha_2, \mu_3, m_h = 125.), \quad m_{h_1} = m_{1A} \quad (2.4.57)$$

Fig. 2.6 exhibits the dependences

$$\lambda_1(t_\beta, s_w^2, \lambda_3, \alpha_1, \alpha_2, \mu_3, m_h = 125.) \quad (2.4.58)$$

Spectrum	Domain	Value
<b>Higgs Spectra</b>		
$m_h$	$\sim \mathcal{O}(100)$ GeV	125.
$m_{h_2}$	$\sim \mathcal{O}(100)$ GeV	278.188
$m_{h_3}$	$= m_{1A} \sim \mathcal{O}(100)$ GeV	827.461
$m_{h_4}$	$\sim \mathcal{O}(1)$ TeV	1406.59
$m_{1\pm}$	$\sim \mathcal{O}(100)$ GeV	422.748
$m_{2\pm}$	$\sim \mathcal{O}(1)$ TeV	1154.63
$m_{A_1}$	$\sim \mathcal{O}(100)$ GeV	827.461
$m_{A_2}$	$\sim \mathcal{O}(1)$ TeV	277.965
<b>Gauge Spectra</b>		
$M_{W'}$	$\sim \mathcal{O}(10)$ TeV	8438.13
$M_{Z'}$	$\sim \mathcal{O}(10)$ TeV	14249.3
$M_W$	SM	80
$M_Z$	SM	90
$M_A$	0	0

Table 2.3: An ALRM benchmark point. Higgs and Gauge spectra.

Higgs Mixing	Value	Higgs Mixing	Value
$Z_{11}^P$	1.	$Z_{12}^P$	0.
$Z_{13}^P$	0.	$Z_{14}^P$	0.
$Z_{21}^P$	0.	$Z_{22}^P$	0.0830402
$Z_{23}^P$	-0.000934876	$Z_{24}^P$	0.996546
$Z_{31}^P$	0.	$Z_{32}^P$	-0.996483
$Z_{33}^P$	0.0112185	$Z_{34}^P$	0.0830455
$Z_{41}^P$	0.	$Z_{42}^P$	0.0112574
$Z_{43}^P$	0.999937	$Z_{44}^P$	$-4.78144 \times 10^{-20}$
$Z_{11}$	0.	$Z_{12}$	0.
$Z_{13}$	1.	$Z_{14}$	0.
$Z_{21}$	-0.990237	$Z_{22}$	0.10587
$Z_{23}$	0.	$Z_{24}$	0.0906771
$Z_{31}$	-0.105227	$Z_{32}$	-0.994378
$Z_{33}$	0.	$Z_{34}$	0.0118526
$Z_{41}$	0.0914221	$Z_{42}$	0.00219516
$Z_{43}$	0.	$Z_{44}$	0.99581
$Z_{11}^\pm$	-0.0830455	$Z_{12}^\pm$	-0.996546
$Z_{13}^\pm$	0.	$Z_{14}^\pm$	0.
$Z_{21}^\pm$	0.996546	$Z_{22}^\pm$	-0.0830455
$Z_{23}^\pm$	0.	$Z_{24}^\pm$	0.
$Z_{31}^\pm$	0.	$Z_{32}^\pm$	0.
$Z_{33}^\pm$	-0.990936	$Z_{34}^\pm$	-0.134337
$Z_{41}^\pm$	0.	$Z_{42}^\pm$	0.
$Z_{43}^\pm$	0.134337	$Z_{44}^\pm$	-0.990936

Table 2.4: An ALRM benchmark. Scalar, Pseudoscalar and Charged Higgs mixing.

### 2.4.3 Higgs Interactions in the ALRM

The interaction terms of the Higgs fields and gauge bosons are contained in the kinetic Lagrangian of the Higgs fields (2.2.14), while the interaction terms of the Higgs fields and fermions are contained in the Yukawa Lagrangian (2.2.16). The third type of the Higgs interactions is that the interactions between Higgs fields themselves. The terms controlling this type are contained in the scalar potential (2.2.15).

### Higgs-Gauge Boson Interactions in the ALRM

In terms of the physical gauge bosons, the covariant derivative (1.3.25) and the kinetic term of the Higgs bidoublet are given in Eqs. (1.6.95) and (1.6.98). The covariant derivative (2.2.12) of the Higgs doublets  $\chi_L$  and  $\chi_R$  are

$$D_\mu \chi_L = \partial_\mu \chi_L - i \frac{g_L}{2} (W_{L\mu} \cdot \sigma) \chi_L - i \frac{g_{BL}}{2} V_\mu \chi_L \\ = \begin{pmatrix} \partial_\mu \chi_L^+ \\ \partial_\mu \chi_L^0 \end{pmatrix} - i \frac{g_L}{\sqrt{2}} \begin{pmatrix} W_{L\mu}^+ \chi_L^0 \\ W_{L\mu}^- \chi_L^+ \end{pmatrix} - \frac{i}{2} \begin{pmatrix} (2eA_\mu + \frac{g_L \cos 2\theta_W}{c_w} Z_{L\mu} - g_Y t_\varphi Z_{R\mu}) \chi_L^+ \\ -(\frac{g_L}{c_w} Z_{L\mu} + g_Y t_\varphi Z_{R\mu}) \chi_L^0 \end{pmatrix}, \quad (2.4.59)$$

$$D_\mu \chi_R = \partial_\mu \chi_R - i \frac{g_R}{2} (W_{R\mu} \cdot \sigma) \chi_R - i \frac{g_{BL}}{2} V_\mu \chi_R \\ = \begin{pmatrix} \partial_\mu \chi_R^+ \\ \partial_\mu \chi_R^0 \end{pmatrix} - i \frac{g_R}{\sqrt{2}} \begin{pmatrix} W_{R\mu}^+ \chi_R^0 \\ W_{R\mu}^- \chi_R^+ \end{pmatrix} - \frac{i}{2} \begin{pmatrix} (2eA_\mu - 2e \tan \theta_W Z_{L\mu} + \frac{2g_Y}{t_{2\varphi}} Z_{R\mu}) \chi_R^+ \\ -\frac{2g_Y}{\sin 2\varphi} Z_{R\mu} \chi_R^0 \end{pmatrix}. \quad (2.4.60)$$

and their kinetic terms are then

$$|D_\mu \chi_L|^2 = \left| \partial_\mu \chi_L^+ - \frac{i}{2} (g_L \sqrt{2} W_{L\mu}^+ \chi_L^0 + (2eA_\mu + \frac{g_L \cos 2\theta_W}{c_w} Z_{L\mu} - g_Y t_\varphi Z_{R\mu}) \chi_L^+) \right|^2 \\ + \left| \partial_\mu \chi_L^0 - \frac{i}{2} (g_L \sqrt{2} W_{L\mu}^- \chi_L^+ - (\frac{g_L}{c_w} Z_{L\mu} + g_Y t_\varphi Z_{R\mu}) \chi_L^0) \right|^2, \quad (2.4.61)$$

$$|D_\mu \chi_R|^2 = \left| \partial_\mu \chi_R^+ - \frac{i}{2} (g_R \sqrt{2} W_{R\mu}^+ \chi_R^0 + (2eA_\mu - 2e \tan \theta_W Z_{L\mu} + \frac{2g_Y}{t_{2\varphi}} Z_{R\mu}) \chi_R^+) \right|^2 \\ + \left| \partial_\mu \chi_R^0 - i (g_R \sqrt{2} W_{R\mu}^- \chi_R^+ - \frac{2g_Y}{\sin 2\varphi} Z_{R\mu} \chi_R^0) \right|^2. \quad (2.4.62)$$

The Higgs-gauge bosons interactions can be extracted by substituting from Eqs. (2.4.4), (2.4.14) and (2.4.40) for the physical Higgs fields in the above set of equations and eq. (1.6.98).

Using eq. (1.6.98), (2.4.61) and (2.4.62), we find that the kinetic Lagrangian (2.2.14) of the Higgs fields contains the following interaction terms ( $l = 0, 2, 3$ ,  $h_0 = h$ )

$$\mathcal{L}_S^{\text{Kin}} \supset g_{lW_L W_L} h_l W_{L\mu}^+ W_L^{-\mu} + g_{lW_R W_R} h_l W_{R\mu}^+ W_R^{-\mu} + e^2 (h_1^+ h_1^- + h_2^+ h_2^-) A_\mu A^\mu \\ + e\rho_{1l} (h_l h_1^+ W_{L\mu}^- A^\mu + h_l h_1^- W_{L\mu}^+ A^\mu) + e\rho_{2l} (h_l h_2^+ W_{R\mu}^- A^\mu + h_l h_2^- W_{R\mu}^+ A^\mu)$$

$$\begin{aligned}
 & + i\rho_{1l}[(\partial_\mu h_1^+)h_l W_L^{-\mu} - (\partial_\mu h_1^-)h_l W_L^{+\mu} - (\partial_\mu h_l)h_1^+ W_L^{-\mu} + (\partial_\mu h_l)h_1^- W_L^{+\mu}] \\
 & + i\rho_{2l}[(\partial_\mu h_2^+)h_l W_R^{-\mu} - (\partial_\mu h_2^-)h_l W_R^{+\mu} - (\partial_\mu h_l)h_2^+ W_R^{-\mu} + (\partial_\mu h_l)h_2^- W_R^{+\mu}]
 \end{aligned} \tag{2.4.63}$$

where the couplings are

$$g_{lW_L W_L} = g_L M_{W_L} (T_{\phi h_l} s_\beta + T_{L h_l} c_\beta) \tag{2.4.64}$$

$$g_{lW_R W_R} = g_R M_{W_R} (T_{\phi h_l} s_\zeta + T_{R h_l} c_\zeta) \tag{2.4.65}$$

$$\rho_{1l} = \frac{g_L}{2} (T_{\phi h_l} c_\beta - T_{L h_l} s_\beta) \tag{2.4.66}$$

$$\rho_{2l} = \frac{g_R}{2} (T_{\phi h_l} c_\zeta - T_{R h_l} s_\zeta) \tag{2.4.67}$$

It is worth mentioning that the kinetic Lagrangian (2.2.14) of the Higgs fields would contain the following interaction terms

$$\mathcal{L}_S^{\text{Kin}} \supset \beta_{1L}(h_1^+ W_{L\mu}^- A^\mu + h_1^- W_{L\mu}^+ A^\mu) + \beta_{2R}(h_2^+ W_{R\mu}^- A^\mu + h_2^- W_{R\mu}^+ A^\mu) \tag{2.4.68}$$

unless they vanish identically because

$$\beta_{1L} = \frac{eg_L}{2} (kc_\beta - v_L s_\beta) = eM_{W_L} (s_\beta c_\beta - c_\beta s_\beta) \equiv 0, \tag{2.4.69}$$

$$\beta_{2R} = \frac{eg_R}{2} (kc_\zeta - v_R s_\zeta) = eM_{W_R} (s_\zeta c_\zeta - c_\zeta s_\zeta) \equiv 0. \tag{2.4.70}$$

where we used Eqs. (2.3.18) and (2.4.4).

Also the scalar potential (2.2.15) of the Higgs fields contains the following trilinear interaction terms between the neutral scalar fields and the charged scalar fields

$$V(\Phi, \chi_L, \chi_R) \supset 2\mu_{ijl} h_l h_i^+ h_j^- \tag{2.4.71}$$

where the mixed couplings vanish ( $\mu_{12l} = \mu_{21l} = 0$ ) and the other couplings are

$$\begin{aligned}
 \mu_{11l} &= T_{\phi h_l} (\lambda_1 k c_\beta^2 - (\alpha_2 - \alpha_3) v_L s_\beta c_\beta + (\alpha_1 + \alpha_3) k s_\beta^2) \\
 &+ T_{L h_l} (\lambda_3 v_L s_\beta^2 - (\alpha_2 - \alpha_3) k s_\beta c_\beta + (\alpha_1 + \alpha_3) v_L c_\beta^2)
 \end{aligned}$$

## 2.4 Higgs Sector in the ALRM

---

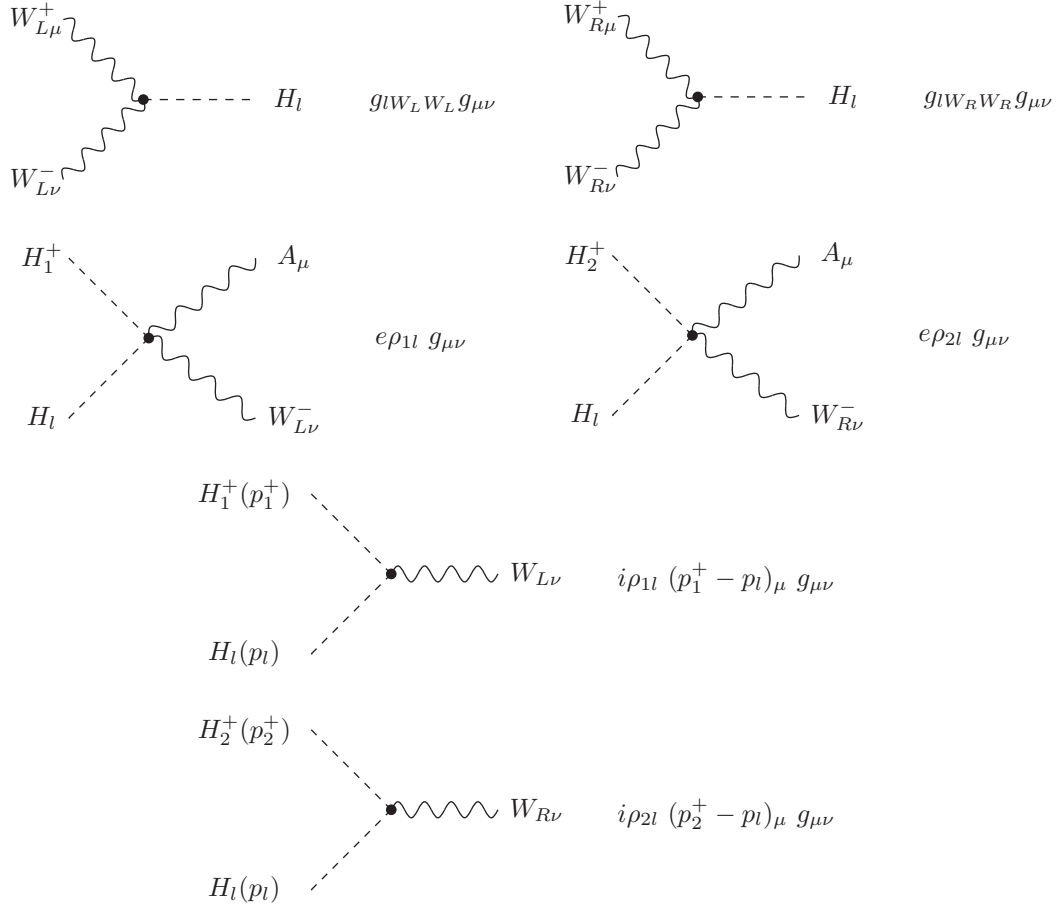


Figure 2.9: Feynman diagrams and rules of Higgs-gauge interactions in the ALRM.

$$+ T_{R h_l} (\lambda_4 v_R s_\beta^2 - \sqrt{2} \mu_3 s_\beta c_\beta + (\alpha_1 + \alpha_2) v_R c_\beta^2), \quad (2.4.72)$$

$$\begin{aligned} \mu_{22l} = & T_{\phi h_l} (\lambda_1 k c_\zeta^2 - (\alpha_2 - \alpha_3) v_R s_\zeta c_\zeta + (\alpha_1 + \alpha_3) k s_\zeta^2) \\ & + T_{R h_l} (\lambda_3 v_R s_\zeta^2 - (\alpha_2 - \alpha_3) k s_\zeta c_\zeta + (\alpha_1 + \alpha_3) v_R c_\zeta^2) \\ & + T_{L h_l} (\lambda_4 v_L s_\zeta^2 - \sqrt{2} \mu_3 s_\zeta c_\zeta + (\alpha_1 + \alpha_2) v_L c_\zeta^2). \end{aligned} \quad (2.4.73)$$

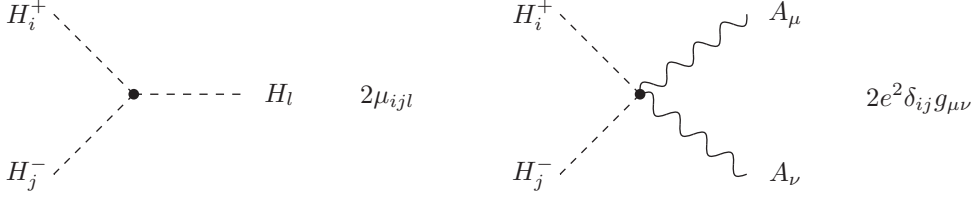


Figure 2.10: Feynman diagram and rule of the trilinear interaction terms between the neutral scalar fields and the charged scalar fields (left) and the four-vertex of two photons and two charged Higgs bosons (right) in the ALRM.

### Higgs-Fermion Interactions in the ALRM

We can invert Eqs. (2.3.46) and (2.3.47) to solve for the Yukawa matrices in terms of the physical masses of fermions after substitution from Eqs. (2.3.48) and (2.3.49) as follows

$$Y^q = \frac{\sqrt{2}}{vs_\beta} V_L^u M_u^{\text{diag}} V_R^{u\dagger}, \quad Y_L^q = \frac{\sqrt{2}}{vc_\beta} V_L^d M_d^{\text{diag}} V_R^{d\dagger}, \quad Y_R^q = \frac{\sqrt{2}}{v_R} V_R^{d'} M_{d'}^{\text{diag}} V_L^{d'\dagger} \quad (2.4.74)$$

$$Y_L^\ell = \frac{\sqrt{2}}{vc_\beta} V_L^\nu \sqrt{M_\nu^{\text{diag}} M_N}, \quad Y^\ell = \frac{\sqrt{2}}{vs_\beta} V_L^e M_e^{\text{diag}} V_R^{e\dagger}, \quad Y_R^\ell = \frac{\sqrt{2}}{v_R} V_R^n M_n^{\text{diag}} V_L^{n\dagger} \quad (2.4.75)$$

where the Yukawa matrix of the neutrinos  $Y_L^\ell$  is expressed as in [24]. From Eqs. (2.3.48), (2.3.48) and (2.3.55), the transformations to the physical fermions are

$$f_{L,R} \rightarrow V_{L,R}^f f_{L,R} \quad (2.4.76)$$

Substituting from Eqs. (2.4.74) and (2.4.75) into the Yukawa Lagrangian (2.2.16) and using the transformations (2.4.76), and then substituting from Eqs. (2.4.4), (2.4.14) and (2.4.1) and writing the Hermitian conjugate terms explicitly, we find that the interaction terms of the neutral scalar and pseudoscalar and charged Higgs bosons with quarks and exotic quarks are

$$\begin{aligned} -\mathcal{L}_{\text{Yuk}} &\supset \frac{1}{vs_\beta} \bar{u} M_u^{\text{diag}} (T_{\phi h_l} h_l - iU_{11} A_2 \gamma^5) u + \frac{1}{vc_\beta} \bar{d} M_d^{\text{diag}} (T_{L h_l} h_l + iU_{21} A_2 \gamma^5) d \\ &+ \frac{1}{v' c_\zeta} \bar{d}' M_{d'}^{\text{diag}} (T_{R h_l} h_l - iU_{31} A_2 \gamma^5) d' \end{aligned}$$

$$\begin{aligned}
 & + \frac{1}{vs_\beta} \bar{d}(V^{L\dagger} M_u^{\text{diag}} V^R (h_1 - iA_1) P_R) d' + h.c. \\
 & - \frac{\sqrt{2}}{v} \bar{u}(ct_\beta M_u^{\text{diag}} V^L P_L + t_\beta V^L M_d^{\text{diag}} P_R) h_1^+ d + h.c. \\
 & - \frac{\sqrt{2}}{v'} \bar{u}(ct_\zeta M_u^{\text{diag}} V^R P_R + t_\zeta V^R M_{d'}^{\text{diag}} P_L) h_2^+ d' + h.c.
 \end{aligned} \tag{2.4.77}$$

where the matrix  $U$  is the rotation matrix of the pseudoscalar Higgs bosons defined in eq. (2.4.14), and  $V^{L,R}$  are the left and right CKM matrices

$$V^L = V_L^{u\dagger} V_L^d, \quad V^R = V_R^{u\dagger} V_R^d \tag{2.4.78}$$

While for leptons we have

$$\begin{aligned}
 -\mathcal{L}_{\text{Yuk}} \supset & \frac{1}{vs_\beta} \bar{e} M_e^{\text{diag}} (T_{\phi h_l} h_l + iU_{11} A_2 \gamma^5) e + \frac{1}{v' c_\zeta} \bar{n} M_n^{\text{diag}} (T_{R h_l} h_l + iU_{31} A_2 \gamma^5) n \\
 & + \frac{1}{vs_\beta} \bar{\nu} (U^L M_e^{\text{diag}} U^{R\dagger} (h_1 + iA_1) P_R) n + h.c. \\
 & + \frac{1}{vc_\beta} \bar{\nu} (\sqrt{M_\nu^{\text{diag}} M_N} (T_{R h_l} h_l - iU_{21} A_2) P_R) N + h.c. \\
 & + \frac{\sqrt{2}}{v} \bar{\nu} (ct_\beta U^L M_e^{\text{diag}} P_R) h_1^+ e + h.c. \\
 & + \frac{\sqrt{2}}{v} \bar{e} (t_\beta U^{L\dagger} \sqrt{M_\nu^{\text{diag}} M_N} P_R) h_1^- N + h.c. \\
 & - \frac{\sqrt{2}}{v'} \bar{e} (ct_\zeta M_e^{\text{diag}} U^{R\dagger} P_R + t_\zeta U^{R\dagger} M_n^{\text{diag}} P_L) h_2^- n + h.c.
 \end{aligned} \tag{2.4.79}$$

where  $U^{L,R}$  are the left and right PMNS matrices

$$U^L = V_L^{\nu\dagger} V_L^e, \quad U^R = V_R^{n\dagger} V_R^e \tag{2.4.80}$$

Note that in contrast to the LRSM, the couplings of the interactions of quarks and leptons with the neutral scalar and pseudoscalar Higgs bosons are diagonal and hence the tree-level FCNC is absent in the ALRM. The couplings of the interactions of quarks and leptons with the charged Higgs bosons are not diagonal since the CKM and PMNS matrices are not diagonal.

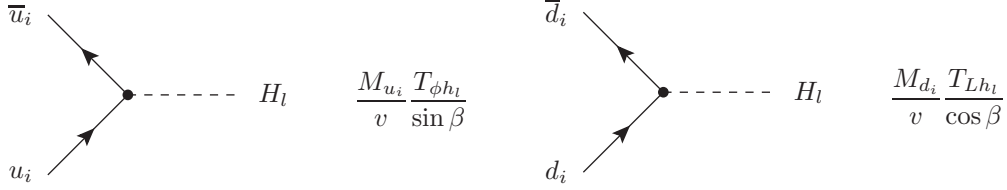


Figure 2.11: Feynman diagrams and rules of quarks and neutral scalar Higgs fields in the ALRM.

### The SM-like Higgs couplings in the ALRM

Here we just adjust our notation for the SM-like Higgs to be comfortable with the next chapter. From now on, we will identify  $H \equiv h_4$  and  $(T_{\phi h}, T_{Lh}, T_{Rh}) \equiv (T_{\phi h3}, T_{4L}, T_{4R})$ .

From Eqs. (2.4.77) and (2.4.79), the SM-like Higgs couplings with fermions in the ALRM are given by

$$Y_{h\bar{u}u} = \frac{m_u}{v} \frac{T_{\phi h}}{s_\beta}, \quad Y_{h\bar{d}d} = \frac{m_d}{v} \frac{T_{Lh}}{c_\beta}, \quad Y_{h\bar{d}'d'} = \frac{m_{d'}}{v'} \frac{T_{Rh}}{c_\zeta}, \quad (2.4.81)$$

$$Y_{h\bar{e}e} = \frac{m_e}{v} \frac{T_{\phi h}}{s_\beta}, \quad Y_{h\bar{n}n} = \frac{m_n}{v'} \frac{T_{Rh}}{c_\zeta}, \quad (2.4.82)$$

where  $m_f = M_f^{\text{diag}}$  and the elements  $T_{\phi h}$ ,  $T_{Lh}$ , and  $T_{Rh}$  are the mixing couplings of the gauge eigenstates  $\phi_2^{0R}$ ,  $\chi_L^{0R}$ , and  $\chi_R^{0R}$ , respectively, with the SM-like Higgs  $h$ . The SM-like Higgs couplings with the charged electroweak gauge bosons are denoted by

$$g_{hWW} = g_{0W_L W_L}, \quad g_{hW'W'} = g_{0W_R W_R}. \quad (2.4.83)$$

Finally, the SM-like Higgs couplings with the charged Higgs bosons are denoted by

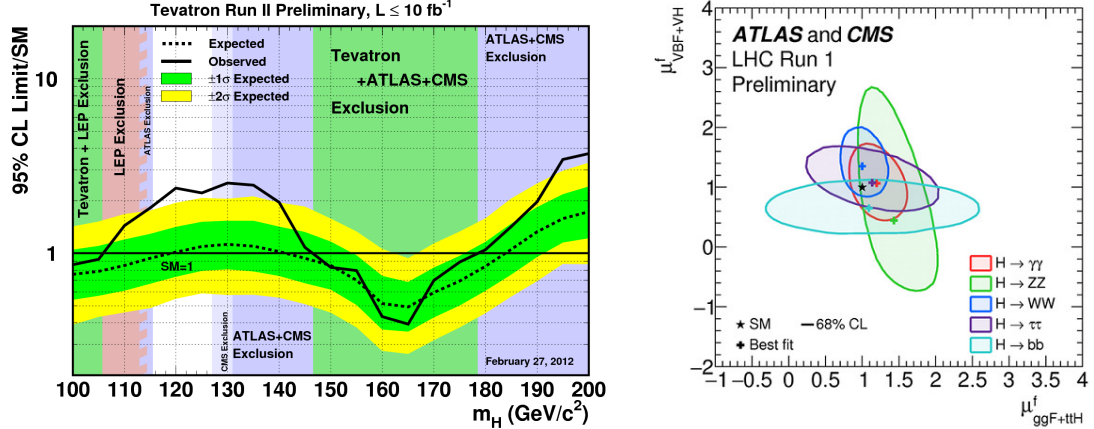
$$\lambda_{hh_1^\pm h_1^\mp} = 2\mu_{114}, \quad \lambda_{hh_2^\pm h_2^\mp} = 2\mu_{224}. \quad (2.4.84)$$

# 3

## PHENOMENOLOGICAL ASPECTS OF THE ALRM

### 3.1 Introduction

The latest results of ATLAS and CMS collaborations [4, 43], confirmed the Higgs discovery with mass around 125 GeV, through Higgs decay channels:  $h \rightarrow \gamma\gamma$ ,  $h \rightarrow ZZ^{(*)} \rightarrow 4l$ , and  $h \rightarrow WW^{(*)} \rightarrow l\nu l\nu$  at integrated luminosities of  $5.1 \text{ fb}^{-1}$  taken at energy  $\sqrt{s} = 7 \text{ TeV}$  and  $19.6 \text{ fb}^{-1}$  taken at  $\sqrt{s} = 8 \text{ TeV}$ . These results still indicate possible discrepancies between their results for signal strengths in these channels [1, 2, 29, 30]. We show that our ALRM has a rich Higgs sector, and consists of one bidoublet and two LH and RH doublets. Therefore, one obtains four neutral  $CP$ -even and two  $CP$ -odd Higgs bosons, in addition to two charged Higgs bosons. It turns out that most of these Higgs bosons can be light, of the order the electroweak scale, and can be accessible at the LHC. We also find that the contributions of the charged Higgs bosons to the decay rate of  $h \rightarrow \gamma\gamma$  are not significant. Furthermore, we show that, due to the mixing among the neutral  $CP$ -even Higgs bosons, the couplings of the SM-like Higgs, which is the lightest one, with the top quark and  $W$ -gauge boson are slightly modified respect to the SM ones. Therefore, the ALRM predictions for signal



(a) Higgs masses excluded by ATLAS, CMS, LEP and Tevatron experiments. (b) Combined ATLAS and CMS limits on Higgs production and decays.

Figure 3.1: Higgs boson mass, production and decays.

strengths of Higgs decays, in particular,  $h \rightarrow \gamma\gamma$  and  $h \rightarrow W^+W^-$ , are consistent with the SM expectation.

Another salient feature of ALRM is the presence of an extra down-type quark,  $d'$ . We analyze the striking signature of this exotic quark at the LHC. We show that the most promising  $d'$ -production channel is  $gg \rightarrow \bar{d}'d'$ , due to the direct coupling of  $d'$  to gluons with a strong coupling constant and color factor. Then,  $d'$  decays to a jet and lepton plus missing energy. We find that the cross section of this process is of  $\mathcal{O}(1)$  fb, which can be probed at the LHC with 14 TeV center-of-mass energy.

### 3.2 The $h \rightarrow \gamma\gamma$ Decay in the ALRM

As advocated in the Introduction, CMS and ATLAS collaborations observed a SM-like Higgs boson with mass around 125 GeV and signal decay strengths as given in Eqs. (3.2.1)-(3.2.6). For instance, ATLAS found [2, 4, 29]

### 3.2 The $h \rightarrow \gamma\gamma$ Decay in the ALRM

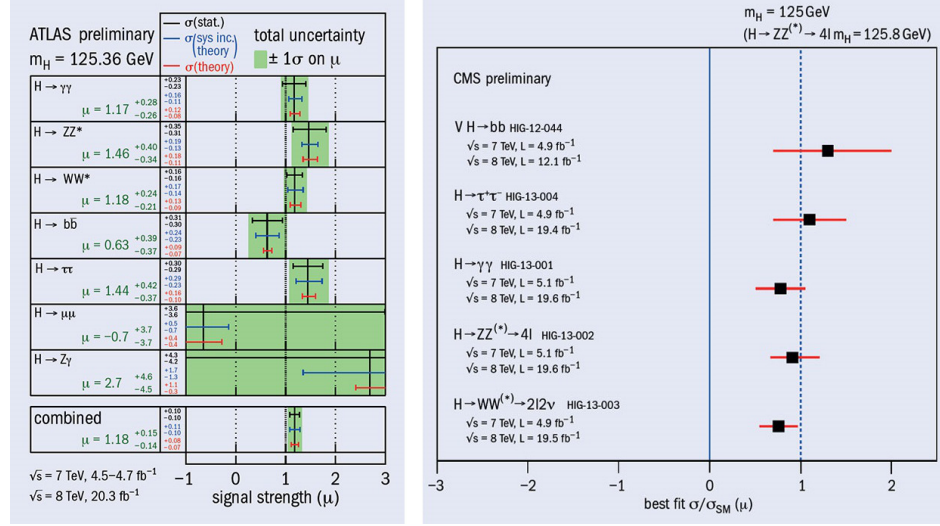


Figure 3.2: ATLAS and CMS signal strength of Higgs decays.

$$\mu_{\gamma\gamma} = \mu(h \rightarrow \gamma\gamma) = 1.17 \pm 0.27, \quad (3.2.1)$$

$$\mu_{ZZ} = \mu(h \rightarrow ZZ) = 0.8 \pm 0.29, \quad (3.2.2)$$

$$\mu_{WW} = \mu(h \rightarrow WW) = 1.01 \pm 0.31, \quad (3.2.3)$$

while the CMS experiment reported that the signal strength of these decays are given by [1, 30, 43]:

$$\mu_{\gamma\gamma} = \mu(h \rightarrow \gamma\gamma) = 1.14^{+0.26}_{-0.23}, \quad (3.2.4)$$

$$\mu_{ZZ} = \mu(h \rightarrow ZZ) = 0.91^{+0.3}_{-0.24}, \quad (3.2.5)$$

$$\mu_{WW} = \mu(h \rightarrow WW) = 0.76 \pm 0.21. \quad (3.2.6)$$

These results indicate enhancement in the diphoton decay channel, with more than  $2\sigma$  deviation, which could be a very important signal for possible new physics beyond the SM. Much work has been done to accommodate these results in different extensions of the SM [15, 17, 18, 22, 23, 25, 26, 39, 45, 70].

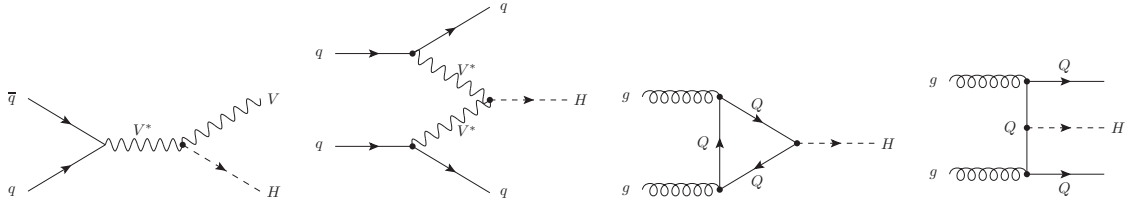


Figure 3.3: The dominant SM Higgs production mechanisms in hadronic collisions.

### 3.2.1 Higgs Production

The Higgs boson couplings to the SM particles are proportional to their masses. Hence, it couples preferentially to the heavy particles, that is the massive weak vector bosons  $W$  and  $Z$  (eq. (1.2.67)) and the top quark and, to a lesser extent, the bottom quark (eq. (1.2.68)). Accordingly, the main production mechanisms for Higgs particles at hadron colliders make use of this fact. Feynmann diagrams of the main four production processes are shown in Fig. 3.3, they are thus [34]:

1. the associated production with  $W/Z$  bosons:

$$q\bar{q} \rightarrow V^* \rightarrow V + h, \quad (3.2.7)$$

2. the weak vector boson fusion processes:

$$qq \rightarrow V^*V^* \rightarrow qq + h, \quad (3.2.8)$$

3. the gluon-gluon fusion mechanism:

$$gg \rightarrow h, \quad (3.2.9)$$

4. the associated Higgs production with heavy top or bottom quarks:

$$gg \rightarrow q\bar{q} + h. \quad (3.2.10)$$

Parton distribution functions (PDFs)  $q_i(x, Q^2)$  describe the momentum distribution of a parton  $q_i$  in the proton, where  $x$  is the parton momentum fraction and  $Q^2$  is the squared center of mass energy at which a process takes place. They play a central role at hadron colliders to precisely predict the production cross sections of the various signal and background processes. They are estimated from a global fit to the available data from deep-inelastic scattering, Drell-Yan and hadronic data and hence they are plagued by uncertainties arising from this fitting distributions. Other uncertainties arise from the scale evolution relevant to the scattering processes together with the effects of unknown perturbative higher-order corrections [34]. Many collaborations CTEQ [46, 72], MRST [56, 80], Alekhin [5] and others [20] provide schemes to precisely estimate the uncertainties on the prediction of physical observables at hadron colliders.

We discuss briefly the Higgs production cross section in the gluon-gluon fusion mechanism, as it's the dominant among the others, due to the contributions from the PDFs. To lowest order (LO), the partonic cross section can be expressed by the gluonic width of the Higgs boson

$$\hat{\sigma}_{\text{LO}}(gg \rightarrow h) = \sigma_0^h m_h^2 \delta(\hat{s} - m_h^2) = \frac{\pi^2}{8m_h} \Gamma_{\text{LO}}(h \rightarrow gg) \delta(\hat{s} - m_h^2) \quad (3.2.11)$$

where  $\hat{s}$  is the  $gg$  invariant energy squared. Substituting in this LO approximation the Breit-Wigner form of the Higgs boson width, in place of the zero-width  $\delta$  distribution

$$\delta(\hat{s} - m_h^2) \rightarrow \frac{1}{\pi} \frac{\hat{s}\Gamma_h/m_h}{(\hat{s} - m_h^2)^2 + (\hat{s}\Gamma_h/m_h)^2} \quad (3.2.12)$$

and recalling the lowest-order two-gluon decay width of the Higgs boson

$$\Gamma(h \rightarrow gg) = \frac{G\alpha_s^2 m_h^3}{36\sqrt{2}\pi^3} \left| \frac{3}{4} \sum_Q F_{1/2}(x_Q) \right|^2, \quad (3.2.13)$$

one finds for the cross section

$$\sigma_0^h = \frac{G\alpha_s^2}{288\sqrt{2}\pi} \left| \frac{3}{4} \sum_Q F_{1/2}(x_Q) \right|^2, \quad (3.2.14)$$

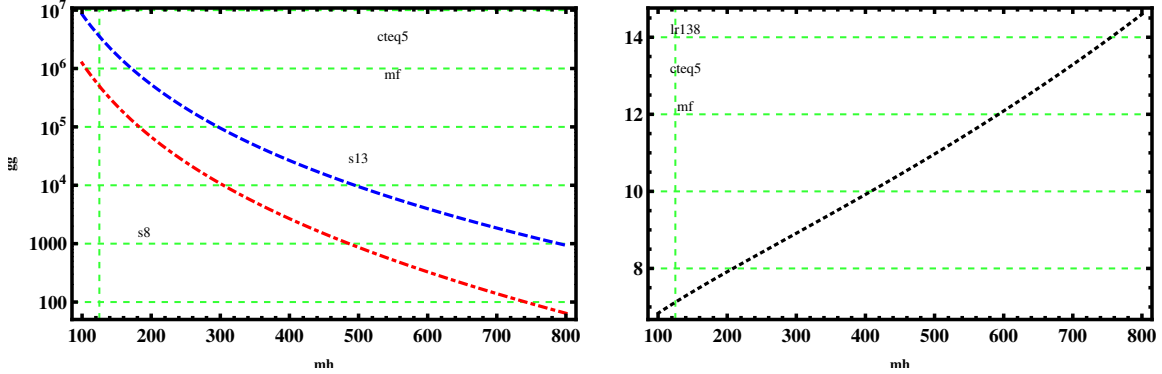


Figure 3.4: Gluon luminosity for Higgs production at the LHC.

where  $x_Q = m_h^2/4m_Q^2$  and the loop functions  $F_i(x)$  are given by [23, 36]

$$F_1(x) = -[2x^2 + 3x + 3(2x - 1) \arcsin^2(\sqrt{x})]x^{-2}, \quad (3.2.15)$$

$$F_{1/2}(x) = 2[x + (x - 1) \arcsin^2(\sqrt{x})]x^{-2}, \quad (3.2.16)$$

$$F_0(x) = -[x - \arcsin^2(\sqrt{x})]x^{-2}. \quad (3.2.17)$$

The proton-proton cross section at LO in the narrow-width approximation reads

$$\sigma_{\text{LO}}(pp \rightarrow h) = \sigma_0^h \tau_h \frac{d\mathcal{L}^{gg}}{d\tau_h}, \quad (3.2.18)$$

where the gluon luminosity is defined in terms of the gluon density  $g(x, \mu_F^2)$  at a factorization scale  $\mu_F$  by

$$\frac{d\mathcal{L}^{gg}}{d\tau} = \int_\tau^1 \frac{dx}{x} \{g(x, \mu_F^2)g(\frac{\tau}{x}, \mu_F^2)\}, \quad (3.2.19)$$

and the Drell-Yan variable is defined as usual by  $\tau_h = m_h^2/s$  with  $s$  being the invariant collider energy squared. Figure 3.4 illustrates the gluon luminosity using the CTEQ5 PDFs gluon density  $g(x, \mu_F^2)$  at the factorization scale  $\mu_F = 125$  GeV and the collider center of mass energies  $\sqrt{s} = 8$  TeV and  $\sqrt{s} = 13$  TeV (left) and the luminosity ratio (right) vs running Higgs mass  $m_h$ . We notice that the gluon luminosity increases with

### 3.2 The $h \rightarrow \gamma\gamma$ Decay in the ALRM

---

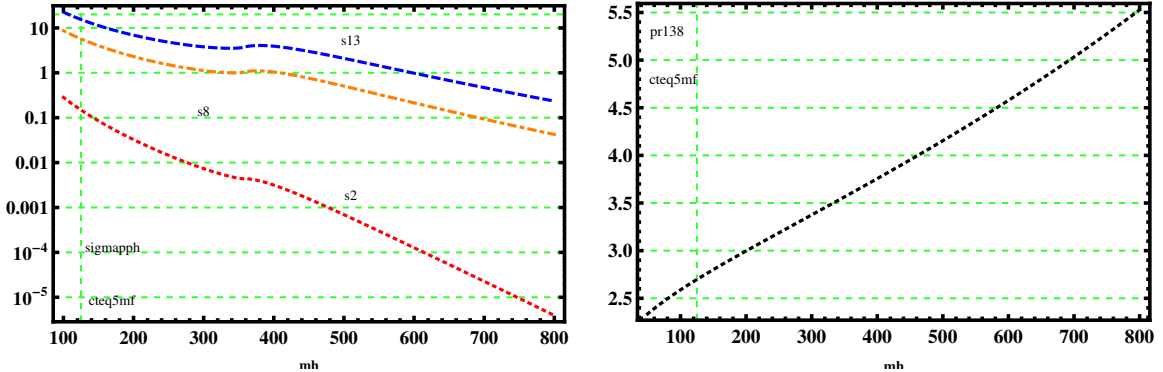


Figure 3.5: Higgs production cross section at the LHC and Tevatron.

the center of mass collider energy while it decreases with heavier Higgs produced. At the fixed Higgs mass  $m_h = 125$  GeV, the gluon luminosity value is about  $0.498 \times 10^6$  at  $\sqrt{s} = 8$  TeV while it's  $3.549 \times 10^6$  at  $\sqrt{s} = 13$  TeV.

Figure 3.5 illustrates the hadronic production cross section for the  $gg$  fusion process at LO as a function of  $m_h$  at the LHC and the Tevatron. The CTEQ5 set of PDFs has been used and the factorization scale is fixed to  $\mu_F = 125$  GeV and the collider center of mass energies  $\sqrt{s} = 8$  TeV and  $\sqrt{s} = 13$  TeV at the LHC and  $\sqrt{s} = 1.96$  TeV at the Tevatron. We notice that the production cross section increases with the center of mass collider energy while it decreases with heavier Higgs produced. At the fixed Higgs mass  $m_h = 125$  GeV, the production cross section value is about 5.704 pb at  $\sqrt{s} = 8$  TeV and 15.387 at  $\sqrt{s} = 13$  TeV at the LHC, while it's 0.148529 pb at  $\sqrt{s} = 1.96$  TeV.

For more details about NLO and NNLO production cross section and other Higgs production mechanisms, visit [34].

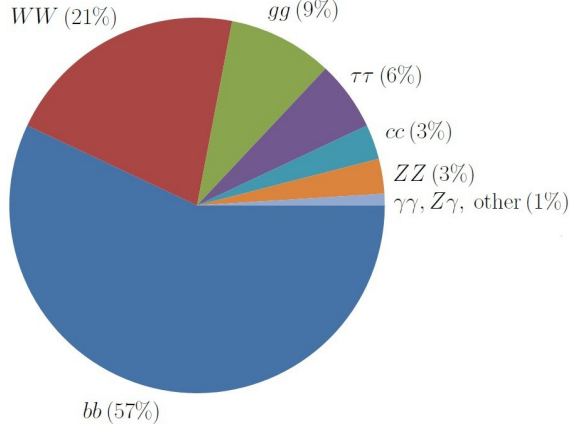


Figure 3.6: SM Higgs decays at  $m_h = 125$  GeV.

### 3.2.2 Higgs Decays

Depending on the fact that, in the SM the Higgs couplings to gauge bosons and fermions are directly proportional to the masses of the particles, the Higgs boson will have the tendency to decay into the heaviest ones allowed by phase space.

For instance, the partial decay width of the Higgs boson decays into fermion pairs is given by [34]

$$\Gamma(h \rightarrow f\bar{f}) = \frac{n_c |Y_{hff}|^2}{8\pi} m_h (1 - x_f)^{3/2}, \quad x_f = \frac{4m_f^2}{m_h^2}. \quad (3.2.20)$$

According to fermion mass hierarchy, decays to heaviest fermion pairs are dominant. In the lepton case, only decays into  $\tau^+\tau^-$  pairs (Fig. 3.7) and, to a much lesser extent, decays into muon pairs are relevant, while in the quark case, the relevant decays are those into pairs of bottom (Fig. 3.8) and, to a much lesser extent, charm quarks quarks. For further information about the QCD corrections of the decays into light quarks, see [34].

After the confirmation of the Higgs mass to be about 125 GeV, Higgs boson decays also to the massive electroweak gauge bosons  $V = W^\pm, Z$  in two different manners,

### 3.2 The $h \rightarrow \gamma\gamma$ Decay in the ALRM

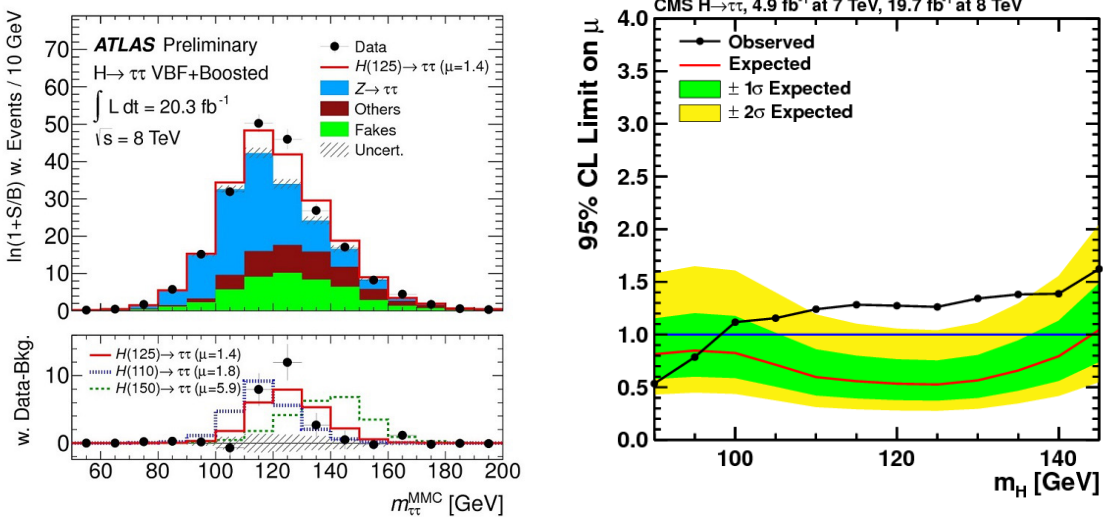


Figure 3.7: ATLAS and CMS Higgs decay channel  $h \rightarrow \tau\tau$ .

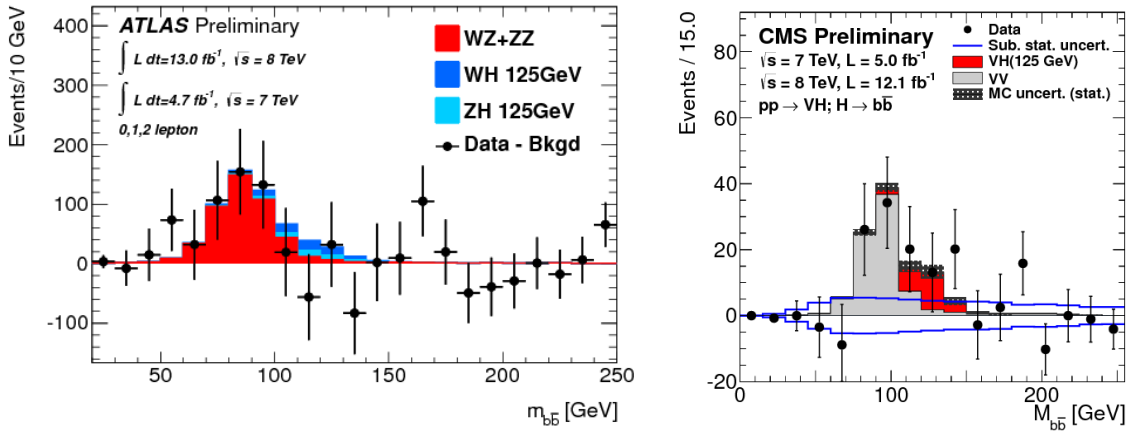


Figure 3.8: ATLAS and CMS Higgs decay channel  $h \rightarrow b\bar{b}$ .

either to have three or four physical final states. In the case of three body decay, the Higgs boson decays into a physical gauge boson and a virtual one that decays into two leptons or two quarks. Otherwise, the Higgs boson rather decays into two virtual vector bosons each of which decays to leptons (Fig. 3.9 and Fig. 3.10) or/and quarks,

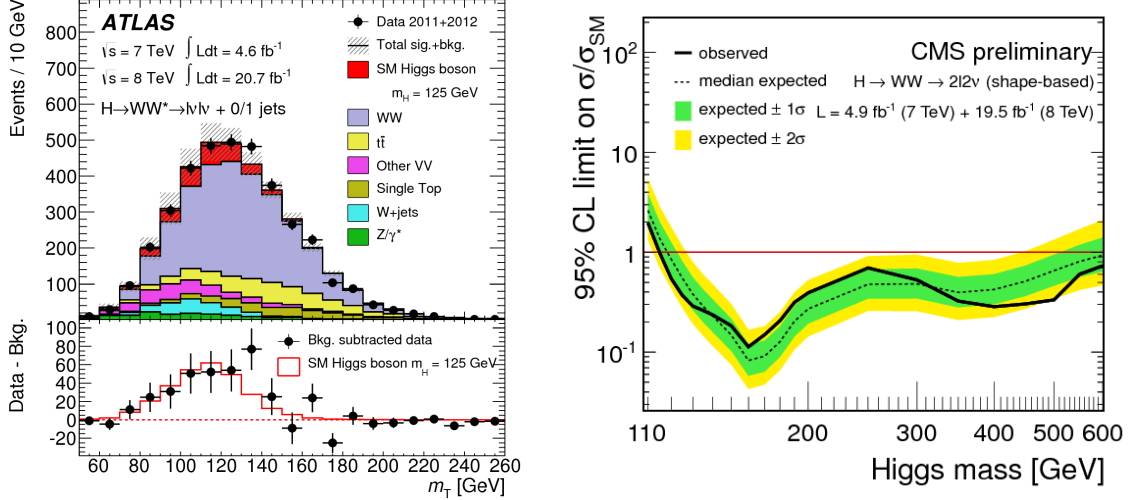


Figure 3.9: ATLAS and CMS Higgs decay channels  $h \rightarrow WW^* \rightarrow 2l2\nu$ .

and we have four body decay for the Higgs boson. In the case of three body decay of the Higgs boson into vector bosons, the decay width is [34]

$$\Gamma(h \rightarrow VV^*) = \frac{9G^2 m_V^4 |g_{hVV}|^2}{16\pi^3} m_h \delta'_V R_T(x_V), \quad x_V = \frac{4M_V^2}{m_h^2}, \quad (3.2.21)$$

where

$$R_T(x_V) = \frac{3(1 - 2x_V + \frac{5}{4}x_V^2)}{\sqrt{x_V - 1}} \arccos \frac{3x_V - 4}{x_V^{3/2}} - \frac{4 - x_V}{2x_V} \left( 2 - \frac{13}{4}x_V + \frac{47}{16}x_V^2 \right) - \frac{3}{4} \left( 1 - \frac{3}{2}x_V + \frac{1}{4}x_V^2 \right) \log x_V, \quad (3.2.22)$$

and in the case of four body decay, it is [34]

$$\Gamma(h \rightarrow V^*V^*) = \frac{|g_{hVV}|^2}{\pi^2} \int_0^{m_h^2} \frac{dq_1^2 M_V \Gamma_V}{(q_1^2 - M_V^2)^2 + M_V^2 \Gamma_V^2} \int_0^{(m_h - q_1)^2} \frac{dq_2^2 M_V \Gamma_V}{(q_2^2 - M_V^2)^2 + M_V^2 \Gamma_V^2} \Gamma_0, \quad (3.2.23)$$

where  $\Gamma_V$  is the  $V$  decay width and the matrix element squared  $\Gamma_0$  is

$$\Gamma_0 = \frac{G m_h^3}{16\sqrt{2}\pi} \delta_V \sqrt{\lambda(q_1^2, q_2^2; m_h^2)} \{ \lambda(q_1^2, q_2^2; m_h^2) + \frac{12q_1^2 q_2^2}{m_h^4} \}, \quad (3.2.24)$$

### 3.2 The $h \rightarrow \gamma\gamma$ Decay in the ALRM

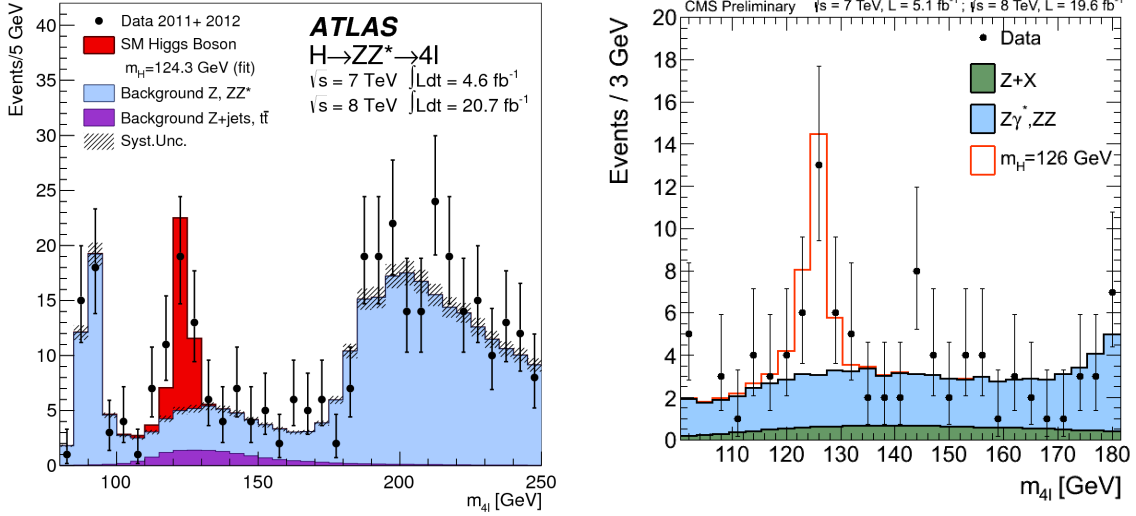


Figure 3.10: ATLAS and CMS Higgs decay channels  $h \rightarrow ZZ^* \rightarrow 4l$ .

where  $\lambda(x, y; z) = (1 - x/z - y/z)^2 - 4xy/z^2$ ,  $\delta_V = 2(1)$  for  $V = W(Z)$ .

Since gluons and photons are massless, the Higgs boson can't not decay two photons or gluons at tree level, however, this is possible but on the loop level. The lowest-order two-gluon, two-photon and  $Z$ -photon decay widths of the Higgs boson are, respectively

$$\Gamma(h \rightarrow gg) = \frac{G\alpha_s^2 m_h^3}{36\sqrt{2}\pi^3} \left| \frac{3}{4} \sum_Q F_{1/2}(x_Q) \right|^2, \quad (3.2.25)$$

$$\Gamma(h \rightarrow \gamma\gamma) = \frac{\alpha^2 m_h^3}{1024\pi^3} \left| \sum_f N_{c,f} Q_f^2 \frac{2Y_{h\bar{f}f}}{m_f} F_{1/2}(x_f) + \frac{g_{hWW}}{M_W^2} Q_W^2 F_1(x_W) \right|^2, \quad (3.2.26)$$

$$\Gamma(h \rightarrow Z\gamma) = \frac{G^2 M_W^2 \alpha m_h^3}{64\pi^4} (1 - \frac{1}{4}x_Z)^3 \left| \sum_f (N_{c,f} Q_f \hat{v}_f / c_W) \frac{2Y_{h\bar{f}f}}{m_f} F_{1/2}(x_f, \lambda_f) + \frac{g_{hWW}}{M_W^2} Q_W^2 F_1(x_W, \lambda_W) \right|^2, \quad (3.2.27)$$

where

$$F_{1/2}(x, \lambda) = I_1(x, \lambda) - I_2(x, \lambda), \quad (3.2.28)$$

$$I_1(x, \lambda) = c_W \left\{ 4 \left( 3 - \frac{s_W^2}{c_W^2} \right) I_2(x, \lambda) + \left[ \left( 1 + \frac{2}{\tau} \right) \frac{s_W^2}{c_W^2} - \left( 5 + \frac{2}{\tau} \right) \right] I_1(x, \lambda) \right\}, \quad (3.2.29)$$

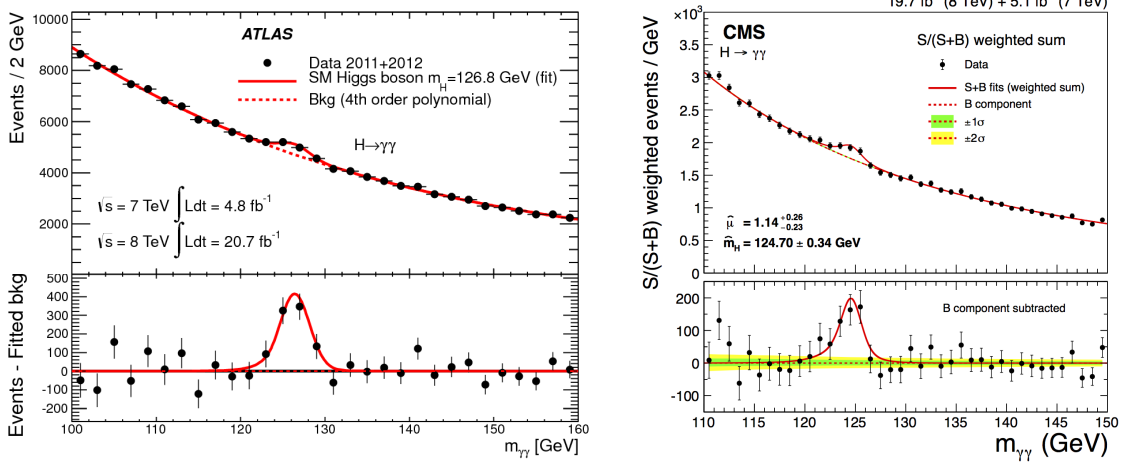


Figure 3.11: ATLAS and CMS Higgs discovery via the decay channel  $h \rightarrow \gamma\gamma$ .

$$I_1(x, \lambda) = \frac{\tau\lambda}{2(\tau - \lambda)} + \frac{\tau^2\lambda^2}{2(\tau - \lambda)^2}[f(\tau^{-1}) - f(\lambda^{-1})] + \frac{\tau^2\lambda}{2(\tau - \lambda)^2}[g(\tau^{-1}) - g(\lambda^{-1})], \quad (3.2.30)$$

$$I_2(x, \lambda) = -\frac{\tau\lambda}{2(\tau - \lambda)}[f(\tau^{-1}) - f(\lambda^{-1})], \quad (3.2.31)$$

$$g(x) = \frac{\sqrt{1-x^{-1}}}{2}[\log \frac{1+\sqrt{1-x^{-1}}}{1-\sqrt{1-x^{-1}}} - i\pi] \quad (3.2.32)$$

where

$$x_f = \frac{4m_f^2}{m_h^2}, \quad x_V = \frac{4M_V^2}{m_h^2}, \quad \lambda_f = \frac{4m_f^2}{M_Z^2}, \quad \lambda_W = \frac{4M_W^2}{M_Z^2}. \quad (3.2.33)$$

### 3.2.3 The $h \rightarrow \gamma\gamma$ Decay

The Higgs signal strength of the decay channel,  $h \rightarrow \gamma\gamma$ , relative to the SM expectation is defined as

$$\mu_{\gamma\gamma} = \frac{\sigma(pp \rightarrow h \rightarrow \gamma\gamma)}{\sigma(pp \rightarrow h \rightarrow \gamma\gamma)^{\text{SM}}} = \frac{\sigma(pp \rightarrow h)}{\sigma(pp \rightarrow h)^{\text{SM}}} \frac{\text{BR}(h \rightarrow \gamma\gamma)}{\text{BR}(h \rightarrow \gamma\gamma)^{\text{SM}}}$$

$$= \frac{\Gamma(h \rightarrow gg)}{\Gamma(h \rightarrow gg)^{\text{SM}}} \frac{\Gamma_{\text{tot}}^{\text{SM}}}{\Gamma_{\text{tot}}} \frac{\Gamma(h \rightarrow \gamma\gamma)}{\Gamma(h \rightarrow \gamma\gamma)^{\text{SM}}} = \kappa_{gg} \cdot \kappa_{\text{tot}}^{-1} \cdot \kappa_{\gamma\gamma}, \quad (3.2.34)$$

where  $\sigma(pp \rightarrow h)$  is the total Higgs production cross section and  $\text{BR}(h \rightarrow \gamma\gamma)$  is the branching ratio of the corresponding channel. The total Higgs decay width is given by the sum of the dominant Higgs partial decay widths,  $\Gamma_{\text{tot}} = \Gamma_{\bar{b}b} + \Gamma_{WW} + \Gamma_{ZZ} + \Gamma_{gg} + \Gamma_{\bar{\tau}\tau}$ . Other partial decay widths are much smaller and can be safely neglected. In the SM with 125 GeV Higgs mass, these partial decay widths are given by:  $\Gamma_{\bar{b}b} = 2.3 \times 10^{-3}$  GeV,  $\Gamma_{WW} = 8.7 \times 10^{-4}$  GeV,  $\Gamma_{ZZ} = 1.1 \times 10^{-4}$  GeV,  $\Gamma_{gg} = 3.5 \times 10^{-4}$  and  $\Gamma_{\bar{\tau}\tau} = 2.6 \times 10^{-4}$  GeV. As shown in the previous section, the Higgs couplings  $g_{hWW}$  and  $Y_{h\bar{b}b}$  may slightly change from the SM values. Hence, the total decay width of the Higgs boson remains very close to the SM result. This has been confirmed numerically, and to a very good approximation, one can consider  $\kappa_{\text{tot}} \simeq 1$ .

As the photon is massless, the first contribution to the decay  $h \rightarrow \gamma\gamma$  is that from the one-loop level. For problem construction, we give the only four relevant Feynman rules of the SM in Fig. 3.12. These four Feynman rules lead to only three one  $W$ -loop diagrams for the  $h \rightarrow \gamma\gamma$  decay through a  $W$  loop. The three diagrams in the unitary gauge are shown in Fig. 3.13. It is now straightforward to write down the amplitudes corresponding to these three diagrams. The corresponding amplitudes are [40]

$$\begin{aligned} \mathcal{M}_1 = & \frac{-ie^2 g M}{(2\pi)^4} \int d^4 k \left[ g_\alpha^\beta - \left(k + \frac{k_1 + k_2}{2}\right)_\alpha \left(k + \frac{k_1 + k_2}{2}\right)^\beta / M^2 \right] \\ & \times \left[ g^{\rho\sigma} - \left(k + \frac{-k_1 + k_2}{2}\right)^\rho \left(k + \frac{-k_1 + k_2}{2}\right)^\sigma / M^2 \right] \\ & \times \left[ g^{\alpha\gamma} - \left(k - \frac{k_1 + k_2}{2}\right)^\alpha \left(k - \frac{k_1 + k_2}{2}\right)^\gamma / M^2 \right] \\ & \times \left[ \left(k + \frac{3k_1 + k_2}{2}\right)_\rho g_{\beta\mu} + \left(k + \frac{-3k_1 + k_2}{2}\right)_\beta g_{\mu\rho} + (-2k - k_2)_\mu g_{\rho\beta} \right] \\ & \times \frac{\left(k - \frac{k_1 + 3k_2}{2}\right)_\sigma g_{\gamma\nu} + \left(k + \frac{-k_1 + 3k_2}{2}\right)_\gamma g_{\nu\sigma} + (-2k + k_1)_\nu g_{\sigma\gamma}}{\left[\left(k + \frac{k_1 + k_2}{2}\right)^2 - M^2 + i\epsilon\right] \left[\left(k + \frac{-k_1 + k_2}{2}\right)^2 - M^2 + i\epsilon\right] \left[\left(k - \frac{k_1 + k_2}{2}\right)^2 - M^2 + i\epsilon\right]} \end{aligned} \quad (3.2.35)$$

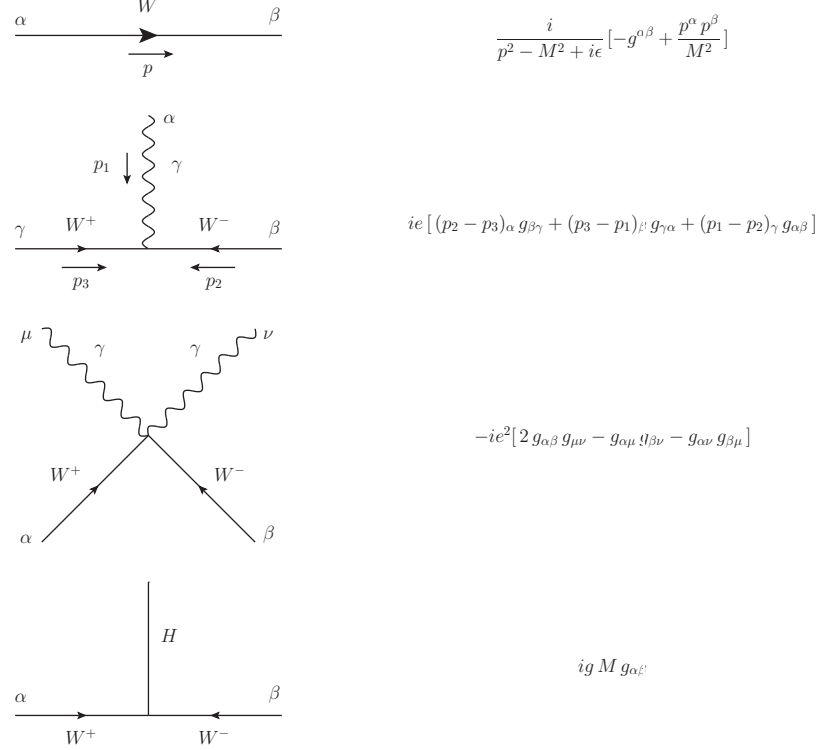


Figure 3.12: Feynman rules in the unitary gauge for the decay  $h \rightarrow \gamma\gamma$  at the one W-loop level in the SM.

$$\begin{aligned}
 \mathcal{M}_2 &= \frac{ie^2 g M}{(2\pi)^4} \int d^4 k [ g_\alpha^\beta - (k + \frac{k_1 + k_2}{2})_\alpha (k + \frac{k_1 + k_2}{2})^\beta / M^2 ] \\
 &\times [ g^{\alpha\gamma} - (k - \frac{k_1 + k_2}{2})^\alpha (k - \frac{k_1 + k_2}{2})^\gamma / M^2 ] \\
 &\times \frac{2 g_{\mu\nu} g_{\beta\gamma} - g_{\mu\beta} g_{\nu\gamma} - g_{\mu\gamma} g_{\nu\beta}}{[(k + \frac{k_1 + k_2}{2})^2 - M^2 + i\epsilon] [(k - \frac{k_1 + k_2}{2})^2 - M^2 + i\epsilon]} \quad (3.2.36) \\
 \mathcal{M}_3 &= \frac{-ie^2 g M}{(2\pi)^4} \int d^4 k [ g_\alpha^\beta - (k + \frac{k_1 + k_2}{2})_\alpha (k + \frac{k_1 + k_2}{2})^\beta / M^2 ] \\
 &\times [ g^{\rho\sigma} - (k + \frac{k_1 - k_2}{2})^\rho (k + \frac{k_1 - k_2}{2})^\sigma / M^2 ] \\
 &\times [ g^{\alpha\gamma} - (k - \frac{k_1 + k_2}{2})^\alpha (k - \frac{k_1 + k_2}{2})^\gamma / M^2 ]
 \end{aligned}$$

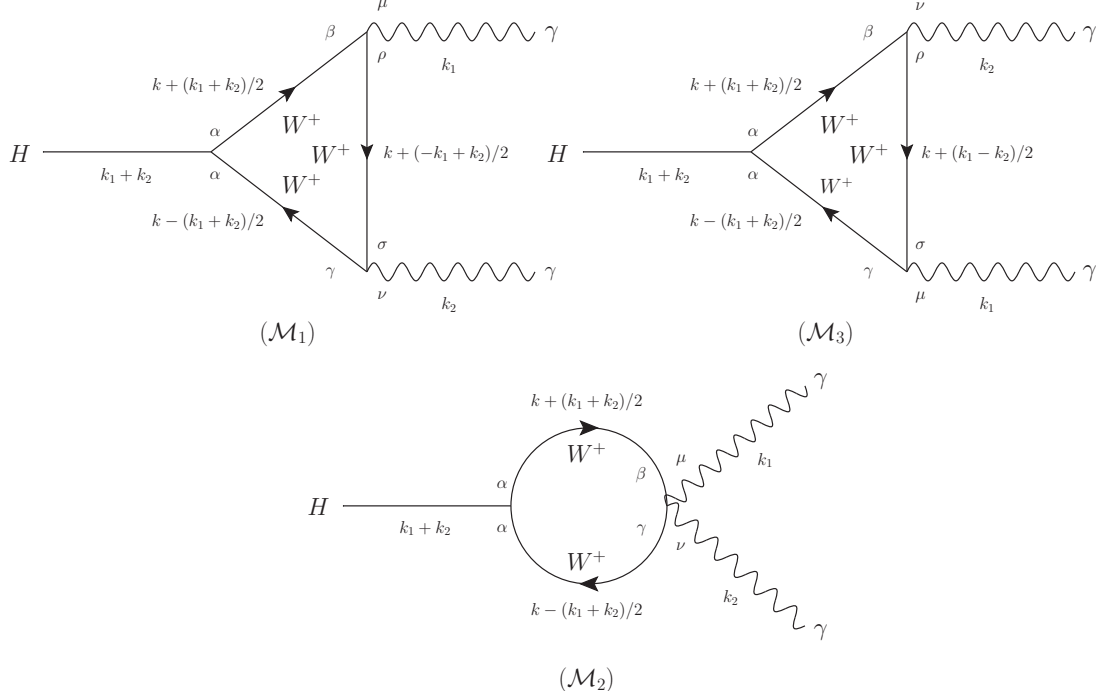


Figure 3.13: The one-loop diagrams with virtual  $W$ 's in the unitary gauge that contribute to the amplitude for  $h \rightarrow \gamma\gamma$  in the SM.

$$\begin{aligned}
 & \times \left[ (k + \frac{k_1 + 3k_2}{2})_\rho g_{\beta\nu} + (k + \frac{k_1 - 3k_2}{2})_\beta g_{\nu\rho} + (-2k - k_1)_\nu g_{\rho\beta} \right] \\
 & \times \frac{\left( k - \frac{3k_1 + k_2}{2} \right)_\sigma g_{\gamma\mu} + \left( k + \frac{3k_1 - k_2}{2} \right)_\gamma g_{\mu\sigma} + (-2k + k_2)_\mu g_{\sigma\gamma}}{\left[ \left( k + \frac{k_1 + k_2}{2} \right)^2 - M^2 + i\epsilon \right] \left[ \left( k + \frac{k_1 - k_2}{2} \right)^2 - M^2 + i\epsilon \right] \left[ \left( k - \frac{k_1 + k_2}{2} \right)^2 - M^2 + i\epsilon \right]}.
 \end{aligned} \tag{3.2.37}$$

where  $M$  is the  $W$ -mass. Following Feynman calculus, these amplitudes lead to the loop function (3.2.15) [23]. Similarly deduced the loop functions for the fermions and the charged scalar loops (3.2.16) and (3.2.17) [36].

Now, we turn to the SM-like Higgs decay into a diphoton,  $W^+W^-$  and  $ZZ$  in our ALRM. As shown in the previous section, the low-energy effective theory of the ALRM contains two charged Higgs bosons that can be light, of  $\mathcal{O}(100)$  GeV, and may

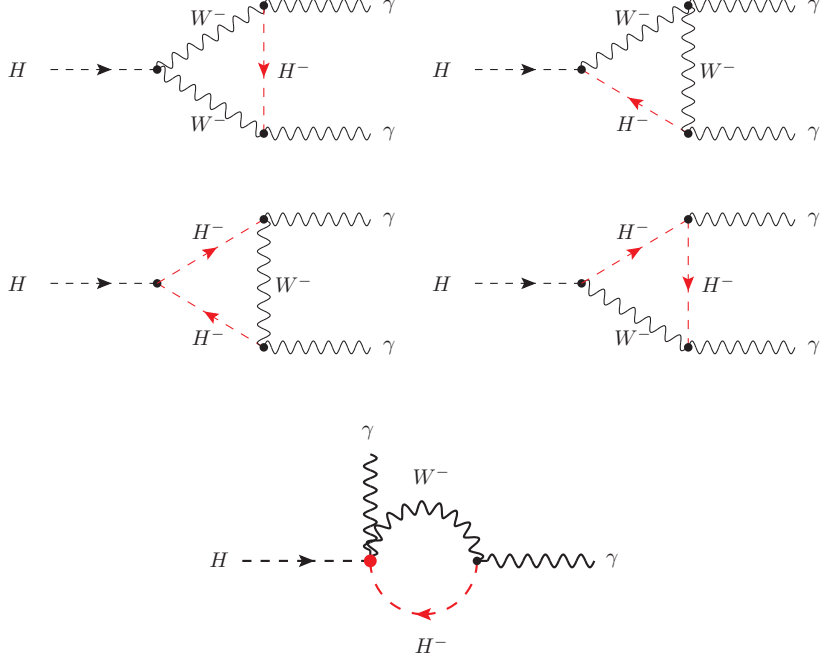


Figure 3.14: Feynman diagrams for the Higgs decay  $h \rightarrow \gamma\gamma$  mediated by gauge bosons  $W^\pm$  and scalars  $h^\pm$  which vanish in the ALRM.

give relevant contributions to the SM-like Higgs decay into a diphoton. In addition, the couplings of the SM-like Higgs with a top quark and  $W$  gauge boson may be suppressed or even flipped, which would lead to significant enhancement/suppression in  $\Gamma(h \rightarrow \gamma\gamma)$ . The Feynman diagrams of the Higgs decay  $h \rightarrow \gamma\gamma$ , mediated by the gauge bosons  $W^\pm$ , top quark, and light-charged Higgs bosons are shown in Fig. 3.16. Note that in the conventional LRSM there are interaction vertices among charged Higgs, the  $W$ -boson and neutral Higgs/photon; therefore, another four diagrams with  $W^\pm$  and  $h^\pm$  running in the loop of triangle diagrams can be generated. In our ALRM, these vertices identically vanish due to the discrete  $S$  symmetry according to Eqs. (2.4.68), (2.4.69) and (2.4.70). These vanishing diagrams are shown Fig. 3.14. In this case, the one-loop partial decay width of the  $H$  decay into two photons is given

### 3.2 The $h \rightarrow \gamma\gamma$ Decay in the ALRM

---

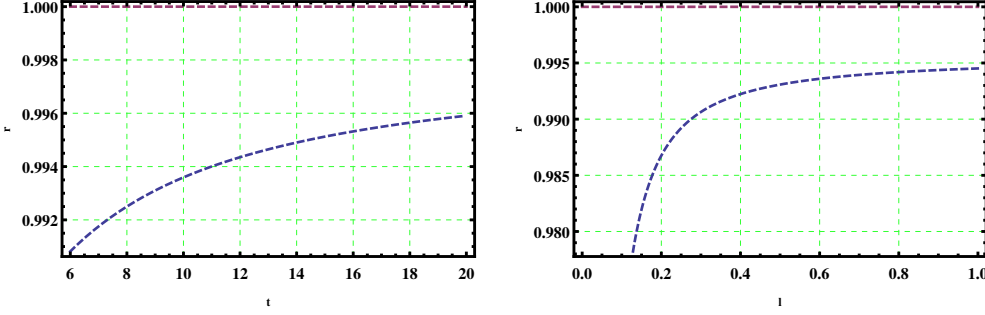


Figure 3.15: The Higgs decay width  $\Gamma(h \rightarrow \gamma\gamma)$  of the SM like Higgs with mass  $m_h = 125$  GeV as function of  $t_\beta$  (left) and  $\lambda_3$  (right) at fixed values of  $\mu_3, \alpha_1, \alpha_2, \alpha_3, s_w^2$ .

by [23, 34–36]

$$\Gamma(h \rightarrow \gamma\gamma) = \frac{\alpha^2 m_H^3}{1024\pi^3} \left| \frac{g_{hWW}}{M_W^2} Q_W^2 F_1(x_W) + N_{c,t} Q_t^2 \frac{2Y_{h\bar{t}t}}{m_t} F_{1/2}(x_t) + \sum_{i=1}^2 Q_{h_i^\pm}^2 \frac{\lambda_{hh_i^\pm h_i^\mp}}{m_{h_i^\pm}^2} F_0(x_{h_i^\pm}) \right|^2, \quad (3.2.38)$$

where  $x_k = m_h^2/4m_k^2$ ,  $m_k = m_t, M_W, m_{h_{1,2}^\pm}$ . The color factor and electric charges are given by  $N_{c,t} = 3$ ,  $Q_W = Q_{h_i^\pm} = 1$ , and  $Q_t = 2/3$ . Recall that the relevant Higgs couplings in the ALRM are given by  $g_{hWW}$ ,  $Y_{h\bar{t}t}$ , and  $\lambda_{hh_i^\pm h_i^\mp}$  in Eqs. (2.4.81), (2.4.82), (2.4.83) and (2.4.84), with  $T_{\phi h} \sim T_{Lh} \gg T_{Rh}$ . Finally, the loop functions  $F_i(x)$  are given by [23, 36]

$$F_1(x) = -[2x^2 + 3x + 3(2x - 1) \arcsin^2(\sqrt{x})]x^{-2}, \quad (3.2.39)$$

$$F_{1/2}(x) = 2[x + (x - 1) \arcsin^2(\sqrt{x})]x^{-2}, \quad (3.2.40)$$

$$F_0(x) = -[x - \arcsin^2(\sqrt{x})]x^{-2}. \quad (3.2.41)$$

For Higgs mass of order 125 GeV and charged Higgs mass of order 200 GeV, the loop functions  $F_1(x_W)$ ,  $F_{1/2}(x_t)$ , and  $F_0(x_{h^\pm})$  are of order  $-8.32$ ,  $+1.38$ , and  $+0.43$ , respectively. Therefore, the partial decay width  $\Gamma(h \rightarrow \gamma\gamma)$  can be enhanced through one of the following possibilities: (i) large charged Higgs couplings such that  $\lambda_{hh^\pm H^\mp}/m_{h^\pm}^2$  is of order  $g_{hWW}/M_W^2$ , and with an opposite sign to compensate the difference in

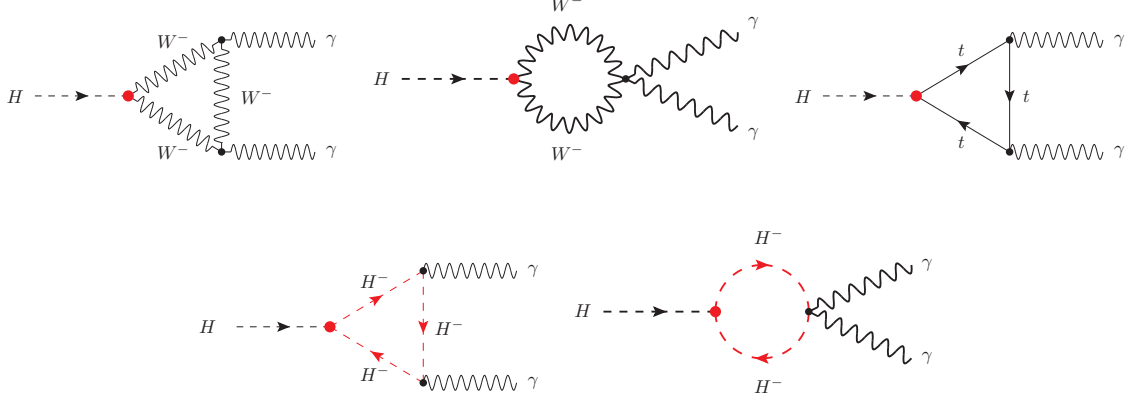


Figure 3.16: Feynman diagrams for the Higgs decay  $h \rightarrow \gamma\gamma$  mediated by gauge bosons  $W^\pm$ , a top quark, and charged scalars  $h^\pm$ .

sign between  $F_1(x_W)$  and  $F_0(x_{h^\pm})$ ; (ii) either the sign of the top Yukawa coupling,  $Y_{h\bar{t}t}$ , or the sign of the coupling between the  $W$  boson and the SM-like Higgs,  $g_{hWW}$ , is flipped so that a constructive interference between  $W$ -gauge boson and top-quark contributions takes place; and (iii) a significant reduction for the top Yukawa coupling,  $Y_{h\bar{t}t}$ , to minimize the destructive interference between  $W$  and  $t$  contributions. In Fig. 3.19, we display the changes in  $g_{hWW}$  and  $Y_{h\bar{t}t}$ , normalized to their SM values. As can be seen from this figure, both couplings are slightly changed from their expectations in the SM. In addition, both  $g_{hWW}$  and  $Y_{h\bar{t}t}$  may flip their sign simultaneously, and hence the usual destructive interference between  $W$ -gauge boson and top-quark contributions remains intact. Therefore, one would not expect any enhancement of  $\Gamma(h \rightarrow \gamma\gamma)$ . The sign correlation between the coupling ratios can be understood from the fact that the parameters  $T_{\phi h}$  and  $T_{Lh}$  in Eqs. (2.4.81), (2.4.82) and (2.4.83), which lead to the modifications of these couplings, have the same sign in the allowed region of ALRM parameter space, as shown in Fig. 3.19.

The Higgs boson production at the LHC is dominated by gluon-gluon fusion. As in the SM, this channel is mediated by top quarks via a one-loop triangle diagram.

### 3.2 The $h \rightarrow \gamma\gamma$ Decay in the ALRM

---

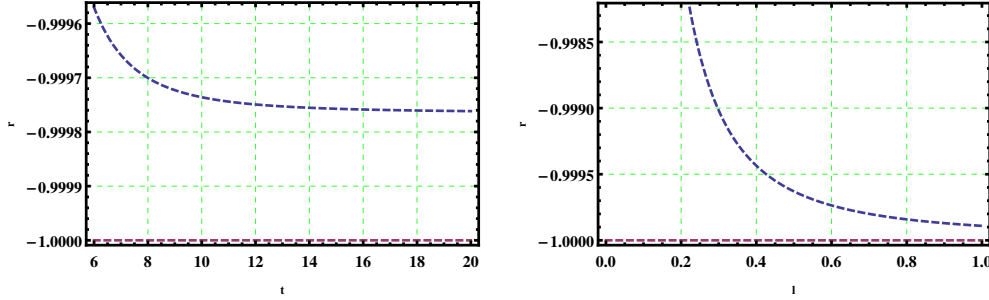


Figure 3.17: Higgs coupling ratios.

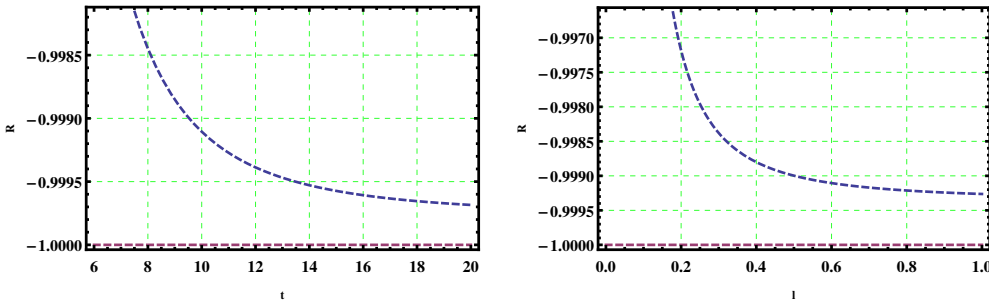


Figure 3.18: Higgs coupling ratios.

The extra quark  $d'$  gives a negligible contribution to  $\sigma(gg \rightarrow h)$  due to the suppression of its coupling with the SM-like Higgs and also its large mass. As mentioned, the top Yukawa coupling can be slightly different from the SM coupling; therefore, the ratio  $\kappa_{gg} = \Gamma(h \rightarrow gg)/\Gamma(h \rightarrow gg)^{\text{SM}}$  can be slightly deviated from 1.

In Fig. 3.20, we display the results of  $\kappa_{\gamma\gamma} = \Gamma(h \rightarrow \gamma\gamma)/\Gamma(h \rightarrow \gamma\gamma)^{\text{SM}}$  and  $\kappa_{gg}$  as function of  $\tan \beta$  for  $0 < \lambda_1, \lambda_3, \lambda_4 < \sqrt{4\pi}$ ,  $-\sqrt{4\pi} < \lambda_2 < 0$ ,  $-\sqrt{4\pi} < \alpha_1, \alpha_2, \alpha_3 < \sqrt{4\pi}$ ,  $100 < m_{h_{1,2}^\pm} < 300$ , and  $\mu_3 < 0$ , to be consistent with the perturbative unitarity and the minimization and boundedness from below conditions (2.3.2)–(2.3.6). It is worth mentioning that for  $\mu_3 < 0$ , one finds, from the minimization conditions, that  $\lambda_4 - \lambda_3 > 0$ , and from (2.3.2),  $\lambda_3 \geq 0$  and hence  $\lambda_4 > \lambda_3 \geq 0$ . In our numerical analysis, we express the parameters  $\mu_1^2$ ,  $\mu_2^2$ , and  $\lambda_4$  in terms of the three vevs  $v_L$ ,  $v_R$ , and  $k$  (or  $v$ ,  $t_\beta$ , and  $M_{W'}$ ). We also substitute the parameters  $\mu_3$  and  $\alpha_3$  in terms of the

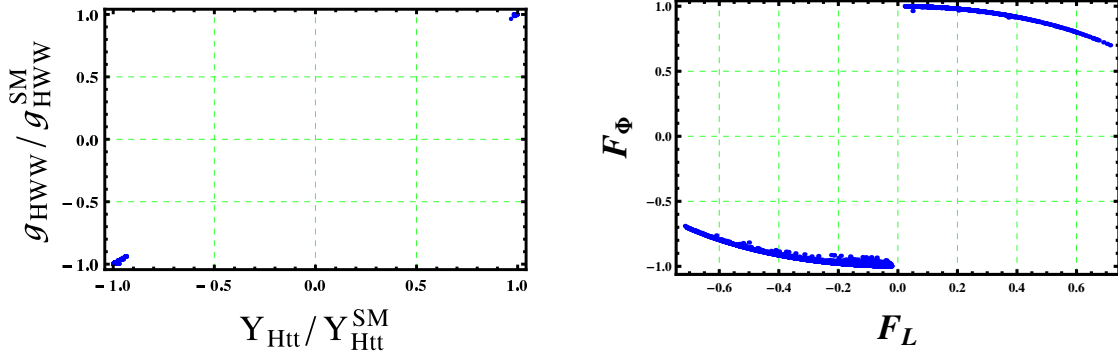


Figure 3.19: (Left) The relation between the coupling ratios  $g_{hWW}/g_{hWW}^{\text{SM}}$  and  $Y_{H\bar{t}t}/Y_{H\bar{t}t}^{\text{SM}}$ . (Right) The relation between the mixing parameters  $F_\Phi = T_{\phi h}$  and  $F_L = T_{Lh}$ .

charged Higgs masses  $m_{h_{1,2}^\pm}$  and the parameter  $\lambda_1$  in terms of the SM-like Higgs mass  $M_H = 125$  GeV. Thus, one can write the matrix  $T \equiv T(t_\beta, M_{W'}, m_{h_{1,2}^\pm}, \lambda_3, \alpha_1, \alpha_2)$ . This figure confirms our theoretical expectation and shows that both of  $\kappa_{\gamma\gamma}$  and  $\kappa_{gg}$  can slightly deviate from 1.

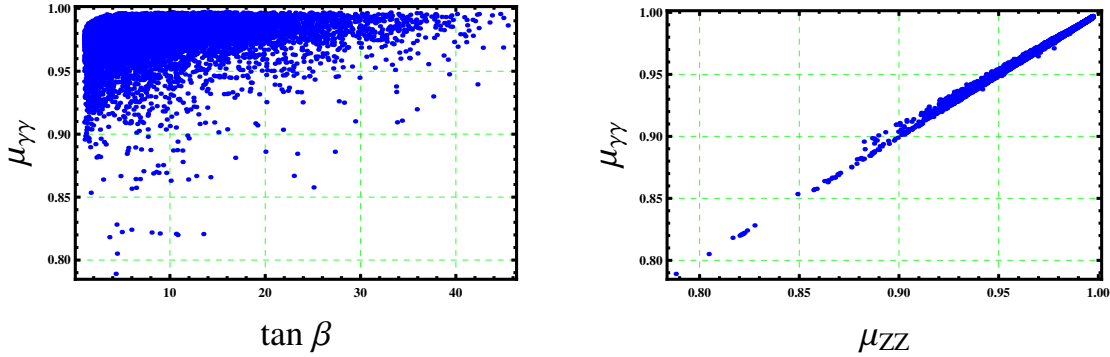


Figure 3.21: (Left) The signal strength  $\mu_{\gamma\gamma}$  as a function of  $t_\beta$  and the parameters  $\lambda_3, \alpha_1, \alpha_2$  and  $m_{h_{1,2}^\pm}$ . (Right) Correlation between  $\mu_{\gamma\gamma}$  and  $\mu_{ZZ}$  in the ALRM.

In this case, it is clear that the signal strength  $\mu_{\gamma\gamma}$  is also close to the SM expectation and can be still consistent with both ATLAS and CMS experimental results.

### 3.2 The $h \rightarrow \gamma\gamma$ Decay in the ALRM

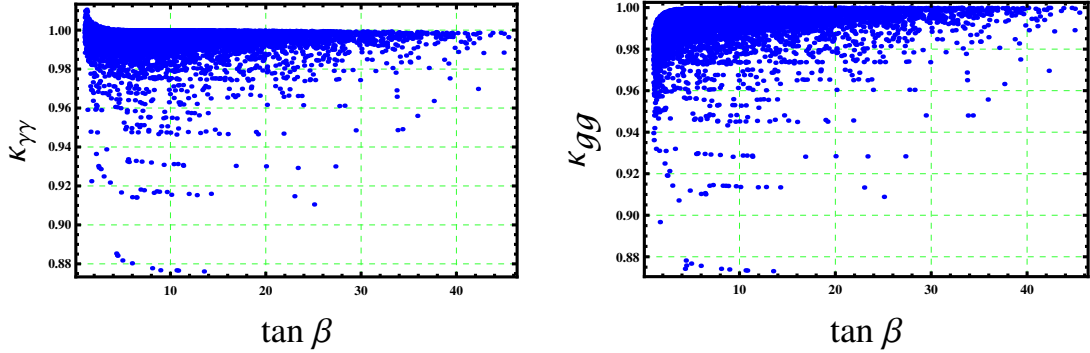


Figure 3.20:  $\kappa_{\gamma\gamma}$  and  $\kappa_{gg}$  as functions of  $t_\beta$  and the parameters  $\lambda_3$ ,  $\alpha_1$ ,  $\alpha_2$  and  $m_{h_{1,2}^\pm}$ .

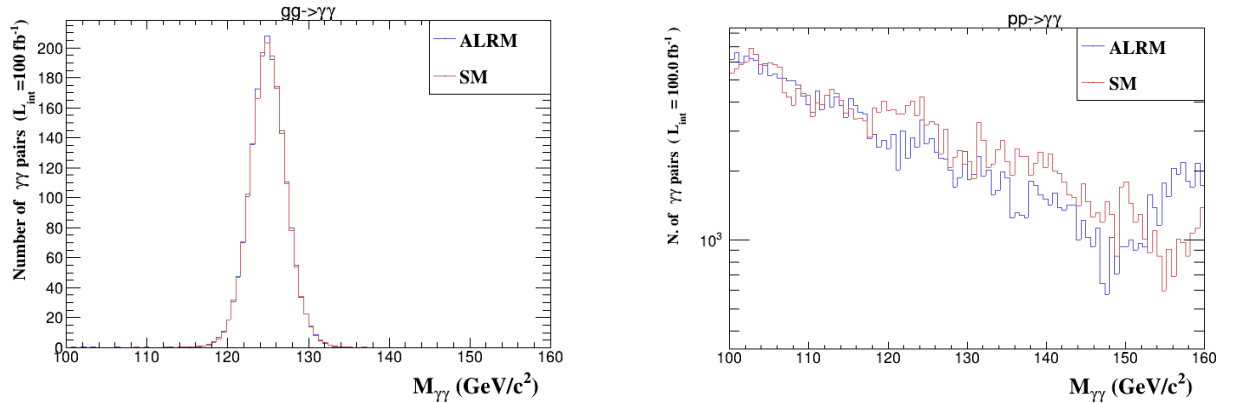


Figure 3.22:  $gg \rightarrow h \rightarrow \gamma\gamma$  and  $pp \rightarrow \gamma\gamma$  in the ALRM and the SM.

In Fig. 3.21, we show the signal strength as a function of  $\tan \beta$ , where other parameters are scanned in the regions mentioned above. For completeness, we also present the correlation between  $\mu_{\gamma\gamma}$  and  $\mu_{ZZ}$ . It is remarkable that all signal strengths of Higgs decay channels in the ALRM are slightly less than the SM results. The effective loop-induced  $h \rightarrow gg$  and  $h \rightarrow \gamma\gamma$  decays at leading order (LO) were implemented into FEYNRULES and CALCHEP [6, 16]. For the complete  $pp \rightarrow \gamma\gamma$  analysis, MADGRAPH [7, 31] is used as the MONTECARLO (MC) event generator (EG), PYTHIA [65, 75–77] is used for parton showering (PS), matrix element (ME) and PS

merging, hadronization and jet matching, then DELPHES [32] is used as a detector simulator and finally MADANALYSIS and ROOT [8, 21, 31] is used for event file analysis, recasting the LHC results and to produce the histogram figures in Fig. 3.22 and Fig. 3.23.

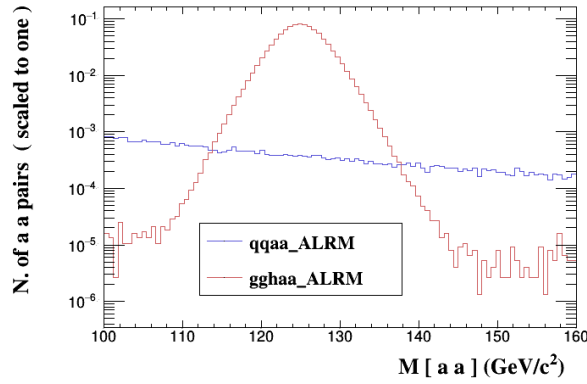
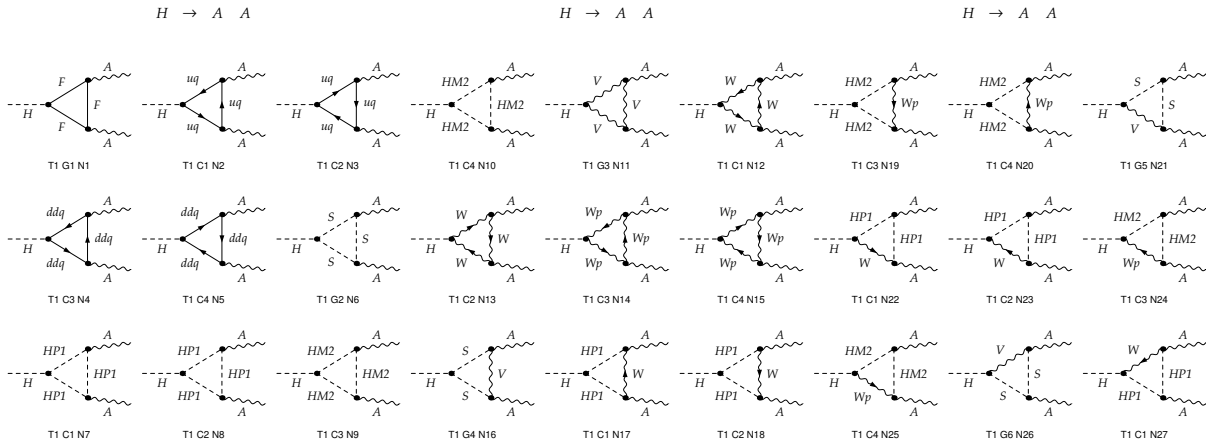


Figure 3.23:  $qq \rightarrow \gamma\gamma$  and  $gg \rightarrow h \rightarrow \gamma\gamma$  in the ALRM.



### 3.2 The $h \rightarrow \gamma\gamma$ Decay in the ALRM

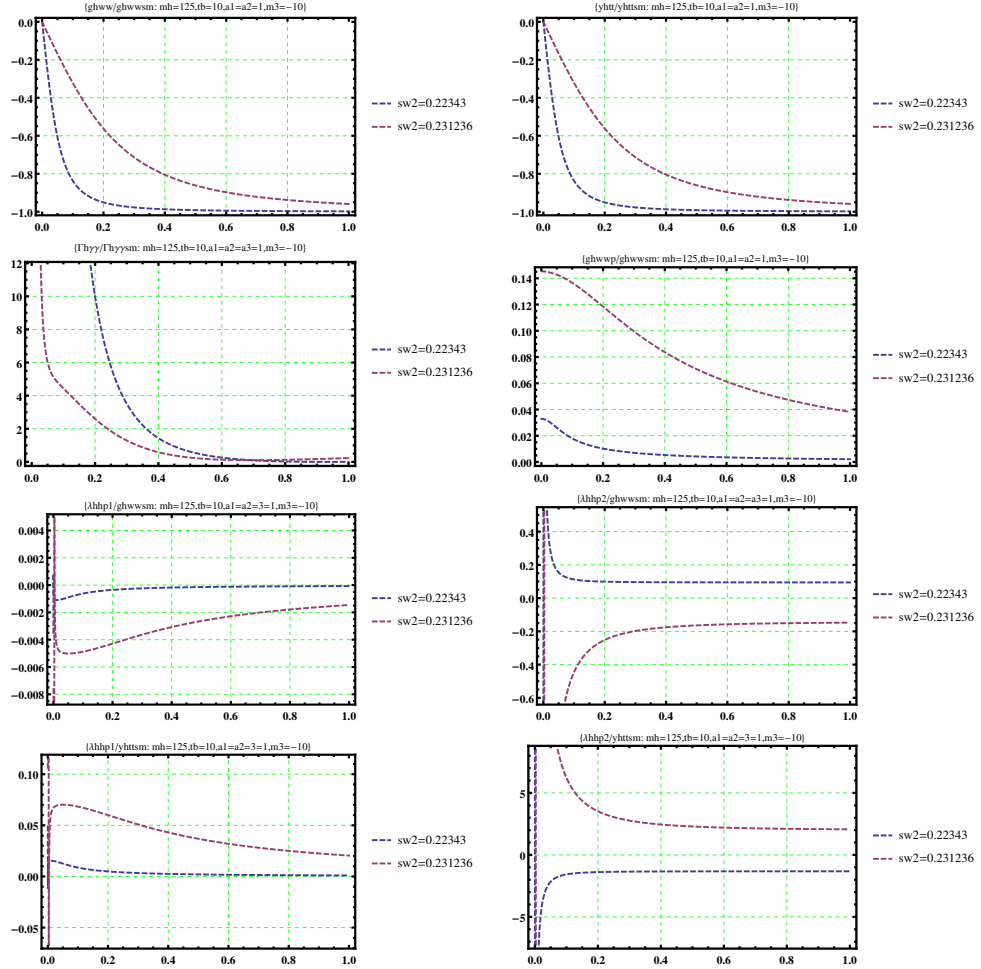
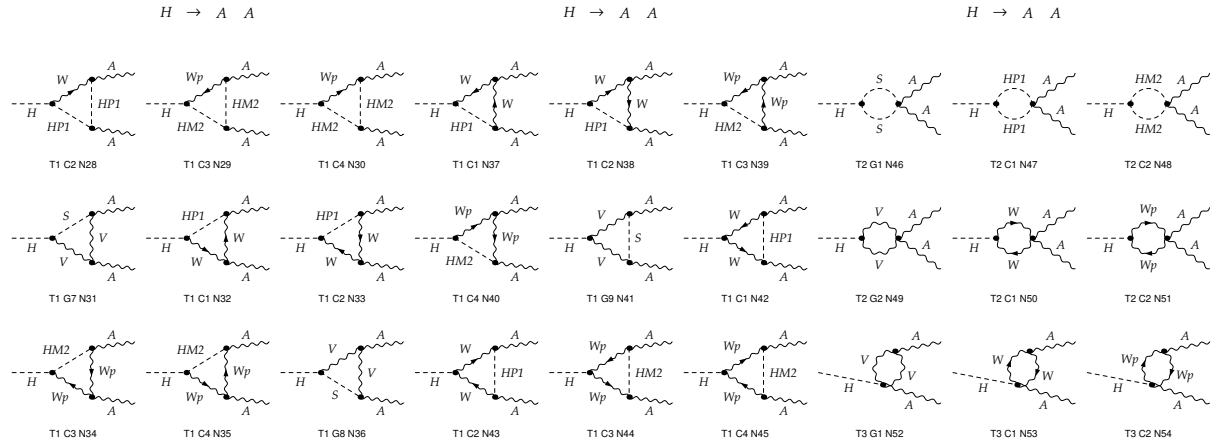
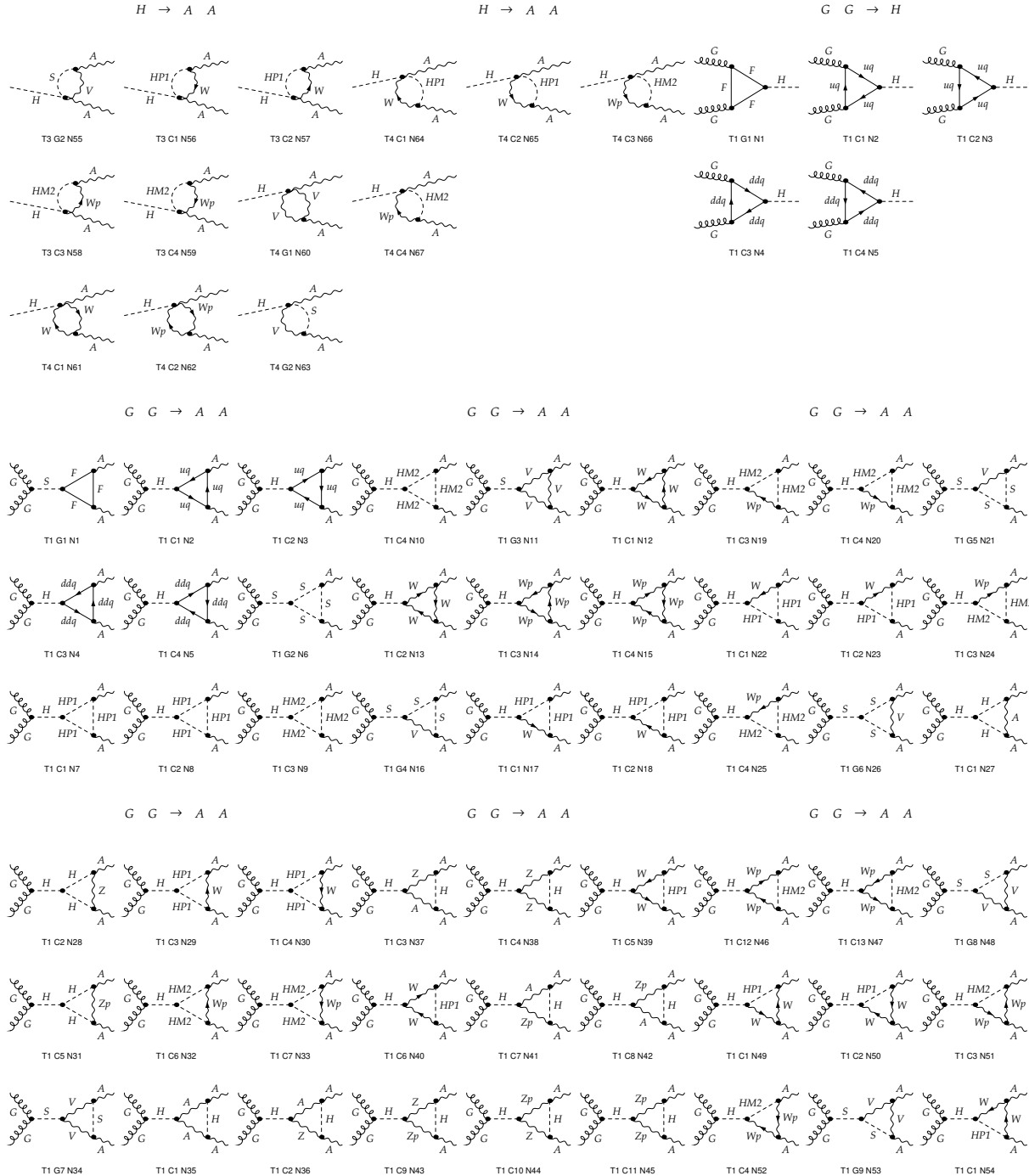


Figure 3.24: Higgs coupling ratios.

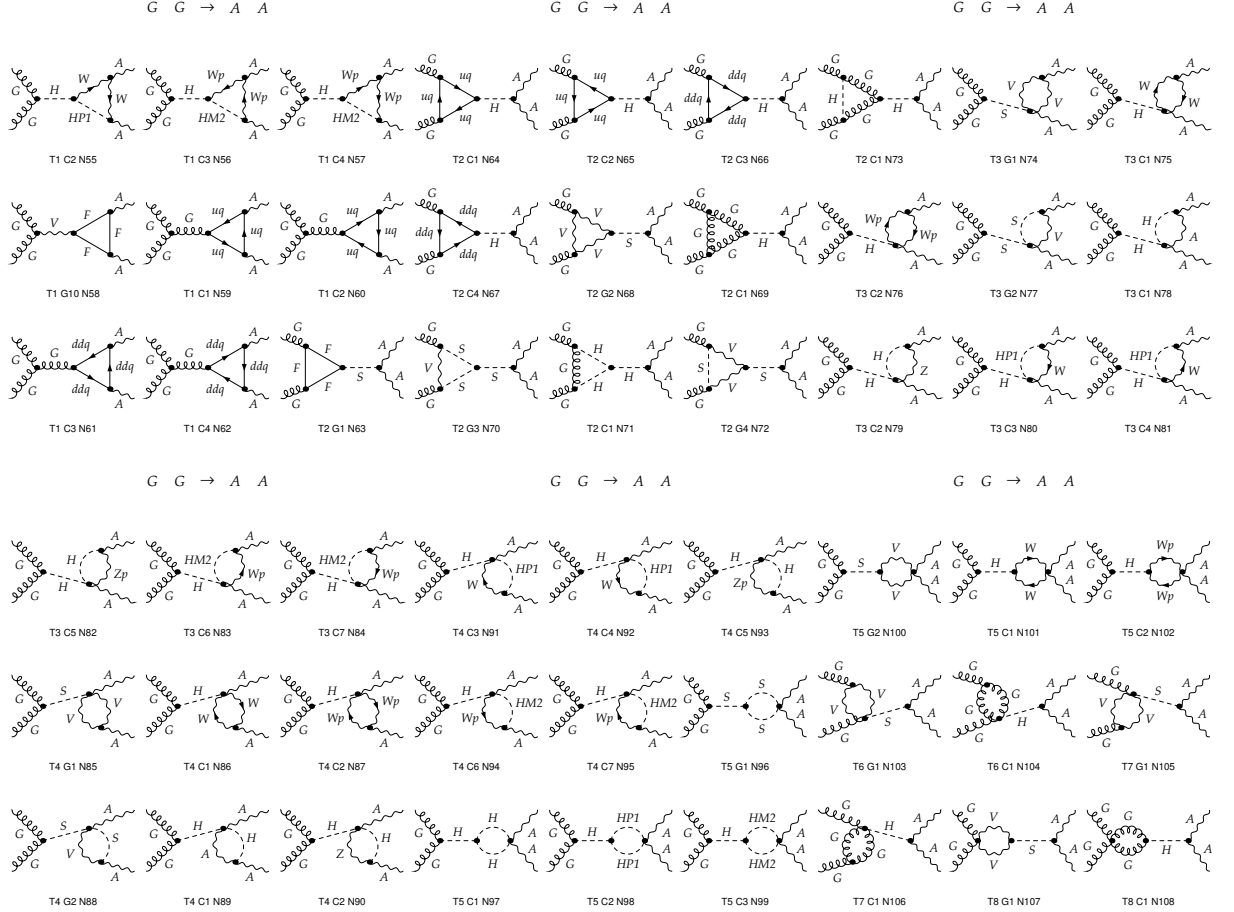


### Chapter 3: PHENOMENOLOGICAL ASPECTS OF THE ALRM

---



### 3.3 ALRM Signatures at the LHC



### 3.3 ALRM Signatures at the LHC

In this section we study the interesting signatures of the exotic quark  $d'$  associated with our ALRM at the LHC. In particular, we will analyze and compute the cross section for the production of this heavy quark and its subsequent decays into jets, leptons and missing energy. The Lagrangian of  $d'$  interactions with the SM quarks can be seen from (2.4.77) as

$$\mathcal{L}_{\text{Yuk}}^{d'} = -\frac{\sqrt{2}}{v'} \bar{u} (\cot \zeta M_u^{\text{diag}} V^R P_R + \tan \zeta V^R M_{d'}^{\text{diag}} P_L) h_2^+ d' + h.c. \quad (3.3.1)$$

In addition, the kinetic Lagrangian of  $d'$  leads to the following interactions with the gauge bosons

$$\begin{aligned} \mathcal{L}_{\text{gauge}}^{d'} = & -\frac{ig_s}{2}\bar{d}'\gamma^\mu\lambda_aG_\mu^ad' - \frac{ig}{\sqrt{2}}\bar{u}P_R\gamma^\mu W'^+_\mu V^R d' - \frac{ig}{\sqrt{2}}\bar{d}'\gamma^\mu P_R W'^-_\mu V^{R\dagger} u \\ & + \frac{i}{3}e\bar{d}'\gamma^\mu\{A_\mu + (\hat{P}\sin\vartheta - \frac{1}{2}\tan\theta_W\cos\vartheta)Z_\mu + (\hat{P}\cos\vartheta + \frac{1}{2}\tan\theta_W\sin\vartheta)Z'_\mu\}d', \end{aligned} \quad (3.3.2)$$

where

$$\hat{P} = \frac{3\cos 2\theta_W - \sin^2\theta_W}{6\sin\theta_W\cos\theta_W\sqrt{\cos 2\theta_W}}P_R + \frac{\sin\theta_W}{\cos\theta_W\sqrt{\cos 2\theta_W}}P_L, \quad (3.3.3)$$

where  $\vartheta$  is given in (2.3.41). Accordingly, in this case the pair production of  $d'$  at the LHC is dominated by the following channel:  $gg \rightarrow d'\bar{d}'$ . Considering all contributions from s,t, and u-channels, the squared amplitude of this process is given by

$$\begin{aligned} |\mathcal{M}(gg \rightarrow d'\bar{d}')|^2 = & \frac{g_s^4}{24\hat{s}^2} \frac{(9m_{d'}^4 - 9m_{d'}^2(\hat{s} + 2\hat{t}) + 4\hat{s}^2 + 9\hat{s}\hat{t} + 9\hat{t}^2)}{(m_{d'}^2 - \hat{t})^2(-m_{d'}^2 + \hat{s} + \hat{t})^2} \\ & \times \{m_{d'}^2(\hat{s}^3 + 2\hat{s}^2\hat{t} + 8\hat{s}\hat{t}^2 + 8\hat{t}^3) + \hat{t}(\hat{s} + \hat{t})(\hat{s}^2 + 2\hat{s}\hat{t} + 2\hat{t}^2) - 2m_{d'}^8 + 8m_{d'}^6\hat{t} - m_{d'}^4(3\hat{s}^2 + 4\hat{s}\hat{t} + 12\hat{t}^2)\}. \end{aligned} \quad (3.3.4)$$

In addition the squared amplitude of the pair production of  $d'$  through the channel  $q\bar{q} \rightarrow \gamma/g \rightarrow d'\bar{d}'$  is given by

$$|\mathcal{M}(q\bar{q} \rightarrow \gamma/g \rightarrow d'\bar{d}')|^2 = \frac{4(2g^4 + 9g_s^4)}{81\hat{s}^2}(2\hat{s}\hat{t} - 4(m_q^2 + m_{d'}^2)\hat{t} + 2(m_q^2 + m_{d'}^2)^2 + 2\hat{t}^2 + \hat{s}^2), \quad (3.3.5)$$

where  $\hat{s}, \hat{t}$  are the partonic Mandelstam variables. The differential cross section is given by

$$\frac{d\hat{\sigma}}{d\cos\theta} = \frac{B}{16\pi\hat{s}^2}|\mathcal{M}|^2, \quad (3.3.6)$$

where  $B = \sqrt{1 - (4m_{d'}^2/\hat{s})}$ . The cross section of  $pp \rightarrow d'd'$  is given by

$$\frac{d\sigma}{d\cos\theta} = \sum_{i,j} \int_{x_0}^1 dx f_i(x) f_j\left(\frac{4m_{d'}^2}{sx}\right) \frac{d\hat{\sigma}}{d\cos\theta}, \quad (3.3.7)$$

### 3.3 ALRM Signatures at the LHC

---

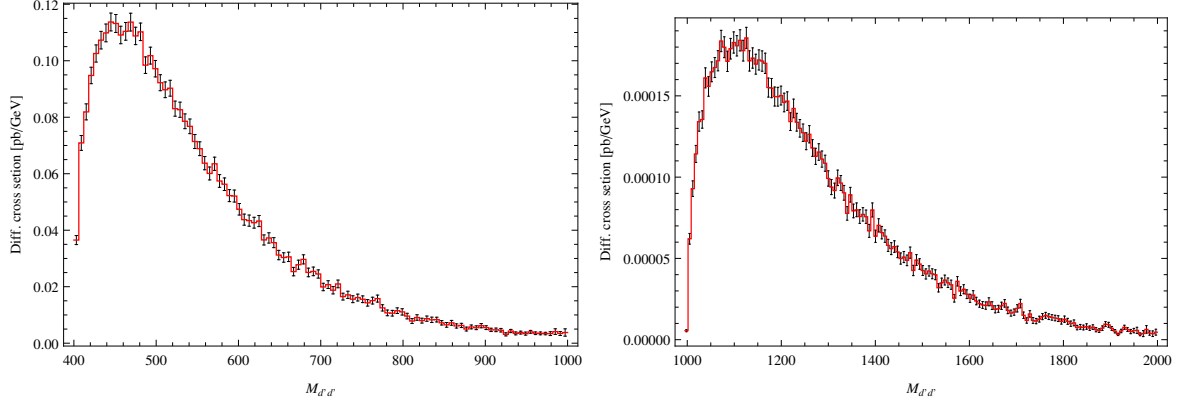


Figure 3.25: Differential production cross section of exotic quark  $d'$  as a function of the invariant mass  $M_{d'd'}$  with  $m_{d'} = 300$  GeV (left) and  $m_{d'} = 500$  GeV (right).

where  $i, j$  refer to the partons. The partons energy fractions are given by  $x_1 x_2 = \hat{s}/s$ , so that the minimum parton energy fraction to produce the  $d'd'$  pair is  $x_0 = 2m_{d'}/\sqrt{s}$ . Also,  $\hat{t} = -\frac{1}{2}\hat{s}(1-B \cos \theta) + M_{d'}^2$ . Therefore, one finds that the production cross section is given by

$$\frac{d\hat{\sigma}}{d\hat{t}} = \frac{1}{8\pi\hat{s}^3} |\mathcal{M}|^2. \quad (3.3.8)$$

In Fig. 3.25, we display the differential cross section of the  $d'$  pair production at the LHC with  $\sqrt{s} = 14$  TeV as a function of the invariant mass  $M_{d'd'}$  for two choices of  $m_{d'}$ , namely,  $m_{d'} = 300$  and 500 GeV. As can be seen from this figure, the typical value of the  $d'$  production cross section is of  $\mathcal{O}(1)$  fb, which was quite accessible at the LHC during its second run. The dominant decay channel of the produced  $d'$  quark is given by  $d' \rightarrow h_2^+ u$ , as indicated in (3.3.1). One can show that the corresponding decay rate is given by

$$\Gamma(d'_i \rightarrow u_j h_2^+) = \frac{|V_{ij}^{R}|^2}{8\pi\hbar v'^2} (M_{u_j}^2 \cot^2 \zeta + M_{d'_i}^2 \tan^2 \zeta) m_{d'} (1 - \frac{m_{h_2^+}^2}{m_{d'}^2})^2. \quad (3.3.9)$$

Here, we assumed that  $m_u \ll m_{d'}$ . On the other hand, the charged Higgs boson  $h_2^+$

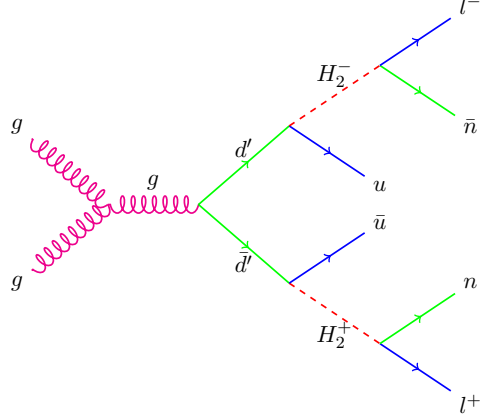


Figure 3.26: Creation and decay of an exotic quark  $d'$ .

decays into a lepton and scotino through the interactions

$$\mathcal{L}_{\text{Yuk}}^{h_2^{\pm}} = -\frac{\sqrt{2}}{v'} \bar{e} (\cot \zeta M_e^{\text{diag}} U^{R\dagger} P_R + \tan \zeta U^{R\dagger} M_n^{\text{diag}} P_L) h_2^- n + h.c. \quad (3.3.10)$$

Thus, the decay rate of  $h_2^- \rightarrow e^- n$ , for  $m_e \ll m_{h_2^\pm}$ , is given by

$$\Gamma(h_2^- \rightarrow e_i n_j) = \frac{|U_{ji}^R|^2}{8\pi \hbar v'^2} (M_{e_i}^2 \cot^2 \zeta + M_{n_j}^2 \tan^2 \zeta) m_{h_2^\pm} (1 - \frac{m_n^2}{m_{h_2^\pm}^2})^2. \quad (3.3.11)$$

In Fig. 3.26, we show the total cross section of this process with an opposite-sign dilepton, which is the most striking signature for this exotic quark at the LHC. This cross section can be approximately written as

$$\begin{aligned} \sigma(gg \rightarrow g \rightarrow d'\bar{d}' \rightarrow l^\mp l^\pm + E_T^{\text{miss}} + \text{jets}) &\simeq \sigma(gg \rightarrow g \rightarrow d'\bar{d}') \\ &\times \text{BR}(d' \rightarrow h_2^\mp + \text{jets})^2 \text{BR}(h_2^\mp \rightarrow l^\mp + E_T^{\text{miss}})^2. \end{aligned} \quad (3.3.12)$$

Since the dominant decay channel of  $d'$  is  $d' \rightarrow u h_2^-$  and the charged Higgs decays mainly to  $l^\pm + n$ , one finds  $\text{BR}(d' \rightarrow u h_2^-) \simeq 1$  and  $\text{BR}(h_2^\pm \rightarrow l^\pm n) \simeq 1$ . Therefore,  $\sigma(gg \rightarrow g \rightarrow d'\bar{d}' \rightarrow l^\mp l^\pm + E_T^{\text{miss}} + \text{jets}) \simeq \sigma(gg \rightarrow g \rightarrow d'\bar{d}') \simeq \mathcal{O}(1) \text{ fb}$ , which can

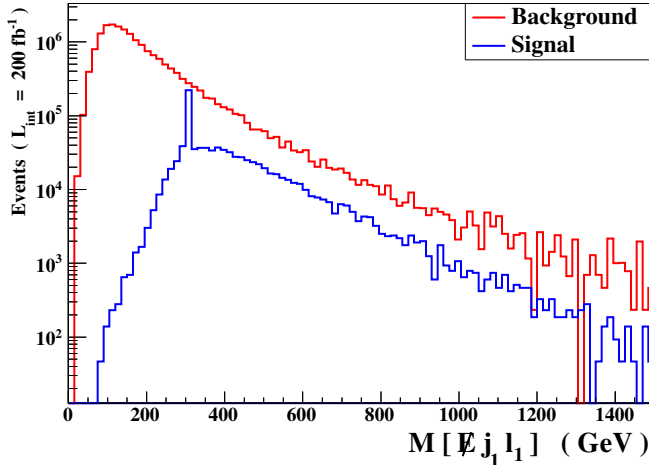


Figure 3.27: The reconstructed invariant mass of an exotic quark  $d'$  decaying to  $l + \text{jet} + \text{missing energy}$  and its background for  $m_{d'} = 300$  GeV and without cuts.

be accessible at the LHC with  $\sqrt{s} \simeq 14$  TeV. In Fig. 3.27, we show the reconstructed invariant mass of the extra quark  $d'$ , which decays into  $l + n$  (scotino) + jet, with all possible background. In this figure, we have not imposed any cut yet. Therefore, the background is clearly dominated the signal. Here, we assume  $m_{d'} = 300$  GeV, the charged Higgs mass is of order 200 GeV, and the LHC integrated luminosity is of order  $200 \text{ fb}^{-1}$ .

In Fig. 3.28 (left), we plot the number of reconstructed events per bin of the invariant mass of  $d'$  of the above process for signal and SM background at  $\cancel{E}_T \text{ cut} > 200$  GeV, where  $\cancel{E}_T$  is the missing transverse energy,  $\cancel{E}_T = \|\sum_{\text{visible particles}} \vec{p}_T\|$ , with  $m_{d'} = 300$  GeV and  $\sqrt{s} = 14$  TeV. This figure shows that it is possible to extract a good significance for the extra-quark signal in this channel. In addition, we also impose a cut,  $H_T < 200$  GeV, where  $H_T$  is the total transverse hadronic energy:  $H_T = \sum_{\text{hadronic particles}} \|\vec{p}_T\|$ . It is remarkable that with  $H_T$  cuts the signal can be much larger than the background. We have used FEYNRULES [6] to generate the

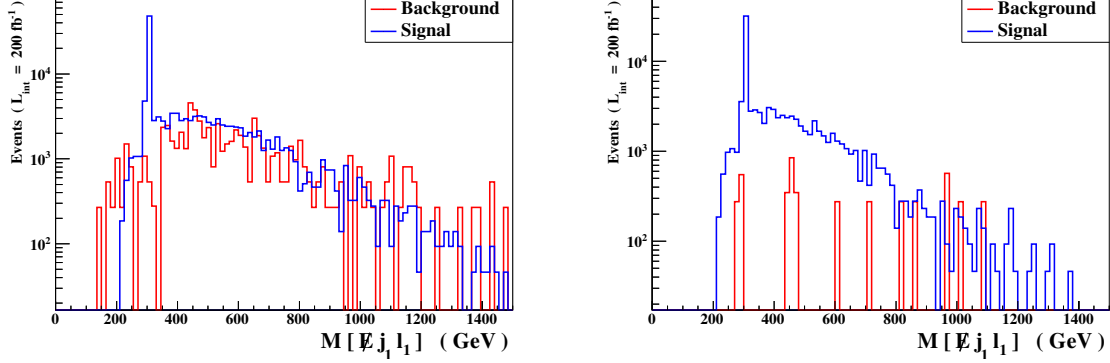


Figure 3.28: The reconstructed invariant mass of an exotic quark  $d'$  decaying to  $l + \text{jet} + \text{missing energy}$  for  $m_{d'} = 300$  GeV, with cuts  $\cancel{E}_T > 200$  GeV (left) and  $H_T < 200$  GeV (right).

model files and CALCHEP [16] and MADEVENT [7, 31] to calculate the numerical values of the cross sections and number of events, respectively.

Cuts (GeV)	Signal (S)	Background (B)	S vs B
Initial (no cut)	$463999$	$9309732 \pm 21646$	$0.049840 \pm 0.000116$
Cut 1 ( $\cancel{E}_T > 200$ )	$72291 \pm 247$	$33523 \pm 198$	$2.1564 \pm 0.0148$
Cut 2 ( $H_T < 200$ )	$47977 \pm 207$	$1942.7 \pm 44.3$	$24.696 \pm 0.573$

Table 3.1: Signal vs background for the process  $pp \rightarrow d'\bar{d}' \rightarrow (l^-l^+) + (u\bar{u}) + (nn)$  with/without cuts.

Finally, we provide in Table 3.1 some details for the used cuts on  $P_T$  and  $H_T$  on the signal and background for the process  $pp \rightarrow d'\bar{d}' \rightarrow (l^-l^+) + (u\bar{u}) + (nn)$ . As can be seen from the results in this table, the signal of this process can be much larger than the background if one imposes the proper  $H_T$  cuts. It is worth mentioning that

the Higgs sector of our model is very similar to the two Higgs doublets in the minimal supersymmetric standard model, where one Higgs doublet couples to up quarks and the second couples to down quarks. Therefore, it does not lead to any flavor-changing neutral current problem, and a light charged Higgs is phenomenologically acceptable. The number of events of exotic quark  $d'$  at the LHC may slightly changed if a heavier charged Higgs is considered, but with keeping  $m_{h^+} < m_{d'}$ , to ensure that  $\text{BR}(d' \rightarrow h^+ + \text{jets}) \sim 1$ .

# 4

## Conclusion

In this thesis, we have analyzed some phenomenological aspects of the alternative left-right model, motivated by the superstring-inspired  $E_6$  model. We provided a detailed analysis for the symmetry breaking and Higgs sector of this model, which consists of four neutral  $CP$ -even Higgs, two  $CP$ -odd Higgs and two charged Higgs bosons. We emphasized that three neutral  $CP$ -even Higgs and two  $CP$ -odd Higgs in addition to two charged Higgs can be light, of  $\mathcal{O}(100)$  GeV. We also found that the contributions of charged Higgs bosons and the extra exotic quark  $d'$  to  $h \rightarrow \gamma\gamma$  are quite negligible. Therefore, our model predicts signal strengths of Higgs decay, in particular, of  $h \rightarrow \gamma\gamma$  and  $h \rightarrow W^+W^-$  that coincide with the SM expectations.

Finally, we studied the striking signatures of the exotic down-type quark at the LHC. In particular, we computed the cross section of  $d'$ -pair production . We showed that the typical value of this cross section is of  $\mathcal{O}(1)$  fb, which is quite accessible at the LHC. The decay of  $d'$  into a jet, lepton, and missing energy provides an important signature for this class of models at the LHC.

# A

## Pauli, Dirac and Gell-Mann Matrices

### Pauli Matrices

The Pauli vector is defined by  $\sigma = (\sigma^1, \sigma^2, \sigma^3)$ , where the Pauli matrices are the set of the three  $2 \times 2$  complex matrices which are Hermitian and unitary

$$\sigma^1 = \begin{pmatrix} 0 & 1 \\ 1 & 0 \end{pmatrix}, \quad \sigma^2 = \begin{pmatrix} 0 & -i \\ i & 0 \end{pmatrix}, \quad \sigma^3 = \begin{pmatrix} 1 & 0 \\ 0 & -1 \end{pmatrix}. \quad (\text{A.0.1})$$

The Pauli matrices obey the following commutation relations

$$[T^i, T^j] = i\epsilon^{ijk}T^k, \quad T^i = \frac{1}{2}\sigma^i, \quad i = 1, 2, 3. \quad (\text{A.0.2})$$

where  $\epsilon^{ijk}$  is the totally antisymmetric Levi-Civita symbol. We also define

$$T^\pm = T^1 \pm iT^2. \quad (\text{A.0.3})$$

## Dirac Matrices

In Weyl representation, the four contravariant gamma matrices are

$$\gamma^0 = \begin{pmatrix} 0 & I_2 \\ I_2 & 0 \end{pmatrix}, \quad \gamma^i = \begin{pmatrix} 0 & \sigma^i \\ -\sigma^i & 0 \end{pmatrix}, \quad i = 1, 2, 3. \quad (\text{A.0.4})$$

Where  $I_2$  is the  $2 \times 2$  unit matrix.

The fifth gamma matrix is defined as the product of the four gamma matrices

$$\gamma^5 = \gamma_5 = i\gamma^0\gamma^1\gamma^2\gamma^3 = \begin{pmatrix} -I_2 & 0 \\ 0 & I_2 \end{pmatrix}. \quad (\text{A.0.5})$$

This matrix is useful in discussions of quantum mechanical chirality.

A Dirac field  $\psi = \psi_L + \psi_R$  can be projected onto its LH and RH components

$$\psi_L = P_L \psi = \frac{1}{2}(1 - \gamma_5)\psi, \quad \psi_R = P_R \psi = \frac{1}{2}(1 + \gamma_5)\psi. \quad (\text{A.0.6})$$

The Dirac conjugate and charge conjugate fields are defined, respectively, as

$$\bar{\psi} = \psi^\dagger \gamma^0, \quad \psi^c = C\psi^*, \quad C = i\gamma^2. \quad (\text{A.0.7})$$

## Gell-Mann Matrices

The Gell-Mann matrices are

$$\lambda^1 = \begin{pmatrix} 0 & 1 & 0 \\ 1 & 0 & 0 \\ 0 & 0 & 0 \end{pmatrix}, \quad \lambda^2 = \begin{pmatrix} 0 & -i & 0 \\ i & 0 & 0 \\ 0 & 0 & 0 \end{pmatrix}, \quad \lambda^3 = \begin{pmatrix} 1 & 0 & 0 \\ 0 & -1 & 0 \\ 0 & 0 & 0 \end{pmatrix}, \quad (\text{A.0.8})$$

$$\lambda^4 = \begin{pmatrix} 0 & 0 & 1 \\ 0 & 0 & 0 \\ 1 & 0 & 0 \end{pmatrix}, \quad \lambda^5 = \begin{pmatrix} 0 & 0 & -i \\ 0 & 0 & 0 \\ i & 0 & 0 \end{pmatrix}, \quad \lambda^6 = \begin{pmatrix} 0 & 0 & 0 \\ 0 & 0 & 1 \\ 0 & 1 & 0 \end{pmatrix}, \quad (\text{A.0.9})$$

---


$$\lambda^7 = \begin{pmatrix} 0 & 0 & 0 \\ 0 & 0 & -i \\ 0 & i & 0 \end{pmatrix}, \quad \lambda^8 = \frac{1}{\sqrt{3}} \begin{pmatrix} 1 & 0 & 0 \\ 0 & 1 & 0 \\ 0 & 0 & -2 \end{pmatrix}. \quad (\text{A.0.10})$$

The Gell-Mann matrices obey the following commutation relations

$$[\Lambda^a, \Lambda^b] = if^{abc}\Lambda^c, \quad \Lambda^a = \frac{1}{2}\lambda^a, \quad a = 1, \dots, 8. \quad (\text{A.0.11})$$

The  $SU(3)$  Lie algebra structure constants  $f^{abc}$  are completely antisymmetric and have values

$$f^{123} = 1, \quad f^{147} = f^{165} = f^{246} = f^{257} = f^{345} = f^{376} = \frac{1}{2}, \quad f^{458} = f^{678} = \frac{\sqrt{3}}{2}. \quad (\text{A.0.12})$$

# B

## The Electric Charge Formula and Gauge Coupling Relations

### The Electric Charge Formula

The remaining of only one massless gauge field after the two stages of SSB means that there is still one linear combination of the generators that leaves the vacuum invariant. This corresponds to the electric charge.

We know that  $\Phi$  and  $\Delta_\hbar$  transform like  $\Phi \rightarrow U_L \Phi U_R^\dagger$  and  $\Delta_\hbar \rightarrow U_\hbar \Delta_\hbar U_\hbar^\dagger$  and we may wonder whether we can find a set of transformations that leaves the vacuum invariant:

$$U_L \langle \Phi \rangle U_R^\dagger = \langle \Phi \rangle, \quad U_\hbar \langle \Delta_\hbar \rangle U_\hbar^\dagger = \langle \Delta_\hbar \rangle. \quad (\text{B.0.1})$$

---

The generator of the desired set of transformations can be identified with the electric charge. With the parameterizations  $U_{\mathcal{H}} = \exp[-i\alpha_{\mathcal{H}}^a T_{\mathcal{H}}^a]$  for an element of the group  $SU(2)_{\mathcal{H}}$  and  $\exp[-iQ_{BL}\beta]$  for an element of the  $U(1)_{B-L}$  group, we need to find a set of real  $\alpha$ 's and a  $\beta$  such that (B.0.1) is satisfied. Consider the infinitesimal form of the gauge transformation, starting with  $\langle \Delta_R \rangle$ :

$$\begin{aligned} e^{-i\beta} e^{-i\alpha_R^a T_R^a} \langle \Delta_R \rangle e^{i\alpha_R^a T_R^a} &\approx (1 - i\beta)(1 - i\alpha_R^a T_R^a) \langle \Delta_R \rangle (1 + i\alpha_R^a T_R^a) \\ &\approx \langle \Delta_R \rangle - i\beta \langle \Delta_R \rangle - i[\alpha_R^a T_R^a, \langle \Delta_R \rangle] \\ &= \langle \Delta_R \rangle - \frac{iv_R}{2} \begin{pmatrix} \alpha_R^1 - i\alpha_R^2 & 0 \\ 2(\beta - \alpha_R^3) & i\alpha_R^2 - \alpha_R^1 \end{pmatrix}. \end{aligned} \quad (\text{B.0.2})$$

With the constraint that the parameters of the transformations must be real, we find  $\alpha_R^1 = 0 = \alpha_R^2$  and  $\alpha_R^3 = \beta$ . At this stage of SSB we see that transformations with  $\alpha_R^3 = \beta$  are that of type we were looking for. As for the bidoublet  $\Phi$

$$e^{-i\alpha_L^a T_L^a} \langle \Phi \rangle e^{i\alpha_R^a T_R^a} \approx \langle \Phi \rangle - i(\alpha_L^a T_L^a \langle \Phi \rangle - \langle \Phi \rangle \alpha_R^a T_R^a). \quad (\text{B.0.3})$$

The second term on the right hand side should vanish, leading to the constraint  $\alpha_L^3 = \alpha_R^3$ .

We see that transformations with  $\alpha_L^3 = \alpha_R^3 = \beta$  are that of type we were looking for. This means the combination  $T_L^3 + T_R^3 + Q_{BL}$  is the only unbroken generator and hence corresponds to the electric charge [63]

$$Q = T_L^3 + T_R^3 + Q_{BL}. \quad (\text{B.0.4})$$

This is the equivalent of Gell-Mann Nishijima relation for the electric charge in the standard model:  $Q = T^3 + Y$ . We can check the above relation by calculating e.g.,

$$Q(\Phi) = T_L^3(\Phi) + T_R^3(\Phi) + Q_{BL}(\Phi) = T_L^3\Phi - \Phi T_R^3 = \begin{pmatrix} 0\Phi_1^0 & +\Phi_1^+ \\ -\Phi_2^- & 0\Phi_2^0 \end{pmatrix}, \quad (\text{B.0.5})$$

$$Q(\Delta_{\mathcal{H}}) = T_L^3(\Delta_{\mathcal{H}}) + T_R^3(\Delta_{\mathcal{H}}) + Q_{BL}(\Delta_{\mathcal{H}}) = [T_{\mathcal{H}}^3, \Delta_{\mathcal{H}}] + \Delta_{\mathcal{H}} = \begin{pmatrix} \frac{+\Delta^+}{\sqrt{2}} & +2\Delta^{++} \\ 0\Delta^0 & +(-\frac{\Delta^+}{\sqrt{2}}) \end{pmatrix}_{\mathcal{H}} \quad (\text{B.0.6})$$

and comparing it with the charge assignments in Table 1.2, which now turn out to be consistent. Note that sofar we did not invoke the VEV of the triplet field  $\Delta_L$ . It seems it is not needed to break the EW gauge group down to  $U(1)_{EM}$  which leaves the possibility of a vanishing  $v_L$ , as may be desirable. Now it is clear that the hypercharge is

$$Y = T_R^3 + Q_{BL}. \quad (\text{B.0.7})$$

The triplet  $\Delta_R$  is already a singlet under the group  $SU(2)_L$  and we can make sure that  $Y(\Delta_R^0) = 0$  by calculating

$$Y(\Delta_R) = T_R^3(\Delta_R) + Q_{BL}(\Delta_R) = [T_R^3, \Delta_R] + \Delta_R = \begin{pmatrix} \frac{+\Delta^+}{\sqrt{2}} & +2\Delta^{++} \\ 0\Delta^0 & +(-\frac{\Delta^+}{\sqrt{2}}) \end{pmatrix}_R. \quad (\text{B.0.8})$$

Also, as we intend to break the SM EW symmetry by the VEVs of the bidoublet  $\Phi$ , we show that  $\Phi$  has nontrivial transformation under  $U(1)_Y$  by calculating

$$Y(\Phi) = T_R^3(\Phi) + Q_{BL}(\Phi) = -\Phi T_R^3 = \frac{1}{2} \begin{pmatrix} -\Phi_1^0 & +\Phi_1^+ \\ -\Phi_2^- & +\Phi_2^0 \end{pmatrix}. \quad (\text{B.0.9})$$

## Gauge Coupling Relations

For any gauge theory, if the electric charge operator is given by the combination

$$Q = \sum_n a_n T_n, \quad (\text{B.0.10})$$

where  $T_n$ 's are the generators of the factors of the gauge group and  $a_n$ 's are numerical coefficients, then the EM charge  $e$  is given by

$$\frac{1}{e^2} = \sum_n \frac{a_n^2}{g_n^2}, \quad (\text{B.0.11})$$

where  $g_n$  is the coupling constant accompanying  $T_n$  [48].

# C

## Gauge Transformations and Covariant Derivatives

In this appendix [28, 81] some conventions regarding the signs occurring in the gauge field transformations and covariant derivatives are stated and motivated.

The following example covers all the cases that are present in this thesis. All the fields appearing are possibly matrices, so we must keep an eye on the ordering. Consider a field  $\phi$  that transforms like:

$$\phi \rightarrow \phi' = U\phi V^\dagger \quad (\text{C.0.1})$$

where  $U$  and  $V$  are elements of some unitary gauge groups. We will show that the

covariant derivative

$$D_\mu \phi = \partial_\mu \phi - ig A_\mu^U \phi + ig' \phi A_\mu^V \quad (\text{C.0.2})$$

gives rise to acceptable transformation rules of the gauge fields  $A_\mu^{U,V}$  when we demand that this derivative transforms the way  $\phi$  does:

$$\text{if } (\phi, A_\mu^{U,V}) \rightarrow (\phi', A'_\mu^{U,V}), \quad \text{then} \quad D_\mu \phi \rightarrow (D_\mu \phi)' = U(D_\mu \phi)V^\dagger \quad (\text{C.0.3})$$

The ‘then’ statement means  $D'_\mu \phi' = (D_\mu \phi)'$ , where  $D'_\mu \phi'$  is the primed version of (C.0.2). Writing out this condition explicitly:

$$\begin{aligned} D'_\mu \phi' &= \partial_\mu \phi' - ig A'_\mu^U \phi' + ig' \phi' A'_\mu^V \\ &= \partial_\mu (U \phi V^\dagger) - ig A'_\mu^U \phi' + ig' \phi' A'_\mu^V \\ &= (\partial_\mu U) \phi V^\dagger + U(\partial_\mu \phi) V^\dagger + U \phi (\partial_\mu V^\dagger) - ig A'_\mu^U \phi' + ig' \phi' A'_\mu^V \\ &= [(\partial_\mu U) U^\dagger] \phi' + U(\partial_\mu \phi) V^\dagger + \phi' [V(\partial_\mu V^\dagger)] - ig A'_\mu^U \phi' + ig' \phi' A'_\mu^V \\ &= [(\partial_\mu U) U^\dagger - ig A'_\mu^U] \phi' + U(\partial_\mu \phi) V^\dagger + \phi' [V(\partial_\mu V^\dagger) + ig' A'_\mu^V]. \end{aligned} \quad (\text{C.0.4})$$

On the other hand,

$$\begin{aligned} (D_\mu \phi)' &= U(\partial_\mu \phi - ig A_\mu^U \phi + ig' \phi A_\mu^V) V^\dagger \\ &= U(\partial_\mu \phi) V^\dagger - ig U A_\mu^U \phi V^\dagger + ig' U \phi A_\mu^V V^\dagger \\ &= U \partial_\mu \phi V^\dagger - ig(U A_\mu^U U^\dagger) \phi' + ig' \phi' (V A_\mu^V V^\dagger). \end{aligned} \quad (\text{C.0.5})$$

Comparing the RHSs of both (C.0.4) and (C.0.5) gives the equality

$$[(\partial_\mu U) U^\dagger + ig(U A_\mu^U U^\dagger) - ig A'_\mu^U] \phi' = \phi' [-V(\partial_\mu V^\dagger) + ig'(V A_\mu^V V^\dagger) - ig' A'_\mu^V]. \quad (\text{C.0.6})$$

If  $U$  and  $V$  are independent of each other (the case of the bidoublet  $\Phi$ ), both sides must be a constant. The easiest option is zero, yielding the transformation rule:

$$A'_\mu^U = U A_\mu^U U^\dagger - \frac{i}{g} (\partial_\mu U) U^\dagger. \quad (\text{C.0.7})$$

---

Using  $0 = \partial_\mu(VV^\dagger) = (\partial_\mu V)V^\dagger + V\partial_\mu V^\dagger$ , one arrives at a completely analogous expression for  $A_\mu^V$ . If  $U = V$  (the case of the triplets  $\Delta_h$ ), eq. (C.0.6) is the commutator

$$[((\partial_\mu U)U^\dagger + ig(UA_\mu^U U^\dagger) - igA_\mu^U), \phi'] = 0, \quad (\text{C.0.8})$$

which is read again as eq. (C.0.7). We have seen that Eqs. (C.0.1), (C.0.2) and (C.0.7) are mutually consistent.

We can apply the above results to fields that transform according to the rule:  $\phi' = U\phi$  by leaving out the  $V$ 's and the corresponding gauge fields. Of special interest are the  $U(1)$  transformations. Suppose we have for a field with charge  $q$

$$\phi' = e^{-iq\alpha(x)}\phi. \quad (\text{C.0.9})$$

In this case the gauge field is not a matrix so it simply commutes with  $U$  and  $U^\dagger$ . Applying the rule from (C.0.7) we find

$$A'_\mu = A_\mu - \frac{q}{g}\partial_\mu\alpha(x) \quad (\text{wrong!}) \quad (\text{C.0.10})$$

This is of course unacceptable. The transformation of the gauge field cannot be dependent on the charge of the field  $\phi$ . In QED for example, there is one gauge field with one and only one transformation rule. The inconsistency can be remedied by redefining the coupling constant  $g$ . A factor  $q$  should be pulled out: replace  $g$  by  $qg$  to get this consistent (and acceptable) set of equations:

$$\phi' = e^{-iq\alpha(x)}\phi, \quad D_\mu\phi = (\partial_\mu\phi - iqgA_\mu)\phi, \quad A'_\mu = A_\mu - \frac{1}{g}\partial_\mu\alpha(x). \quad (\text{C.0.11})$$

# D

## The Higgs Potential in the ALRM

### D.1 Boundedness From Below Conditions of the ALRM Potential

To study the boundedness from below, and hence the stability, of the potential (2.2.15) we use the following theorem [42, 71] to ensure that the matrix of the quartic terms, which are dominant at higher values of the fields, is copositive:

**Theorem 1** (Copositivity Criteria). *Let  $a \in \mathbb{R}$ ,  $b \in \mathbb{R}^{n-1}$  and  $C \in \mathbb{R}^{(n-1) \times (n-1)}$ . The*

*symmetric matrix  $M \in \mathbb{R}^{n \times n}$*

$$M = \begin{pmatrix} a & b^T \\ b & C \end{pmatrix}, \quad (\text{D.1.1})$$

*is copositive if and only if*

1.  $a \geq 0$ ,  $C$  is copositive,

2. for any nonzero vector  $y \in \mathbb{R}^{(n-1)}$ , with  $y \geq 0$ , if  $b^T y \leq 0$ , it follows that

$$y^T(aC - bb^T)y \geq 0.$$

The quartic terms of the potential (2.2.15) can be written as

$$\begin{aligned} {}^{4F}V(\phi_{1,2}^{0,+}, \chi_{L,R}^{0,+}) &= \lambda_1(|\phi_1^0|^4 + |\phi_1^+|^4 + |\phi_2^0|^4 + |\phi_2^+|^4) + \lambda_3(|\chi_L^0|^4 + |\chi_L^+|^4 + |\chi_R^0|^4 + |\chi_R^+|^4) \\ &+ 2|\phi_1^0|^2[\lambda_1(|\phi_1^+|^2 + |\phi_2^+|^2) + \lambda_{12}|\phi_2^0|^2 + \alpha_{13}(|\chi_L^0|^2 + |\chi_R^0|^2) + \alpha_{12}(|\chi_L^+|^2 + |\chi_R^+|^2)] \\ &+ 2|\phi_1^+|^2[\lambda_1|\phi_2^0|^2 + \lambda_{12}|\phi_2^+|^2 + \alpha_{13}(|\chi_L^0|^2 + |\chi_R^+|^2) + \alpha_{12}(|\chi_L^+|^2 + |\chi_R^0|^2)] \\ &+ 2|\phi_2^0|^2[\lambda_1|\phi_2^+|^2 + \alpha_{12}(|\chi_L^0|^2 + |\chi_R^0|^2) + \alpha_{13}(|\chi_L^+|^2 + |\chi_R^+|^2)] \\ &+ 2|\phi_2^+|^2[\alpha_{12}(|\chi_L^0|^2 + |\chi_R^+|^2) + \alpha_{13}(|\chi_L^+|^2 + |\chi_R^0|^2)] \\ &+ 2|\chi_L^0|^2(\lambda_3|\chi_L^+|^2 + \lambda_4|\chi_R^0|^2 + \lambda_4|\chi_R^+|^2) + 2|\chi_L^+|^2(\lambda_4|\chi_R^0|^2 + \lambda_4|\chi_R^+|^2) \\ &+ 2\lambda_3|\chi_R^0|^2|\chi_R^+|^2 - 8\lambda_2 \operatorname{Re}[\phi_1^0 \phi_1^- \phi_2^0 \phi_2^+] \\ &+ 4(\alpha_2 - \alpha_3) \operatorname{Re}[(\phi_1^0 \phi_2^+ + \phi_2^{0*} \phi_1^+) \chi_L^0 \chi_L^- + (\phi_2^0 \phi_2^+ + \phi_1^{0*} \phi_1^+) \chi_R^0 \chi_R^-], \end{aligned} \quad (\text{D.1.2})$$

where  $\alpha_{12} = \alpha_1 + \alpha_2$ ,  $\alpha_{13} = \alpha_1 + \alpha_3$  and  $\lambda_{12} = \lambda_1 + 2\lambda_2$ . We have

$$\phi_{1,2}^{0,+} = |\phi_{1,2}^{0,+}| \exp[i\theta_{1,2}^{0,+}], \quad \chi_{L,R}^{0,+} = |\chi_{L,R}^{0,+}| \exp[i\theta_{L,R}^{0,+}]. \quad (\text{D.1.3})$$

By the following redefinitions of the fields' components

$$\phi_1^+ \rightarrow \phi_1^+ \exp[i(\theta_1^0 - \theta_1^+)], \quad \phi_2^0 \rightarrow \phi_2^0 \exp[i(\theta_1^0 - \theta_2^0)], \quad (\text{D.1.4})$$

$$\phi_2^+ \rightarrow \phi_2^+ \exp[-i(\theta_1^0 + \theta_2^+)], \quad \chi_{L,R}^+ \rightarrow \chi_{L,R}^+ \exp[i(\theta_{L,R}^0 - \theta_{L,R}^+)], \quad (\text{D.1.5})$$

we can write

$$\begin{aligned} {}^{4F}V(\phi_{1,2}^{0,+}, \chi_{L,R}^{0,+}) &= X^T {}^{4F}V X - 8\lambda_2 |\phi_1^0| |\phi_1^-| |\phi_2^0| |\phi_2^+| \\ &\quad + 4(\alpha_2 - \alpha_3) \left[ (|\phi_1^0| |\phi_2^+| + |\phi_2^0| |\phi_1^+|) |\chi_L^0| |\chi_L^+| + (|\phi_2^0| |\phi_2^+| + |\phi_1^0| |\phi_1^+|) |\chi_R^0| |\chi_R^+| \right], \end{aligned} \quad (\text{D.1.6})$$

where

$$X^T = \begin{pmatrix} |\phi_1^0|^2 & |\phi_1^+|^2 & |\phi_2^0|^2 & |\phi_2^+|^2 & |\chi_L^0|^2 & |\chi_L^+|^2 & |\chi_R^0|^2 & |\chi_R^+|^2 \end{pmatrix}, \quad (\text{D.1.7})$$

$${}^{4F}V = \begin{pmatrix} \lambda_1 & \lambda_1 & \lambda_{12} & \lambda_1 & \alpha_{13} & \alpha_{12} & \alpha_{13} & \alpha_{12} \\ \lambda_1 & \lambda_1 & \lambda_1 & \lambda_{12} & \alpha_{13} & \alpha_{12} & \alpha_{12} & \alpha_{13} \\ \lambda_{12} & \lambda_1 & \lambda_1 & \lambda_1 & \alpha_{12} & \alpha_{13} & \alpha_{12} & \alpha_{13} \\ \lambda_1 & \lambda_{12} & \lambda_1 & \lambda_1 & \alpha_{12} & \alpha_{13} & \alpha_{13} & \alpha_{12} \\ \alpha_{13} & \alpha_{13} & \alpha_{12} & \alpha_{12} & \lambda_3 & \lambda_3 & \lambda_4 & \lambda_4 \\ \alpha_{12} & \alpha_{12} & \alpha_{13} & \alpha_{13} & \lambda_3 & \lambda_3 & \lambda_4 & \lambda_4 \\ \alpha_{13} & \alpha_{12} & \alpha_{12} & \alpha_{13} & \lambda_4 & \lambda_4 & \lambda_3 & \lambda_3 \\ \alpha_{12} & \alpha_{13} & \alpha_{13} & \alpha_{12} & \lambda_4 & \lambda_4 & \lambda_3 & \lambda_3 \end{pmatrix}. \quad (\text{D.1.8})$$

For the potential (D.1.2) to be bounded from below, it must happen that the matrix  ${}^{4F}V$  is copositive and  $\lambda_2 \leq 0$  and  $\alpha_2 - \alpha_3 \geq 0$ . The pseudoscalar Higgs mass (2.4.15) implies that  $\mu_3 < 0$ . With the minimization condition (2.3.4), both imply that  $\lambda_4 > \lambda_3$ . The copositivity implies that the diagonal elements  $\lambda_1, \lambda_3 \geq 0$ . Accordingly,  $\lambda_4 > \lambda_3 \geq 0$ . It is remarkable that the copositivity of the matrix  ${}^{4F}V$  significantly depends on the signs of the parameters  $\alpha_{12}$ ,  $\alpha_{13}$ , and  $\lambda_{12}$ . Here we present the cases depending on these signs:

1.  $\alpha_{12} \geq 0$ ,  $\alpha_{13} \geq 0$ , and  $\lambda_{12} \geq 0$ : In this case, the matrix  ${}^{4F}V$  is copositive, and the potential is bounded from below.

2.  $\alpha_{12} \geq 0$ ,  $\alpha_{13} \geq 0$ , and  $\lambda_{12} \leq 0$ : The copositivity conditions are

$$\lambda_1 + \lambda_2 \geq 0, \quad \lambda_1^2 + 8\lambda_1\lambda_2 + 4\lambda_2^2 \leq 0. \quad (\text{D.1.9})$$

We deduce these conditions in detail considering the case assumptions and using Theorem 1. To make the  $8 \times 8$  matrix  ${}^{4F}V$  be copositive, we shall make that first with the  $7 \times 7$  matrix,  $C$ , arising from the matrix  ${}^{4F}V$  by eliminating the first row and the first column. In our case, it is sufficient to stop at this level, since the  $6 \times 6$  matrix,  $C_1$ , arising from the matrix  ${}^{4F}V$  by eliminating the first two rows and the first two columns is already copositive; being a matrix of nonnegative elements. Now,

$${}^{4F}V = \begin{pmatrix} \lambda_1 & b^T \\ b & C \end{pmatrix}, \quad b^T = \begin{pmatrix} \lambda_1 & \lambda_{12} & \lambda_1 & \alpha_{13} & \alpha_{12} & \alpha_{13} & \alpha_{12} \end{pmatrix}, \quad (\text{D.1.10})$$

$$C = \begin{pmatrix} \lambda_1 & b_1^T \\ b_1 & C_1 \end{pmatrix}, \quad b_1^T = \begin{pmatrix} \lambda_1 & \lambda_{12} & \alpha_{13} & \alpha_{12} & \alpha_{12} & \alpha_{13} \end{pmatrix}. \quad (\text{D.1.11})$$

Let  $y_1^T = (x_1 \ x_2 \ x_3 \ x_4 \ x_5 \ x_6)$  be a vector that satisfies Theorem 1 requests, *i.e.*, a nonzero and a nonnegative vector. Taking  $x_2 \neq 0$ ,  $x_{1,3,\dots,6} = 0$ , makes the linear form  $b_1^T y_1 = \lambda_{12} x_2 \leq 0$  and its corresponding quadratic form

$$y_1^T (\lambda_1 C_1 - b_1 b_1^T) y_1 = -4\lambda_2(\lambda_1 + \lambda_2)x_2^2.$$

Since we have  $\lambda_2 \leq 0$ , we impose the condition

$$\lambda_1 + \lambda_2 \geq 0 \quad (\text{D.1.12})$$

to make the quadratic form  $y_1^T (\lambda_1 C_1 - b_1 b_1^T) y \geq 0$  and hence as a necessary condition for the copositivity.

Let us assume that  $x_i \neq 0$ ,  $i = 1, \dots, 6$ . Then, the linear form

$$b_1^T y_1 \leq 0 \longleftrightarrow x_2 \geq x_2^{\min} = \frac{1}{-\lambda_{12}}(\lambda_1 x_1 + \alpha_{13} x_3 + \alpha_{12} x_4 + \alpha_{12} x_5 + \alpha_{13} x_6).$$

The copositivity condition (D.1.12) makes the corresponding quadratic form be increasing in  $x_2$  (for any fixed values of the other  $x_i$ 's), and hence we deduce that

$$\begin{aligned}
 y_1^T(\lambda_1 C_1 - b_1 b_1^T) y_1 &\geq y_1^T(\lambda_1 C_1 - b_1 b_1^T) y_1 \Big|_{x_2=x_2^{\min}} \\
 &= \frac{\lambda_1}{\lambda_{12}^2} \left[ 4\lambda_1\lambda_2^2 x_1^2 - 2\lambda_2(\alpha_{13}\lambda_1 - \alpha_{12}\lambda_{12})x_1x_3 - 2\lambda_2(\alpha_{12}\lambda_1 - \alpha_{13}\lambda_{12})x_1x_4 \right. \\
 &\quad + 2x_1((\alpha_{12}x_5 + \alpha_{13}x_6)(\lambda_1^2 + 2\lambda_1\lambda_2 + 4\lambda_2^2) - 2(\alpha_{13}x_5 + \alpha_{12}x_6)\lambda_1\lambda_{12}) \\
 &\quad + x_3((\alpha_{13}^2\lambda_1 - 2\alpha_{12}\alpha_{13}\lambda_{12})(x_3 + 2x_6) + \lambda_{12}^2(\lambda_3x_3 + 2\lambda_4x_6)) \\
 &\quad + 2x_3((\alpha_{12}\alpha_{13}\lambda_1 - \lambda_{12}(\alpha_{12}^2 + \alpha_{13}^2))(x_4 + x_5) + \lambda_{12}^2(\lambda_3x_4 + \lambda_4x_5)) \\
 &\quad + x_4((\alpha_{12}^2\lambda_1 - 2\alpha_{12}\alpha_{13}\lambda_{12})(x_4 + 2x_5) + \lambda_{12}^2(\lambda_3x_4 + 2\lambda_4x_5)) \\
 &\quad + 2x_6((\alpha_{12}\alpha_{13}\lambda_1 - \lambda_{12}(\alpha_{12}^2 + \alpha_{13}^2))(x_4 + x_5) + \lambda_{12}^2(\lambda_4x_4 + \lambda_3x_5)) \\
 &\quad \left. + (\alpha_{12}^2\lambda_1 - 2\alpha_{12}\alpha_{13}\lambda_{12} + \lambda_{12}^2\lambda_3)x_5^2 + (\alpha_{13}^2\lambda_1 - 2\alpha_{12}\alpha_{13}\lambda_{12} + \lambda_{12}^2\lambda_3)x_6^2 \right] \\
 &\tag{D.1.13}
 \end{aligned}$$

By the case assumptions and the copositivity condition (D.1.12), the quadratic form (D.1.13) is non-negative termwise and the theorem is satisfied.

For the copositivity of the matrix  ${}^4FV$ , let  $y^T = (x_1 \ x_2 \ x_3 \ x_4 \ x_5 \ x_6 \ x_7)$  be a nonzero and a non-negative vector. Let  $x_{1,2,3} \neq 0$ ,  $x_{4,\dots,7} = 0$ . Then the linear form

$$b^T y = \lambda_1(x_1 + x_3) + \lambda_{12}x_2 \leq 0 \longleftrightarrow x_2 \geq x_2^{\min} = \frac{\lambda_1}{-\lambda_{12}}(x_1 + x_3).$$

Condition (D.1.12) makes the corresponding quadratic form

$$y^T(\lambda_1 C - bb^T)y = -4\lambda_2(x_1(x_2 - x_3)\lambda_1 + x_2(x_3\lambda_1 + x_2(\lambda_1 + \lambda_2)))$$

be increasing in  $x_2$  (for any fixed values of  $x_{1,3}$ ), and hence we deduce that

$$y^T(\lambda_1 C - bb^T)y \geq y^T(\lambda_1 C - bb^T)y \Big|_{x_2=x_2^{\min}}$$

$$\begin{aligned}
 &= \frac{4\lambda_1}{\lambda_{12}^2} (\lambda_1 \lambda_2^2 x_1^2 + \lambda_2 (\lambda_1^2 + 6\lambda_1 \lambda_2 + 4\lambda_2^2) x_1 x_3 + \lambda_1 \lambda_2^2 x_3^2) \geq 0 \\
 &= \frac{4\lambda_1}{\lambda_{12}^2} X_{13}^T M_{13} X_{13} \geq 0, \quad \forall x_{1,3},
 \end{aligned} \tag{D.1.14}$$

where

$$M_{13} = \begin{pmatrix} \lambda_1 \lambda_2^2 & \frac{1}{2} \lambda_2 (\lambda_1^2 + 6\lambda_1 \lambda_2 + 4\lambda_2^2) \\ \frac{1}{2} \lambda_2 (\lambda_1^2 + 6\lambda_1 \lambda_2 + 4\lambda_2^2) & \lambda_1 \lambda_2^2 \end{pmatrix}, \quad X_{13} \begin{pmatrix} x_1 \\ x_3 \end{pmatrix}.$$

Now,  $y^T(\lambda_1 C - bb^T)y \Big|_{x_2=x_2^{\min}} \geq 0$  is equivalent to the copositivity of the matrix  $M_{13}$ . Equivalently,

$$\lambda_1^2 + 8\lambda_1 \lambda_2 + 4\lambda_2^2 \leq 0. \tag{D.1.15}$$

Now, assume that  $x_i \neq 0$ ,  $i = 1, \dots, 7$ . Then, the linear form

$$b^T y \leq 0 \longleftrightarrow x_2 \geq x_2^{\min} = \frac{1}{-\lambda_{12}} (\lambda_1 x_1 + \lambda_1 x_3 + \alpha_{13} x_4 + \alpha_{12} x_5 + \alpha_{13} x_6 + \alpha_{12} x_7).$$

As before, conditions (D.1.12, D.1.15) make

$$y^T(\lambda_1 C - bb^T)y \geq y^T(\lambda_1 C - bb^T)y \Big|_{x_2=x_2^{\min}} \geq 0, \quad \forall x_{1,3,\dots,6}.$$

Hence, the theorem is satisfied, and, finally, the only imposed conditions for the matrix  ${}^{4F}V$  to be copositive in this case are those in (D.1.9). The same procedure is followed to extract the copositivity conditions in the following cases:

3.  $\alpha_{12} \geq 0$ ,  $\alpha_{13} \leq 0$ , and  $\lambda_{12} \geq 0$ : The following conditions are necessary for the copositivity:

$$\lambda_1 \lambda_3 - \alpha_{13}^2 \geq 0, \quad \alpha_{13}^2 (\lambda_3 - \lambda_4) \geq 0.$$

Since  $\lambda_4 - \lambda_3 > 0$ , then we must have  $\alpha_{13} = 0$ . Finally, in this case, the copositivity conditions are

$$\alpha_{12} \geq 0, \quad \alpha_{13} = 0, \quad \lambda_{12} \geq 0. \tag{D.1.16}$$

4.  $\alpha_{12} \leq 0$ ,  $\alpha_{13} \geq 0$ , and  $\lambda_{12} \geq 0$ : The following conditions are necessary for the copositivity:

$$\lambda_1\lambda_3 - \alpha_{12}^2 \geq 0, \quad \alpha_{12}^2(\alpha_{12} - \alpha_{13})^2\lambda_1^2(\lambda_3^2 - \lambda_4^2) \geq 0.$$

Again, either  $\alpha_{12} = 0$ ,  $\alpha_{12} = \alpha_{13}$ , or  $\lambda_1 = 0$ . But the minimal copositivity conditions in this case are

$$\alpha_{12} = 0, \quad \alpha_{13} \geq 0, \quad \lambda_{12} \geq 0. \quad (\text{D.1.17})$$

5.  $\alpha_{12} \geq 0$ ,  $\alpha_{13} \leq 0$ , and  $\lambda_{12} \leq 0$ : The copositivity conditions are

$$\alpha_{12} \geq 0, \quad \alpha_{13} = 0, \quad \lambda_{12} \leq 0, \quad \lambda_1 + \lambda_2 \geq 0, \quad \lambda_1^2 + 8\lambda_1\lambda_2 + 4\lambda_2^2 \leq 0. \quad (\text{D.1.18})$$

6.  $\alpha_{12} \leq 0$ ,  $\alpha_{13} \geq 0$ , and  $\lambda_{12} \leq 0$ : The copositivity conditions are

$$\alpha_{12} = 0, \quad \alpha_{13} \geq 0, \quad \lambda_{12} \leq 0, \quad \lambda_1 + \lambda_2 \geq 0, \quad \lambda_1^2 + 8\lambda_1\lambda_2 + 4\lambda_2^2 \leq 0. \quad (\text{D.1.19})$$

7.  $\alpha_{12} \leq 0$ ,  $\alpha_{13} \leq 0$ , and  $\lambda_{12} \geq 0$ : The following conditions are necessary for the copositivity:

$$\lambda_1\lambda_3 - \alpha_{12}^2 \geq 0, \quad \lambda_1\lambda_3 - \alpha_{13}^2 \geq 0, \quad \alpha_{12}^2(\lambda_3 - \lambda_4) \geq 0, \quad \alpha_{13}^2(\lambda_3 - \lambda_4) \geq 0. \quad (\text{D.1.20})$$

Hence, in this case, the copositivity conditions are

$$\alpha_{12} = \alpha_{13} = 0, \quad \lambda_{12} \geq 0. \quad (\text{D.1.21})$$

8.  $\alpha_{12} \leq 0$ ,  $\alpha_{13} \leq 0$ , and  $\lambda_{12} \leq 0$ : The copositivity conditions are

$$\alpha_{12} = \alpha_{13} = 0, \quad \lambda_{12} \leq 0, \quad \lambda_1 + \lambda_2 \geq 0, \quad \lambda_1^2 + 8\lambda_1\lambda_2 + 4\lambda_2^2 \leq 0. \quad (\text{D.1.22})$$

## D.2 Minimization of the ALRM Potential

The minimization of the Higgs potential (2.2.15) leads to obtaining the different VEVs in terms of the potential parameters. The procedure is to insert the VEVs in the potential which gives  $V(k', k, v_L, v_R) = V(\langle \Phi \rangle, \langle \chi_R \rangle, \langle \chi_L \rangle)$ . Written out in full:

$$\begin{aligned} 4V(k', k, v_L, v_R) &= (k^4 + k'^4)\lambda_1 + 2k^2k'^2(\lambda_1 + 2\lambda_2) + 2k^2((\alpha_1 + \alpha_2)(v_L^2 + v_R^2) - \mu_1^2) \\ &\quad + 2\sqrt{2}k\mu_3v_Lv_R + 2k'^2((\alpha_1 + \alpha_3)(v_L^2 + v_R^2) - \mu_1^2) + \lambda_3(v_L^4 + v_R^4) \\ &\quad + 2\lambda_4v_L^2v_R^2 - 2\mu_2^2(v_L^2 + v_R^2). \end{aligned} \quad (\text{D.2.1})$$

For minimization, we solve the following equations

$$\frac{\partial V}{\partial k'} = k'(k^2(\lambda_1 + 2\lambda_2) + k'^2\lambda_1 - \mu_1^2 + (\alpha_1 + \alpha_3)(v_L^2 + v_R^2)) = 0, \quad (\text{D.2.2})$$

$$\frac{\partial V}{\partial k} = k^3\lambda_1 + k(k'^2(\lambda_1 + 2\lambda_2) - \mu_1^2 + (\alpha_1 + \alpha_2)(v_L^2 + v_R^2)) + \frac{\mu_3v_Lv_R}{\sqrt{2}} = 0, \quad (\text{D.2.3})$$

$$\frac{\partial V}{\partial v_L} = k^2v_L(\alpha_1 + \alpha_2) + \frac{k\mu_3v_R}{\sqrt{2}} + v_L(k'^2(\alpha_1 + \alpha_3) - \mu_2^2 + \lambda_3v_L^2 + \lambda_4v_R^2) = 0, \quad (\text{D.2.4})$$

$$\frac{\partial V}{\partial v_R} = k^2v_R(\alpha_1 + \alpha_2) + \frac{k\mu_3v_L}{\sqrt{2}} + v_R(k'^2(\alpha_1 + \alpha_3) - \mu_2^2 + \lambda_3v_R^2 + \lambda_4v_L^2) = 0. \quad (\text{D.2.5})$$

The value  $k' = 0$  satisfies the first equation. Substituting in the remaining three equations

$$k^3\lambda_1 + k((\alpha_1 + \alpha_2)(v_L^2 + v_R^2) - \mu_1^2) + \frac{\mu_3v_Lv_R}{\sqrt{2}} = 0, \quad (\text{D.2.6})$$

$$\frac{k\mu_3v_R}{\sqrt{2}} + v_L(k^2(\alpha_1 + \alpha_2) - \mu_2^2 + \lambda_3v_L^2 + \lambda_4v_R^2) = 0, \quad (\text{D.2.7})$$

$$\frac{k\mu_3v_L}{\sqrt{2}} + v_R(k^2(\alpha_1 + \alpha_2) - \mu_2^2 + \lambda_3v_R^2 + \lambda_4v_L^2) = 0. \quad (\text{D.2.8})$$

Multiply the second equation by  $v_R$  and the third one by  $v_L$ . Sum the resulting equations to each other and then subtract one from the other. We obtain

$$v_L^2 + v_R^2 = \frac{\mu_2^2 - k^2(\alpha_1 + \alpha_2)}{\lambda_3}, \quad v_Lv_R = \frac{-k\mu_3}{\sqrt{2}(\lambda_4 - \lambda_3)}. \quad (\text{D.2.9})$$

From which we obtain

$$v_L^2 = \frac{1}{2} \left( \frac{\mu_2^2 - k^2(\alpha_1 + \alpha_2)}{\lambda_3} - \sqrt{\frac{(\mu_2^2 - k^2(\alpha_1 + \alpha_2))^2}{\lambda_3^2} - \frac{2k^2\mu_3^2}{(\lambda_4 - \lambda_3)^2}} \right), \quad (\text{D.2.10})$$

$$v_R^2 = \frac{1}{2} \left( \frac{\mu_2^2 - k^2(\alpha_1 + \alpha_2)}{\lambda_3} + \sqrt{\frac{(\mu_2^2 - k^2(\alpha_1 + \alpha_2))^2}{\lambda_3^2} - \frac{2k^2\mu_3^2}{(\lambda_4 - \lambda_3)^2}} \right). \quad (\text{D.2.11})$$

From eq. (D.2.6), we have

$$k^2 = \frac{2(\lambda_3\mu_1^2 - (\alpha_1 + \alpha_2)\mu_2^2)(\lambda_4 - \lambda_3) + \lambda_3\mu_3^2}{2(\lambda_1\lambda_3 - (\alpha_1 + \alpha_2)^2)(\lambda_4 - \lambda_3)}. \quad (\text{D.2.12})$$

# E

## Mass Matrix Diagonlization

### E.1 Eigenvalues

For a (symmetric)  $n \times n$  (mass) matrix  $M = (m_{ij})_{i,j=1,\dots,n}$  whose eigenvalues  $x_i$ ,  $i = 1, \dots, n$ , we have

$$T = \text{Tr}(M) = \sum_{i=1}^n x_i, \quad D = \text{Det}(M) = \prod_{i=1}^n x_i. \quad (\text{E.1.1})$$

If  $D = 0$ , for  $x_1 = \dots = x_s = 0$ , for some  $s < n$ , we have

$$x_n = T - \sum_{i=s+1}^{n-1} x_i. \quad (\text{E.1.2})$$

Otherwise, i.e., if all the eigenvalues are nonzero, we have

$$x_n = T - \sum_{i=1}^{n-1} x_i = \frac{D}{\prod_{i=1}^{n-1} x_i}. \quad (\text{E.1.3})$$

From the second equality in (E.1.3), we obtain

$$x_{n-1}^2 - (T - \sum_{i=1}^{n-2} x_i)x_{n-1} + \frac{D}{\prod_{i=1}^{n-2} x_i} = 0, \quad (\text{E.1.4})$$

i.e.,

$$x_{n-1} = \frac{1}{2} \left( T - \sum_{i=1}^{n-2} x_i \pm \sqrt{(T - \sum_{i=1}^{n-2} x_i)^2 - \frac{4D}{\prod_{i=1}^{n-2} x_i}} \right). \quad (\text{E.1.5})$$

Substituting from eq. (E.1.5) into eq. (E.1.3), we obtain

$$x_n = \frac{1}{2} \left( T - \sum_{i=1}^{n-2} x_i \mp \sqrt{(T - \sum_{i=1}^{n-2} x_i)^2 - \frac{4D}{\prod_{i=1}^{n-2} x_i}} \right). \quad (\text{E.1.6})$$

Thus from eq. (E.1.5) and eq. (E.1.6) we have the two eigenvalues  $x_{n-1}, x_n$  in terms of the other eigenvalues  $x_1, \dots, x_{n-2}$ , the trace  $T$  and the determinant  $D$  of the matrix  $M$ . Notice that the  $\pm$  signs in the expressions of  $x_{n-1}, x_n$  in eq. (E.1.5) and eq. (E.1.6) just interchange the roles between the numerical values of both  $x_{n-1}$  and  $x_n$ .

It's worth mentioning that the  $CP$ -even neutral Higgs mass matrix is an example for the case in which all eigenvalues are nonzero. The  $CP$ -odd neutral Higgs, charged Higgs, where it appears a set of Goldstone bosons eaten by corresponding gauge bosons for acquiring masses, and the Electroweak neutral gauge boson mass matrix, where the photon appears, are examples for the case in which some eigenvalues are zeros.

The characteristic polynomial can be written as

$$P_n(x) = \sum_{k=0}^n D_{n-k}(-x)^k, \quad (\text{E.1.7})$$

where

$$D_0 = 1, \quad D_{n-k} = \sum_{i_1 < \dots < i_k} \text{Det}(M_{n-k}^{(i_1 \dots i_k)}), \quad k = 0, \dots, n-1. \quad (\text{E.1.8})$$

$M_{n-k}^{(i_1 \dots i_k)}$  is the  $(n-k) \times (n-k)$  submatrix of  $M$  which results by eliminating the  $i_1, \dots, i_k$  rows and columns. Notice that  $D_1 = \text{Tr}(M)$  and  $D_n = \text{Det}(M)$ . Moreover, since  $x_i$ 's are the zeros of the characteristic polynomial, and if the coefficients  $D_{n-k}$  ( $k = 0, \dots, n$ ) are linear in some parameter, say  $\lambda$  of the theory, then we have<sup>1</sup>

$$\lambda = -\frac{\sum_{k=0}^n D_{n-k}^{(0)} (-x_i)^k}{\sum_{k=0}^n D_{n-k}^{(1)} (-x_i)^k}, \quad D_{n-k} = D_{n-k}^{(1)} \lambda + D_{n-k}^{(0)}. \quad (\text{E.1.9})$$

## E.2 Nonsingular Mass Matrix Diagonlization

An  $n$  nonsingular symmetric mass matrix  $M$  has a number of  $n(n+1)/2$  independent variable

$$m_{ij}, \quad i = 1, \dots, n, \quad i \leq j \leq n, \quad (\text{E.2.1})$$

and the other inputs are given by the symmetry condition

$$m_{ij} = m_{ji}, \quad j < i \leq n. \quad (\text{E.2.2})$$

A typical matrix element of the rotation matrix  $V$  is given by

$$V_{jk} = \frac{f_{jk}^{(k)}}{\sqrt{\sum_{l=1}^n (f_{lk}^{(k)})^2}}, \quad j, k = 1, \dots, n, \quad (\text{E.2.3})$$

where the numbers  $f_{ij}^{(k)}$ 's are defined recursively by

$$f_{ij}^{(k)} = f_{ij}^{(k-1)} - \frac{f_{i,k-1}^{(k-1)} \sum_{l=1}^n (f_{lj}^{(1)} f_{l,k-1}^{(k-1)})}{\sum_{l=1}^n (f_{l,k-1}^{(k-1)})^2}, \quad i = 1, \dots, n, \quad j = k, \dots, n, \quad (\text{E.2.4})$$

---

<sup>1</sup>Based on a notice by my late colleague A. Elsayed, and I dedicate its usage to his smart soul.

where we define  $f_{ij}^{(1)} = f_{ij} = f_i(x_j)$ , and the base functions  $f_i$ 's for a nonsingular matrix  $M$  are given by

$$f_i(x) = (-1)^{n+i} \frac{D(x)_{n-1}^{(i1)}}{D(x)_{n-1}^{(n1)}}, \quad D(x)_{n-1}^{(i_1 i_2)} = \text{Det}(M(x)_{n-1}^{(i_1 i_2)}), \quad i = 1, \dots, n, \quad (\text{E.2.5})$$

where  $M(x)_{n-1}^{(i_1 i_2)}$  is the  $(n-1) \times (n-1)$  submatrix of  $M - Ix$  which results by eliminating the  $i_1^{\text{th}}$  row and the  $i_2^{\text{th}}$  column. We notice that  $f_n(x) \equiv 1$ .

In fact, the diagonalization matrix  $V_{jk}$  is just the orthonormalization of the matrix  $f_{ij}$  of the eigenvectors of the mass matrix  $M$ . So the formula of  $V_{jk}$  does not change according to whether  $M$  is a singular or nonsingular matrix. However, if the matrix  $M$  is singular for having a number of  $s$  ( $< n$ ) zero eigenvalues, the set of base functions is devided into two sets corresponding to the zero and nonzero eigenvalues. The base functions of the set corresponding to the nonvanishing are given again by (E.2.5), while the other set arise from the consistency conditions of singularity and symmetry of  $M$  (See App. E.3).

### E.2.1 Example: $n = 2$

The characteristic polynomial

$$P_2(x) = x^2 - Tx + D, \quad (\text{E.2.6})$$

whose eigenvalues are

$$x_1 = \frac{1}{2}(T \pm \sqrt{T^2 - 4D}), \quad x_2 = T - x_1 = \frac{D}{x_1} = \frac{1}{2}(T \mp \sqrt{T^2 - 4D}). \quad (\text{E.2.7})$$

If  $D = 0$ , then  $x_1 = T$  and  $x_2 = 0$ . The rotation matrix (E.2.3) is

$$V = \begin{pmatrix} \frac{f_{11}}{\sqrt{1+f_{11}^2}} & \frac{\text{sgn}}{\sqrt{1+f_{11}^2}} \\ \frac{1}{\sqrt{1+f_{11}^2}} & -\frac{\text{sgn}f_{11}}{\sqrt{1+f_{11}^2}} \end{pmatrix}, \quad (\text{E.2.8})$$

where  $\text{sgn} = \text{sign}(f_{12} - f_{11})$ , and the base function (E.2.5) is

$$f_1(x) = -\frac{m_{22} - x}{m_{12}}. \quad (\text{E.2.9})$$

### E.2.2 Example: $n = 3$

This is the case considered already in details in subsection 2.4.1 for the  $CP$ -even Higgs bosons' mass matrix (2.4.17). The mass squared eigenvalues are the roots of the characteristic polynomial

$$P_3(x) = -x^3 + Tx^2 - D_2x + D. \quad (\text{E.2.10})$$

The Higgs mass squared eigenvalues are [37, 38, 50, 73, 82]

$$x_k = \frac{1}{3} \left( T - \xi^{k-1} C - \frac{\Delta_0}{\xi^{k-1} C} \right), \quad \xi = \frac{-1 + \sqrt{3}i}{2}, \quad k = 1, \dots, 3, \quad (\text{E.2.11})$$

where

$$\Delta_0 = T^2 - 3D_2, \quad (\text{E.2.12})$$

$$\Delta_1 = 2T^3 - 9TD_2 + 27D, \quad (\text{E.2.13})$$

$$C = \sqrt[3]{\frac{1}{2} \left( -\Delta_1 + \sqrt{\Delta_1^2 - 4\Delta_0^3} \right)}. \quad (\text{E.2.14})$$

The discriminant is

$$\Delta = 18TD_2D - 4T^3D + T^2D_2^2 - 4D_2^3 - 27D^2. \quad (\text{E.2.15})$$

If  $\Delta = 0$  and  $\Delta_0 = 0$ , then the equation has a single root (which is a triple root)  $\frac{T}{3}$ .

If  $\Delta = 0$  and  $\Delta_0 \neq 0$ , then there are both a double root  $\frac{TD_2 - 9D}{2\Delta_0}$  and a simple root  $\frac{4TD_2 - 9D + D_2^2}{-\Delta_0}$ .

Explicitly, the rotation coefficients of the diagonalization matrix (E.2.3) is

$$V_{11} = \frac{f_{11}}{\sqrt{f_{11}^2 + f_{21}^2 + 1}}, \quad (\text{E.2.16})$$

$$V_{12} = \frac{f_{12}(1 + f_{21}^2) - f_{11}(1 + f_{21}f_{22})}{\sqrt{(1 + f_{11}^2 + f_{21}^2)\{(f_{11} - f_{12})^2 + (f_{21} - f_{22})^2 + (f_{12}f_{21} - f_{11}f_{22})^2\}}}, \quad (\text{E.2.17})$$

$$V_{13} = \frac{(\text{sgn})(f_{22} - f_{21})}{\sqrt{(f_{11} - f_{12})^2 + (f_{21} - f_{22})^2 + (f_{12}f_{21} - f_{11}f_{22})^2}}, \quad (\text{E.2.18})$$

$$V_{21} = \frac{f_{21}}{\sqrt{f_{11}^2 + f_{21}^2 + 1}}, \quad (\text{E.2.19})$$

$$V_{22} = \frac{f_{22}(1 + f_{11}^2) - f_{21}(1 + f_{11}f_{12})}{\sqrt{(1 + f_{11}^2 + f_{21}^2)\{(f_{11} - f_{12})^2 + (f_{21} - f_{22})^2 + (f_{12}f_{21} - f_{11}f_{22})^2\}}}, \quad (\text{E.2.20})$$

$$V_{23} = \frac{(\text{sgn})(f_{11} - f_{12})}{\sqrt{(f_{11} - f_{12})^2 + (f_{21} - f_{22})^2 + (f_{12}f_{21} - f_{11}f_{22})^2}}, \quad (\text{E.2.21})$$

$$V_{31} = \frac{1}{\sqrt{f_{11}^2 + f_{21}^2 + 1}}, \quad (\text{E.2.22})$$

$$V_{32} = \frac{f_{11}(f_{11} - f_{12}) + f_{21}(f_{21} - f_{22})}{\sqrt{(1 + f_{11}^2 + f_{21}^2)\{(f_{11} - f_{12})^2 + (f_{21} - f_{22})^2 + (f_{12}f_{21} - f_{11}f_{22})^2\}}}, \quad (\text{E.2.23})$$

$$V_{33} = \frac{(\text{sgn})(f_{12}f_{21} - f_{11}f_{22})}{\sqrt{(f_{11} - f_{12})^2 + (f_{21} - f_{22})^2 + (f_{12}f_{21} - f_{11}f_{22})^2}}, \quad (\text{E.2.24})$$

where

$$\text{sgn} = \text{sign}\{f_{11}(f_{23} - f_{22}) + f_{12}(f_{21} - f_{23}) + f_{13}(f_{22} - f_{21})\}, \quad (\text{E.2.25})$$

and the base functions  $f_i$ 's (E.2.5) are

$$f_1(x) = \frac{(m_{22} - x)(m_{33} - x) - m_{23}^2}{m_{12}m_{23} - m_{13}(m_{22} - x)}, \quad (\text{E.2.26})$$

$$f_2(x) = -\frac{m_{12}(m_{33} - x) - m_{13}m_{23}}{m_{12}m_{23} - m_{13}(m_{22} - x)}. \quad (\text{E.2.27})$$

### E.2.3 Example: $n = 4$

The mass squared eigenvalues are the roots of the characteristic polynomial

$$P_4(x) = x^4 - Tx^3 + D_2x^2 - D_3x + D. \quad (\text{E.2.28})$$

The Higgs mass squared eigenvalues are [37, 38, 50, 73, 82]

$$x_k = \frac{T}{4} - S \mp \frac{1}{2}\sqrt{-2p + \frac{q}{S} - 4S^2}, \quad \frac{T}{4} + S \mp \frac{1}{2}\sqrt{-2p - \frac{q}{S} - 4S^2}, \quad k = 1, \dots, 4, \quad (\text{E.2.29})$$

where

$$p = \frac{1}{8} (8D_2 - 3T^2), \quad (\text{E.2.30})$$

$$q = \frac{1}{8} (-T^3 + 4TD_2 - 8D_3), \quad (\text{E.2.31})$$

$$S = \frac{1}{2} \sqrt{\frac{1}{3} \left( \frac{\Delta_0}{Q} + Q \right) - \frac{2p}{3}}, \quad (\text{E.2.32})$$

$$Q = \sqrt[3]{\frac{1}{2} \left( \sqrt{\Delta_1^2 - 4\Delta_0^3} + \Delta_1 \right)}, \quad (\text{E.2.33})$$

$$\Delta_0 = -3TD_3 + D_2^2 + 12D, \quad (\text{E.2.34})$$

$$\Delta_1 = 27T^2D - 9TD_2D_3 + 2D_2^3 - 72D_2D + 27D_3^2. \quad (\text{E.2.35})$$

The base functions  $f_i$ 's (E.2.5) are

$$f_1(x) = -\frac{(m_{22}-x)((m_{33}-x)(m_{44}-x)-m_{34}^2) - m_{23}(m_{23}(m_{44}-x)-m_{24}m_{34}) + m_{24}(m_{23}m_{34}-m_{24}(m_{33}-x))}{m_{12}(m_{23}m_{34}-m_{24}(m_{33}-x)) - m_{13}(m_{34}(m_{22}-x)-m_{23}m_{24}) + m_{14}((m_{22}-x)(m_{33}-x)-m_{32}^2)}, \quad (\text{E.2.36})$$

$$f_2(x) = \frac{m_{12}((m_{33}-x)(m_{44}-x)-m_{34}^2) - m_{13}(m_{23}(m_{44}-x)-m_{24}m_{34}) + m_{14}(m_{23}m_{34}-m_{24}(m_{33}-x))}{m_{12}(m_{23}m_{34}-m_{24}(m_{33}-x)) - m_{13}(m_{34}(m_{22}-x)-m_{23}m_{24}) + m_{14}((m_{22}-x)(m_{33}-x)-m_{32}^2)}, \quad (\text{E.2.37})$$

$$f_3(x) = -\frac{m_{12}(m_{23}(m_{44}-x)-m_{24}m_{34}) - m_{13}((m_{22}-x)(m_{44}-x)-m_{24}^2) + m_{14}(m_{34}(m_{22}-x)-m_{23}m_{24})}{m_{12}(m_{23}m_{34}-m_{24}(m_{33}-x)) - m_{13}(m_{34}(m_{22}-x)-m_{23}m_{24}) + m_{14}((m_{22}-x)(m_{33}-x)-m_{32}^2)}. \quad (\text{E.2.38})$$

## E.3 Singular Mass Matrix Diagonlization

An  $n$  singular symmetric mass matrix  $M$  with a number  $s$  of zero eigenvalues has a number of  $(n-s)(n+s+1)/2$  independent variable

$$m_{ij}, \quad i = 1, \dots, n-s, \quad i \leq j \leq n, \quad (\text{E.3.1})$$

and the other inputs are given by the symmetry and singularity conditions

$$m_{ij} = m_{ji}, \quad i = 1, \dots, n, \quad j = 1, \dots, n-s, \quad j < i, \quad (\text{E.3.2})$$

and

$$m_{n-s+r, n-s+j} = \sum_{q=1}^{n-s} x_{rq} m_{n-s+j, q}, \quad r, j = 1, \dots, s, \quad (\text{E.3.3})$$

where  $x_{rq}$ 's are the solutions of the linear systems of the singularity and symmetry consistency conditions of  $M$  (E.3.5).

For an  $n$  singular symmetric mass matrix  $M$  with a number  $s$  of zero eigenvalues, a typical matrix element of the rotation matrix is given again by (E.2.3) and (E.2.4) where we define  $f_{ij}^{(1)} = f_{ij}$ . However, in the case of a singular matrix, the numbers  $f_{ij}$ 's are devided this time into two sets according to the zero and nonzero eigenvalues as follows. The first set does not depend on the eigenvalues, but they rather arise from the singularity and symmetry consistency conditions of  $M$ . They are

$$f_{qr} = -x_{s-r+1, q}, \quad f_{n-s+u, r} = \delta_{n-s+u, n-r+1}, \quad q = 1, \dots, n-s, \quad u, r = 1, \dots, s, \quad (\text{E.3.4})$$

where  $x_{rq}$ 's are the solutions of the linear systems of the singularity and symmetry consistency conditions of  $M$

$$\sum_{q=1}^{n-s} x_{rq} m_{tq} = m_{t, n-s+r}, \quad t = 1, \dots, n-s, \quad r = 1, \dots, s, \quad (\text{E.3.5})$$

and the second set depends on the nonzero eigenvalues and it is given again as (E.2.5)

$$f_{ij} = f_i(x_j) = (-1)^{n+i} \frac{D(x_j)_{n-1}^{(i1)}}{D(x_j)_{n-1}^{(n1)}}, \quad D(x)_{n-1}^{(i_1 i_2)} = \text{Det}(M(x)_{n-1}^{(i_1 i_2)}), \quad i = 1, \dots, n, \quad j = s+1, \dots, n, \quad (\text{E.3.6})$$

where  $x_j$  ( $j = s+1, \dots, n$ ) are the nonzero eigenvalues.

### E.3.1 Example: $n = 2$

The general form of a symmetric  $2 \times 2$  mass matrix with one zero eigenvalue ( $s = 1$ ) (say, the charged Higgs matrices (2.4.2) and (2.4.3)) is

$$\begin{pmatrix} m_{11} & m_{12} \\ m_{12} & \frac{m_{12}^2}{m_{11}} \end{pmatrix}, \quad (\text{E.3.7})$$

and  $x_{11} = m_{12}/m_{11}$ .

### E.3.2 Example: $n = 3$

**Case:**  $s = 1$

The general form of a symmetric  $3 \times 3$  mass matrix with only one zero eigenvalue (say, the  $ZZ'A$  gauge mass matrix (2.3.21)) is

$$\begin{pmatrix} m_{11} & m_{12} & m_{13} \\ m_{12} & m_{22} & m_{23} \\ m_{13} & m_{23} & x_{11}m_{13} + x_{12}m_{23} \end{pmatrix} \quad (\text{E.3.8})$$

such that from (E.3.5)

$$x_{11}m_{11} + x_{12}m_{12} = m_{13}, \quad x_{11}m_{12} + x_{12}m_{22} = m_{23}. \quad (\text{E.3.9})$$

i.e.,

$$x_{11} = \frac{m_{22}m_{13} - m_{12}m_{23}}{m_{11}m_{22} - m_{12}^2}, \quad x_{12} = \frac{m_{11}m_{23} - m_{12}m_{13}}{m_{11}m_{22} - m_{12}^2}. \quad (\text{E.3.10})$$

**Case:**  $s = 2$

The general form of a symmetric  $3 \times 3$  mass matrix with two zero eigenvalues (say, the pseudoscalar Higgs matrix (2.4.11)) is

$$\begin{pmatrix} m_{11} & m_{12} & m_{13} \\ m_{12} & \frac{m_{12}^2}{m_{11}} & \frac{m_{12}m_{13}}{m_{11}} \\ m_{13} & \frac{m_{12}m_{13}}{m_{11}} & \frac{m_{13}^2}{m_{11}} \end{pmatrix}, \quad (\text{E.3.11})$$

and we have directly from (E.3.5)

$$x_{11} = \frac{m_{12}}{m_{11}}, \quad x_{21} = \frac{m_{13}}{m_{11}}. \quad (\text{E.3.12})$$

### E.3.3 Example: $n = 4$

**Case:**  $s = 1$

The general form of a symmetric  $4 \times 4$  mass matrix with one zero eigenvalue is

$$\begin{pmatrix} m_{11} & m_{12} & m_{13} & m_{14} \\ m_{12} & m_{22} & m_{23} & m_{24} \\ m_{13} & m_{23} & m_{33} & m_{34} \\ m_{14} & m_{24} & m_{34} & x_{11}m_{14} + x_{12}m_{24} + x_{13}m_{34} \end{pmatrix} \quad (\text{E.3.13})$$

such that from (E.3.5), the  $x_{ij}$ 's are the solutions of the system

$$\begin{aligned} x_{11}m_{11} + x_{12}m_{12} + x_{13}m_{13} &= m_{14}, \\ x_{11}m_{12} + x_{12}m_{22} + x_{13}m_{23} &= m_{24}, \\ x_{11}m_{13} + x_{12}m_{23} + x_{13}m_{33} &= m_{34}. \end{aligned} \quad (\text{E.3.14})$$

**Case:**  $s = 2$

The general form of a symmetric  $4 \times 4$  mass matrix with two zero eigenvalues (say, the pseudoscalar or the charged Higgs matrices in the LRSM [59]) is

$$\begin{pmatrix} m_{11} & m_{12} & m_{13} & m_{14} \\ m_{12} & m_{22} & m_{23} & m_{24} \\ m_{13} & m_{23} & x_{11}m_{13} + x_{12}m_{23} & x_{11}m_{14} + x_{12}m_{24} \\ m_{14} & m_{24} & x_{21}m_{13} + x_{22}m_{23} & x_{21}m_{14} + x_{22}m_{24} \end{pmatrix} \quad (\text{E.3.15})$$

such that

$$x_{11}m_{11} + x_{12}m_{12} = m_{13}, \quad x_{11}m_{12} + x_{12}m_{22} = m_{23}, \quad (\text{E.3.16})$$

$$x_{21}m_{11} + x_{22}m_{12} = m_{14}, \quad x_{21}m_{12} + x_{22}m_{22} = m_{24}, \quad (\text{E.3.17})$$

i.e.,

$$x_{11} = \frac{m_{22}m_{13} - m_{12}m_{23}}{m_{11}m_{22} - m_{12}^2}, \quad x_{12} = \frac{m_{11}m_{23} - m_{12}m_{13}}{m_{11}m_{22} - m_{12}^2}. \quad (\text{E.3.18})$$

$$x_{21} = \frac{m_{22}m_{14} - m_{12}m_{24}}{m_{11}m_{22} - m_{12}^2}, \quad x_{22} = \frac{m_{11}m_{24} - m_{12}m_{14}}{m_{11}m_{22} - m_{12}^2}. \quad (\text{E.3.19})$$

**Case:**  $s = 3$

The general form of a symmetric  $4 \times 4$  mass matrix with three zero eigenvalues is

$$\begin{pmatrix} m_{11} & m_{12} & m_{13} & m_{14} \\ m_{12} & \frac{m_{12}^2}{m_{11}} & \frac{m_{12}m_{13}}{m_{11}} & \frac{m_{12}m_{14}}{m_{11}} \\ m_{13} & \frac{m_{12}m_{13}}{m_{11}} & \frac{m_{13}^2}{m_{11}} & \frac{m_{13}m_{14}}{m_{11}} \\ m_{14} & \frac{m_{12}m_{14}}{m_{11}} & \frac{m_{13}m_{14}}{m_{11}} & \frac{m_{14}^2}{m_{11}} \end{pmatrix}, \quad (\text{E.3.20})$$

and from (E.3.5)

$$x_{11} = \frac{m_{12}}{m_{11}}, \quad x_{21} = \frac{m_{13}}{m_{11}}, \quad x_{31} = \frac{m_{14}}{m_{11}}. \quad (\text{E.3.21})$$

## E.4 Mathematica® Codes

Since FEYNRULES is a MATHEMATICA® package, I was interested to make these two MATHEMATICA® codes for diagonalization. The first code defines the functions  $f_{ij}$ 's (E.2.5) and hence the diagonalization matrix elements (E.2.3), and the second code composes the coefficients of the characteristic polynomial of the mass matrix so that it can be solved for (E.1.9). I used these codes in testing their purposes before implementing the procedure into FEYNRULES.

### A Mathematica® Code for Diagonalization

(\*\*\* Inputs \*\*\*)

```

dim=n;

msub=Module[{i,j},Flatten[Table[ToExpression["m"<>ToString[i]<>ToString[j]]->
RandomReal[],{i,dim},{j,i,dim}]]];

M=Table[If[i<=j,ToExpression["m"<>ToString[i]<>ToString[j]],

ToExpression["m"<>ToString[j]<>ToString[i]]],{i,dim},{j,dim}];

Mx[x_]:=M-x IdentityMatrix[dim];

d[i1_,i2_,x_]:=Det[Drop[Mx[x], i1, i2]];

(***  $f_i(x)$  ***)

f[i_,x_]:=(-1)(dim+i) d[i,1,x]/d[dim,1,x];

(*** Eigenvalues ***)

x[j_]:=Eigenvalues[M][[j]];

(*** Diagonalization ***)

(***  $f_{ij}^{(k)}$  ***)

f[k_,i_,j_]:=If[k==1,f[i,x[j]],f[k-1,i,j]-f[k-1,i,k-1]

(Sum[f[1,l,j]f[k-1,l,k-1],{l,dim}]/Sum[f[k-1,l,k-1]2,{l,dim}])];

(***  $v_{jk}$  ***)

v[j_,k_]:=f[k,j,k]/Sqrt[Sum[f[k,l,k]2,{l,dim}]];

(*** Outputs ***)

V=Table[v[i,j],{i,dim},{j,dim}];

V//MatrixForm

V†.M.V//MatrixForm//Chop

```

$V^\dagger \cdot V // \text{MatrixForm} // \text{Chop}$

$V \cdot V^\dagger // \text{MatrixForm} // \text{Chop}$

### A Mathematica® Code for a Singular Diagonalization

```
(*** Inputs ***)

dim=n;mul=s;

msub=Module[{i,j},Flatten[Table[ToExpression["m"<>ToString[i]<>ToString[j]]->
RandomReal[],{i,dim},{j,i,dim}]]];

Mns=Table[If[i<=j,ToExpression["m"<>ToString[i]<>ToString[j]],

ToExpression["m"<>ToString[j]<>ToString[i]]],{i,dim-mul},{j,dim}];

Mx[x_]:=M-x IdentityMatrix[dim];

d[i1_,i2_,x_]:=Det[Drop[Mx[x], i1, i2]];

lm[j_]:=Eigenvalues[M][[j]];

x[r_, q_]:=ToExpression["x" <> ToString[r] <> ToString[q]];

m[t_, q_]:=If[t <= q, ToExpression["m" <> ToString[t] <> ToString[q]],

ToExpression["m" <> ToString[q] <> ToString[t]]];

A[r_, t_]:=Sum[x[r, q] m[t, q], {q, dim - s}];

x1[r_]:=Table[A[r, t]==m[t, dim - s + r], {t, dim - s}];

x2[r_]:=Flatten[Solve[x1[r], Table[x[r, q1], {q1, dim - s}]]];

x3[r_, q_]:=x[r, q] /. x2[r][[q]];

f0[q_, r_]:=If[1 <= r <= s, If[1 <= q <= dim - s, -x3[s - r + 1, q],
```

```

If[dim - s + 1 <= q <= dim, KroneckerDelta[q, dim - r + 1]]];

f[i_, j_] := If[1 <= j <= s, f0[i, j], f1[i, lm[j]]];

msuba = Module[r, q, Flatten[Table[ToExpression["x" <> ToString[r] <> ToString[q]]
-> x3[r, q], r, s, q, dim - s]]];

Ms = Table[A[r, t], r, s, t, dim] /. msuba;

Msns[i_, j_] := If[i <= dim - s, Mns[[i, j]], Ms[[i - (dim - s), j]]];

Mn = Table[Msns[i, j], i, dim, j, dim];

(** Diagonalization **)

(** fij(k) **)

f[k_, i_, j_] := If[k == 1, f[i, x[j]], f[k - 1, i, j] - f[k - 1, i, k - 1]
(Sum[f[1, l, j] f[k - 1, l, k - 1], {l, dim}]/Sum[f[k - 1, l, k - 1]2, {l, dim}])];

(** vjk **)

v[j_, k_] := f[k, j, k]/Sqrt[Sum[f[k, l, k]2, {l, dim}]];

(** Outputs **)

V = Table[v[i, j], {i, dim}, {j, dim}];

V//MatrixForm

V†.Mn.V//MatrixForm//Chop

V†.V//MatrixForm//Chop

V.V†//MatrixForm//Chop

```

### A Mathematica® Code for the Characteristic Polynomial

```

(*** Inputs ***)

dim=n;

msub=Module[{i,j},Flatten[Table[ToExpression["m"<>ToString[i]<>ToString[j]]->
RandomReal[],{i,dim},{j,i,dim}]]];

M=Table[If[i<=j,ToExpression["m"<>ToString[i]<>ToString[j]],

ToExpression["m"<>ToString[j]<>ToString[i]]],{i,dim},{j,dim}]/.msub;

(*** Test *** )

SymmetricMatrixQ[M]

True

(*** Rows and Columns ***)

brkts[x__]:=Table[{x[[i]]},{i,Length[x]}];

p[k_,i_]:=Sort[Permutations[Table[j,{j, dim}],{k}] [[i]]];

p1[k_]:=DeleteDuplicates[Table[p[k,i],{i,dim!/(dim - k)!}]]];

tx[k_,r_]:=If[MemberQ[Range[dim],k]&&MemberQ[Range[Length[p1[k]]],r],

brkts[p1[k][[r]]],Print["Error, enter 0<=k<="<>ToString[dim]<>",

and 1<=r<="<>ToString[Length[p1[k]]]]];

(***  $M_{n-k}^{i_1 \dots i_k}$  *** )

md[m_,k_,r_]:=If[k==0,m,Delete[m,tx[k,r]]];

md1[m_,k_,r_]:=If[k==0||k==dim,md[m,k,r],

Transpose[Delete[Transpose[md[m,k,r]],tx[k,r]]]];


```

```
(*** Dn-k *** )
dt[m_,k_,r_]:=If[k==dim,1,Det[md1[m,k,r]]];
dt1[m_,k_]:=Sum[dt[m,k,r],{r,Length[p1[k]]}];
(* Characteristic Polynomial *)
Pn[m_,x_]:=Sum[dt1[m,k](-x)k,{k,0,dim}];
(* Test *)
In[1]:=CharacteristicPolynomial[m,x]-Pn[m,x]//FullSimplify
Out[1]=0
```

# Bibliography

- [1] Talk by Christophe Ochando, on behalf of the CMS collaboration at Rencontres de Moriond, QCD Session March 9-16, 2013: <http://moriond.in2p3.fr/QCD/2013/ThursdayMorning/Ochando.pdf>.
- [2] Talk by Eleni Mountricha, on behalf of the ATLAS collaboration at Rencontres de Moriond, QCD Session March 9-16, 2013: <http://moriond.in2p3.fr/QCD/2013/ThursdayMorning/Mountricha2.pdf>.
- [3] Aad, G., et al. *Search for dilepton resonances in  $pp$  collisions at  $\sqrt{s} = 7$  TeV with the ATLAS detector*. Phys.Rev.Lett. **107** (2011), 272002.
- [4] Aad, G., et al. *Measurement of Higgs boson production in the diphoton decay channel in  $pp$  collisions at center-of-mass energies of 7 and 8 TeV with the ATLAS detector*. Phys. Rev. **D90** (2014), 112015.
- [5] Alekhin, S. *Parton distributions from deep inelastic scattering data*. Phys. Rev. **D68** (2003), 014002.
- [6] Alloul, A., Christensen, N. D., Degrande, C., Duhr, C., and Fuks, B. *FeynRules 2.0 - A complete toolbox for tree-level phenomenology*. Comput. Phys. Commun. **185** (2014), 2250–2300.
- [7] Alwall, J., Herquet, M., Maltoni, F., Mattelaer, O., and Stelzer, T. *MadGraph 5 : Going Beyond*. JHEP **1106** (2011), 128.

- [8] Antcheva, I., et al. *ROOT: A C++ framework for petabyte data storage, statistical analysis and visualization.* Comput. Phys. Commun. **180** (2009), 2499–2512.
- [9] Ashry, M. *TeV Scale Left-Right Symmetric Model With Minimal Higgs Sector.* Msc thesis, Cairo University, Cairo, 2015.
- [10] Ashry, M. *TeV Scale Left-Right Symmetric Model with Minimal Higgs Sector.* Master’s thesis, Faculty of Science, Cairo University, 2015.
- [11] Ashry, M., and Khalil, S. *Phenomenological aspects of a TeV-scale alternative left-right model.* Phys. Rev. **D91** (2015), 015009.
- [12] Aulakh, C. S., Melfo, A., and Senjanovic, G. *Minimal supersymmetric left-right model.* Phys.Rev. **D57** (1998), 4174–4178.
- [13] Babu, K., He, X.-G., and Ma, E. *New Supersymmetric Left-Right Gauge Model: Higgs Boson Structure and Neutral Current Analysis.* Phys.Rev. **D36** (1987), 878.
- [14] Barenboim, G., Gorbahn, M., Nierste, U., and Raidal, M. *Higgs sector of the minimal left-right symmetric model.* Phys.Rev. **D65** (2002), 095003.
- [15] Basak, T., and Mohanty, S. *130 GeV gamma ray line and enhanced Higgs diphoton rate from Triplet-Singlet extended MSSM.* JHEP **1308** (2013), 020.
- [16] Belyaev, A., Christensen, N. D., and Pukhov, A. *CalcHEP 3.4 for collider physics within and beyond the Standard Model.* Comput.Phys.Commun. **184** (2013), 1729–1769.
- [17] Berg, M., Buchberger, I., Ghilencea, D., and Petersson, C. *Higgs diphoton rate enhancement from supersymmetric physics beyond the MSSM.* Phys.Rev. **D88** (2013), 025017.

## BIBLIOGRAPHY

---

- [18] Bhupal Dev, P., Ghosh, D. K., Okada, N., and Saha, I. *125 GeV Higgs Boson and the Type-II Seesaw Model.* JHEP **1303** (2013), 150.
- [19] Borah, D., Patra, S., and Sarkar, U. *TeV scale Left Right Symmetry with spontaneous D-parity breaking.* Phys.Rev. **D83** (2011), 035007.
- [20] Botje, M. *Error estimates on parton density distributions.* Journal of Physics G: Nuclear and Particle Physics **28** (2002), 779.
- [21] Brun, R., and Rademakers, F. *ROOT: An object oriented data analysis framework.* Nucl. Instrum. Meth. **A389** (1997), 81–86.
- [22] Cao, J., Wan, P., Yang, J. M., and Zhu, J. *The SM extension with color-octet scalars: diphoton enhancement and global fit of LHC Higgs data.* JHEP **1308** (2013), 009.
- [23] Carena, M., Low, I., and Wagner, C. E. *Implications of a Modified Higgs to Diphoton Decay Width.* JHEP **1208** (2012), 060.
- [24] Casas, J., and Ibarra, A. *Oscillating neutrinos and muon to e, gamma.* Nucl.Phys. **B618** (2001), 171–204.
- [25] Chang, W.-F., Ng, J. N., and Wu, J. M. *Constraints on New Scalars from the LHC 125 GeV Higgs Signal.* Phys.Rev. **D86** (2012), 033003.
- [26] Chao, W., Zhang, J.-H., and Zhang, Y. *Vacuum Stability and Higgs Diphoton Decay Rate in the Zee-Babu Model.* JHEP **1306** (2013), 039.
- [27] Chatrchyan, S., et al. *Search for Resonances in the Dilepton Mass Distribution in pp Collisions at  $\sqrt(s) = 7$  TeV.* JHEP **1105** (2011), 093.
- [28] Cheng, T. P., and Li, L. F. *GAUGE THEORY OF ELEMENTARY PARTICLE PHYSICS.* Oxford, Uk: Clarendon ( 1984) 536 P. ( Oxford Science Publications), 1984.

- [29] Collaboration, A. *Combined coupling measurements of the Higgs-like boson with the ATLAS detector using up to  $25 \text{ fb}^{-1}$  of proton-proton collision data* (2013).
- [30] Collaboration, C. *Combination of standard model Higgs boson searches and measurements of the properties of the new boson with a mass near 125 GeV* (2013).
- [31] Conte, E., Fuks, B., and Serret, G. *MadAnalysis 5, A User-Friendly Framework for Collider Phenomenology*. Comput. Phys. Commun. **184** (2013), 222–256.
- [32] de Favereau, J., Delaere, C., Demin, P., Giannanco, A., Lemaître, V., Mertens, A., and Selvaggi, M. *DELPHES 3, A modular framework for fast simulation of a generic collider experiment*. JHEP **02** (2014), 057.
- [33] Deshpande, N., Gunion, J., Kayser, B., and Olness, F. I. *Left-right symmetric electroweak models with triplet Higgs*. Phys.Rev. **D44** (1991), 837–858.
- [34] Djouadi, A. *The Anatomy of electro-weak symmetry breaking. I: The Higgs boson in the standard model*. Phys.Rept. **457** (2008), 1–216.
- [35] Djouadi, A. *The Anatomy of electro-weak symmetry breaking. II. The Higgs bosons in the minimal supersymmetric model*. Phys.Rept. **459** (2008), 1–241.
- [36] Ellis, J., Gaillard, M. K., and Nanopoulos, D. *A phenomenological profile of the Higgs boson*. Nuclear Physics B **106** (1976), 292 – 340.
- [37] Euler, L. *Elements of algebra. Transl. from the French by John Hewlett. Reprinted from the fifth edition, Longman, Orme, and Co., London 1840. With an introduction by C. Truesdell*. New York etc.: Springer-Verlag. LX, 593 p. DM 88.00; \$ 30.90 (1984)., 1984.
- [38] Faucette, W. M. *A Geometric Interpretation of the Solution of the General Quartic Polynomial*. The American Mathematical Monthly **103** (1996), 51–57.

## BIBLIOGRAPHY

---

- [39] Feng, W.-Z., and Nath, P. *Higgs diphoton rate and mass enhancement with vector-like leptons and the scale of supersymmetry.* Phys.Rev. **D87** (2013), 075018.
- [40] Gastmans, R., Wu, S. L., and Wu, T. T. *Higgs Decay into Two Photons, Revisited* (2011).
- [41] Guadagnoli, D., and Mohapatra, R. N. *TeV Scale Left Right Symmetry and Flavor Changing Neutral Higgs Effects.* Phys.Lett. **B694** (2011), 386–392.
- [42] Kannike, K. *Vacuum Stability Conditions From Copositivity Criteria.* Eur.Phys.J. **C72** (2012), 2093.
- [43] Khachatryan, V., et al. *Observation of the diphoton decay of the Higgs boson and measurement of its properties.* Eur. Phys. J. **C74** (2014), 3076.
- [44] Khalil, S., Lee, H.-S., and Ma, E. *Bound on Z' Mass from CDMS II in the Dark Left-Right Gauge Model II.* Phys.Rev. **D81** (2010), 051702.
- [45] Khalil, S., and Salem, S. *Enhancement of in model with -plet.* Nuclear Physics B **876** (2013), 473 – 492.
- [46] Lai, H. L., Huston, J., Kuhlmann, S., Morfin, J., Olness, F. I., Owens, J. F., Pumplin, J., and Tung, W. K. *Global QCD analysis of parton structure of the nucleon: CTEQ5 parton distributions.* Eur. Phys. J. **C12** (2000), 375–392.
- [47] Langacker, P. *Bounds on Mixing Between Light and Heavy Gauge Bosons.* Phys.Rev. **D30** (1984), 2008.
- [48] Langacker, P. *The standard model and beyond.* Thesis (2010).
- [49] Langacker, P., and Sankar, S. U. *Bounds on the Mass of W(R) and the W(L)-W(R) Mixing Angle xi in General SU(2)-L x SU(2)-R x U(1) Models.* Phys.Rev. **D40** (1989), 1569–1585.

- [50] Lazard, D. *Quantifier elimination: Optimal solution for two classical examples.* Journal of Symbolic Computation **5** (1988), 261 – 266.
- [51] Ma, E. *Particle Dichotomy and Left-Right Decomposition of  $E(6)$  Superstring Models.* Phys.Rev. **D36** (1987), 274.
- [52] Ma, E. *Dark Left-Right Model: CDMS, LHC, etc.* J.Phys.Conf.Ser. **315** (2011), 012006.
- [53] Ma, E. *Dark-matter fermion from left-right symmetry.* Phys. Rev. D **85** (2012), 091701.
- [54] Maiezza, A., Nemevsek, M., Nesti, F., and Senjanovic, G. *Left-Right Symmetry at LHC.* Phys.Rev. **D82** (2010), 055022.
- [55] Maiezza, A., and Università degli studi dell’Aquila. Facoltà di scienze matematiche, f. e. n. *Left-right Symmetry at LHC and Phenomenological Implications.* Università degli studi dell’Aquila. Facoltà di scienze matematiche, fisiche e naturali, 2012.
- [56] Martin, A. D., Roberts, R. G., Stirling, W. J., and Thorne, R. S. *MRST partons and uncertainties.* In *Proceedings, 11th International Workshop on Deep Inelastic Scattering (DIS 2003)* (2003), pp. 150–154.
- [57] Messier, M. D. *Review of neutrino oscillations experiments.* eConf **C060409** (2006), 018.
- [58] Mohapatra, R. *Unification and Supersymmetry. Third edition.* Springer, New York, 2003.
- [59] Mohapatra, R., and Pati, J. C. *A Natural Left-Right Symmetry.* Phys.Rev. **D11** (1975), 2558.

## BIBLIOGRAPHY

---

- [60] Mohapatra, R. N. *UNIFICATION AND SUPERSYMMETRY. THE FRONTIERS OF QUARK - LEPTON PHYSICS*. Springer, Berlin, 1986.
- [61] Mohapatra, R. N., Paige, F. E., and Sidhu, D. *Symmetry Breaking and Naturalness of Parity Conservation in Weak Neutral Currents in Left-Right Symmetric Gauge Theories*. Phys.Rev. **D17** (1978), 2462.
- [62] Mohapatra, R. N., and Senjanovic, G. *Neutrino Mass and Spontaneous Parity Violation*. Phys.Rev.Lett. **44** (1980), 912.
- [63] Mohapatra, R. N., and Senjanovic, G. *Neutrino Masses and Mixings in Gauge Models with Spontaneous Parity Violation*. Phys.Rev. **D23** (1981), 165.
- [64] Mohapatra, R. N., and Sidhu, D. P. *Gauge Theories of Weak Interactions with Left-Right Symmetry and the Structure of Neutral Currents*. Phys.Rev. **D16** (1977), 2843.
- [65] Mrenna, S., and Richardson, P. *Matching matrix elements and parton showers with HERWIG and PYTHIA*. JHEP **05** (2004), 040.
- [66] Nemevsek, M., Senjanovic, G., and Tello, V. *Left-Right Symmetry: from Majorana to Dirac*. Phys.Rev.Lett. **110** (2013), 151802.
- [67] Pati, J. C., and Salam, A. *Lepton Number as the Fourth Color*. Phys.Rev. **D10** (1974), 275–289.
- [68] Patrignani, C., et al. *Review of Particle Physics*. Chin. Phys. **C40** (2016), 100001.
- [69] Peskin, M. E., and Schroeder, D. V. *An Introduction to quantum field theory*. Addison-Wesley Publishing Company, 1995.
- [70] Picek, I., and Radovcic, B. *Enhancement of  $h \rightarrow \gamma\gamma$  by seesaw-motivated exotic scalars*. Phys.Lett. **B719** (2013), 404–408.

- [71] Ping, L., and Yu, F. Y. *Criteria for copositive matrices of order four.* Linear Algebra and its Applications **194** (1993), 109 – 124.
- [72] Pumplin, J., Stump, D. R., Huston, J., Lai, H. L., Nadolsky, P. M., and Tung, W. K. *New generation of parton distributions with uncertainties from global QCD analysis.* JHEP **07** (2002), 012.
- [73] Rees, E. L. *Graphical Discussion of the Roots of a Quartic Equation.* The American Mathematical Monthly **29** (1922), 51–55.
- [74] Senjanovic, G., and Mohapatra, R. N. *Exact Left-Right Symmetry and Spontaneous Violation of Parity.* Phys.Rev. **D12** (1975), 1502.
- [75] Sjostrand, T., Lonnblad, L., Mrenna, S., and Skands, P. Z. *Pythia 6.3 physics and manual* (2003).
- [76] Sjostrand, T., Mrenna, S., and Skands, P. Z. *PYTHIA 6.4 Physics and Manual.* JHEP **05** (2006), 026.
- [77] Sjostrand, T., Mrenna, S., and Skands, P. Z. *A Brief Introduction to PYTHIA 8.1.* Comput. Phys. Commun. **178** (2008), 852–867.
- [78] Tanabashi, M., et al. *Review of Particle Physics.* Phys. Rev. **D98** (2018), 030001.
- [79] Tello, V. *Connections between the high and low energy violation of Lepton and Flavor numbers in the minimal left-right symmetric model.* PhD thesis, SISSA, Trieste, 2012.
- [80] Thorne, R. S., Martin, A. D., and Stirling, W. J. *MRST parton distributions: Status 2006.* In *Deep inelastic scattering. Proceedings, 14th International Workshop, DIS 2006, Tsukuba, Japan, April 20-24, 2006* (2006), pp. 81–84.
- [81] Van der Hoek, D. J. *Massive neutrinos and their occurrence in a left-right symmetric model.* Master's thesis, Groningen U., 2007.

## BIBLIOGRAPHY

---

- [82] Van der Waerden, B. L. *Algebra. Volume I. Based in part on lectures by E. Artin and E. Noether. Transl. from the German 7th ed. by Fred Blum and John R. Schulenberger.* New York etc.: Springer-Verlag, 1991.
- [83] Yao, W., et al. *Review of Particle Physics.* J.Phys. **G33** (2006), 1–1232.